Chapter III

Photocatalytic Reactions Using Semiconductors as Photocatalysts.

§1 Hydrogen Production from Water with Hydrocarbons and Fossil Fuels.

[Abstract]

Photocatalytic hydrogen productions from several aliphatic and aromatic compounds with water were investigated with powdered Pt/TiO_2 catalyst suspended in the solution. Various fossil fuels such as coal, tar-sand and pitch whose model structures are composed of aromatic compounds connected by aliphatic hydrocarbons, also reacted with water , producing both hydrogen and carbon dioxide from an early stage of irradiation.

[Introduction]

Recently, photocatalytic reactions such as water splitting[1-8], carbon dioxide fixation[9,10] and nitrogen fixation[1] with powdered semiconductors were studied in connection to solar energy conversion. Our studies have concentrated on hydrogen production from water and various organic compounds using metal or metal oxide loaded TiO_2 as a photocatalyst[11-18], where organic compounds serve as electron donors and hydrogen is produced from water. It was demonstrated that hydrogen was produced very efficiently in the case of some alcohols[11,14,18], glucose[12] and urea resin[15] as reducing agents. These organic compounds were oxidized to carbon dioxide finally when platinized TiO_2 was used as a photocatalyst. One of the most efficient systems can be composed of methanol and water, in which the quantum yield of the hydrogen production is more than 50 % for 380 nm light. The photocatalytic activity depends on the size of the semiconductor particle and also on the irreversibility of the reaction[18]. We also reported that a solid carbon (charcoal) reacted with water or water vapor in the presence of TiO_2/RuO_2 as a photocatalyst[16,17]. The solid carbon was oxidized to carbon monoxide and carbon dioxide with reducing water to hydrogen.

Here we investigated the hydrogen-producting reactions of aliphatic and aromatic compounds with water. In these cases carbon dioxide was also produced besides hydrogen even at an early stage of irradiation. This phenomenon is quite different from that for the alcohol-water system in which the main oxidation product is aldehyde at the early stage and carbon dioxide is produced only after irradiation for a long time.

We have also extended this subject to the photocatalytic hydrogen production from liquid water and some natural fossil fuels such as coal, tar-sand and pitch, since these fossil fuels are composed of aliphatic and aromatic hydrocarbons.[19]

[Experimental]

Several kinds of powdered TiO_2 ([1] Nippon Aerosil Co.,LTD, P-25, anatase, average grain size 300 Å, [2] Katayama Kagaku Co.,LTD, rutile, 1000 Å, [3] Kojundo Kagaku Co.,LTD, rutile, several μm) were used. The results obtained were almost same regardless the species of TiO_2. The surface of these TiO_2 powders was modified with Pt (4 wt %) photochemically.[20,21]

A bituminous coal produced in Japan was ground into powder (0.1 g) and physically mixed with Pt/TiO_2 (0.3 g) in an agate mortar. Athabasca tar-sand (Syncrude) adhering to the surface of sands, produced in Canada and a pitch (the residue on distillation of Kafuji oil) produced in China were used without any treatments. The various aliphatic hydrocarbons and aromatic compounds were purchased from Katayama Kagaku or Tokyo Kasei (special grade), and were used without further purification.

The photocatalyst (0.3 g) and a fossil fuel (0.1 g) or a hydrocarbon (0.1-1 g) were suspended in a deaerated water (30 ml) in 280 ml Pyrex glass flask which passes light of wavelength longer than 320 nm. The glass flask was irradiated from the bottom side for several hours to several tens of hours with the white light from a 500-W Xe lamp (USHIO,

UXL500). All the experiments were done at room temperature. The temperature of the solution was about 40 - 50 °C during the irradiation.

The gaseous reaction products were trapped at -196°C or -55°C and analyzed by a quadrupole mass spectrometer (Anelva, AGA-360) and a sensitive manometer (Data metrics, barocel pressure sensor) as described in Chapter I.

[Results and Discussion]

Aliphatic Compounds

In Table I are shown the rates of hydrogen production from mixtures of water and several aliphatic hydrocarbons with a white light (λ > 320 nm) from the 500-W Xe lamp. The rates in alkaline solution are about 2-4 times larger than those in neutral solution. The quantum yields of the hydrogen production in these systems are in the order of 10^{-2}-10^{-3}. One of the characteristic features of these systems is that

TABLE I : Hydrogen Production Rates from Water with an Aliphatic Hydrocarbon

Reactant	H_2 Production Rate (μmol/h)	
	Neutral	Alkaline (5N)
n-pentane	4.4	8.4
n-heptane	6.6	11
iso-octane	2.4	9.4
n-paraffine	1.2	2.3
polyethylene	1.0	3.9

Light source:500 W Xe lamp
Photocatalyst:Pt/TiO_2

carbon dioxide is produced even from an early stage of irradiation. This point is quite different from that of photocatalytic reaction of alcohols and water in which the main oxidation products were aldehydes at the early stage and carbon dioxide was observed only after long time irradiation. This will be discussed later.

These are the reactions of water with organic compounds, in which the organic compounds are oxidized eventually to carbon dioxide and the water is reduced producing hydrogen.[11-18] A typical example is the reaction of sugar. Sugar reacts with water completely producing hydrogen and carbon dioxide with the aid of semiconductor photocatalysts and light energy[12]. Here we tried the complete decomposition of n-hexadecane ($C_{16}H_{34}$), one of the linear saturated hydrocarbons which are difficult to oxidize. The expected reaction is described by the following equation.

$$C_{16}H_{34} + 32\ H_2O \longrightarrow 16\ CO_2 + 49\ H_2 \qquad (1)$$

$$\Delta G^0 = 1232\ kJ/mol$$

In this experiment, 25 μl (85 μmol) of n-hexadecane, 30 ml of distilled water and Pt/TiO_2 were mixed in a flask and irradiated after evacuation. The gaseous products were analyzed and purged from the cell after an irradiation of every several tens of hours. It took about 700 hours for the complete decomposition. The result is shown in Figure 1. The

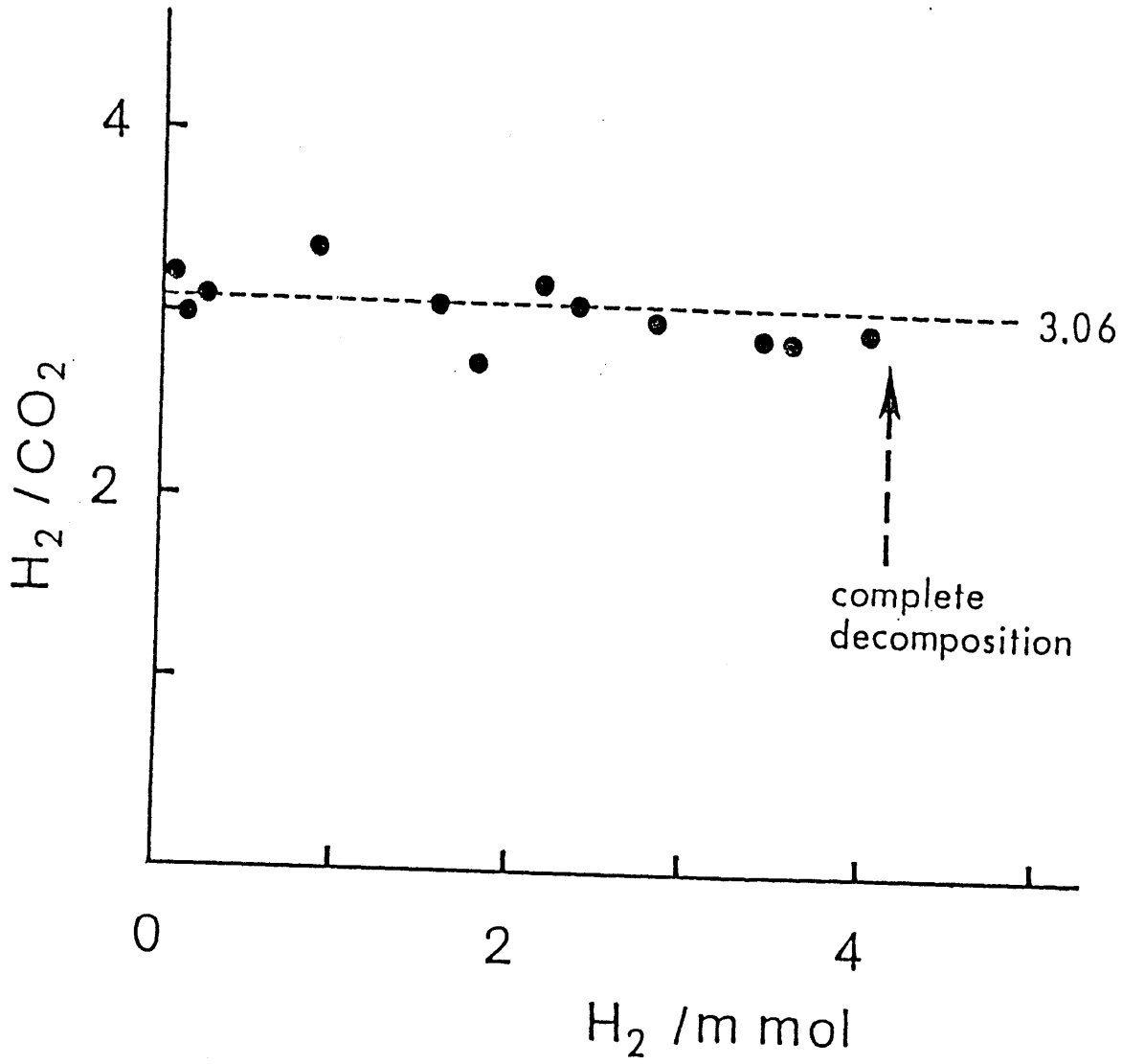

Figure 1. Ratio of hydrogen to carbon dioxide produced during the complete decomposition of n-hexadecane ($C_{16}H_{34}$). Neutral aq. solution, light source: 1 KW Xe lamp, photocatalyst: Pt/TiO_2, total irradiation time: ∿700 hours

gaseous products are hydrogen and carbon dioxide as is expected from eq. 1. Other products were not detected in the gas phase. The total amounts of hydrogen and carbon dioxide produced are 4.14 mmol and 1.3 mmol, respectively. The amounts of hydrogen and carbon dioxide predicted by eq. (1) and the initial amount of n-hexadecane, 85 μmol, are 4.16 mmol and 1.36 mmol respectively, in excellent with the experiment. This supports the reaction scheme (1) for the complete decomposition of n-hexadecane. Another interesting result is that the ratio of hydrogen to carbon dioxide is always about 3 at each sampling point as seen in this figure. This implies that the ratio of hydrogen to carbon dioxide is constant, about 3, during the decomposition of the reaction intermediates of n-hexadecane.

Bard et al. demonstrated the formation of ·OH radical on TiO_2 photocatalyst under illumination by using the spin trapping method[22]. The ·OH radical was produced on the surface of TiO_2 by the oxidation of water and it was suggested to play an important role in the oxidation of hydrocarbons, such as benzene and toluene[22-27]. Alcohols are reported to be formed during the photocatalytic oxidation of aliphatic hydrocarbons[23]. Assuming the involvement of the ·OH radical, our result for n-hexadecane could be explained by the following reaction schemes.

I) Formation of the alcohol and carboxylic acid.

$$H_2O + p \longrightarrow \cdot OH + H^+ \quad (2)$$

$$H^+ + e \longrightarrow 1/2\ H_2 \quad (3)$$

$$RCH_2CH_3 + 2\cdot OH \longrightarrow RCH_2CH_2OH + H_2O \quad (4)$$

$$RCH_2CH_2OH \longrightarrow RCH_2CHO + H_2 \quad (5)$$

$$RCH_2CHO + H_2O \longrightarrow RCH_2COOH + H_2 \quad (6)$$

2 x [(2)+(3)] + (4) + (5) + (6)

$$RCH_2CH_3 + 2H_2O \longrightarrow RCH_2COOH + 3H_2 \quad (7)$$

II) Decomposition of the carboxylic acid (photo-Kolbe reaction)[28-31]

$$RCH_2COOH \longrightarrow RCH_3 + CO_2 \quad (8)$$

III) Total reaction

$$RCH_2CH_3 + 2H_2O \longrightarrow RCH_3 + 3H_2 + CO_2 \quad (9)$$

As seen in eq. (9), three hydrogen and one carbon dioxide molecules are produced along with the decrease of one in the carbon number. When the above reactions (eq. (4), (5), (6) and (8)) are assumed to proceed successively, the result in Figure 1 is explained well. This assumption means that the intermediate products of this reaction, RCH_2CH_2OH, RCH_2CHO and RCH_2COOH, are oxidized much faster than the saturated hydrocarbons. This will be discussed in §2.

Aromatic Compounds

Several aromatic compounds also served as the electron donors for the reaction of the present photocatalytic hydrogen production with Pt/TiO_2 as is shown in Table II. The rates in alkaline region are also about 5 to 10 times larger than those in neutral region. They depend on the concentration of the hydrocarbons. For example, the rate takes a maximum value at a volume ratio of about 30 for the benzene - water mixture. As the ratio decreases, the rate decreases remarkably and hydrogen can not be detected with a pure benzene system. The alcohol-water mixture is in marked contrast to the benzene-water mixture, because the rate increases with larger concentrations of the alcohols and it takes a maximum value for the pure alcohol such as methanol and ethanol.

TABLE II : Hydrogen Production Rates from Water with an Aromatic Compound

Reactant	H_2 Production Rate (μmol/h)	
	Neutral	Alkaline (5N)
benzene	4.0	36
phenol	4.1	33
pyridine	2.7	31

Light source:500 W Xe lamp
Photocatalyst:Pt/TiO_2

In these cases carbon dioxide also produced from as early stage of irradiation. For example, in the case of benzene the ratio of hydrogen to carbon dioxide was about 2.5 in the neutral condition, and a trace amount of phenol (H_2/phenol > 1000) was produced in the alkaline condition. This will be discussed in §2.

Fossil Fuels

We applied the present hydrogen-producting method to the gacification of natural fossil fuels, that is, the fossil fuels were used as the electron donors for the photocatalytic reaction. The model compounds of the fossil fuels are composed of unit structures connected by aliphatic hydrocarbons. The unit structures consist of aromatic and condensed aromatic compounds.[19] Thus it can be considered that these photocatalytic reactions are the extensions of the present subject.

In Table III are shown the initial hydrogen production rates from mixtures of fossil fuels and water. The rates were about 1 μmol/h in the neutral region in the case of any coal, tar-sand or pitch. However, the rate icreased remarkably ,about 10 times, when NaOH was added to the solution. The quantum yields of these hydrogen-producting reactions in the alkaline region correspond to about 0.5 % at 380 nm.

TABLE III: Initial Rate of Hydrogen Production from Water with a Fossil Fuel

Reactant	H_2 Production Rate (μmol/h)	
	Neutral	Alkaline (5N)
coal	1.3	9.0
oil sand	0.5	10
pitch	1.0	10

Light source:500 W Xe lamp
Photocatalyst:Pt/TiO_2

When D_2O was used instead of H_2O for the aqueous suspension of coal, D_2 was 86 % of the produced hydrogen gas, DH 10 % and H_2 4 %. This result indicates that water is reduced through the photocatalytic process and the fossil fuels serve as electron donors. Hydrogen was the only gaseous reaction product in alkaline solutions, while carbon dioxide was also produced in neutral solutions. The ratio of hydrogen to carbon dioxide was also about two to three during the early stages of irradiation. However, the reaction rate decreases gradually under irradiation. This tendency is quite different from that of a pure organic compound. Figure 2 represents the hydrogen production from the aqueous solution of phenol versus time (solid line). In this case the rate does not decrease remarkably after 30 hours irradiation. Furthermore, the rate

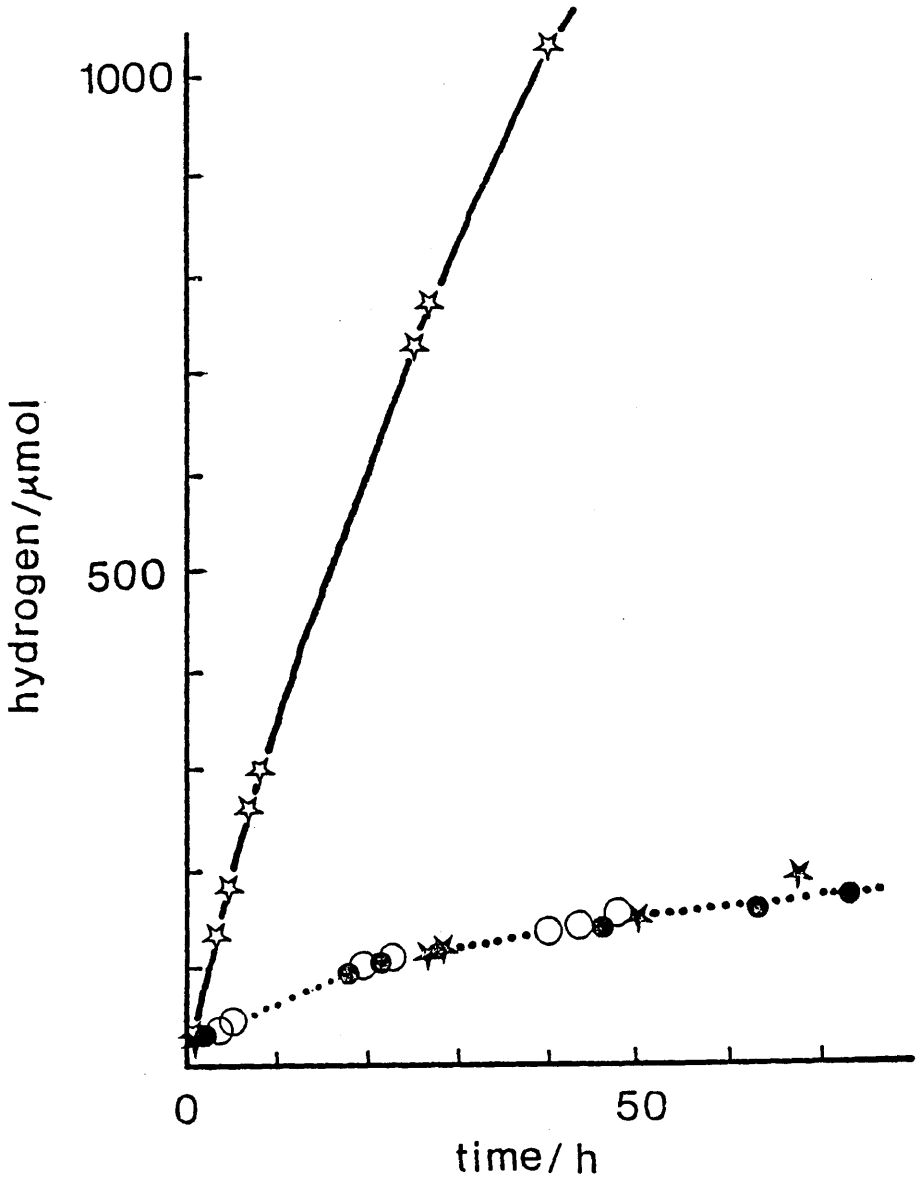

Figure 2. Hydrogen productions from water with phenol and fossil fuels.
☆:phenol, ★:pitch, ○:tar-sand, ●:coal, 1N NaOH solution, light source:500-W Xe lamp, photocatalyst:Pt/TiO_2.

did not show any change after leaving this reaction flask as it was for over one month under room light. This some property is observed for the alcohol-water and the glucose-water mixtures, and suggests that this photocatalyst is rather stable under irradiation even in a concentrated alkaline solution. However, the situation is quite different for a fossil fuel-water mixture. The dotted line in Figure 2, which represents the hydrogen production from a fossil fuel-water mixture, shows that the rate decreases gradually under irradiation. The rates after 40 hours irradiation were 10 times smaller than those during an early stage of irradiation. Even after the photocatalyst was filtered and was mixed again with a fresh coal, the rate did not recover. These results suggest that the activity of the photocatalyst itself was reduced in these cases. One of the main reasons for these results may be explained by the effect of various metal ions, for instance Fe ion, which are contained in fossil fuels. They might be adsorbed on the surface of TiO_2 and serve as a recombination center of electrons and holes, which would decrease the photocatalytic activity. For example, the rate of hydrogen production from an ethanol-water mixture with Fe adsorbed TiO_2 (Fe/TiO_2) was about half of that with TiO_2 alone.

[Conclusion]

It was shown that fossil fuels and hydrocarbons can produce hydrogen by reacting with water at room temperature with the aid of light energy and a semiconductor photocatalyst. At present, the efficiency of these reactions is low and the poisoning of the photocatalyst is a serious problem for the decomposition of fossil fuels. However, if we can succeed in exploiting a new photocatlyst which can decompose fossil fuels efficiently with visible light and the poisoning problem of photocatlyst is solved, this method could be attractive for the use of fossil fuels for hydrogen production and organic synthesis.

[References]

(1) G.N. Shrauzer, and T.D. Guth, J. Am. Chem. Soc., 99, 7189 (1977).

(2) F.T. Wagner, and G.A. Somorjai, Nature, 285, 559 (1980).

(3) S. Sato, and J.M. White, Chem. Phys. Lett., 72, 83 (1980).

(4) T. Kawai, and T. Sakata, Chem. Phys. Lett., 72, 87 (1980).

(5) J.M. Lehn, J.P. Sauvage, and R. Ziessel, Nouv. J. Chim., 4, 623 (1980).

(6) K. Domen, S. Naito, M. Soma, T. Ohnishi, and T. Tamaru, J. Chem. Soc. Chem. Commun., 1980, 543

(7) D. Duonghong, E. Borgarello, and M. Grätzel, J. Amer. Chem. Soc., 103, 4685 (1981).

(8) K. Kalyanasundaram, E. Borgarello, and M. Grätzel, Helv. Chim. Acta, 64, 362 (1981).

(9) T. Inoue, A. Fujishima, and K. Honda, Nature, 277, 637 (1979).

(10) B. Aurian-Blajeni, M. Halmann, and J. Manassen, Solar Energy, 25, 165 (1980).

(11) T. Kawai, and T. Sakata, J. Chem. Soc. Chem. Commun., 1980, 695.

(12) T. Kawai, and T. Sakata, Nature, 286, 5772 (1980).

(13) T. Sakata, and T. Kawai, Nouv. J. Chim., 5, 279 (1981).

(14) T. Sakata, and T. Kawai, Chem. Phys. Lett., 80, 341

(1981).

(15) T. Kawai, and T. Sakata, Chem. Lett., 1981, 81.

(16) T. Kawai, and T. Sakata, J. Chem. Soc. Chem. Commun., 1979, 1047.

(17) T. Kawai, and T. Sakata, Nature, 282, 5736 (1979).

(18) T. Sakata, T. Kawai and K. Hashimoto, Chem. Phys. Lett., 88, 50 (1982).

(19) For example, (a) H.H. Lowry, "Chemistry of Coal Utilization", Vol. 1, p 2 (1945), Supplement, John Wiley (1962). (b) P.L. Walker,Jr., F. Rusinko,Jr., and L.G. Austin, "Advances in Catalysis", Vol. 11, p 133, Academic Press (1959).

(20) B. Kraeutler, and A.J. Bard, J. Am. Chem. Soc., 100, 2239 (1978).

(21) K. Hashimoto, T. Kawai, and T. Sakata, Nouv. J. Chim., 7, 249 (1983).

(22) C.D. Jaeger, and A.J. Bard, J. Phys. Chem., 83, 3146 (1979).

(23) I. Izumi, W.W. Duun, K.O. Wilbiurn, Fu-Rien F. Fun, and A.J. Bard, J. Phys. Chem., 84, 3207 (1980).

(24) M. Fujihira, Y. Satoh, and T. Osa, Nature, 293, 5829 (1981).

(25) M. Fujihira, Y. Satoh, and T. Osa, J. Electroanal. Chem., 126, 277 (1981).

(26) M. Fujihira, Y. Satoh and T. Osa, Chem. Lett., 1981,

1053.

(27) I. Izumi, Fu-Ren F. Fun, and A.J. Bard, J. Phys. Chem., 85, 218 (1981).

(28) B. Kraeutler, and A.J. Bard, J. Am. Chem. Soc., 100, 2239 (1978).

(29) B. Kraeutler, and A.J. Bard, J. Am. Chem. Soc., 100, 4903 (1978).

(30) B. Kraeutler, and A.J. Bard, J. Am. Chem. Soc., 100, 5985 (1978).

(31) T. Sakata, T. Kawai, and K. Hashimoto, J. Phys. Chem., in press.

§2 Photocatalytic Oxidations of Hydrocarbons.

[Abstract]

The photocatalytic oxidations of linear hydrocarbons and benzene were studied in the presence of a semiconductor powder and silver ion as a photocatalyst and an electron acceptor, respectively. For aliphatic hydrocarbons, they are oxidized to alcohols, aldehydes and carboxylic acids, successively. Carbon dioxide was found to be produced through photo-Kolbe reaction of carboxylic acids produced, which explained well the result of the complete decomposition of n-hexadecane described in §1. For the decomposition of benzene, we could detect phenol, catecohol, hydroquinone and muconic acid. Based on these results, the possibility of the direct oxidation of benzene by photogenerated holes and its ring opening process peculiar to the photocatalytic reaction are dicussed. The main reaction path for carbon dioxide production was suggested in which benzene ring opens not by way of phenol and catecohol, but by way of the intermediates whose reactivities are much larger than that of benzene.

[Introduction]

The photocatalytic oxidation of hydrocarbons in the presence of oxygen as an electron acceptor is reported by several researchers.[1-6] For aliphatic hydrocarbons, Bard et.al. reported that small amount of alcohols was produced and carbon dioxide was the main product. For the oxidation of aromatic hydrocarbon it has been considered that the photogenerated holes are scavenged by water at first forming ·OH radical, and the oxidation begins by the hydroxylation of aromatic ring with ·OH radical for benzene, and proceeds to carbon dioxide production eventually [1-6] However, no detailed consideration on the mechanism of oxidation process has been proposed. In those cases, hydrogen was not produced and the oxidation rate was much larger than that without oxygen since oxygen serves as a good electron acceptor compared to the proton. However, oxygen may form $\cdot O_2^-$ and $\cdot HO_2$ which might contribute to the oxidation process of a hydrocarbon. Moreover oxygen itself sometimes participates in the oxidation process.[1-6] Thus we used silver ion as an electron acceptor instead of oxygen in the experiment of photocatalytic oxidation reaction. Silver ion is reduced to silver metal and does not affect the oxidation of these compounds. Consequently this electron acceptor seems a good choice for

investigation of the mechanism of oxidation reaction.

Here we investigated the oxidation of these aliphatic and aromatic compounds with water. In these cases carbon dioxide was the main product and produced even at an early stage of irradiation. This phenomenon is quite different from that for the alcohol - water system in which carbon dioxide is produced only after irradiation for a long time.

In order to elucidate this phenomenon, we carried out the product analysis for the photocatalytic reaction of the aliphatic and aromatic hydrocarbons. Based on those results, we discuss their oxidation processes. Especially for benzene the following two points will be discussed : (a) the possibility that direct oxidation of benzene by the photogenerated holes occurs in considerable ratio to that by ·OH radical, and (b) the mechanism of oxidation processes that carbon dioxide is produced mainly by the direct ring opening of benzene by way of not phenol as the intermediate product but non-aromatic alcohols and aldehydes whose reactivities are much larger than that of benzene.

[Experimental]

Several kinds of powdered TiO_2 ([1] Nippon Aerosil Co.,LTD, P-25, anatase, average grain size 300 Å, [2] Katayama Kagaku Co.,LTD, rutile, 1000 Å, [3] Kojundo Kagaku Co.,LTD, rutile, several μm) were used. The results obtained were almost same regardless the species of TiO_2. Other powdered semiconductors ($SrTiO_3$, WO_3, SnO_2, Fe_2O_3) were purchased from Kojundo Kagaku Co.,LTD. These were used without any treatment. The various aliphatic hydrocarbons and aromatic compounds were purchased from Katayama Kagaku or Tokyo Kasei (special grade), and were used without further purification. $AgNO_3$ or Ag_2SO_4 (Wako Pure Chemical Industries,LTD.) was also used without further purification.

The photocatalyst (0.3 g) and a hydrocarbon (0.1-1 g) were suspended in a dearated water (30 ml) with silver ion (1-5 mmol) in 280 ml Pyrex glass flask which passes light of wavelength longer than 320 nm. The glass flask was irradiated from the bottom side for several hours to several tens of hours with the white light from a 500-W Xe lamp (USHIO, UXL500). All the experiments were done at room temperature. The temperature of the solution was about 40 - 50 °C during the irradiation.

The gaseous reaction products were trapped at -196°C or

-55°C and analyzed by a quadrupole mass spectrometer (Anelva, AGA-360) and a sensitive manometer (Data metrics, barocel pressure sensor) as described in Chapter I. The reaction products in the aqueous phase were analyzed by a steam gas chromatograph (S-GC:Okura Denki, Model 103), a liquid chromatograph (LC:Japan Spectroscopic Co.,Ltd.,Familic-100) and a gas chromatograph (GC:Okura Denki, Model 701).

[Results and Discussion]

Aliphatic Compounds

In the previous section (§1), we showed the result of complete decomposition of a linear saturated hydrocarbon, in which the ratio of hydrogen to carbon dioxide produced was always about 3 during the photolysis. Based on these results we speculated the reaction process. In order to find evidence to support the reaction scheme (§1 eq.(2)-(8)), we carried out the photocatalytic reaction of n-pentane, one of the simpler hydrocarbons, in an aqueous medium. Only a small amount of products could be detected in aqueous phase under the condition of hydrogen production, as was expected in §1. However, if the excited electrons in the conduction band of TiO_2 are consumed quickly, a large number of holes will be left on TiO_2 and the oxidation reaction will occur efficiently. Consequently silver ion (5 mmol) was added as an electron accepter to the 20 wt% of pentane aqueous solution (50 ml). In this case oxygen production was observed at an early stage of irradiation. The total amount of oxygen produced was 0.83 mmol after 14 h irradiation. This indicates that the oxidation of n-pentane is not efficient and is in competition with the oxidation of water. By contrast, oxygen

production was not observed in the absence of silver ion. In this case, ·OH radical, the first oxidation product of water, would not be produced efficiently because the reduction of proton is not so fast. This situation is not favorable for oxygen production, since a high density of ·OH radicals on the surface and fast recombination are necessary for efficient oxygen production. A low density of ·OH radicals will be consumed by reacting with the hydrocarbon. Another reason of the lack of oxygen production, as observed in the complete decomposition of n-hexadecane, is that the oxidation products of water such as ·OH, H_2O_2, $\cdot O_2H$ and O_2 are reduced again under the condition of hydrogen production. Actually, in the photocatalytic reactions of various organic compounds with water, hydrogen and carbon dioxide were produced, but no oxygen was observed in the gas phase, unless a strong electron acceptor such as Fe^{3+} and Ag^{+} was added to the reaction system.

Besides oxygen, carbon dioxide was produced in the decomposition of n-pentane and the amount was increased with time. The reaction products in aqueous phase were detected by S-GC. The main product was acetic acid with about 60 μmol produced after 40 h irradiation. A small amount of propionic acid, acetaldehyde, ethanol, methanol and several unknown products were also detected. This result seems to support the reaction scheme described in §1 (eq. (2)-(8)).

We also investigated the decomposition of n-butyric acid ($n\text{-}C_3H_7COOH$, 10 vol%) in an aqueous medium in the presence of silver ion (5 mmol). After 19 h irradiation, n-propyl alcohol (75 μmol), propionaldehyde (102 μmol) and propionic acid (34 μmol) were produced as the main products as well as propane (1.7 mmol) and carbon dioxide (3.6 mmol). This result is shown in Figure 1.

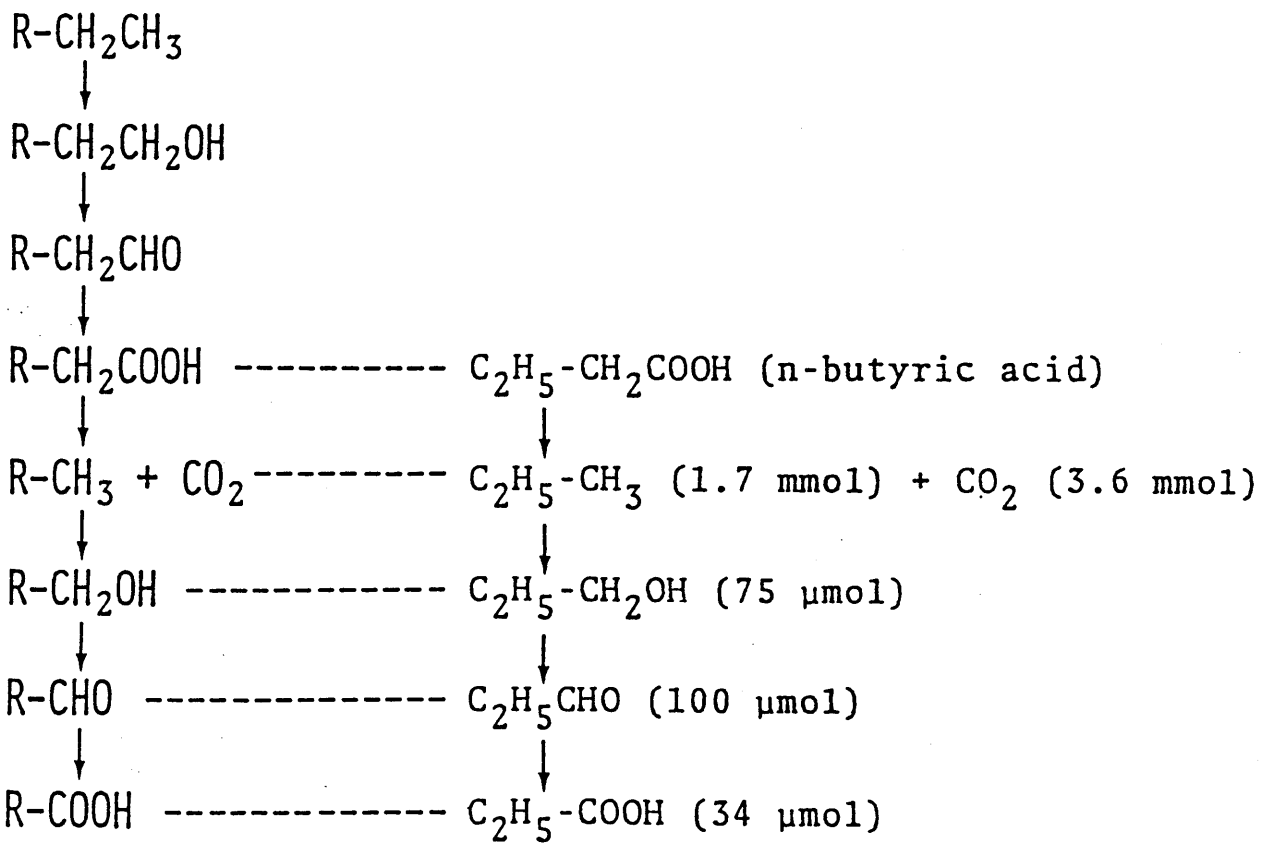

Figure 1. Photocatalytic oxidation process of a linear saturated hydrocarbon and the oxidation products from n-butyric acid. Neutral aq. solution, light source: 1 kw Xe lamp, photocatalyst: TiO_2 in the presence of $AgNO_3$, irradiation time: 19 hours.

Besides the above products, a small amount of ethanol (0.92 μmol), acetaldehyde (6.0 μmol) and acetic acid (4.6 μmol) were detected. These results show clearly how the decomposition proceeds. Moreover oxygen was not produced for the decomposition of n-butyric acid. Since a large amount of oxygen was produced by the reaction of n-pentane, this indicates that n-butyric acid is oxidized more easily than n-pentane through the photocatalytic process. Taking all these results into account, we conclude that an aliphatic hydrocarbon is oxidized mainly according eq. (2)-(8) in §1 successively, because the intermediate products are much more reactive than the starting material, so that one oxidation cycle makes three hydrogen and one carbon dioxide molecules.

We have described above only the simplest and probably the main path. There might be many other paths besides that. For example, according to the reaction scheme, simple hydrocarbons such as methane, ethane and propane are expected to be produced in the gas phase. However, such hydrocarbons were barely detected even at the last stage of reaction for the complete decomposition of n-hexadecane. This fact suggests that the hydrogen attached to a carbon chain are attacked rather randomly by ·OH radicals to produce various alcohols with many OH groups. Such a reaction is more favorable to hydrogen production than to hydrocarbon production[7,8]. We also analysed the reaction products of the photocatalytic oxidation

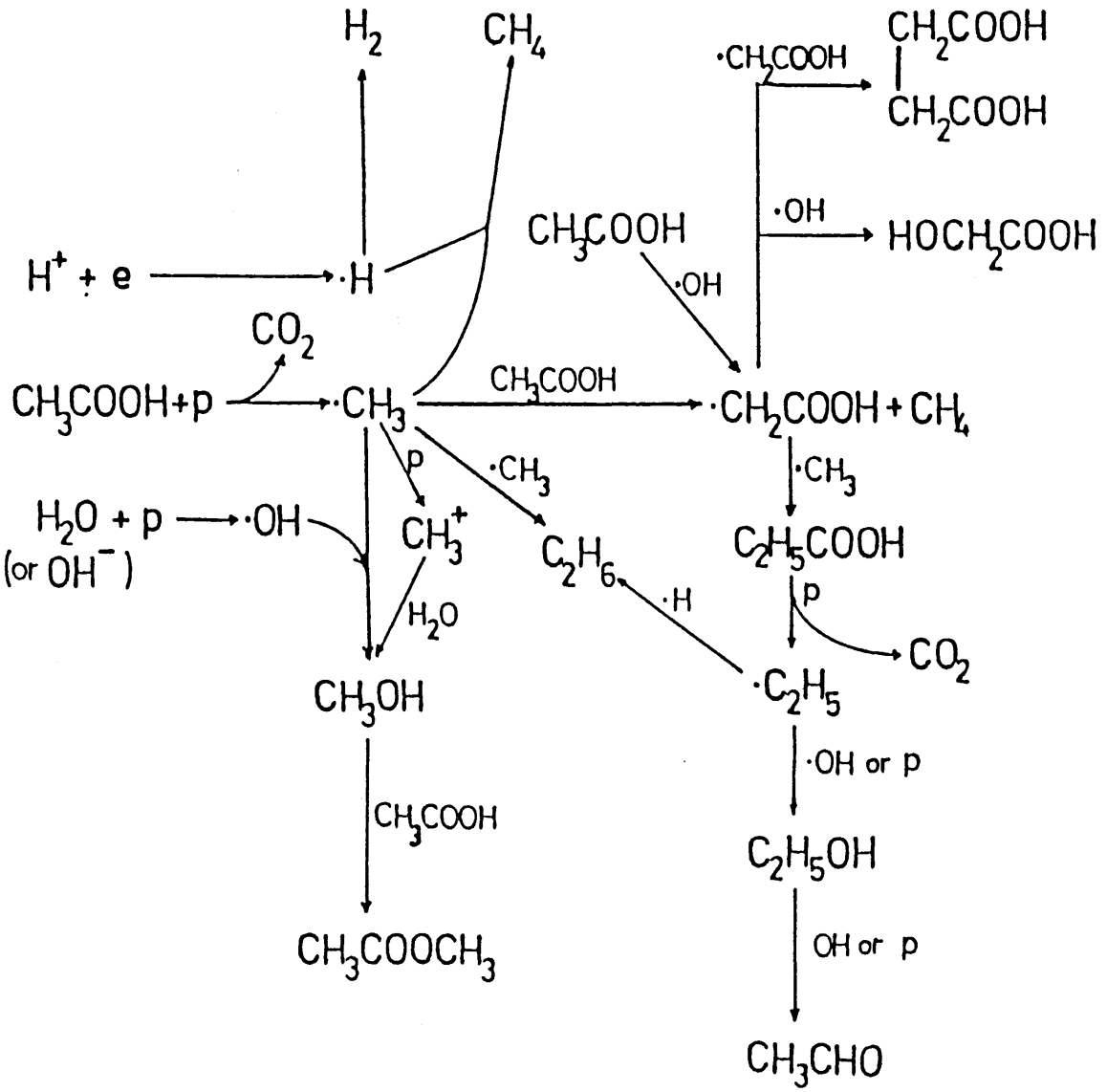

Figure 2. Reaction scheme of photocatalytic reactions of acetic acid in aqueous medium with powdered TiO_2 photocatalysts.

of acetic acid and propionic acid, and we could elucidate the reaction processes as shown in Figure 2 and Figure 3.

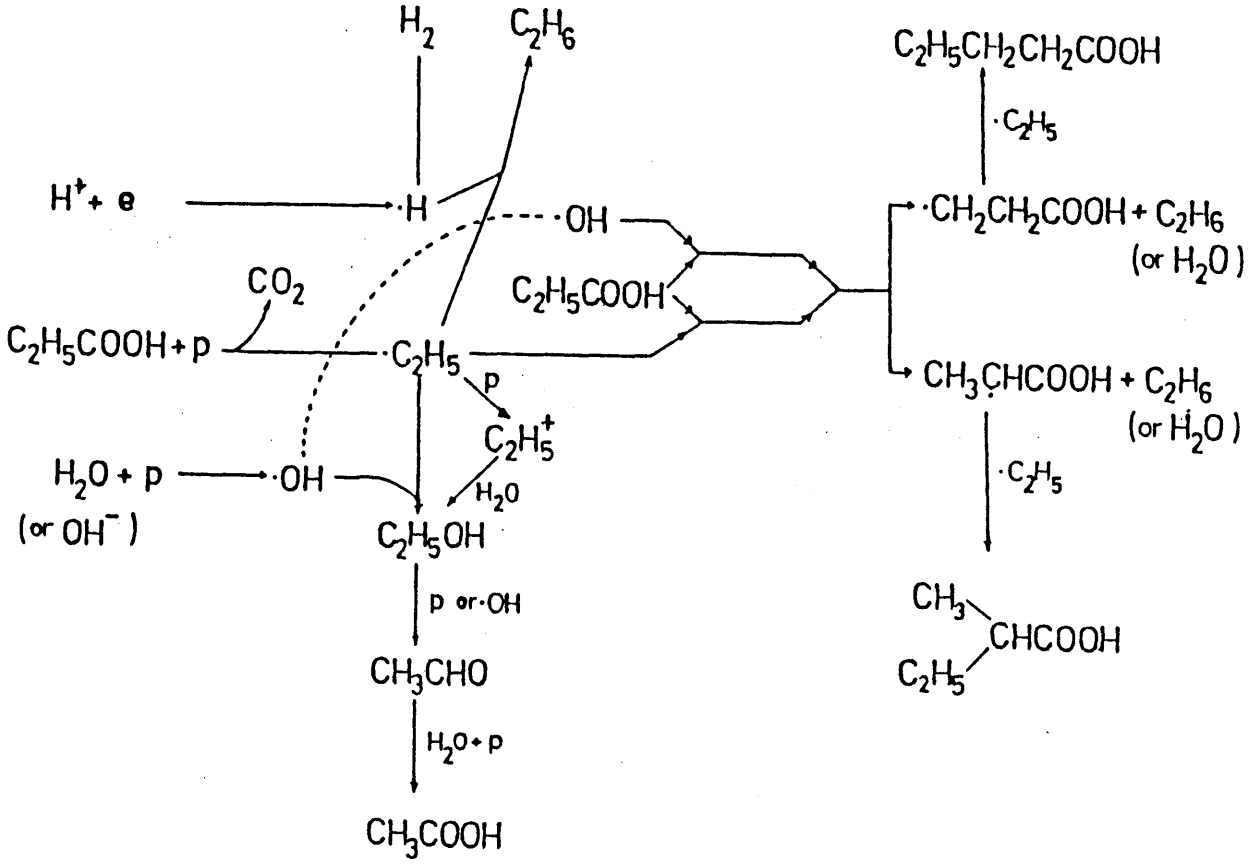

Figure 3. Reaction scheme of photocatalytic reactions of propionic acid in aqueous medium with powdered TiO_2 photocatalysts.

Aromatic Compounds

(A) Direct Oxidation of Benzene

As was described in the introduction, it has been considered that the oxidation of benzene also starts by the hydroxylation of the benzene ring as same as the oxidation of aliphatic hydrocarbons.[1-5] However, we will propose the possibility of the direct oxidation of benzene by photogenerated holes of TiO_2. It can be insured from several reasons described below. At first, biphenyl (180 μmol) was produced from deaerated pure benzene with Ag_2SO_4 (0.5 mmol) and TiO_2 powder after 170 h irradiation, although no gaseous product was detected in this case. The production rate of biphenyl was slow, which can be explained by the following two reasons. (a) The ionization potential of pure benzene is much larger than that in aqueous solution because of the small stabilization energy of benzene cation radical in pure benzene. (b) The concentration of silver ion is small because Ag_2SO_4 is hardly dissolved in it. Thus it is considered that the direct oxidation in water occurs more easily and faster. Secondly, Aikawa and Sukigara reported the measurement of the mobility and electrical charge of photosensitive particle in a dielectric liquid with a photoelectrical transient technique[9]. They observed that a negative charge was accumlated on TiO_2 powder suspended either in benzene-water mixture or in pure

benzene under UV light irradiation. The magnitude of the electrical negative charge of TiO_2 powder in water-benzene mixture was two times larger than that in pure benzene. This suggests that photogenerated holes were scavenged by both water and benzene molecules, and that the ratio of hole consumption by water to by benzene is the same order in the case of TiO_2. On the other hand the half-wave potential of the anodic oxidation for benzene in acetonitrile was reported to be 2.54-2.62 V vs NHE[10,11]. The potential value starting an oxidation is about 0.3 V more negative than a half wave potential in general. Thus if the value is assumed to be approximately the same as that in a neutral aqueous solution, the oxidation of benzene would start from around 2.2-2.3 V vs NHE. The value of the ionization potential of benzene in a neutral aqueous solution can be approximately calculated to be 2.2 V vs NHE with the aid of Born's equation (eq.2) assuming that benzene cation radical is a sphere with a radius of 2.7 Å.

$$P[\text{adiabatic}] = \frac{Q^2}{2R}(1 - 1/\varepsilon) \qquad (1)$$

Here, P,R,Q, and ε represent the polarization energy, the radius of a sphere, the electric charge, and the dielectric constant, respectively. By using the following values, R = 2.7 Å, $Q = 1.6\times10^{-19}$ C, ε = 78 for water, the polarization energy of benzene cation, $P(C_6H_6^+)$, in water is calculated

approximately to be 2.6 eV. The ionization potential of benzene in gas phase, $I_p[C_6H_{6gas}]$, is 9.24 eV[12] so that the value 6.7 eV, is obtained as the ionization potential of benzene in water ($I_p[C_6H_{6aq}]$) using the approximate equation.

$$I_p[C_6H_{6aq.}] = I_p[C_6H_{6gas}] - P[C_6H_6^+] \qquad (2)$$

The ionization potential of 6.7 eV corresponds to 2.2 V vs NHE assuming that the electron energy for normal hydrogen electrode (NHE) is -4.5 eV from the vacuum[13]. This result is

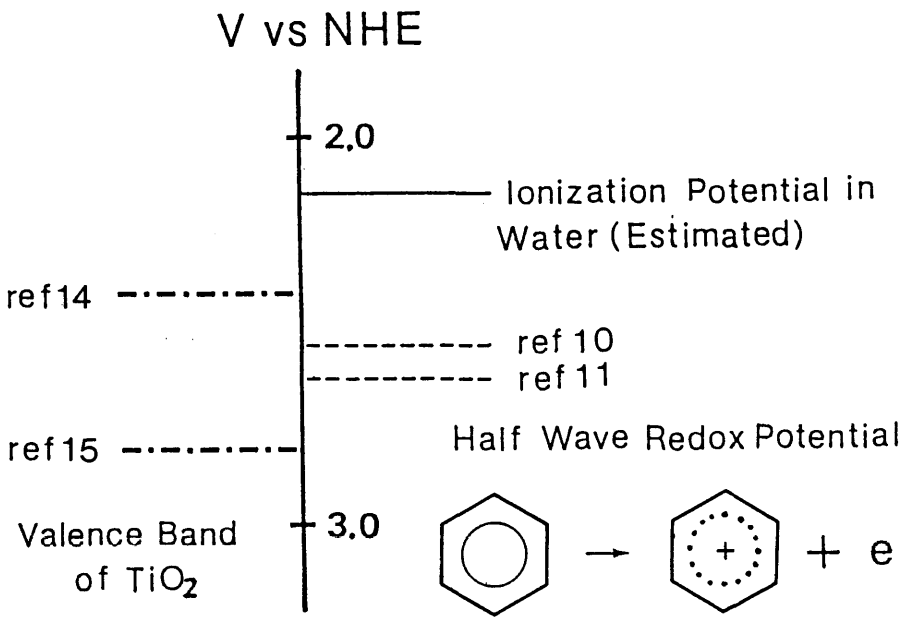

Figure 4. Valence band position of TiO_2,[14 15] half-wave redox potential of benzene in acetonitrile[10 11] and estimated ionization potential of benzene in water. pH = 7.0, vs NHE[26].

in good agreement with the value estimated previously from the oxidation potential. Since the valence band edge position of TiO_2 is reported to be 2.4[14] - 2.8[15] V vs NHE at pH = 7,[16] the direct electron transfer from benzene molecule in a neutral aqueous solution to the photogenerated holes in TiO_2 seems to be possible. A schematic energy diagram is shown in Figure 4.

It has been established by pulse radiolysis that benzene radical cation reacts rapidly ($\leq$ 0.1 μs) with water to give hydroxycyclohexadienyl radical,[17] which in turn dissociates to benzene and ·OH radical, or leads to simultaneous formation of phenol[18,19] and hydroxymucondialdehyde(HMD)[20-23] (see eq.9) in the presence of oxygen. Taking all these facts into

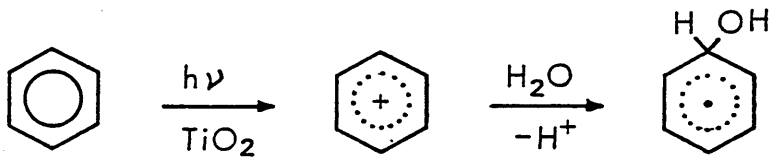

(3)

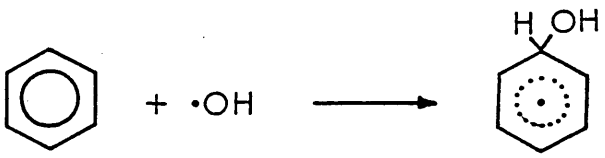

(4)

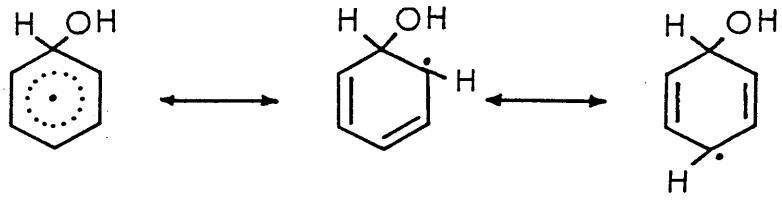

(5)

a b

consideration, we conclude that the direct oxidation of benzene by photogenerated holes (eq.3) also proceeds in competition with ·OH radical addition to benzene ring (eq.4). Both reactions yield the hydroxycyclohexadienyl radical which is the primary intermediate of the present photocatalytic reaction.

(B) Oxidation Process of Benzene

Benzene is oxidized mainly to carbon dioxide and several other minor products with near UV light by the present photocatalytic reaction, although benzene itself is known to be very stable against near UV light. The property of the carbon dioxide production is very similar to that for aliphatic compounds, that is, carbon dioxide is produced from an early stage of irradiation. Thus the intermediate oxidation products should be much more reactive than benzene by the same reasoning as was done for the decomposition of aliphatic compounds. We carried out product analysis for several aromatic compounds. Here we also used silver ion as the electron acceptor and controlled the amount of silver ion added to the solution. Since only the reduction of silver ion proceeds instead of proton, the number of holes consumed during a reaction can be controlled by knowing the amount of silver ions and finishing the irradiation just at the time when the hydrogen production starts. The relative

reactivities of these compounds can be also determined from the rates of oxygen production which is in competition with oxidation of these compounds.

We examined the oxidation products carefully in the presence of 1 mmol silver ion (0.5 mmol of Ag_2SO_4) as an electron acceptor[24]. The results are shown in Table I.[25]

TABLE I: Photocatalytic Oxidation Products after Consuming 1 mmol of Silver Ion

Reactant	Gas Phase (μmol)		Liquid Phase (μmol)
	O_2	CO_2	
Benzene	8.0	110	Biphenyl (3.0) Phenol (21) Catecohol (1) Hydroquinone (13) Muconic acid (1.0)
Phenol	24	27	Catecohol (17) Hydroquinone (23) Muconic acid (none)
Catecohol	0.6	38	Muconic acid (3.5)
Hydroquinone	3.4	98	Muconic acid (none)
Muconic acid	5.0	380	

Neutral aq. solution, light source:1 KW Xe lamp
Irradiation time:50 ∿ 100 hours, Photocatalyst:TiO_2
Ag_2SO_4:0.5 mmol

In these experiments the concentrations of the reactants were equal each other in order to compare their reactivities, and products were analyzed with S-GC, GC and LC. Although there were other unknown peaks in the chromatographs, only the species which could be assigned are shown. Phenol, catecohol and muconic acid were obtained as oxidation products from an aqueous solution of benzene. Muconic acid and catecohol were detected as the oxidation products of catecohol and phenol, respectively. Since muconic acid produces carbon dioxide by the photo-Kolbe reaction,these results suggest that the oxidation proceeds partially by way of phenol, catecohol and muconic acid [Figure 3. path 7 → 8 → 9], and that muconic acid is oxidized to produce carbon dioxide. In fact it is known that phenol is easily oxidized to muconic acid via catecohol by metal-catalyzed peracetic acid.[26] However, it can be considered that the main path of carbon dioxide production exists besides that. This is expected by the following three reasons. (a) Muconic acid could not be detected for the photocatalytic reaction of phenol although it could for that of benzene. (b) Much more hydroquinone was produced than catecohol for the decomposition of benzene whereas these quantities were nealy equal each other for that of phenol. (c) The total amount of carbon dioxide produced for the photocatalytic reaction of benzene is about three times larger than those for phenol and catecohol. Moreover,

the initial production rate of carbon dioxide from saturated aqueous solution of benzene is also two or three times larger than those from aqueous solution of phenol and catecohol. In Table II are shown the initial rates of carbon dioxide and oxygen production for aqueous solution of various compounds in the presence of 1 mmol of silver ion. Due to the poor activity of these compounds, oxygen was also produced. Here the solubility of muconic acid in water is much lower than that of benzene so that the reactivity of muconic acid can not be compared to the others by the oxygen production rate[25]. Even in this situation the rate of carbon dioxide production from muconic acid is much larger than those from

TABLE II: Initial Rates of Carbon Dioxide and Oxygen Production in the Presence of Silver Ion

Reactant (1 mmol)	Initial Production Rate (μmol/h)	
	O_2	CO_2
Benzene	2.1	13
Phenol	7.8	5.4
Catecohol	0.3	7.9
Hydroquinone	0.4	2.4
Muconic acid	(5.0)	71

Neutral aq. solution, Ag_2SO_4:0.5 mmol,
Reactant:1.3 mmol (see Table I),
Light source:1 KW Xe lamp, Photocatalyst:TiO_2

other aromatic compounds as shown in Table II, so that if the benzene ring opening occurs accompanied with muconic acid formation, carbon dioxide will be produced easily by successive decomposition of muconic acid. The experimental result shows that a lot of carbon dioxide is produced at an early stage of the reaction. This suggests that the intermediate products should be much more reactive than the staring material. Therefore if the benzene ring opening occurs mainly by way of phenol and catecohol, it has to be assumed that the reactivities of phenol and catecohol should be much larger than that of benzene. However, the order of rectivities of these compounds which is determined from the oxygen production rates is in the order of

Catecohol > Benzene > Phenol (6).

This means that the above assumption is not reasonable and the path 7 → 8 → 9 is a minor one. Consequently these results suggest that the main path of carbon dioxide production is that benzene ring does not open by way of phenol and catecohol but opens by way of intermediate products whose reactivities are much larger than that of benzene.

On the other hand, in the radiolysis of the aqueous benzene solution under oxygen, it is known that oxygen is added to hydroxycyclohexadienyl radical and the ring opens to form hydroxymucondialdehyde (HMD).[20-23] This ring opening

process is in competition with the phenol formation. Phenol and HMD are both "primary" products in the sense that their formation does not involve any of the stable reaction products as intermediates. The existence of oxygen is indispensable for the benzene ring opening, and only a small amount of biphenyl forms in the absence of oxygen.[20] The mechanisms have been referred as follows.[21,22]

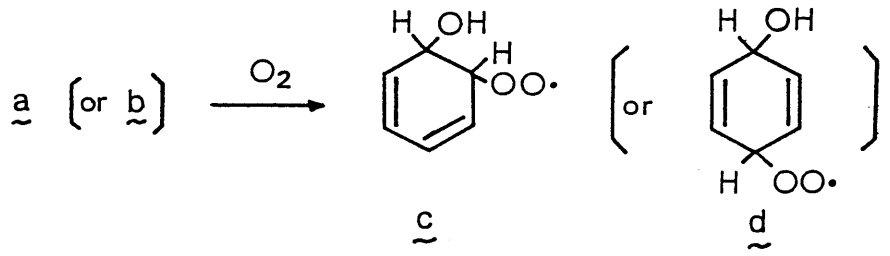

(7)

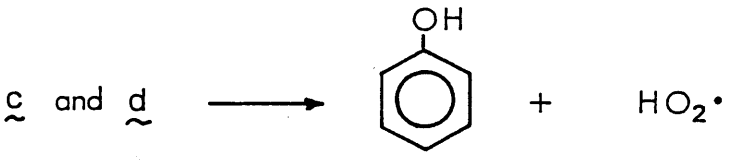

(8)

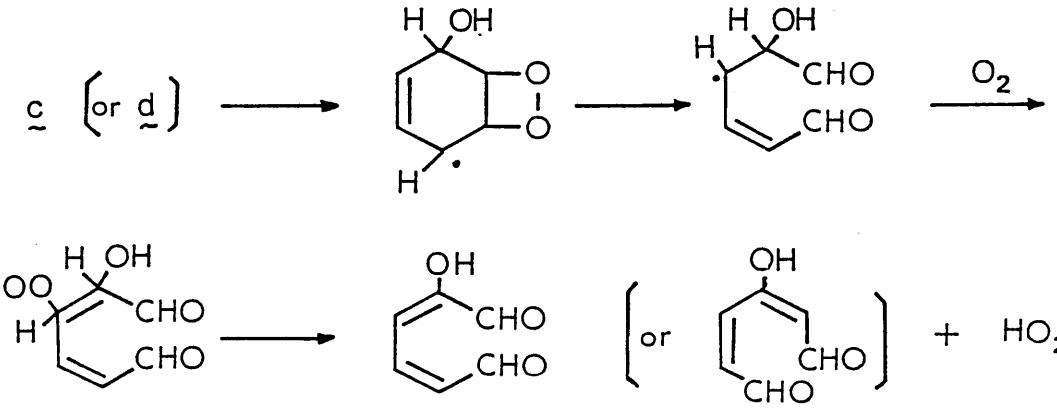

(9)

(HMD)

Thus in the case of the present photocatalytic oxidation reaction, it may be considered that a similar direct ring opening path also exists (Figure 3, path 11 → 12) besides phenol formation. In this case when intermediate products do not have an aromatic nature but are alcohols, aldehydes and acids, they are oxidized to carbon dioxide successively as is the same as the case described in the previous section because the latter products are much more easily oxidized than benzene. These processes are different from those for radiolysis because muconic acid forms from benzene even in the absence of oxygen. Although it may be premature to speculate on the detailed mechanism, all the experimental results could be explained well with the following process, that is, the hydroxycyclohexadienyl radical is oxidized further by photogenerated holes of TiO_2 and the reaction proceeds as follows.

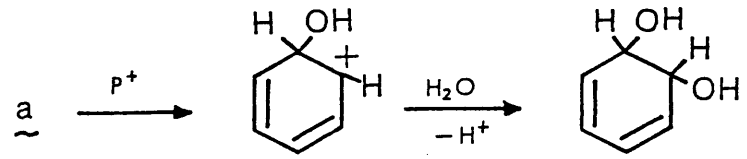

(10)

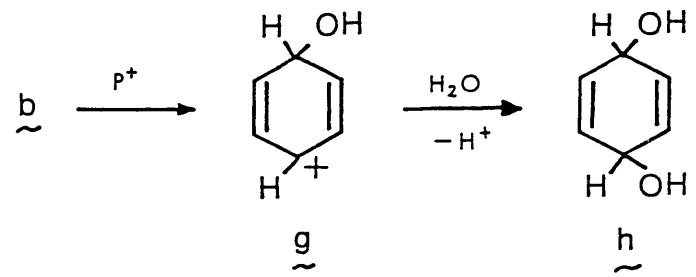

(11)

Eq.(10) and (11) correspond to eq.(7) for the radiolysis, but here hydroxycyclohexadienyl radical is oxidized by photogenerayted holes instead of oxygen.

As is well known 1,2-diol is easily oxidized breaking the C-C bond to yield an aldehyde which is much more easily oxidized than benzene. Thus muconic acid forms from f as follows.

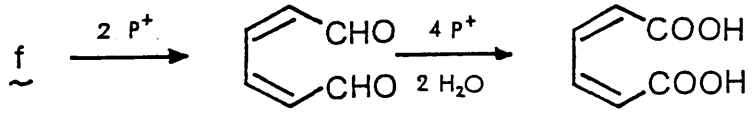

(12)

The muconic acid thus formed is easily oxidized to carbon dioxide.

1,4 diol (h) may be also decomposed partially, but the main reaction is probably the formation of hydroquinone.

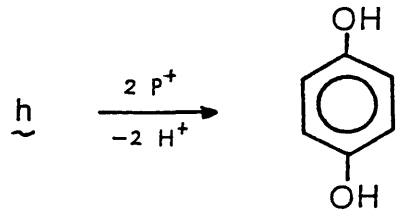

(13)

Eq.(12) and (13) also correspond to eq.(8). The experimental result that much more hydroquinone was produced than catecohol can be also explained well by the above consideration. If catecohol and hydroquinone are produced by

the hydroxylation of phenol, their quantities must be nearly equal since the reactivities of these two are of the same order (see Table II).

The formation of phenol can be thought to proceed mainly by the direct oxidation of hydroxycyclohexadienyl radical by photogenerated holes as follows

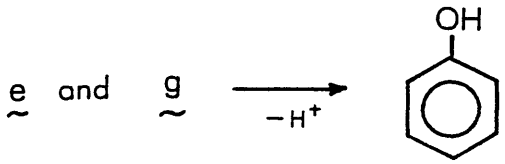

(14)

since in the radiolysis experiment phenol is hardly produced in the absence of oxygen suggesting that hydrogen atom extraction by ·OH radical is very difficult.

Fujihira et al. reported that phenol is the main product of the photocatalytic oxidation of acidic aqueous benzene solution in the presence of oxygen.[2] This is quite different from the present result, in which the main product is carbon dioxide (110 μmol) more than phenol (21 μmol) in neutral water as is seen in Table I. This discrepancy might be explained as follows, that is, the reactions (7),(8) are also proceeding in the presence of oxygen besides the reaction (10),(11), and the reactions (7),(8) may be catalyzed by acids.[26]

Various oxidation processes of benzene are schematically illustrated in Figure 5, and are summarized as follows.

Benzene forms hydroxycyclohexadianyl radical with both the ·OH radical addition (path 1,2) and the direct oxidation by photogenerated holes (path 4,5) proceeding in parallel, and that this radical is oxidized to phenol (path 7) or muconic acid (path 11 → 12 → 13) by holes. Muconic acid is oxidized to carbon dioxide. Carbon dioxide is also produced partially by the further oxidation of phenol (path 7 → 8 → 9 → 11).

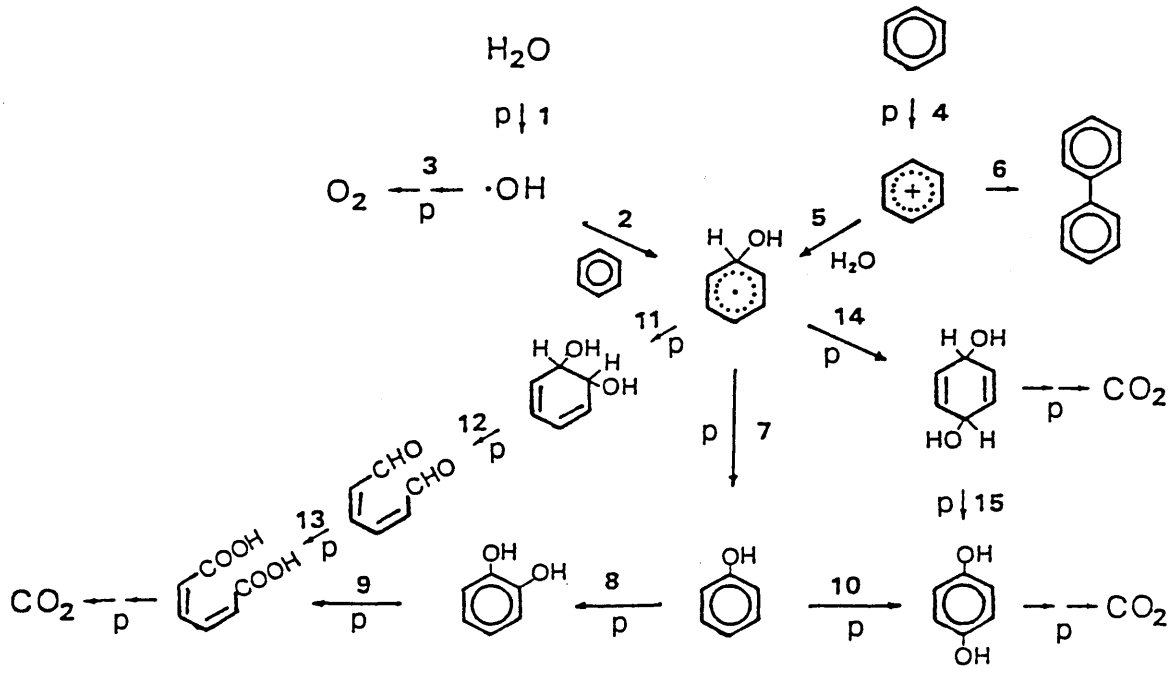

Figure 5. Reaction scheme of photocatalytic oxidation of benzene in water.

(C) Photocatalytic Oxidation of Benzene with Various Powdered Semiconductor

An aqueous solution of benzene in the presence of Ag^+ was also oxidized producing carbon dioxide and oxygen simultaneously, when certain type of powdered semiconductors were used instead of TiO_2. The results and the energy levels of the semiconductors used are shown in Table III and Figure 6, respectively. In addition to the energy levels of semiconductor, the efficiencies of these reactions were also dependent on the lifetimes of the minority carriers, surface states, and the adsorption and catalytic properties of the surface of reaction site. Roughly speaking, however, the comparison between the rates of the carbon dioxide production and the energy levels of the semiconductors indicates that a semiconductor having a stronger oxidation power (the valence band position is more positive) leads to a higher yield of carbon dioxide. This may be explained using the result obtained in the previous section. Namely, the direct oxidation of both benzene and the hydroxycyclohexadienyl radical by photogenerated holes is easier with a semiconductor possessing a deeper valence band, and this results in the carbon dioxide production.[27] Moreover, the ratio of carbon dioxide production to oxygen production is also dependent on the type of semiconductor. These reactions compete each other. According to the mechanism described previously, a

semiconductor with a deeper valence band should give a higher ratio of carbon dioxide to oxygen, since the direct oxidation of benzene (path 4) becomes more efficient in this condition. In fact the general tendency in table III agrees with this explanation.

TABLE III: Amounts of Carbon Dioxide and Oxygen Produced by the Photocatalytic Decomposition of Aqueous Solution of Benzene in the Presence of Silver Ion

	SnO_2	WO_3	TiO_2	$SrTiO_3$	Fe_3O_3
CO_2 (μmol)	140	160	110	30	3
O_2 (μmol)	0	60	10	70	0

Neural aq. solution, Light source:1 KW Xe lamp
Irradiation time:65 hours, Ag_2SO_4:0.5 mmol

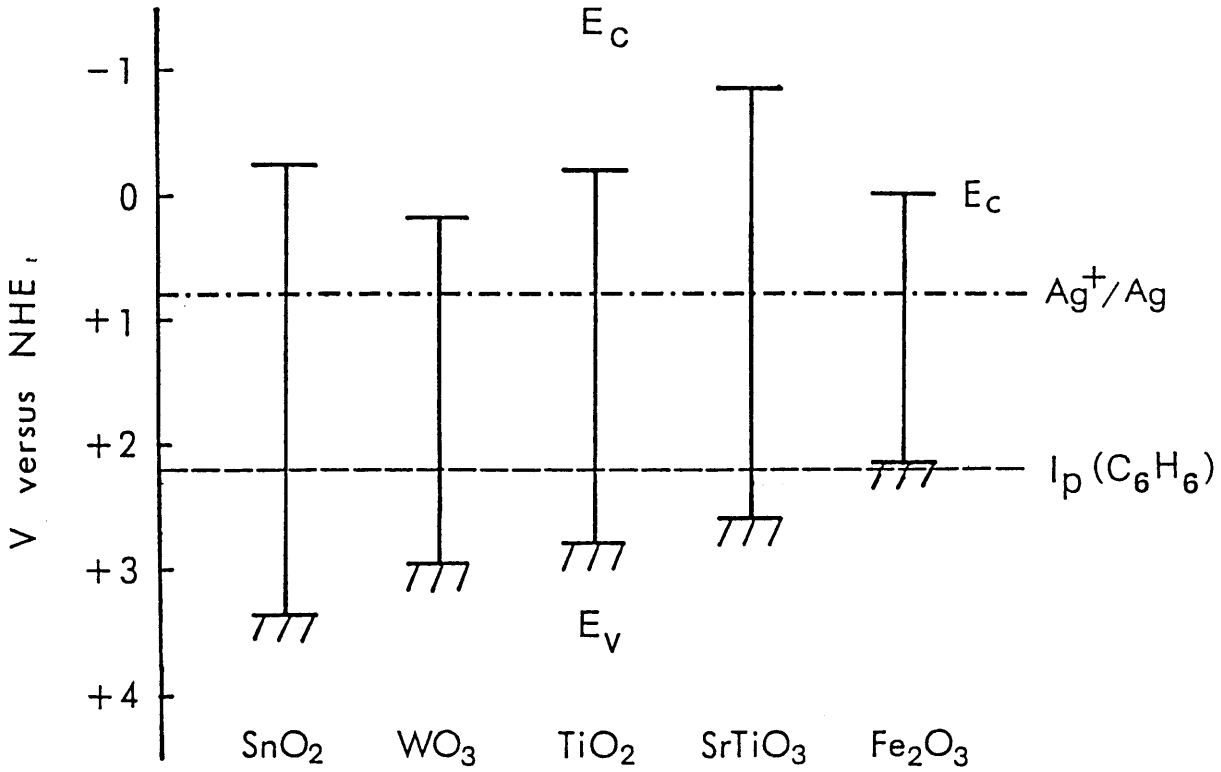

Figure 6. Band edge positions of various semiconductors at pH = 7 vs NHE. Redox potential of Ag^+ and estimated ionization potential of benzene in water are also illustrated.

[Conclusion]

Several interesting organic compounds are found to be produced for the photocatalytic reactions of hydrocarbons.

The mechanisms of carbon dioxide production from the aqueous solution of a linear saturated hydrocarbon or benzene are presented. These compounds are oxidized to acids and the "photo – Kolbe" type of reactions occur producing carbon dioxide. Generally speaking if the intermediate products from a hydrocarbon to a corresponding acid are more reactive than the starting material, they are oxidized successively resulting in carbon dioxide as a main product.

[References and Notes]

(1) I. Izumi, W.W. Duun, K.O. Wilbiurn, Fu-Rien F. Fun, and A.J. Bard, J. Phys. Chem., 84, 3207 (1980).

(2) M. Fujihira, Y. Satoh, and T. Osa, Nature, 293, 5829 (1981).

(3) M. Fujihira, Y. Satoh, and T. Osa, J. Electroanal. Chem., 126, 277 (1981).

(4) M. Fujihira, Y. Satoh and T. Osa, Chem. Lett., 1981, 1053.

(5) I. Izumi, Fu-Rien F. Fun, and A.J. Bard, J. Phys. Chem., 85, 218 (1981).

(6) C.D. Jaeger, and A.J. Bard, J. Phys. Chem., 83, 3146 (1979).

(7) T.Sakata, and T.Kawai, Chem. Phys. Lett ., 80, 341 (1981).

(8) T. Sakata, T. Kawai, and K. Hashimoto, submitted to J. Phys. Chem.

(9) Y. Aikawa, and M. Sukigara, Proceedings of Annual Meeting of Electro. Chem. Soc. Jpn., Sendai, Japan, 1982 (Spring), p 65.

(10) J.W. Loveland, and G.R. Dimeler, Anal. Chem., 33, 1196 (1961).

(11) E.S. Pysh, and N.C. Yang, J. Am. Chem. Soc., 20, 2124

(1963).

(12) R.W. Kiser, "Introduction to Mass Spectrometry and Its Applications", Prentice-Hall, Englewood Cliffs, N.J., 1965, p 308.

(13) F.Lohmann, Z.Naturforsh, A,22, 843 (1967).

(14) K. Honda, A. Fujishima, and T. Inoue, "Hydrogen Energy Progress", T.N. Veziroglu, K. Fueki, and T. Ohta, Eds., Proceedings of the 3rd World Hydrogen Energy Conference, Tokyo, Japan, Pergamon, Oxford, 1980, p 753-63.

(15) H. Gerischer, "Solar Energy Conversion" Topics in Applied Physics, vol. 31, Eds. B.O. Seraphin, Springer (1979).

(16) In these experiments, the solution was not buffered, so that the pH changes continuously during the photolysis. For example, in the case of benzene with silver ion, the pH changed from 5.0 to 1.5 for 100 h irradiation. Therefore the valence band edge is more positive than the value in the text under thus condition, but this small shift is not so serious in the present discussion.

(17) P. Neta and R.W. Fessenden, J. Am. Chem. Soc., 99, 163 (1977).

(18) M.K. Eberhardt, J. Am. Chem. Soc., 103, 3876 (1981).

(19) M.P. Irion, W. Fuβ, and K.-L. Kompa, Appl. Phys., B27, 191 (1982).

(20) I. Loeff, and G. Stein, J. Chem. Soc., 2623 (1963).

(21) L. M. Dorfman, I.A. Taub, and R.E. Bühler, J. Chem. Phys., 36, 3051 (1962).

(22) I. Balakrishnan, and M.P. Reddy, J. Phys. Chem., 76, 1273 (1972).

(23) N. Jacob, I. Balakrishnan, and M.P. Reddy, J. Phys. Chem., 81, 17 (1977).

(24) In these experiments 1 mmol of silver ion was added to the solution. First oxygen and carbon dioxide were produced, and hydrogen started evolving instead of oxygen and carbon dioxide after 50 ~ 100 hours irradiation. We analyzed the products in the liquid phase at this time.

(25) The solubility of benzene in water is about 0.205 wt% at 50 °C (J.A. Riddick and W.B. Bunger, "Organic Solvents" 3rd. Edition John Wiley and Sons, Inc., New York, 1970, p 107.) which corresponds to 1.3 mmol/50 ml aqueous solution, so that the same molar amount of the other compounds were added to 50 ml of neutral water. However, the solubility of muconic acid in water is very lower than that of benzene, so that the reactivity of muconic acid can not be compared to those of others by the oxygen production rate.

(26) A.J. Pandell, J. Org. Chem., 41, 3992 (1976).

(27) For rigorous comparison of the oxidation rates, we have to use the quantum yields of the reactions, although their measurements are difficult in these systems. For

example, the band gap of SnO_2 is much larger than those of the others, so that the absorbed photon number is smaller. This means that the quantum yield of CO_2 production rate for SnO_2 system may be much larger than those for other systems. However, this tendency agrees with the consideration in the text.

[Acknowlegements]

I would like to express my sincerest gratitude to Professor T. Sakata for the continuing encouragement and suggestions throughout this work.

Particular thanks are due to Professor H. Kuroda at University of Tokyo for his kind instructions and careful reading of this thesis.

My greatful thanks are also due to Professor T. Kawai at Osaka University for his valuable suggestions and discussions.

I am grateful to Professor T. Kajiwara at Toho University for his helpful discussions and collaboration on the experiment described in Chapter I, section 2.

I cannot help expressing my many thanks to all the members of the Chemistry of Excited States Laboratory at the Institute for Molecular Science, and of the Physical Organic Chemistry Laboratory of the Institute of Physical and Chemical Research for their encouragement, providing a stimulating and friendly atomosphere.

I wish to thank Drs. D.V. O'Connor and R.D. McKelvey, visitors to the Institute for Molecular Science, for the careful reading of the manuscript.

And last, but of course never least, I am deeply grateful to Professor S. Nagakura, director general of the Institute for Molecular Science for his continuous guidance and constant encouragement throughout this work.

[List of publications]

Chapter I.

(1) "Hydrogen Production with Visible Light by Using Dye-Sensitized TiO_2 Powder"
K.Hashimoto, T.Kawai, and T.Sakata,
Nouv. J. Chim., 7, 249 (1983).

(2) "Dynamics of Luminescence from $Ru(bpy)_3Cl_2$ Adsorbed on Semiconductor Surface"
T.Kajiwara, K.Hashimoto, T.Kawai, and T.Sakata,
J. Phys. Chem., 86, 4516 (1982).

Chapter II.

(3) "Efficient Hydrogen Production from Water by Visible Light Excitation of Fluorescein-Type Dyes in the Presence of a Redox Catalyst and a Reducing Agent"
K.Hashimoto, T.Kawai, and T.Sakata,
Chem. Lett., 1983, 709.

(4) "The Mechanism of Photocatalytic Hydrogen Production with Halogenated Fluorescein Derivatives"
K.Hashimoto, T.Kawai, and T.Sakata,
Nouv. J. Chim., 8, in press.

Chapter III.

(5) "Photocatalytic Reactions of Hydrocarbons and Fossil Fuels with Water : Hydrogen Production and Oxidation"
K.Hashimoto, T.Kawai, and T.Sakata,
J. Phys. Chem., 88, 4083 (1984).

(6) "Heterogeneous Photocatalytic Reactions of Organic Acids and Water : New Reaction Paths besides the Photo-Kolbe Reaction"
T.Sakata, T.Kawai, and K.Hashimoto,
J. Phys. Chem., 88, 2344 (1984).

Reference papers.

(7) "Magnetic Field Effect on the Fluorescence of Methylglyoxal"
K.Hashimoto, S.Nagakura, J.Nakamura, and S.Iwata,
Chem. Phys. Lett., 74, 228 (1980).

(8) "External Magnetic Field Effect on the Fluorescence of Glyoxal"
J.Nakamura, K.Hashimoto, and S.Nagakura,
J. Luminescence, 24/25, 763 (1981).

(9) "Photochemical Diode Model of Pt/TiO_2 Particle and Its Photocatalytic Activity"
T.Sakata, T.Kawai, and K.Hashimoto.
Chem. Phys. Lett., 88, 50 (1982).

(10) "Neutral Particle Emission from Zinc Oxide Surface Induced by High-Density Electronic Excitation"
T.Nakayama, N.Itoh, T.Kawai, K.Hashimoto, and T.Sakata,
Radiation Effects Lett., 67, 129 (1982).

(11) "The Catalytic Properties of RuO_2 and Pt on n-Type Semiconductors"
T.Sakata, T.Kawai, and K.Hashimoto,
Denki Kagaku, 51, 79 (1983), (in Japanese)

(12) "The Structures and Reactivities of Powdered Semiconductor Photocatalysts"
T.Kawai, T.Sakata, K.Hashimoto, and M.Kawai,
Nippon Kagakukaishi, 1984, 277 (in japanese).

(13) "The Catalytic Properties of RuO_2 on n-Type Semiconductors Under Illumination"
T.Sakata, K.Hashimoto, and T.Kawai,
J.Phys Chem., 88, in press.

(14) "Photocatalysis of Zinc Sulfide Microcrystals in Reductive Hydrogen Evolution in Water/Methanol Systems"
S.Yanagida, H.Kawakami, K.Hashimoto, T.Sakata, and H.Sakurai,
Chem. Lett., 1984, 1449.

(15) "Analysis of the Transient Response of a Semiconductor-Electrolyte Circuit to a Short Light Pulse : Application to CdSe Electrodes"
R.H.Wilson, T.Sakata, T.Kawai, and K.Hashimoto,
J. Electrochem. Soc., submitted.

(16) "Highly Efficient Photocatalytic Production of Amino Acids from Organic Acids - Ammonia - Water by Use of Dye or Semiconductor"
T.Sakata, and K.Hashimoto,
J. Am. Chem. Soc., submitted.

HYDROGEN PRODUCTION WITH VISIBLE LIGHT BY USING DYE-SENSITIZED TiO_2 POWDER.

Kazuhito Hashimoto, Tomoji Kawai, and Tadayoshi Sakata

Institute for Molecular Science, Myodaiji, Okazaki 444, Japan.
Received July 21, 1982.

RÉSUMÉ. — De l'hydrogène est produit à partir de l'eau par excitation à la lumière visible de plusieurs colorants organiques fixés sur TiO_2 ou Pt/TiO_2 en présence de réducteurs. Le rendement quantique de la production d'hydrogène a été estimé à environ 10^{-1} pour $Ru(bipy)_3^{2+}$ avec l'EDTA comme agent réducteur. On admet que l'hydrogène est produit par réduction de l'eau par l'intermédiaire d'un processus de sensibilisation du colorant.

ABSTRACT. — Hydrogen was produced from water by exciting various organic dyes on TiO_2 or Pt/TiO_2 with visible light in the presence of reducing agent. The quantum efficiency of hydrogen production was estimated to be in the order of 10^{-1} for $Ru(bipy)_3^{2+}$ with EDTA as the reducing agent. It is postulated that hydrogen is produced by the reduction of water through a dye-sensitized process.

Introduction

The photo-induced water splitting reaction in which TiO_2 or $SrTiO_3$ are used as a photocatalyst has been investigated by many researchers [1-7]. Hydrogen production has also been reported in the photocatalytic reaction of water with various organic compounds in which powdered semiconductors are used [8-11]. However, most semiconductors which are stable under irradiation in an electrolyte solution have wide band-gaps. They absorb mainly UV light. The utilization of dye-sensitization appears to be a promising means of extending the effective wavelength into the visible region. There have also been many reports of hydrogen production with visible light using dyes such as $Ru(bipy)_3^{2+}$ or water soluble zinc porphyrin in a homogeneous system [12]. In such a system, an electron relay such as methylviologen plays an important role in charge separation. We here report a system for hydrogen production by dye sensitization of a semiconductor (TiO_2) in which an electron relay is not necessary; rather, excited dye molecules near the semiconductor powder inject electrons to the conduction band. Grätzel *et al.* reported the complete water splitting reaction with the same electron relay free system by using $Ru(bipy)_3^{2+}$ analogues [12j] or $Ru(bipy)_3^{2+}$ [12l] as sensitizer.

Experimental

As a semiconductor, very fine powdered TiO_2 (anatase, average grain size: 300 Å, Aerosil P-25) with a large surface area, 50 m^2/g, was used. Pt was deposited photochemically on the surface of TiO_2. Powdered TiO_2 (3 g) suspended in a water-ethanol solution (20% aq. soln, 100 ml) of K_2PtCl_6 (0.3 g) was illuminated with a 500 W Xe lamp (Ushio, UXL 500) [13]. The particle size of platinum on TiO_2, which is prepared with this photochemical method, is known to be about 20-100 Å [11, 14]. $Ru(bipy)_3Cl_2$, various water soluble porphyrins and some other organic dyes served as sensitizers. EDTA or methanol was the reducing agent. In the liquid phase experiment, platinized TiO_2 powder (0.1 g) was suspended in an aqueous solution of each dye (10^{-4} M, 50 ml) with a reducing agent (EDTA : 5×10^{-2} M or methanol: 50 vol/vol %) in a 280 ml Pyrex glass bulb. The pH of the solution was adjusted to 5 with HCl or NaOH. After deaeration the bulb was irradiated from the bottom with visible light (500 W Xe lamp; a Toshiba sharp cut filter eliminated UV light). After irradiation for several hours, the gas produced was analysed by a quadrupole mass spectrometer as described previously [8]. In the vapor phase experiment, $Ru(bipy)_3Cl_2$ was adsorbed as follows. The TiO_2 powder was soaked in a methanol solution of the dye and the solvent was evaporated by evacuation ($Ru(bipy)_3Cl_2/TiO_2$: 0.01 wt/wt %). This semiconductor-dye photocatalyst was put into the bulb described above and methanol-water vapor was introduced from a side glass bulb. For the measurement of the apparent quantum yield of hydrogen production in $Ru(bipy)_3^{2+}$-TiO_2/Pt, monochromatic light at 460 nm, provided by a 500 W Xe lamp and a monochromator (Nikon G250), was used to excite only the dye molecules. The photon number was determined by using a thermopile (Eppley Inc.). The amount of $Ru(bipy)_3^{2+}$ adsorbed on the TiO_2 powder was estimated by measuring the change of the absorption intensities of the solution before and after addition of the TiO_2 powder. The absorption spectra were measured on a Hitachi 556 spectrometer. In order to avoid scattered light effects, the spectrum of the solution to which TiO_2 was added was measured after the powder was removed by using an ultracentrifuge (40 000 rpm, 30 min. Beckmann Co.).

Results and discussion

In Table I are shown the results of the liquid phase experiments. When methanol was used as the reducing agent, the hydrogen production rate did not increase upon addition of $Ru(bipy)_3^{2+}$ into the solution [Run Nos. 12, 13]. However, when EDTA was used as the reducing agent, the rate in the presence of $Ru(bipy)_3^{2+}$ was about 8 times larger than that in the absence of the dye [Nos 9, 10]. When D_2O was used instead of H_2O, D_2 was 90% of the evolved hydrogen gas, DH 5% and H_2 5%. This result indicates that hydrogen is generated through the reduction of protons from water in this Dye-Pt/TiO_2 system as well as in Pt/TiO_2 systems in which band gap irradiation of the semiconductor is employed [8, 9, 15]. Small amounts of hydrogen could be produced in the presence of Pt/TiO_2 even without dyes [Nos. 8, 13], probably because of the absorption of visible light by the surface states of TiO_2. Besides $Ru(bipy)_3^{2+}$, several dyes in Table I were found to be effective for hydrogen production. The hydrogen production rate was increased by more than a factor of 10 [Nos. 1-8]. Since it is known that they are able to sensitize semiconductor electrodes (ZnO, SnO_2 and TiO_2) [16], the present results

suggest that hydrogen is produced *via* a dye-sensitization effect.

Table I. – Rate of hydrogen production on Dye-Pt/TiO_2 system in the liquid phase. Light source: 500 W Xe lamp. (*) Pt/SiO_2 instead of Pt/TiO_2.

Run	Dye	Red. agent	Rate (μmol/h)	Light
1	Zn-TPPS	EDTA	1.6	
2	Pd-TPPS	EDTA	<0.4	
3	H_2-TPPS	EDTA	<0.4	
4	Safranine T	EDTA	3.4	λ>480 nm
5	Rhodamine B	EDTA	1.0	(filter Y-48)
6	Rhodamine 6G	EDTA	3.0	
7	Rose Bengal	EDTA	5.6	
8	none	EDTA	0.4	
9	$Ru(bipy)_3^{2+}$	EDTA	4.6	
10	none	EDTA	0.6	λ>440 nm
11	$Ru(bipy)_3^{2+}$ (*)	EDTA	0.0	(filter Y-44)
12	$Ru(bipy)_3^{2+}$	methanol	<0.5	
13	none	methanol	0.5	
14	none	EDTA	220	white light
15	none	methanol	270	(no filter)

For dye-sensitization, the reaction scheme of hydrogen production is written as,

$$\text{Dye} \xrightarrow{h\nu} \text{Dye}^*, \quad (1)$$

$$\text{Dye}^* \rightarrow \text{Dye}^{+\cdot} + e^-(TiO_2), \quad (2)$$

$$e^-(TiO_2) + H^+ \xrightarrow{\text{Pt on } TiO_2} 1/2\,H_2, \quad (3)$$

$$\text{Dye}^{+\cdot} + \text{Red} \rightarrow \text{Dye} + \text{Red}^{+\cdot}, \quad (4)$$

$$\text{Red}^{+\cdot} \rightarrow \text{Oxidation products}. \quad (5)$$

Here $e^-(TiO_2)$ and Red represent an electron in the conduction band of TiO_2 and a reducing agent, respectively. The figure illustrates the hydrogen production process resulting from dye sensitization of the TiO_2 semiconductor. This process is quite similar to that of the dye-sensitized semiconductor electrode in a photoelectrochemical cell [16]. Another mechanism of hydrogen production is possible. It involves reductive quenching of the excited dye as follows:

$$\text{Dye} \xrightarrow{h\nu} \text{Dye}^*, \quad (6)$$

$$\text{Dye}^* + \text{Red} \rightarrow \text{Dye}^{-\cdot} + \text{Red}^{+\cdot}, \quad (7)$$

$$\text{Dye}^{-\cdot} + H^+ \xrightarrow{\text{Pt or Pt/}TiO_2} \text{Dye} + 1/2\,H_2, \quad (8)$$

$$\text{Red}^{+\cdot} \rightarrow \text{oxidation products}. \quad (9)$$

This possibility is ruled out especially for $Ru(bipy)_3^{2+}$-EDTA in Table I for the following reasons. Firstly, hydrogen was not produced when Pt/SiO_2 was used instead of Pt/TiO_2 as seen in No. 11 of Table I. If the mechanism of reductive quenching, i. e. equations (6)-(9), is true in this case, hydrogen should be produced even for Pt/SiO_2. Actually, for fluorescein derivatives, which are reduced according to equation (7) with triethanolamine (TEOA) as a reducing agent [17], hydrogen is produced very efficiently with colloidal Pt or Pt/SiO_2 (hydrogen evolution rate: 320 μmol/h for dibromofluoresceine), since hydrogen production is possible without a semiconductor in this case. This fact indicates that the dye sensitization is indispensable for $Ru(bipy)_3^{2+}$-EDTA-Pt/TiO_2.

Secondly, the luminescence of $Ru(bipy)_3^{2+}$ is quenched by TiO_2 [18, 19] as well as by MV^{2+} [12d, i, 19] through an electron transfer process from the excited dye to these electron acceptors, although it is not quenched by EDTA [12d, i]. This means that the rate of reduction of $Ru(bipy)_3^{2+*}$ is very slow compared with oxidative quenching. The mechanism of reductive quenching of excited dye can also be distinguished from the dye sensitization mechanism by using an electrochemical method, since the reductive quenching corresponds to a photogalvanic process in which electroactive species are accumulated in the bulk solution. For instance, in a photoelectrochemical cell with fluorescein derivatives and TEOA, the rise and decay time of the short circuit current and open voltage is quite slow (several ten seconds to several minutes) and depends on the thickness of the solution layer between a glass window and the metal (Pt) or semiconductor (ZnO, TiO_2) electrode [17]. This slow response can be explained by a gradual accumulation and diffusion of long-lived electroactive species which are generated by a photochemical redox reaction in the homogeneous solution. On the other hand, the rise time of the photocurrent in a photoelectrochemical cell based on dye sensitization is very rapid [16, 20, 21]. Such a rapid response was observed for an electrochemical cell with $Ru(bipy)_3^{2+}$-H_2O and Rose Bengal-hydroquinone, I_2 or EDTA. All these facts indicate that the hydrogen production from $Ru(bipy)_3^{2+}$-EDTA-Pt/TiO_2 occurs through

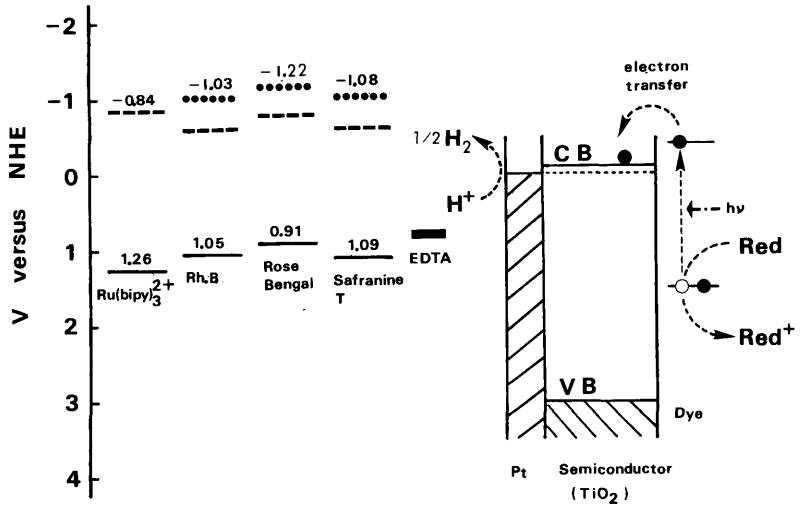

Figure. – Schematic mechanism of dye sensitization of semiconductor and the oxidation potentials of the ground state and the first excited state dyes.
——— D^+/D (the ground state) [25, 26];
. . . $D^+/{}^1D^*$ (the first excited singlet state) [27];
--- $D^+/{}^3D^*$ (the excited triplet state) [28, 29]. The TiO_2 energy level diagram is also drawn according to the scale at the lhs.

a dye sensitization process. The hydrogen production by dye sensitization seems to be applicable also to the cases with other dyes (Nos. 1, 4, 5, 6, 7 in Table I), since it is well known that all these dyes are able to sensitize semiconductor electrodes (ZnO, SnO_2, TiO_2) in electrochemical cells [16]. Generally speaking for the dyes, which are soluble in an aqueous medium, hydrogen is produced more efficiently for the photogalvanic cases than for dye sensitization of semiconductor, since in the former cases the reduced species, responsible for hydrogen production, are formed in the bulk solution, whereas, in the latter cases, only the dyes near the semiconductor surface are involved in the electron transfer to the semiconductor.

Besides $Ru(bipy)_3^{2+}$, Rose Bengal, Safranine T and Rhodamine 6G showed rather a good effect (Nos. 4, 6, 7 in Table I). Rose Bengal, however, was not stable under long-time irradiation. The hydrogen production rate decreased gradually and became zero after 10 to 20 hours irradiation. Safranine T and Rhodamine 6G were relatively stable compared to Rose Bengal, but the rates also decreased gradually. $Ru(bipy)_3^{2+}$ was very stable and the rate did not change after more than 40 hours irradiation. For Pd-TPPS and H_2-TPPS, the effect was negative (Nos. 2 and 3 in Table I). It suggests that it is difficult for these dyes to sensitize TiO_2 and that the number of photons absorbed by the surface states of TiO_2 is decreased by the absorption by these dye molecules.

Since a hydrogen production rate of 0.1 μmol/hour corresponds to 5.3 μA of photocurrent in a photochemical cell, the rate for Rose Bengal-Pt/TiO_2 given in Table I, 5.6 μmol/hour, corresponds to a photocurrent of 300 μA. This value is quite large compared to even the largest photocurrent in a dye-sensitized semiconductor photochemical cell [16]. On the other hand, the hydrogen production rates achieved by dye-sensitization of platinized TiO_2 powder are about a hundred times smaller than those achieved by band gap excitation of platinized TiO_2 powder [Nos. 14, 15]. The apparent quantum efficiency of hydrogen production (2 × the number of H_2 molecules produced/the number of the incident photons) in the dye sensitization system listed in Table I is quite small, in the order of 10^{-3}. It was measured to be 1.7×10^{-3} for $Ru(bipy)_3^{2+}$-TiO_2/Pt by using monochromatic light at 460 nm, where $Ru(bipy)_3^{2+}$ shows an absorption maximum. However, this low value does not mean that the actual quantum yield of hydrogen production (2 × the number of H_2 molecules produced/the number of photons which were absorbed by the dye molecules involved in the dye-sensitized electron transfer reaction) is much smaller than that achieved by direct excitation of TiO_2, because only a relatively small number of dye molecules are able to participate in hydrogen production and only a small fraction of the incident light is absorbed by these molecules.

Actually the quantum yield for the $Ru(bipy)_3^{2+}$-TiO_2/Pt system is probably larger than 0.3. This value was estimated as follows. As was outlined in the Experimental section, the amount of $Ru(bipy)_3^{2+}$ adsorbed on the powdered TiO_2 was estimated by measuring the change of the absorption intensities of the solutions before and after addition of the powdered TiO_2. The change of absorbance in the dye solution (1.0×10^{-4} M, 50 ml) was less than 0.005 after addition of powdered TiO_2 (1.0 g, 50 m^2/g surface area). This value corresponds to less than 2.5×10^{-8} mol of adsorbed dye, and constitutes a 1/4 000 monolayer on TiO_2. Here we assumed that $Ru(bipy)_3^{2+}$ was a sphere with a radius of 5 Å. In our hydrogen production experiment, it is less than 2.5×10^{-9} mol since 0.1 g of TiO_2 was used. The absorbance of these adsorbed molecules can be calculated with the aid of the Beer-Lambert equation [equation (10)]:

$$\log(I_0/I) = \varepsilon cd, \qquad \varepsilon = 10\,000 \text{ cm}^{-1}.1^{-1} \text{ (at 460 nm)} \qquad (10)$$

The concentration (c mol/l) is given by equation (11), in which it is assumed that the dye molecules are uniformly distributed in the total volume of TiO_2 powder (V.cm^3). The path length (d cm) is calculated from equation (12):

$$c = N_{ad.}/(10^{-3} \times V) = (2.5 \times 10^{-9})/(10^{-3} \times V), \qquad (11)$$

$$d = V/A = V/20. \qquad (12)$$

Here, $N_{ad.}$ (mol) and A (cm^2) represent the number of adsorbed dye molecules and the irradiated surface area (20 cm^2), respectively. Using these equations the absorbance of adsorbed dye is calculated to be below 1.3×10^{-3}, so that less than 0.3% of the incident light is absorbed by the adsorbed molecules. In addition to these adsorbed molecules, it is possible for excited molecules in the bulk solution to inject electrons into the semiconductor by diffusing to the surface during their lifetime. Since the excited state of $Ru(bipy)_3^{2+}$ has a relatively long lifetime ($\tau = 6.0 \times 10^{-7}$ s [22]), this contribution cannot be neglected. It can be estimated as follows. The diffusion length (L cm) of the excited molecules is given by $L = \sqrt{\tau \cdot D}$ (D: diffusion coefficient), and is calculated to be 2.5×10^{-6} cm by assuming $D = 10^{-5}$.cm^2.s^{-1}. The adsorbance of this layer is calculated to be 1.0×10^{-3} from equation (10) assuming that the concentration and the path length are given by equations (13) and (14):

$$c = \frac{1}{6} c_1 \text{ [23]} = 10^{-4}/6 \text{ (mol/l)}, \qquad (13)$$

$$d = LS/A = (2.5 \times 10^{-6})\ (5 \times 10^4)/20 \text{ (cm)}, \qquad (14)$$

Here, c_1 and S represent the concentration of the solution (1.0×10^{-4} M) and the surface area of TiO_2 powder (5×10^4 cm^2/0.1 g TiO_2), respectively. Consequently, the ratio of light absorbed by the dye molecules that are involved in the electron transfer to the incident light is given by:

$$\log(I_0/I) < 1.3 \times 10^{-3} + 1.0 \times 10^{-3}, \qquad I/I_0 > 0.995. \qquad (15)$$

The quantum yield is given by:

$$Q.Y. = (I_0/I_0 - I) \times Q.Y._{\text{apparent}} > 0.3 \qquad (16)$$

These results suggest that the efficiencies of electron transfer from the excited state dye to the semiconductor and the hydrogen production are high. This value is close to the yield of electron transfer in dye sensitized photochemical cells. Memming *et al.* reported that the quantum yield of transferred electrons to absorbed photons was 0.15 in a monolayer of $Ru(bipy)_3^{2+}$ analogues on the SnO_2 electrode [20].

In order to investigate this effect further, hydrogen production in the gaseous phase was carried out using $Ru(bipy)_3Cl_2$ and methanol as sensitizer and reducing agent, respectively. The result is shown in Table II. A comparison with the rates obtained without dye or TiO_2, clearly indicates that hydrogen production in the TiO_2-$Ru(bipy)_3^{2+}$ system results mainly from the sensitization effect of $Ru(bipy)_3^{2+}$. The rate is about ten times smaller than that resulting from direct band gap excitation of TiO_2 in the gas phase experiment. It is interesting that methanol is effective as a reducing agent in the gas phase [24].

Hydrogen production with visible light where $Ru(bipy)_3^{2+}$ or Zn-TPPS was used as photocatalysts has been reported [12]. This method is, however, based on the reaction in a homogeneous system in which methylviologen is necessary as an electron relay. The principal reaction scheme may be written as:

Table II. – Sensitization effect on hydrogen production from saturated methanol-water vapor by $Ru(bipy)_3Cl_2$ on powdered TiO_2. Light source: 500 W Xe lamp with filter Y-44 ($\lambda > 440$ nm) (*) 30 hours irradiation. (**) White light from Xe lamp. Dye concentration: 0.01 wt/wt % (1/600 monolayer).

Photocatalyst	Quantity of H_2 (μmol) (*)
TiO_2	2.1
TiO_2-$Ru(bipy)_3Cl_2$	26
SiO_2-$Ru(bipy)_3Cl_2$	0
TiO_2 (**)	340

$$Dye \xrightarrow{h\nu} Dye^*, \quad (17)$$

$$Dye + MV^{2+} \rightarrow Dye^{+\cdot} + MV^{+\cdot}, \quad (18)$$

$$MV^{+\cdot} + H^+ \xrightarrow{Pt} MV^{2+} + 1/2H_2, \quad (19)$$

$$Dye^{+\cdot} + Red \rightarrow Dye + Red^{+\cdot}, \quad (20)$$

$$Red^{+\cdot} \rightarrow \text{oxidation products}. \quad (21)$$

Here MV^{2+} is methylviologen.

The system reported in this paper is quite different from this system as mentioned before. The dye is used as a sensitizer of semiconductor powders and electrons are transferred from excited dye molecules to the conduction band of the semiconductor.

One of the characteristic features to which attention should be given is the weak oxidation power of the dye. As illustrated in Figure 1, the valence orbital of the sensitizing dyes is at a higher energy than the valence band of the semiconductor. Oxidation of a reducing agent such as EDTA or methanol in the dye sensitization process may therefore be more difficult than oxidation by direct excitation of TiO_2. Furthermore, the rate of hole consumption by the reducing agent may decrease as a result of the weak oxidation power of these oxidized dyes, resulting in an increased recombination. Actually the hydrogen production rate with methanol as a reducing agent was much smaller than the rate with EDTA in the case of the dye sensitization system [Table I Run Nos. 9, 12], whereas in the case of direct excitation of TiO_2 the rates achieved with methanol and EDTA were almost equal [Nos. 14, 15].

The hydrogen production rates listed in Tables I and II are rather small. As described previously, these small rates result from the fact that only a small portion of the incident light is absorbed by the dyes near the semiconductor in the liquid phase. In the vapor phase, the concentration of reacting molecules is small and some dye molecules such as $Ru(bipy)_3^{2+}$ are not attached closely to the semiconductor surface under the presence of water vapor [19]. Therefore, highly efficient hydrogen production would be possible under the following conditions.

(1) The sensitizing dye molecules should be adsorbed tightly on the semiconductor surface with a consequent increase in the electron transfer interaction and in the amount of light absorbed by the dye molecules participating in hydrogen production.

(2) The dye should have an intrinsically long excited state lifetime, so that the probability of photo-redox reactions in the excited state is increased.

(3) The electron energy in the excited state of the dye should be higher than the conduction band of the substrate semiconductor, and the valence orbital of the dye should be low enough to oxidize reactants such as organic compounds or water (or OH^-).

(4) Good catalysts for hydrogen production and also for the oxidation reaction are used.

Acknowlegement

We thank Professor Kenichiro Hatano of Nagoya City University for the gift of water soluble metal porphyrins and Professor Takashi Kajiwara of Toho University for stimulating discussions and Dr. Desmond O'Connor for careful reading of the manuscript.

REFERENCES

[1] G. N. Schrauzer, and T. D. Guth, *J. Amer. Chem. Soc.*, **99**, 7189 (1977).
[2] F. T. Wagner, and G. A. Somorjai, *Nature*, **285**, 559 (1980).
[3] S. Sato, and J. M. White, *Chem. Phys. Lett.*, **72**, 83 (1980).
[4] T. Kawai, and T. Sakata, *Chem. Phys. Lett.*, **72**, 87 (1980).
[5] J. M. Lehn, J. P. Sauvage, and R. Ziessel, *Nouv. J. Chim.*, **4**, 623 (1980).
[6] K. Domen, S. Naito, M. Soma, T. Ohnishi, and T. Tamaru, *J.C.S. Chem. Commun.*, 543 (1980).
[7] D. Duonghong, E. Borgarello, and M. Grätzel, *J. Amer. Chem. Soc.*, **103**, 4685 (1981).
[8] (*a*) T. Kawai, and T. Sakata, *Nature*, **282**, 283 (1979); (*b*) T. Kawai, and T. Sakata, *J.C.S. Chem. Commun.*, 694 (1980); (*c*) T. Kawai, and T. Sakata, *Nature*, **286**, 474 (1980); (*d*) T. Sakata, and T. Kawai, *Nouv. J. Chim.*, **5**, 279 (1981); (*e*) T. Kawai, and T. Sakata, *Chem. Lett.*, 81 (1981); (*f*) T. Sakata, and T. Kawai, *Chem. Phys. Lett.*, **80**, 341 (1981).
[9] (*a*) S. Sato, and J. M. White, *Chem. Phys. Lett.*, **70**, 131 (1981); (*b*) S. Sato, and J. M. White, *J. Amer. Chem. Soc.*, **102**, 7206 (1980); (*c*) S. Sato, and J. M. White, *J. Phys. Chem.*, **85**, 336 (1981).
[10] J. R. Darwent, and G. Porter, *J.C.S. Chem. Commun.*, 145 (1981).
[11] P. Pichat, J.-M. Herrmann, J. Disdier, H. Courbon, and M.-N. Mozzanega, *Nouv. J. Chim.*, **5**, 627 (1981).
[12] For example, (*a*) B. V. Koriakin, T. S. Dzhabiev, and A. E. Shilov, *Dokl. Akad. Nauk. S.S.R.R.*, **233**, 620 (1977); (*b*) J. M. Lehn, and J. P. Sauvage, *Nouv. J. Chim.*, **1**, 449 (1977); (*c*) A. I. Krasna, in *Biological Solar Energy Conversion*, A. San Pietro, and A. Mitsuri, Eds., Academic Press, New York, (1977); (*d*) A. Moradpour, E. Amouyal, P. Keller, and H. Kagan, *Nouv. J. Chim.*, **2**, 547 (1978); (*e*) A. I. Krasna, *Photochem. Photobiol.*, **29**, 267 (1979); (*f*) J. M. Lehn, J. P. Sauvage, and R. Ziessel, *Nouv. J. Chim.*, **3**, 423 (1979); (*g*) K. Kalyanasundaram, and M. Grätzel, *Angew. Chem. Int. Ed. Engl.*, **18**, 701 (1979); (*h*) J. M. Lehn, J. P. Sauvage, and E. Ziessel, *Nouv. J. Chim.*, **4**, 355 (1980); (*i*) P. Keller, A. Moradpour, E. Amouyal, and H. B. Kagan, *Nouv. J. Chim.*, **4**, 377 (1980); (*j*) E. Borgarello, J. Kiwi, E. Pelizzetti, M. Visca, and M. Grätzel, *Nature*, **289**, 158 (1981); (*k*) M. Grätzel, *Acc. Chem. Res.*, **14**, 376 (1981); (*l*) E. Borgarello, J. Kiwi, E. Pelizzetti, M. Visca, and M. Grätzel, *J. Amer. Chem. Soc.*, **103**, 6324 (1981); (*m*) A. Harriman, G. Porter, and M. C. Richoux, *J. Chem. Soc. Trans.*, **77**, 833 (1981).
[13] B. Kraeutler, and A. J. Bard, *J. Amer. Chem. Soc.*, **100**, 2239 (1978).
[14] (*a*) T. Kawai, K. Hashimoto, and T. Sakata, *Proceedings of Annual Meeting of Electro. Chem. Soc. Jpn.*, Tokyo, Japan, 1982

(autum) p. 107; (*b*) P. Pichat, J.-M. Herrmann, M.-N. Mozzanega, H. Courbon, J. Disdier, and L. T. Prahov, *Book of Abstracts of 4th International Conference on Photochemical Conversion and Storage of Solar Energy*, Jerusalem, Israel, J. Rabani (Chairman), 1982, p. 108.

[15] T. Sakata, T. Kawai, and K. Hashimoto, *Chem. Phys. Lett.*, **88**, 50 (1982).

[16] For example, (*a*) H. Gerischer, and H. Tributsch, *Ber. Bunsenges. Phys. Chem.*, **72**, 437 (1968); (*b*) K. Hauffe, and J. Range, *Z. Naturforsch*, **23b**, 736 (1968); (*c*) H. Tributsch, and H. Gerischer, *Ber. Bunsenges. Phys. Chem.*, **73**, 251 (1969); (*d*) R. Memming, *Photochem. Photobiol.*, **16**, 325 (1972); (*e*) T. Watanabe, A. Fujishima, O. Tatsuoki, and K. Honda, *Bull. Chem. Soc. Jpn.*, **49**, 8 (1976); (*f*) H. Tsubomura, M. Matsumura, Y. Nomura, and T. Amamiya, *Nature*, **261**, 402 (1976); (*g*) M. Matsumura, Y. Nomura, and H. Tsubomura, *Bull. Chem. Soc. Jpn.*, **52**, 1599 (1979); (*h*) M. Matsumura; Doctor Thesis at Osaka University (1979).

[17] K. Hashimoto, T. Kawai, and T. Sakata, to be published.

[18] J. Kiwi, *Chem. Phys. Lett.*, **83**, 594 (1981).

[19] T. Kajiwara, K. Hashimoto, T. Kawai, and T. Sakata, *J. Phys. Chem.*, **86**, 4516 (1982).

[20] R. Memming, and F. Schröppel, *Chem. Phys. Lett.*, **62**, 207 (1979).

[21] T. Kojima, T. Ban, K. Kasatani, M. Kawasaki, and H. Sato, *Chem. Phys. Lett.*, submitted for publication.

[22] For example, (*a*) F. E. Lytle, and D. M. Hercules, *J. Amer. Chem. Soc.*, **91**, 253 (1969); (*b*) J. Van. Houten, and R. J. Watts, *J. Amer. Chem. Soc.*, **98**, 4853 (1976); (*c*) C. Creutz, N. Sutin, and B. S. Brunshwig, *J. Amer. Chem. Soc.*, **101**, 1297 (1979).

[23] The factor about 1/6 in equation (5) represents the possibility of the collision between a sphere with a radius of 150 Å (TiO_2) and a dye molecule while the molecule moves in the distance of 250 Å at randum.

[24] The dye sensitization effect of $Ru(bipy)_3^{2+}$ is apparent in the gas phase, whereas this effect is not obvious in the liquid phase experiment when methanol was used as the reducing agent.

[25] C. T. Lin, W. Böttcher, M. Chou, C. Creutz, and N. Sutin, *J. Amer. Chem. Soc.*, **98**, 6536 (1976).

[26] H. Tsubomura, *Photoelectrochemistry and Energy Conversion*, Tokyo Kagaku Dojin, (1980).

[27] The energy difference of the lowest excited singlet state ($^1D^*$) and the ground state (D) was determined by measuring the edge of the absorption spectrum.

[28] The lowest triplet states like these dyes have been known to be separated by 3 000-4 000 cm^{-1} below from the lowest excited singlet states. Thus, we assumed that $^3D^*$ states situated about 0.43 eV lower than $^1D^*$ state, approximately.

[29] S. P. Mcglynn, T. Azumi, and M. Kinoshita, *Molecular Spectroscopy of the Triplet State*, Prentice-Hall, Englewood cliffs, N.J., (1969).

Reprinted from The Journal of Physical Chemistry, 1982, 86, 4516.

Dynamics of Luminescence from $Ru(bpy)_3Cl_2$ Adsorbed on Semiconductor Surfaces

Takashi Kajiwara,*† Kazuhito Hasimoto,‡ Tomoji Kawai,‡ and Tadayoshi Sakata‡

Department of Chemistry, Faculty of Science and Institute of Molecular Science, Toho University, Miyama 2-2-1, Funabashi-shi, Chiba-ken, Japan 274 *(Received: February 24, 1982; In Final Form: June 4, 1982)*

The dynamic spectroscopic properties of the excited state of $Ru(bpy)_3^{2+}$ adsorbed on powdered semiconductors (TiO_2, SnO_2, $SrTiO_3$, and ZrO_2), a powdered insulator (SiO_2), and microcrystalline methylviologen chloride have been investigated by using a pulsed dye laser (6 ns, 450 nm) or a YAG laser (25 ps, 530 nm) as an exciting light source. The time-resolved luminescence spectra of $Ru(bpy)_3^{2+}$ adsorbed on oxide semiconductors were found to be classified into two components. One is blue shifted compared with the normal spectrum and originates from the tightly bound $Ru(bpy)_3^{2+}$ whose excited state decays with a lifetime of 12–20 ns depending on the substrate. The short lifetime can be explained by an electron-transfer interaction between the excited $Ru(bpy)_3^{2+}$ and the oxide semiconductor. The other originates from loosely bound $Ru(bpy)_3^{2+}$ whose luminescent state has a longer lifetime (40–3500 ns) than that of the tightly bound $Ru(bpy)_3^{2+}$. The excited $Ru(bpy)_3^{2+}$ on microcrystalline methylviologen chloride decays very fast with a lifetime of 3.3 ns, indicating a strong electron-transfer interaction. Hydrogen evolved due to the dye sensitization effect on $Ru(bpy)_3^{2+}$ on TiO_2, although the efficiency was not good. This is explained by the poor adsorption ability of $Ru(bpy)_3^{2+}$ onto TiO_2 and by recombination of electrons injected into the conduction band with the oxidized dyes.

Introduction

$Ru(bpy)_3^{2+}$ and related complexes have been intensively investigated as photocatalysts for the water-splitting reaction.[1] A photochemical cell based on electron-transfer quenching of the excited-state $Ru(bpy)_3^{2+}$ gives both H_2 and a photocurrent.[2] Ru(II) complexes have also been used as photosensitizers of semiconductor electrodes.[3] In the dye sensitization of a semiconductor, electron transfer between the exicted dye and the semiconductor has been believed to be the initial process.[3,4] Memming and Shröppel investigated electron-transfer reactions of excited Ru(II) complexes in monolayer assemblies at a SnO_2 electrode by using photoelectrochemical methods.[3a] The photocurrent was interpreted as an electron transfer from a Ru(II) complex, excited to its triplet state, to the conduction band of SnO_2. They suggested an efficient oxidation of water by Ru(III) complex generated in that reaction. Clark and Sutin performed a detailed photoelectrochemical study of sensitization of n-type TiO_2 electrodes by poly(pyridine)ruthenium(II) complexes and showed that the electron transfer from excited states of these complexes can occur efficiently.[3b] The quenching processes involving the excited states of $Ru(bpy)_3^{2+}$ in solution have been well studied by the Stern–Volmer analysis of luminescence intensity and also by flash photolysis experiments.[5] However, transient spectroscopic analysis of quenching of excited $Ru(bpy)_3^{2+}$ by solid material has not been reported to our knowledge. These experiments, we think, can significantly contribute to the understanding of the dye sensitization process of semiconductors because it may be possible to obtain direct data for the rate of electron transfer between the excited dye and the semiconductor that are free from complications caused by various diffusion processes inevitable for experiments using solutions. In the present study under vacuum, methylviologen (MW) and oxide semiconductors (TiO_2, SnO_2, $SrTiO_2$, and ZrO_2) were chosen as the electron acceptor. Since the luminescence of the $Ru(bpy)_3^{2+}$ monolayer adsorbed on the single crystal of these acceptor materials was too weak for the present apparatus to give reliable data, fine powders with large effective surfaces were used as substrates. SiO_2 was used as a reference substrate.

Fine powdered semiconductors are also interesting because of the photocatalytic effects for hydrogen evolution which have been extensively investigated.[6] Here the hydrogen evolution was also investigated by making use of photosensitization by $Ru(bpy)_3^{2+}$ adsorbed on powdered TiO_2 photocatalysts.

Experimental Section

$Ru(bpy)_3Cl_2$ was purchased from Strem Chemicals, Inc., and was purified by several recrystallizations from water. It was sometimes used without purification and no significant difference was observed in the results. Methylviologen was purchased from Sigma Chemical Co. and was used without further purification. TiO_2, SnO_2, ZrO_2, and $SrTiO_3$ powders of 99.9% or 99.99% purity were purchased from Furuuchi Chemical Corp. and were used as received or after reduction under H_2 atmosphere.

$Ru(bpy)_3Cl_2$ (≤1 mg) was dissolved in a small amount of pure water or pure methanol and the solution was mixed with a known amount of a substrate powder. The mixture

† Department of Chemistry, Faculty of Science.
‡ Institute of Molecular Science.

(1) For example: J. M. Lehn and J. P. Sauvage, *Nouv. J. Chim.*, 1, 449 (1977); J. M. Lehn, J. P. Sauvage, and R. Ziessel, *ibid.* 3, 423 (1979); M. Grätzel, *Ber. Bunsenges. Phys. Chem.* 84, 981 (1980); E. Borgarello, J. Kiwi, E. Pelizzetti, M. Visca, and M. Grätzel, *Nature (London)*, 289, 158 (1981), and references therein.

(2) B. Durham, W. J. Dressick, and T. J. Meyer, *J. Chem. Soc., Chem. Commun.*, 381 (1979).

(3) (a) R. Memming and F. Schröppel, *Chem. Phys. Lett.*, 62, 207 (1979); (b) W. D. Clark and N. Sutin, *J. Am. Chem. Soc.*, 99, 4676 (1977).

(4) H. Tsubomura, M. Matsumura, Y. Nomura, and T. Amamiya, *Nature (London)*, 261, 402 (1976); M. Matsumura, K. Mitsuda, N. Yoshizawa, and H. Tsubomura, *Bull. Chem. Soc. Jpn.*, 54, 693 (1981).

(5) C. R. Bock, T. J. Meyer, and D. G. Whitten, *J. Am. Chem. Soc.*, 96, 4710 (1975); R. C. Young, T. J. Meyer, and D. G. Whitten, *ibid.*, 98, 286 (1976); C. T. Lin, W. Böttcher, M. Chou, C. Creutz, and N. Sutin, *ibid.*, 98, 6536 (1976); J. N. Demas and J. W. Addington, *ibid.*, 98, 5800 (1976); P. Natarajan and J. F. Endicott, *J. Phys. Chem.*, 77, 1823 (1973); A. Juris, M. T. Gandorfi, M. F. Manfrin, and V. Balzani, *J. Am. Chem. Soc.*, 98, 1047 (1976).

(6) For example: (a) T. Kawai and T. Sakata, *Nature (London)*, 282, 283 (1979); T. Sakata and T. Kawai, *Nouv. J. Chim.*, 5, 279 (1981); (b) K. Kalyanasundaram, E. Borgarello, and M. Grätsel, *Helv. Chim. Acta*, 64, 362 (1981); S. Sato and J. M. White, *J. Phys. Chem.*, 85, 592 (1981), and references therein; (c) F. T. Wagner and G. Somorjai, *Nature (London)*, 285, 559 (1980); J. M. Lehn, J. P. Sauvage, and R. Ziessel, *Nouv. J. Chim.*, 4, 623 (1980); K. Domen, S. Naito, M. Soma, T. Onishi, and K. Tamaru, *J. Chem. Soc., Chem. Commun.*, 543 (1980).

0022-3654/82/2086-4516$01.25/0

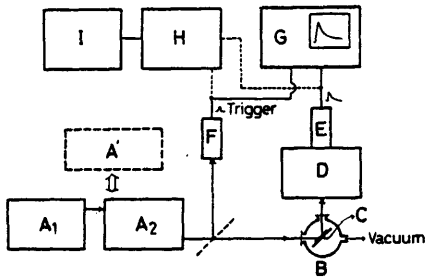

Figure 1. Schematic diagram of experimental apparatus: (A_1) N_2 laser, (A_2) dye laser, (A') YAG laser, (B) cryostat, (C) sample, (D) monochromator, (E) photomultiplier, (F) biplanar phototube, (G) oscilloscope, (H) boxcar integrator, (I) recorder.

was dried under air at room temperature or at somewhat higher temperature and then, in most cases, dried completely by dehydration under vacuum of about 10^{-3} mmHg. The dried sample was placed between two quartz plates and was mounted on the sample holder of an Oxford optical cryostat. Figure 1 shows a schematic diagram of the apparatus. A Molectron DL-II dye laser pumped by a Molectron UV-22 N_2 laser was used as the excitation source. The excitation wavelength was 450 nm throughout the experiment, and the half-width of the excitation pulse was 6 ns. The intensity was 0.5–1 mJ/pulse and the repetition rate was several tens per second.

A Hamamatsu TV R-955 or R-636 photomultiplier was used and the decay curve drawn on the CRT of a Sony-Tektronix 7104 (1 GHz) or 7904 (500 MHz) was photographed with Polaroid type 410 (ASA 10 000) film. The overall time constant of the detecting system was restricted by the rise time of the photomultiplier to 2.6 ns. A quantel YG-500 YAG laser (the second harmonics, 530 nm) and a Hamamatsu TV R-1294U (rise time 350 ps) were also used as a light source and a photomultiplier, respectively. The overall time constant of this system was several hundred picoseconds. The decay characteristics of the luminescence obtained by using this did not show any significant difference from those obtained by using the nanosecond system except for the case of the Ru(bpy)$_3$Cl$_2$/MV system which showed a fast decay component. Measurements were performed at room temperature (25 °C) and at liquid-N_2 temperature under vacuum of $\sim 10^{-3}$ mmHg. The transient phosphorescence spectra of adsorbed Ru(bpy)$_3$Cl$_2$ were also obtained by use of a boxcar detector PAR 162, or reconstructed from the decay curves at different wavelengths.

Hydrogen evolution by making use of dye sensitization was tried as follows: Powdered TiO_2 (300 mg) loaded with Ru(bpy)$_3$Cl$_2$ (Ru(bpy)$_3$Cl$_2$/TiO_2 = 1:10000 by weight, ca. 1/600 monolayer of Ru(bpy)$_3^{2+}$ on TiO_2 surface) was put into a 280-mL Pyrex glass flask. After the flask was evacuated to remove oxygen, a saturated methanol–water vapor was introduced into it. After it was irradiated from the bottom for 30 h by using a 500-W Xe lamp with a VY-44 filter (sharp cuttoff at 440 nm), the evolved hydrogen was detected by a quadrupole mass spectrometer (Anelva, AGA-360) and the quantity was determined from the pressure by using a sensitive manometer[6a] (Datametrics Inc., barocel pressure sensor, Model 1174). As a control experiment, powdered SiO_2, which has the same surface area as TiO_2, was used instead of TiO_2.

Results and Discussion

Ru(bpy)$_3$Cl$_2$ in pure water showed a single exponential decay under air at room temperature. The lifetime was about 400 ns and was similar to the value reported for a solution of 50% H_2SO_4.[7] The decay of the phosphorescence of Ru(bpy)$_3$Cl$_2$ adsorbed on the substrate powders was apparently much faster and was more complicated (see Figure 2). It could be expressed as a sum of exponential decays

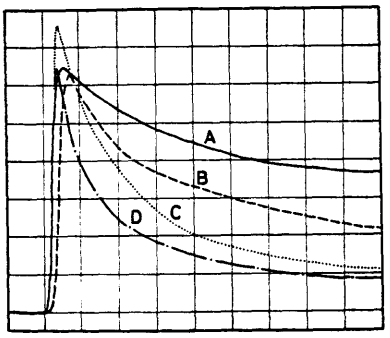

Figure 2. Phosphorescence decay curves of Ru(bpy)$_3$Cl$_2$ adsorbed on various oxide powders. Dye laser excitation, 6 ns, 450 nm. Observed at 620 nm, at 25 °C and under vacuum of 10^{-3} mmHg: (A) SiO_2, (B) ZrO_2, (C) TiO_2, (D) $SrTiO_3$.

$$I(t) = \sum_{i=1}^{N} I_i e^{-t/\tau_i} \quad (1)$$

The slowest decay component (with the largest τ_i) was determined at first, because, when t is large enough, $I(t)$ can be expressed by a single exponential decay as $I_N \exp(-t/\tau_N)$, where τ_N is the largest among the τ_i's. Then the other components were successively determined in order of the magnitude of τ_i, by substracting the already determined components from $I(t)$. This process is illustrated in Figure 3 for the case of Ru(bpy)$_3$Cl$_2$/TiO_2. The preexponential factors depended on the wavelength of the monitored light. Figure 4 shows the typical transient spectra of Ru(bpy)$_3$Cl$_2$. The luminescence seems to be composed of at least two components with different decay constants.

The origin of the photoluminescence of ruthenium(II) complexes has been assigned to three closely spaced charge-transfer levels, dπ^*(a_2);A_2, dπ^*(a_2);E, and dπ^*-(a_2);A_1, of rather singlet nature by Crosby and co-workers.[7a-c] They assumed that Boltzmann distribution between these three levels holds down to 1.6 K owing to strong spin–orbit coupling. On the basis of this assumption, they could successively analyze the temperature dependence of the lifetime and quantum yields of the photoluminescence of Ru(bpy)$_3$Cl$_2$ in poly(methyl methacrylate) film between 77 and 4.2 K and derived the following characteristics of the above-mentioned three levels. The A_1 level is energetically the lowest and both the radiative lifetime (τ_r) and the nonradiative lifetime (τ_{nr}) are very large: τ_r = 1091.5 μs and τ_{nr} = 183.1 μs. The A_2 level is energetically the highest and is located at 61.2 cm^{-1} above the A_1 level. Though thermodynamically unfavorable, this A_2 level is the most important decay channel of the excited Ru(bpy)$_3^{2+}$ both radiatively and nonradiatively due to its relatively short lifetimes; τ_r = 1.69 μs, τ_{nr} = 0.68 μs. Thus, this level contributes more than 90% of the luminescence intensity at 77 K. The degenerate E level is located at 18.8 cm^{-1} above the A_1 level and contributes about 10% of the luminescence intensity at 77 K: τ_r = 81.7 μs and τ_{nr} = 18.8 μs. Allsopp and co-workers gave evidence that the mul-

(7) (a) G. D. Hager and G. A. Crosby, *J. Am. Chem. Soc.*, 97, 7031 (1975); (b) G. D. Hager, R. J. Watts, and G. A. Crosby, *ibid.*, 97, 7037 (1975); (c) K. W. Hipps and G. A. Crosby, *ibid.*, 97, 7042 (1975); (d) D. C. Baker and G. A. Crosby, *Chem. Phys.*, 4, 428 (1974); (e) S. R. Allsopp, A. Cox, T. J. Kemp, and W. J. Reed, *J. Chem. Soc., Faraday Trans. 1*, 74, 1275 (1978); (f) J. Van Houten and R. J. Watts, *J. Am. Chem. Soc.*, 98, 4853 (1976); (g) F. E. Lytle and D. M. Hercules, *ibid.*, 91, 253 (1969).

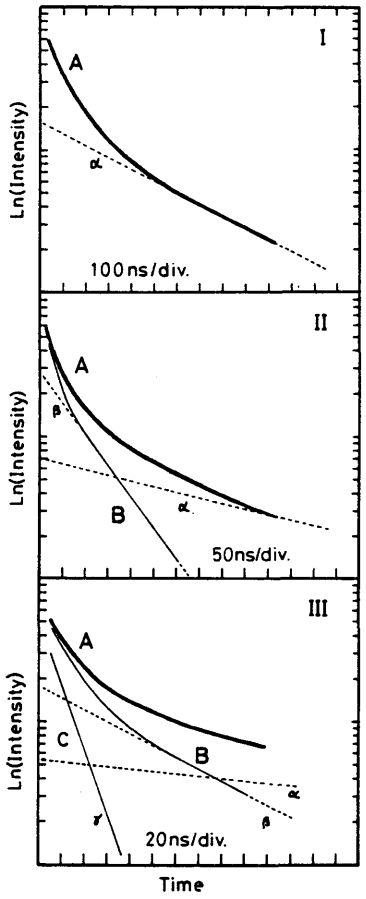

Figure 3. Typical decay curves and decomposition to components. Luminescence decay of $Ru(bpy)_3Cl_2$ on TiO_2 powder observed at 620 nm at liquid-N_2 temperature. See Table I. A: Observed decay curves with different time scales, which are decomposed as described in the text in the order I, II, and III. α 530-ns lifetime component. β = 100-ns lifetime comonent. γ = 20-ns lifetime component If we express the intensity of A by A and so on, $B = A - \alpha$ and $C = B - \beta = \gamma$. Absolute intensities are not the same for I, II, and III, and B, C, α, β, and γ are normalized relative to A.

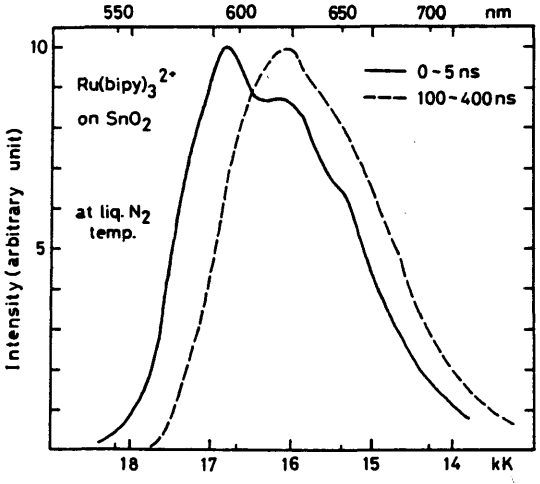

Figure 4. Transient spectra of $Ru(bpy)_3Cl_2$ on SnO_2 detected by boxcar integrator. Light source: pulsed dye laser, 6 ns, 450 nm. Time window of boxcar integrator: (—) 0–5 ns from the instant that the short-wavelength region of the spectra began to decrease; (- - -) 100–400 ns after the excitation pulse. Each spectrum has been normalized to its maximum for comparison of the spectrum shape. The spectra are not corrected for sensitivity of the detecting system.

tiple-state model described above holds also in H_2O, D_2O, and other solvents at temperatures above 77 K.[7e] They showed that the location of the A_2 level relative to the A_1 level (E_2 of ref 7e) is slightly dependent on the solvent. For example, it was 2.64 kJ/mol (221 cm^{-1}) in H_2O in the temperature region from 273 to 373 K, 1.90 kJ/mol (159 cm^{-1}) in 9 M LiCl–H_2O in the temperature region from 178 to 373 K, and 0.63 kJ/mol (52.7 cm^{-1}) in the temperature region from 77 K to the glass transition temperature (143 K). Unfortunately, the data reported by Allsopp et al. are insufficient to determine the relative contributions of three levels to the intensity of luminescence at temperatures above 77 K. However, if we assume that the decay rates reported by Crosby et al. are not significantly dependent on solvent, the contribution of the A_2 level is calculated to be not less than 91% at temperatures between 77 and 373 K. Crosby and co-workers have also reported that the temperature dependence of the luminescence band contours is not significant under 77 K and that vibrational structures of the luminescence spectra originating from these three levels must be similar except for a slight difference in relative intensities of vibrational bands. This observation can be reasonably explained by postulating that the vibrational structure of the luminescence is, according to the Franck–Condon principle, governed by the change of vibrational states of the ligand molecules induced by charge-transfer excitation, which should be similar for the three levels. When the temperature is raised from 77 K to room temperature, the luminescence spectrum broadens and red shifts.[7f,g] The previously stated studies have shown that the A_2 level is the predominant emitting state at temperatures above 77 K, which precludes the possibility of ascribing the temperature dependence of the spectrum above 77 K to alteration of the emitting level. Thus, it seems reasonable to say that this temperature change is caused by the change in the vibrational modes of ligands and consequently to the change of Franck–Condon factors.

All the time-resolved spectra observed in the present study and shown in Figures 4 and 5 fall in the same region as the low-temperature spectra and room-temperature spectra of $Ru(bpy)_3^{2+}$ reported by Van Houten and Watts[7f] and other authors.[7g] The band contours observed in this study are also similar to those reported by these authors. Thus, we think it is reasonable to conclude that the origins of the time-resolved spectra are all the same, that is, a mixture of more than 90% A_2 level and less than 10% E level, and that differences in the band contour are due to differences in circumstances around the ligands. The spectral components that decay rapidly are located in the relatively short wavelength region and their band contours resemble more or less the spectrum of $Ru(bpy)_3^{2+}$ in a low-temperature solution. On the basis of the aforementioned discussion on the band contour we tentatively assign these components to molecules which are rather firmly attached to the surface of the substrate where the molecular motions of ligands are somewhat hindered. Hereafter we will call the corresponding spectrum the F spectrum (the spectrum of firmly attached species). Similarly, the time-resolved components with long lifetimes can be ascribed to more or less loosely held molecules. We will call the corresponding spectrum the L spectrum (the spectrum of loosely attached species). The F spectrum is blue shifted compared with the L spectrum as seen in Figure 5. The firmly attached $Ru(bpy)_3^{2+}$ would be stabilized near the ionic atmosphere of the oxide or methylviologen chloride surface. The stabilization would be larger in the ground state than in the excited state, because the adsorbed molecule in the ground state locates the position of minimum energy on the surface. That must be the reason for the blue shift of the F spectrum. The above interpretations agree with the proposal that the

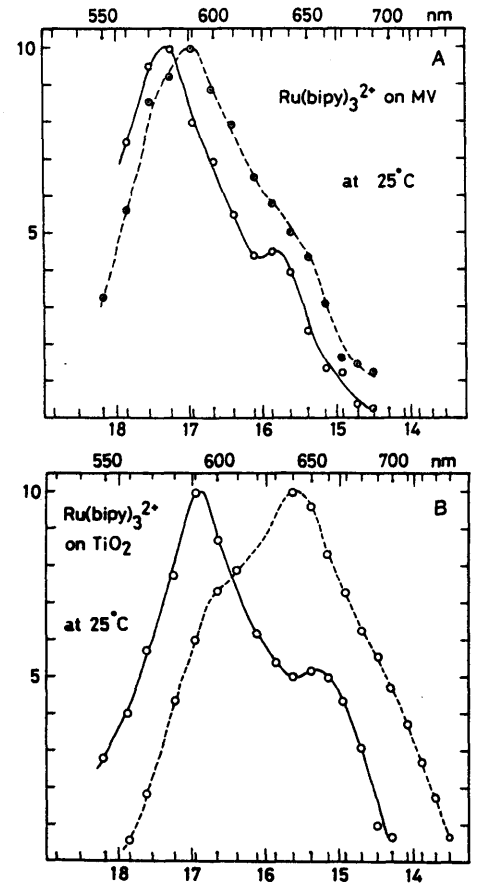

Figure 5. Normalized spectra of respective phosphorescence decay components of $Ru(bpy)_3Cl_2$. The spectra have been constructed from decay data at various wavelengths. They are not corrected for wavelength dependence of sensitivity of the detecting system. (A) $Ru(bpy)_3Cl_2$ (1/1000 w/w) on methylviologen: (—) component of 3.3-ns lifetime; (- - -) component of 13-ns lifetime. (B) $Ru(bpy)_3Cl_2$ (1/1000 w/w) on TiO_2: (—) component of 18-ns lifetime; (— — —) component of 64- and 280-ns lifetime.

relaxation channel responsible for the fast decay is the electron-transfer process from the excited $Ru(bpy)_3Cl_2$ to the substrate, because the probability of this process should depend on the overlap of the wave functions of the donor and the acceptor, which is strongly dependent on the distance between the two. A heavy-atom effect must not be important because Ru itself is a heavy atom.[7c] The decay characteristics are summarized in Table I.

It may seem an attractive conjecture as an alternative interpretation of the different time-resolved spectra that diffeent lifetimes are due to differences in the electron-transfer rate from each level of the multiplet (A_2, E, and A_1) and that the different emitting level gives the different spectrum. However, this interpretation seems to contradict Crosby and co-worker's observation that the thermal equilibration process between the three levels is rather rapid due to strong spin–orbit coupling.[7a-c] If any one of the three levels has a very large electron-transfer rate, it must greatly shorten lifetimes of other levels through the rapid thermal equilibration process. The wide range of observed lifetimes indicates that the conjecture stated above does not apply to the present case.

Van Houten and Watts[7f] and Allsopp et al.[7e] have shown that a certain set of levels which is located about 3600–4000 cm^{-1} above the emitting multiplet works as a significant decay channel at temperatures above 173 K. This set of levels was originally proposed by Van Houten and Watts[7f] as being of d–d parentage to explain the temperature dependence of luminescence lifetime and quantum yield

TABLE I: Lifetime of Decay Component and Relative Weight

sub-strate	concn, w/w	temp	lifetime (rel wt),[d] ns
MV[a]	1/1000	room temp	3.3 (0.81), 13 (0.19)
		liq-N_2 temp	3.1 (0.81), 14 (0.17), 130 (0.02)
TiO_2	1/10000	room temp	18 (0.52), 64 (0.32), 280 (0.16)
		liq-N_2 temp	21 (0.64), 100 (0.28), 530 (0.07)
SnO_2	1/10000	room temp	14 (0.63), 65 (0.30), 260 (0.07)
		liq-N_2 temp	15 (0.59), 140 (0.31), 1000 (0.10)
$SrTiO_3$	1/10000	room temp	12 (0.58), 40 (0.22), 130 (0.13), 500 (0.06)
		liq-N_2 temp	12 (0.50), 60 (0.26), 280 (0.17), 1200 (0.07)
ZrO_2	1/10000	room temp	17 (0.35), 130 (0.38), 530 (0.27)
		liq-N_2 temp	20 (0.25), 240 (0.29), 810 (0.45)
SiO_2	1/10000	room temp	50 (0.33), 420 (0.36), 1200 (0.31)
		liq-N_2 temp	50 (0.25), 1300 (0.26), 3500 (0.60)
in ethanol-methanol (5:1) soln[b]		290 K	0.89 μs
		80 K	4.0 μs
in 50% H_2SO_4[b]		290 K	0.70 μs
		80 K	2.7 μs
in ethanol-methanol (4:1) soln[c]		77 K	5.12–5.37 μs

[a] YAG laser (25 ps, 530 nm) was also used as an exciting light source (see text). [b] Reported by Lytle and Hercules (ref 7g). [c] Reported by Demas and Crosby (ref 14). [d] The precision of the obtained values has not been statistically determined but the rough estimate is ±10% for lifetime and ±5% for relative weight.

between 0 and 100 °C. They reported that it is important for photochemical reaction involving ligand displacement. Apparently, it cannot be a candidate for the origin of our spectra, because not only is the position of the level too high but also it is not luminescent.

Methylviologen. On the surface of microcrystalline powder of methylviologen chloride, $Ru(bpy)_3Cl_2$ showed a fast decay, which is composed of two components with about 3-ns and about 13-ns lifetimes. The decay curve of the former component was unambiguously observed by using the picosecond system. Figure 5A shows the spectra corresponding to the two components. They both belong to the F spectrum. No significant difference was observed between the decay curves at room temperature and at liquid N_2 temperature, except that a small amount (2%) of a slowly decaying component was observed at liquid-N_2 temperature. It may be conjectured that the molecules which give the long-lifetime component at liquid-N_2 temperature have some freedom of movement at room temperature and can take a position where fast electron transfer is possible.

TiO_2 and Other Oxide Semiconductors. On the TiO_2 powder (99.9%, anatase, the surface area of ca. 50 m^2/g, Nippon Aerosil Co.), the decay has three components and the lifetimes of these components are 16, 60, and 280 ns at room temperature and 21, 100, and 520 ns at liquid-N_2 temperature. The fastest decay component is dominant and shows the F spectrum, and the slowest decay component shows the L spectrum. The intermediate decay component seems to belong to the L spectrum, and Figure 5B shows the F and L spectra constructed from the decay curve data at various wavelengths. The relative magnitude of the preexponential factors of the fast, intermediate, and

slow decay components is not significantly dependent on temperature. This naturally leads to the conclusion that each decay component originates from different kinds of sites and the electron-transfer rate from the excited $Ru(bpy)_3Cl_2$ molecule at the respective sites should be one of the important factors that determine the lifetime, especially in the case of the F spectrum. It is probable that thermal reorientational motion of the loosely attached molecules enhances the electron transfer, which may be partly responsible for the rather large temperature dependence of the lifetime of the long-lifetime component.

We performed some experiments on samples loaded with different amounts (1/1000 w/w and 1/100000 w/w) of $Ru(bpy)_3Cl_2$. Contrary to our expectation, these experiments could not give any significant information. When the quantity of $Ru(bpy)_3Cl_2$ was 1/1000 w/w, inspection by sight apparently showed that uniform mixing was not attained, and resultant aggregation of $Ru(bpy)_3Cl_2$ molecules obstructed rational analysis of observed decay curves. A further discussion will be given later on the luminescence decay curve of crystalline powder of $Ru(bpy)_3Cl_2$. On the other hand, when the quantity of $Ru(bpy)_3Cl_2$ was 1/100000 w/w or less, the luminescence intensity was so small that the signal-to-noise ratio of our present apparatus was not sufficient for acquisition of data that can be used for reliable analysis. A rough estimate showed that relative weights of time-resolved components for different concentrations of $Ru(bpy)_3Cl_2$ on TiO_2 were not significantly different from those in Table I. This did not seem to support our expectation that the relative weight of firmly attached species might be larger at lower concentrations of $Ru(bpy)_3Cl_2$. However, we think this result is not fatal to the F- and L-spectrum interpretation, because the ratio of molecules of various kinds of absorption states might be mainly governed by the ratio of different adsorption sites on the surface of the oxide rather than the concentration of $Ru(bpy)_3Cl_2$ at these low concentrations, considering that 1/100000 w/w $Ru(bpy)_3Cl_2$ on the surface of TiO_2 whose surface area is 50 m^2/g corresponds to a mean surface area per $Ru(bpy)_3^{2+}$ molecule of 5×10^4 Å^2 which is much larger than the value for monolayer adsorption (1/600 monolayer).

On SnO_2, $SrTiO_3$, and ZrO_2 surfaces, similar results were obtained, and the lifetime of the fastest decay component was similar to the value for TiO_2. However, in the case of ZrO_2, the weight of the decay component with long lifetime is larger than those for other oxide semiconductors.

SiO_2. On SiO_2 (99.99%, the surface area of ca. 50 m^2/g, Nippon Aerosil Co.), the components with long lifetimes, 420 and 1200 ns at room temperature and 1300 and 3500 ns at liquid-N_2 temperature, are dominant. These values are similar to the values in alcoholic solution or in its rigid glass solution.[7] It is noticeable that there is a component with a very long lifetime up to 1200 ns at room temperature. It is longer than those in the solutions as shown in Table I. It seems to indicate a smaller radiationless process due to the inhibited movement of ligands on the surface. Figure 6 shows the energy levels of the conduction and valence bands for the oxides in solution at pH 7, together with the redox potentials of methylviologen and $Ru(bpy)_3^{2+}$.[8-10] Since our experiments were carried out in the gas phase (10^{-3} mmHg), not in the aqueous medium,

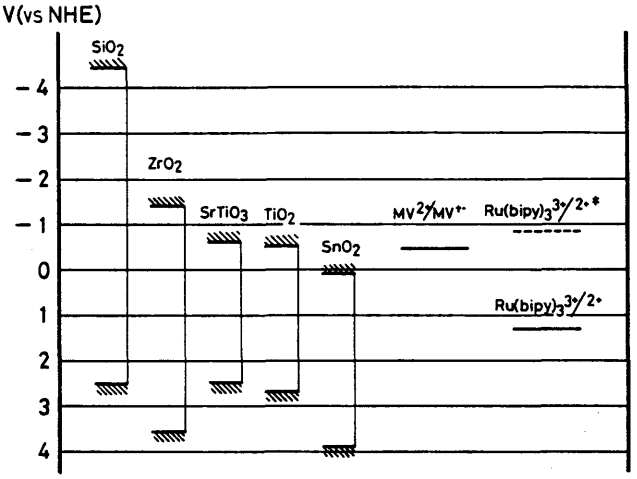

Figure 6. Band energies of oxides at ph 7 and redox potentials of methylviologen and $Ru(bpy)_3Cl_2$: (—) redox potential for ground state; (- - -) redox potential for excited state. See text and ref 8–11.

the energy levels in the gas phase should be used. Moreover, for the redox potential of $Ru(bpy)_3^{2+}$, the value at the oxide surface and also in the gas phase is necessary for a rigorous discussion. But those data are not available at present. Thus, the energy diagram described in Figure 6 should be understood as a rough measure for the present discussion. The position of the conduction band of SiO_2 is estimated by using Scaife's equation[11] and a band gap of 6.9 eV. From this figure the electron transfer from the excited $Ru(bpy)_3^{2+}$ to the conduction band is conjectured to be possible for SnO_2, TiO_2, and $SrTiO_3$. This is supported by the large weight of the fast decay components as seen in Table I. Clark and Sutin[3b] estimated the reorganization parameter λ, the energy required to change the environment of the reduced form to that which exists around the oxidized form at equilibrium for the $Ru(bpy)_3^{3+}/Ru(bpy)_3^{2+*}$ couple in water, to be about 0.25 eV. In the present case of $Ru(bpy)_3^{2+}$ on the surface of oxide powder under vacuum, the value of λ must be much smaller, since polar molecules of solvent do not exist around $Ru(bpy)_3^{2+}$. The small value of λ favors the electron transfer from excited $Ru(bpy)_3^{2+}$ to oxides.

On the other hand, for SiO_2, the decay characteristics are quite different from those for the other oxides: The dominant decay components have very long lifetimes. In the case of ZrO_2, the decay characteristics look intermediate between those of SiO_2 and those of the other three oxides, i.e., SnO_2, TiO_2, and $SrTiO_3$, as seen in Figure 2 and Table I. The weight of the decay component with a short lifetime (17 ns at room temperature) is smaller than those for other oxide semiconductors. This is expected from the fact that the conduction band of ZrO_2 is located, in the aqueous medium, higher than those of $SrTiO_3$, TiO_2, and SnO_2 as shown in Figure 6. In this case, the existence of a considerable amount of a fast decay component (17–20-ns lifetime) as shown in Table I might be explained by assuming that the relative positions of the energy bands of the oxides and the energy levels of $Ru(bpy)_3^{2+}$ are different from those in solution at pH 7. Another explanation would be possible by assuming surface states which interact with the excited $Ru(bpy)_3^{2+}$ through the electron- or energy-transfer processes and reduce its lifetime.

The component with 50 ns in the case of SiO_2 is also controversial, because the electron transfer from the excited $Ru(bpy)_3^{2+}$ to the conduction band is quite difficult as shown in Figure 6. One possible explanation would be

(8) K. Honda, A. Fujishima, and T. Inoue in "Hydrogen Energy Progress", T. N. Veziroglu, K. Fueki, and T. Ohta, Eds., Proceedings of the 3rd World Hydrogen Energy Conference, Tokyo, Japan, Pergamon, Oxford, 1980, pp 753–63.

(9) L. Michaelis and E. S. Hill, *J. Gen. Physiol.*, **16**, 859 (1933).

(10) C. T. Lin, W. Böttchen, M. Chon, C. Creutz, and N. Sutin, *J. Am. Chem. Soc.*, **98**, 6536 (1976).

(11) D. E. Scaife, *Sol. Energy*, **25**, 41 (1980).

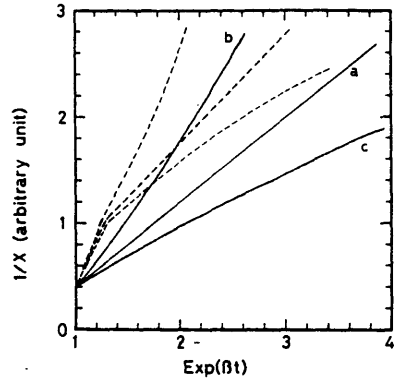

Figure 7. Phosphorescence decay characteristics of $Ru(bpy)_3Cl_2$ crystalline powder compared to general second-order decay curve. (—) The decay that obeys eq 2: (a) $\beta = \beta_0$, (b) $\beta < \beta_0$, (c) $\beta > \beta_0$ where β_0 is the appropriate value of β. (– – –) observed decay for crystalline powder of $Ru(bpy)_3Cl_2$, monitored at 620 nm at liquid-N_2 temperature, excited by a dye laser. Three lines correspond to relatively large, medium, and small values of β, respectively. Similar decay characteristics were also observed at room temperature.

the surface states interacting with $Ru(bpy)_3^{2+*}$ similar to the case of ZrO_2. On the other hand, the following decay channels would not be neglected, if aggregates of $Ru(bpy)_3Cl_2$ are formed on the surface of SiO_2:

$$2Ru(bpy)_3^{2+*} \rightarrow Ru(bpy)_3^{+*} + Ru(bpy)_3^{3+} \quad (2)$$

$$Ru(Bpy)_3^{2+*} + Ru(bpy)_3^{2+} \rightarrow Ru(bpy)_3^{+} + Ru(bpy)_3^{3+} \quad (3)$$

Indeed, crystalline powder of $Ru(bpy)_3Cl_2$ gave a decay curve which was a superposition of several decays just as those for $Ru(bpy)_3Cl_2$ on SnO_2, TiO_2, and $SrTiO_3$, and the lifetime of the fastest component reached sometimes as low as about 20 ns. However, the decay curve showed more complicated characteristics, that is, large temperature dependence in the preexponential factors, than the case of oxide semiconductors. The preexponential factors were also significantly affected by sample conditions that could not be controlled. If we assume rapid random movement of excitation and spatially uniform energy transformations in the crystal, processes 2 and 3 and ordinary first-order radiative and nonradiative processes will give a rate equation like

$$dx/dt = -\alpha x^2 - \beta x \quad (4)$$

where α is the rate constant for process 2 and β is the sum of rate constants for other processes. By integrating eq 4, we obtain

$$1/x = (\alpha/\beta + 1/x_0)e^{\beta t} - \alpha/\beta \quad (5)$$

where x_0 is the initial ($t = 0$) value of x. The three solid lines in Figure 7 exhibits the observed $1/x$ vs. $\exp(\beta t)$ curves that are expected when eq 5 holds, depending on whether the chosen value of β is appropriate, large or small. The observed decay curve is shown by dashed lines for various values of β and it is obvious that eq 5 is not a good approximation. The initial fast decay cannot be reconciled with the posterior slow decay by eq 5. Thus, we have to assume some nonuniform processes in the crystal. It may involve a few kinds of special sites where the molecules are arranged in configurations that are, in various degrees, favorable for charge separation by processes like reactions 2 and 3. The diffusion velocity of molecular excitation must be sufficiently slow and the charge separation may occur rapidly in the vicinity of these sites in comparison with other regular sites. These special sites may involve impurities, defects, and surfce traps, which are not easily controlled and are well-known as the important factors that affect the photoelectric process of solids. accordingly, the present data for crystals can only suggest that processes 2 and 3 are quite probable, though the latter might be unfavorable with regard to free energy change. Further details are beyond the scope of the present work. Anyway, the aggregate formation seems to be a factor that decreases the lifetime of $Ru(bpy)_3^{2+*}$ on SiO_2, and possibly on ZrO_2. The spectrum of the 50-ns component seemed to be F type, but we could not perform the unambiguous decomposition because the weight of this component was relatively small.

TABLE II: Sensitization Effect on Hydrogen Production from Saturated Methanol-Water Vapor by $Ru(bpy)_3Cl_2$ [a]

photocatalyst	quantity of H_2,[b] μmol
TiO_2	2.1
TiO_2-$Ru(bpy)_3Cl_2$ (0.01% w/w)	26
SiO_2-$Ru(bpy)_3Cl_2$ (0.01% w/w)	0

[a] Light source: 500-W Xe lamp with VY-44 filter (sharp cutoff at 440 nm). [b] 30-h irradiation.

The electron-transfer rate from $Ru(bpy)_3^{2+*}$ to SnO_2, TiO_2, $SrTiO_3$, and possibly ZrO_2 is deduced to be about 5×10^7 s^{-1} (=1/20 ns) from the results and discussion so far described. Although this value is not large compared to those for other systems, e.g., for rhodamine B/anthracene, 2.9×10^{10} s^{-1},[12] and for zinc porphyrin/SnO_2, 7.5×10^9 s^{-1},[13] it is sufficient for effective electron transfer, because the rates for the other deactivation channels are small, if the mutual charge-separation processes 2 and 3 are not important. The photoinduced electron transfer from a sensitizing molecule to a semiconductor can be confirmed easily by measuring a photocurrent of the semiconductor electrode immersed in an electrolyte solution of a sensitized dye.[4] However, such a measurement is impossible for a powdered semiconductor in a gaseous medium. So, we tried the hydrogen evolution due to the dye sensitization effect in order to demonstrate the electron transfer from $Ru(bpy)_3^{2+*}$ to TiO_2. Table II shows the results. It indicates clearly the sensitization effect on the hydrogen evolution, although the efficiency is not good. Since the hydrogen evolution rate of 1 μmol/10 h corresponds to 5.3 μA of photocurrent, the evolution rate, 26 μmol/30 h, for TiO_2–$Ru(bpy)_3^{2+}$ in this table corresponds to the photocurrent of 46 μA. The efficiency is rather low contrary to our expectation.

One important reason of this low efficiency seems to be that $Ru(bpy)_3Cl_2$ molecules are not closely attached to the surface of the semiconductor powder under the conditions of the present photocatalytic reactions. The concentration of 1/10000 w/w $Ru(bpy)_3Cl_2$ on TiO_2 is much less than that of monolayer adsorption (~1/600 monolayer) as was previously mentioned. Yet, the preexponential factor of the fastest component for this case is only about 60% as is given in Table I. This implies that TiO_2 is not a good adsorbent of $Ru(bpy)_3Cl_2$. This has been suggested by the observation that fast decay components with less than 100-ns lifetimes decreased extremely when the $Ru(bpy)_3Cl_2/TiO_2$ sample was only slightly wetted by water.

Another reason for the low efficiency may be the recombination of the electrons injected into the conduction band of the semiconductor with the oxidized dyes. This process is considered to be important because of the fol-

(12) N. Nakashima, K. Yoshihara, and F. Willig, *J. Chem. Phys.*, 73, 3553 (1980).
(13) K. Tanimura, T. Kawai, and T. Sakata, *J. Phys. Chem.*, 83, 2641 (1979).
(14) J. N. Demas and G. A. Crosby, *J. Mol. Spectrosc.*, 26, 72 (1968).

lowing characteristics which are common for simple sensitization processes. As shown in Figure 6, the redox potential of $Ru(bpy)_3^{3+}/Ru(bpy)_3^{2+}$ is located higher than the valence band of TiO_2. It means that the oxidation power of $Ru(bpy)_3^{3+}$ is weaker than that of the holes in the valence band of TiO_2. Thus, oxidation of methanol–water by visible irradiation of $Ru(bpy)_3^{2+}/TiO_2$ may be more difficult than the oxidation by direct excitation of TiO_2. This increases the probability of the recombination process. Furthermore, the band bending of TiO_2 is considered to be small under conditions of hydrogen evolution, and this is also unfavorable for charge separation of injected electrons.

Conclusion

We have obtained time-resolved luminescence spectra of $Ru(bpy)_3^{2+}$ which have characteristic features depending on the interaction on the surfaces. Although the decay characteristics are not so simple as we had expected, the origin of more than two decay components of different lifetimes would be mainly assigned to different electron-transfer rates depending on the relative position of $Ru(bpy)_3^{2+}$ on the solid surface. The concentration quenching and the electron and energy transfer to the surface states seem also to contribute to the deactivation process of $Ru(bpy)_3^{2+*}$, though further work is necessary to prove and clarify the details of these mechanisms. Anyway, the electron transfer to the conduction band must be the main deactivation channel for $Ru(bpy)_3^{2+}$ giving the fast decay component with less than 21-ns lifetime, for the following reasons: (i) There is a good correlation between the relative weight of the faster decay component and the energy of the conduction band edge of the substrate semiconductor relative to the redox level of $Ru(bpy)_3^{3+}/Ru(bpy)_3^{2+*}$. (ii) The spectrum of the fastest decay component can be assigned to $Ru(bpy)_3^{2+}$ molecules firmly attached to the surface of semiconductors. (iii) A photosensitization effect on hydrogen evolution has been observed for the $Ru(bpy)_3^{2+}/TiO_2$ system.

Thus, the present study confirms that $Ru(bpy)_3Cl_2$ has a considerable potential ability for sensitization of oxide semiconductors. However, close contact between the sensitizer and the semiconductor surface must be realized and the recombination of injected electrons with the oxidized sensitizer must be somehow prevented to achieve a high overall efficiency for sensitization.

Acknowledgment. We thank Professor T. Ito and Mr. F. Ueno, who kindly provided purified $Ru(bpy)_3Cl_2$, and Professor K. Yoshihara, Dr. N. Nakashima, and Dr. M. Sumitani at the Institute for Molecular Science for valuable advice regarding the lifetime measurements. This work supported by the Joint Studies Programme (1979–1981) of the Institute for Molecular Science.

REPRINTED FROM

CHEMISTRY LETTERS

The Chemical Society of Japan

1983

CHEMISTRY LETTERS, pp. 709-712, 1983.

EFFICIENT HYDROGEN PRODUCTION FROM WATER BY VISIBLE LIGHT EXCITATION OF FLUORESCEIN-TYPE DYES IN THE PRESENCE OF A REDOX CATALYST AND A REDUCING AGENT

Kazuhito HASHIMOTO, Tomoji KAWAI, and Tadayoshi SAKATA*
Institute for Molecular Science, Myodaiji, Okazaki 444

A hydrogen production system for visible light without an electron relay, efficient in the high pH region, is constructed with some fluorescein derivatives in the presence of a redox catalyst and a sacrificial reducing agent.

For H_2 production from water with visible light, only a limited number of dyes such as $Ru(bipy)_3^{2+}$ and water soluble zinc porphyrins have been used as efficient photocatalysts.[1] It is well studied that fluorescein and its halogenated derivatives are photo-reduced in the presence of a reducing agent, forming very stable semi-reduced radicals in high pH region.[2-8] Here, we report that these dyes also serve as efficient photocatalysts in the presence of triethanolamine(TEOA) as a reducing agent by making use of a high reducing power of the semi-reduced radicals, i.e., these radicals can reduce water to produce H_2 with the aid of platinum catalyst. The absorption peaks of these dyes in the visible region are situated at around 500 nm.

As the redox catalyst, platinized TiO_2 powder or colloidal Pt was used. Pt was deposited photochemically on the surface of TiO_2 powder (4 wt%, Aerosil P-25, average grain size 300 Å),[9] and the colloidal Pt catalyst was stabilized with polyvinyl-pyrrolidone(PVP).[10] H_2 was detected by a mass spectrometer and a manometer, as described previously.[11] When an aqueous solution of each dye (5×10^{-3}M, 10 ml, pH= 12.5 adjusted with NaOH) in the presence of Pt/TiO_2 (0.3 g) and TEOA (5×10^{-1}-10^{-2}M) was irradiated with visible light from a 500 W Xe lamp filtered with a 460 nm cutoff glass filter, the H_2 gas produced was observed as streams of bubbles in a 280 ml Pyrex glass bulb. In Table 1 are shown the initial rates of H_2 production in these systems. When D_2O was used instead of H_2O, D_2 was 79% of the produced H_2 gas, DH 19% and H_2 2%. This result suggests that H_2 is produced from water.

These systems are so-called two-component systems, i.e., electron relay free systems.[12,13,14] The most efficient system was obtained with dibromofluorescein and

the H_2 production rate was 7.1 ml/h with the visible light. In a recent study,[15] we determined the quantum efficiency of H_2 production in $Ru(bipy)_3^{2+}$-Pt/TiO_2 system to be 1.7×10^{-3}. This corresponded to a rate of H_2 production of 0.10 ml/h under the visible light illumination. The spectral profile of the present system is similar to that of $Ru(bipy)_3^{2+}$ system, so that from the rate of the production of 7.1 ml/h, we can infer a quantum efficiency of about 0.1. This value is almost equal to that of one of the most efficient three-component systems, $Ru(bipy)_3^{2+}$-methylviologen(MV^{2+})-collodial Pt in the presence of ethylene-diamine-tetra-acetic acid (EDTA), 0.13.[16]

Table 1. Initial Rates of H_2 Production

Dye	Initial rate of H_2 production (ml/h)
(a) fluorescein	0.5
(b) gallein	0.0
(c) dichlorofluorescein	1.2
(d) dichlorofluorescein diacetate	1.4
(e) dibromofluorescein	7.1
(f) mercurochrome	2.3

dye (5×10^{-3}M), Pt/TiO_2 (0.3g), TEOA (10^{-1}M), pH=12.5, visible light (λ>460nm) from a 500 W Xe lamp.

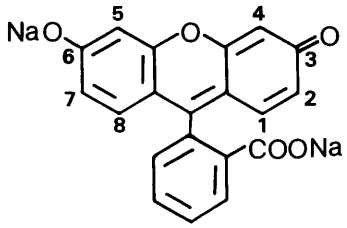

(a) fluorescein Na salt
(b) 4,5 : OH
(c) 2,7 : Cl
(d) 2,7 : Cl, 3,6 : $OCOCH_3$
(e) 4,5 : Br
(f) 2,7 : Br, 5 : HgOH

Although the system with Pt/TiO_2 was efficient and the results reproducible, collodial Pt also served as the reducing catalyst. Consequently, these two-component systems are quite different from those based on the dye sensitization of a semiconductor. For instance, in the system $Ru(bipy)_3^{2+}$-Pt/TiO_2 and EDTA, the existence of TiO_2 is indispensable for H_2 production.[15] Moreover, the H_2 production rates increase with heavier halogen substitution, indicating a heavy atom effect on the intersystem crossing. It is known that these fluorescein-type dyes in alkaline aqueous solution are photo-reduced in the presence of a reducing agent via the lowest triplet states and form very stable semi-reduced dyes.[2-8] By taking these facts into account, we assume the following reaction scheme for this H_2 production reaction

$$\text{Dye} \xrightarrow{h\nu} {}^1\text{Dye}^* \quad \text{(excitation)} \qquad (1)$$

$$ {}^1\text{Dye}^* \longrightarrow {}^3\text{Dye}^* \quad \text{(intersystem crossing)} \qquad (2)$$

$$^3Dye^* + Red \longrightarrow Dye^{\cdot-} + Red^{\cdot+} \quad \text{(formation of semi-reduced dye)} \quad (3)$$

$$Red^{\cdot+} \longrightarrow \text{decomposition} \quad (4)$$

$$Dye^{\cdot-} + H_2O \xrightarrow{Pt} Dye + 1/2\ H_2 + OH^- \ (H_2 \text{ production}) \quad (5)$$

This reaction is analogous to that of other two-component systems without an electron relay such as $Ru(bipy)_3^{2+}$-PtO_2,[12] proflavine-Pt/PVA[13] and chromium(III) complexes-Pt/PVA[14] in the presence of triethylamine, EDTA or TEOA, and EDTA, respectively. However, H_2 production for dibromofluorescein is more efficient than it is in other relatively stable two-component systems. For instance, the rate for dibromofluorescein is several times larger than that for proflavine. The quantum efficiency for the chromium complexes is almost the same as for dibromofluorescein, but the turn-over number of chromium complexes is very small, about 4.[14] Another characteristics of this system is the fact that the reaction is efficient in the high pH region, since the semi-reduced dyes are stable in alkaline solution. A comparison of this system with others is summarized in Table 2. However, the reaction rate decreases gradually over long time irradiation. The turn-over number of dibromofluorescein obtained at present is about 100, but this value might be improved with a choice of better conditions.[17]

Table 2. Comparison of the Characteristics of H_2 Production Systems.

Dye	Absorption peak (nm)	Electron relay	Redox catalyst	H_2 production[(a)] rate (ml/h)	pH	Reducing agent
dibromo-fluorescein	508	——	Pt-PVP	7.1	12.5	TEOA
proflavine [(b)]	445	——	Pt-PVP	2.4	7.0	TEOA
$Ru(bipy)_3^{2+}$ (c)	452	MV^{2+}	Pt-PVP	2.9[18]	5.0	EDTA
$Ru(bipy)_3^{2+}$ (d)	452	——	Pt-TiO_2	0.1	5.0	EDTA

(a) Visible light from a 500 W Xe lamp filtered with a 460 nm cutoff filter for the dibromofluorescein system, a 390 nm filter for the proflavine system and a 440 nm filter for the $Ru(bipy)_3^{2+}$ systems, respectively. (b), (c) The experimental conditions were chosen as same as those of reference 13) and 16), respectively. (d) Dye sensitized Pt/TiO_2 system.[15]

By making use of a high reducing power of the semi-reduced dye, we constructed a relatively efficient photogalvanic cell <semiconductor or Pt (light)|dibromofluorescein, TEOA|Pt (dark)> in which the open voltage was about 800 mV and the short circuit current was about 40 $\mu A/cm^2$.[17]

Because of the long-lived nature of the semi-reduced intermediate species, these dyes play the role of both photocatalysts and electron relays in three-component systems. It is well known that stable semi-reduced dyes can also be formed in the presence of ethanol, 2-propanol or phenol,[4,6] so that these organic compounds might be albe to serve as reducing agents for H_2 production. In fact, we have produced H_2 in the presence of ethanol instead of TEOA, although the production rate was small (0.11 ml/h).[17]

We thank Dr. Desmond O'Connor for careful reading of the manuscript.

References

1) For example, (a) M. Grätzel, Acc. Chem. Res., 14, 376 (1981). (b) A. Harriman, G. Porter, and M.-C. Richoux, J. Chem. Soc., Faraday Trans.2, 77, 833 (1981).
2) A.H. Adelman and G. Oster, J. Am. Chem. Soc., 78, 3977 (1956).
3) M. Imamura and M. Koizumi, Bull. Chem. Soc. Jpn., 29, 913 (1956).
4) M. Imamura, Bull. Chem. Soc. Jpn., 31, 962 (1958).
5) G. Oster, G.K. Oster, and G. Karg, J. Phys. Chem., 66, 2514 (1962).
6) E.F. Zwicker and L.I. Grossweiser, J. Phys. Chem., 67, 549 (1963).
7) Y. Momose, K. Uchida, and M. Koizumi, Bull. Chem. Soc. Jpn., 38, 1601 (1965).
8) K. Kimura, T. Miwa, and M. Imamura, Bull. Chem. Soc. Jpn., 43, 1337 (1970).
9) B. Kraeutler and A.J. Bard, J. Am. Chem. Soc., 100, 2239 (1978).
10) H. Hirai, Y. Nakao, and N. Toshima, J. Macromol. Sci. Chem., A13, 727 (1979).
11) T. Kawai and T. Sakata, J. Chem. Soc., Chem. Commun., 1979, 1047.
12) P.J. Delaive, B.P. Sullivan, T.J. Meyer, and D.A. Whitten, J. Am. Chem. Soc., 401, 4007 (1979).
13) K. Kalyanasundaram and M. Grätzel, J. Chem. Soc., Chem. Commun., 1979, 1137.
14) R. Ballardini, A. Juris, G. Varani, and V. Balzani, Nouv. J. Chem., 4, 563 (1980).
15) K. Hashimoto, T. Kawai, and T. Sakata, Nouv. J. Chem., in press.
16) J. Kiwi and M. Grätzel, (a) J. Am. Chem. Soc., 101, 7214 (1979). (b) Nature, 281, 657 (1979).
17) K. Hashimoto, T. Kawai, and T. Sakata, to be published.
18) The hydrogen production efficiency is rather small compared to that of the literature,[16] probably because of the particle size effect of Pt colloid on the H_2 production efficeincy as was reported by J. Kiwi and M. Grätzel, Nature, 281, 657 (1979).

(Received February 22, 1983)

THE MECHANISM OF PHOTOCATALYTIC HYDROGEN PRODUCTION WITH HALOGENATED FLUORESCEIN DERIVATIVES

Kazuhito Hashimoto, Tomoji Kawai* and Tadayoshi Sakata

Institute for Molecular Science, Myodaiji, Okazaki 444, Japan.
Revised manuscript, receveid June 18, 1984.

RÉSUMÉ. — On constate que les dérivés de la fluorescéine halogénée servent de photocatalyseurs efficaces pour la production d'hydrogène par excitation à la lumière visible en présence de réducteurs. Ces colorants sont stables, et la réaction est efficace dans une région de pH élevés. Les rendements quantiques de la production d'hydrogène pour l'érythrosine sont respectivement 12 et 0,15 % avec la triéthanolamine (TEOA) et l'alcool éthylique comme agents réducteurr. Le spectre d'absorption transitoire et la durée de vie de l'espèce intermédiaire ont été mesurés. Ces colorants sont d'abord photo-réduits en colorants semi-réduits stables via l'état triplet. Le radical intermédiaire a une durée de vie très longue, plus de 10 secondes, par conséquent ces colorants peuvent servir à la fois de sensibilisateurs et de relais d'électrons. Le radical formé au sein de la solution diffuse jusqu'à la surface du catalyseur, en initiant le transfert d'électrons dans le système de production d'hydrogène. Ces processus sont très semblables à ceux du fonctionnement d'une cellule photogalvanique. En fait, la cellule photoélectrochimique composée d'un dérivé de la fluorescéine se comporte typiquement comme une cellule photogalvanique. La différence de potentiel et le rendement quantique du photocourant produit par l'éosine Y agissant comme sensibilisateur en présence de TEOA sont d'environ 1 V et 21 %, respectivement.

ABSTRACT. — Halogenated fluorescein derivatives are found to serve as efficient photocatalysts for hydrogen production with visible light in the presence of a reducing agent. These dyes are stable and the reaction is efficient in the high pH region. The quantum yields of hydrogen production for erythrosin are 12 and 0.15% with triethanolamine (TEOA) and ethanol as the reducing agents, respectively. The transient absorption spectrum and the time behavior of the intermediate species were measured. First, these dyes are photo-reduced to stable semi-reduced dyes via the triplet state. The intermediate radical has a very long lifetime, more than 10 seconds, so that these dyes can serve both as photo-sensitizers and electron relays. The radical formed in the bulk of the solution diffuses to the surface of the catalyst initiating the electron transfer in the hydrogen production system. These processes are very similar to those of a photogalvanic cell. In fact the photoelectrochemical cell composed of a fluorescein derivative shows a photo-response behavior typical to a photogalvanic cell. The open voltage and the quantum yield of the short circuit current for eosin Y as a sensitizer in the presence of TEOA are about 1 V and 21%, respectively.

Introduction

Photochemical and photoelectrochemical energy conversion has been actively investigated over the last years in connection with solar energy utilization. Especially, the photocatalytic water-splitting reaction is well studied [1]. However only a limited number of dyes and semiconductors such as $Ru(bipy)_3^{2+}$ [2], water soluble zinc porphyrins [3] and CdS [4] have been used as efficient photocatalysts for visible light. We reported that several other organic dyes can also serve as photocatalysts in the hydrogen production system based on dye-sensitization of a semiconductor, in which excited dye molecules are quenched by electron transfer to the semiconductor [5]. The efficiencies of hydrogen production, however, are not high since only a relatively small number of dye molecules adsorbed on the semiconductor or located in the distance of diffusion length of the excited-state dye are able to participate in the electron transfer. Consequently, a strong adsorption or a long excited-state lifetime is necessary for an efficient system based on the dye-sensitized semiconductor method [5].

On the other hand, we reported briefly that several halogenated fluorescein derivatives serve as photocatalysts for hydrogen production in the presence of a reduction catalyst and a reducing agent [6]. This hydrogen production system is a so-called two-component system, i. e., non-electron relay system [7]. It is well known that xanthene and thiazine dyes are photo-reduced in the presence of a reducing agent under visible light illumination [8]. Especially, fluorescein and its halogenated derivatives are reduced efficiently to very stable semi-reduced dyes in the high pH region [8, 9].

Here we studied this hydrogen-producing reaction in detail and also found that an efficient photogalvanic cell can be constructed by using these dyes and an irreversible reducing agent. The mechanism, based on reductive quenching of excited dyes [10], will be discussed and compared with that based on the dye sensitized semiconductor system. The absorption peaks in the visible region of these dyes are situated around 500 nm and shift to longer wavelength with substituting heavier halogen atoms.

* Present Address: Osaka University, Institute of Scientific and Industrial Research, Mihogaoka, Ibaraki, Osaka 567, Japan.

Experimental

MATERIALS AND PREPARATION OF A REDUCTION CATALYST

The dyes (fluorescein, dichlorofluorescein, dichrolofluorescein diacetate, dibromofluorescein, mercurochrome, eosin *B*, eosin *Y* and erythrosin) were obtained either from Eastman Kodak Co. Organic Chemicals or from Aldrich Chemical Company, Inc. and were used without further purification. Hereafter, these dyes are reffered to as Fl, $FlCl_2$, $FlCl_2(OCOCH_3)_2$, $FlBr_2$, $FlBr_2Hg$, $FlBr_2(NO_2)_2$, $FlBr_4$ and FlI_4, respectively. The dyes except $FlCl_2(OCOCH_3)_2$ were employed as the sodium salts. Fl, $FlCl_2$ and $FlBr_2$ were available only in the acid form so that in these cases the sodium form was prepared by dissolving the dye in aqueous NaOH solution. The chemical structures of these dyes are shown in Figure 1.

As the reduction catalyst, platinized semiconductor powder, platinized SiO_2 powder or colloidal Pt was used. Commercial semiconductor powders and SiO_2 powders were obtained either from Nippon Aerosil Co., LTD. (TiO_2 : P-25 anatase, average grain size 0.03 μm, surface area 50 m^2/g, SiO_2 : Ox-50, 0.04 μm, 50 m^2/g) or Kojundo Kagaku Co., LTD. [TiO_2 (rutile), SnO_2, $SrTiO_3$, ZrO_2, average grain size, several μm]. Pt was deposied on the surface of the powders either with the photochemical [11], or a conventional impregnation method. The colloidal Pt catalyst was stabilized with polyvinylpyrrolidone (PVP) [12]. Other regents were at least commercial special grade and used without further treatments.

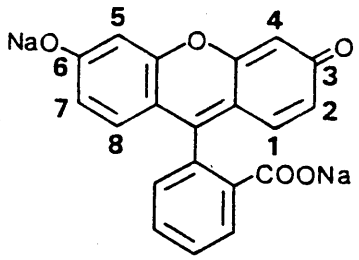

Fl : 1,2,4,5,7,8-H
$FlCl_2$: 2,7-Cl
$FlCl_2(OCOCH_3)_2$: 2,7-Cl, 3,6-$OCOCH_3$
$FlBr_2$: 4,5-Br
$FlBr_2Hg$: 2,7-Br, 5-Hg
$FlBr_2(NO_2)_2$: 2,7-NO_2, 4,5-Br
$FlBr_4$: 2,4,5,7-Br
FlI_4 : 2,4,5,7-I

Figure 1. — Chemical structures of halogenated fluorescein derivatives.

HYDROGEN PRODUCTION AND CHARACTERIZATION OF INTERMEDIATE SPECIES

An aqueous solution of each dye (5×10^{-3}M, 10 ml) with a reducing agent (TEOA, triethylamine (TEA), ethylenediamine-tetra-acetic acid (EDTA), or phenol: 5×10^{-1}-10^{-2}M, or 30 vol% ethanol) and a reduction catalyst (300 mg of platinized powder, or 4 mg of Pt for colloidal Pt/PVP) in a 280-ml Pyrex flask was deaerated. The pH of the solution was adjusted to 8-13.5 with HCl or NaOh. The flask was irradiated from the bottom with visible light from a 500 W Xe lamp (Ushio, UXL 500) filtered with a Toshiba 470-nm sharp cutoff glass filter. After irradiation for about 1 hour, the gas produced was analysed by a quadrupole mass spectrometer and a manometep, as described previously [13]. For the measurement of the quantum yields for $FlBr_2$ and FlI_4, monochromatic light at the wavelength of the absorption peak of each dye, provided by the 500-W Xe lamp and a interference filter (Vacuum Optics Corporation of Japan), was used as an exciting light whose photon number was determined by using a thermopile (Eppley Inc.). A hydrogen production rate of 87 ml/hr. under white light illumination corresponded to a quantum yield of 1.0 with the present equippment. The spectral profiles of the other dyes are similar to those of $FlBr_2$ and FlI_4, so that from the hydrogen production rates under white light illumination we estimated ΦH_2 for the other dyes. The absorption spectra were measured on a Hitachi 556 spectrometer with 1 mm path length cell. The measurements of the time behavior of the transient species were performed with a frequency-doubled (532 nm) YAG laser with a pulse width of 15 ns (Quanta-Ray Inc.) as the exciting light and a DC iodine lamp as the monitor light. The photomultiplier output was recorded and analysed with a 100 MHz transient digitizer (Iwatsu INC., DM901). The details were described elsewhere [14].

PHOTOELECTROCHEMICAL EXPERIMENT

A commercial TiO_2 single crystal which was heated under hydrogen (300 Torr) for 2 hours, a commercial SnO_2 coated glass plate and a ZnO sintered disk, which was prepared from ZnO powder moulded by compression and heated at 1,300°C for 2 hours in the air, were used as working electrodes. The electrochemical measurements were performed in a glass cell containing a working electrode, a Pt plate and a saturated calomel electrode (SCE) as the counter electrode and reference electrode, respectively. The electrolyte solution contained the dye (5×10^{-4}M), TEOA (10^{-2}M) and K_2SO_4 (0.2 M). The pH of the sample solution was adjusted to 12.6 by adding NaOH solution. Nitrogen gas was bubbled into the solution for 10 minutes before each measurement. The open voltage (V_{op}) and the short circuit current (I_{sc}) were measured on a digital voltmeter and a recorder under visible light illumination ($\lambda > 470$ nm from the 500-W Xe lamp). For the measurements of the action spectrum, time response and quantum efficiency of I_{sc}, monochromatic light provided by the 500-W Xe lamp and a monochromator (Nikon G250) was used.

Results and discussion

PHOTOCATALYTIC PROPERTIES

Hydrogen production experiments

It was found that fluorescein and its halogenated derivatives serve as good sensitizers for hydrogen production from water in the presence of Pt/TiO_2 and TEOA as the reduction catalyst and the reducing agent, respectively [6]. When an aqueous solution of dye-Pt/TiO_2-TEOA system was irradiated with visible light, the hydrogen gas produced was observed as streams of bubles. When D_2O was used instead of H_2O, D_2 was 79% of the produced gas, DH 19% and H_2 2%. This result suggests that hydrogen is produced from water. In Table I are shown rates and quantum yields of hydrogen production in these systems. Here the quantum yield, Φ_{H_2}, was defined as follows.

$$\Phi_{H_2} = 2 \times \frac{\text{(number of hydrogen molecules produced)}}{\text{(number of incident photons)}} \qquad (1)$$

Φ_{H_2} values for $FlBr_2$ and FlI_4 were determined directly to be 0.082 and 0.12, respectively, and those for the other dyes were estimated with the method described in the experimental

Table II. – Effect of reduction catalysts on hydrogen production. Dye: $FlBr_2$ (5×10^{-3} M), Reducing agent: TEOA (10^{-1} M). Powders of (*a*) and (*b*) were purchased from Kojundo Kagaku Co., LTD. (grain size: several μm) and Nippon Aerosil Co., LTD. (300 Å), respectively. (*c*) The rate for Pt/TiO_2 (300 Å) was normalized to 100. These values were averaged from several experiments.

Reduction catalyst	Ratio of initial hydrogen production rates (c)
Pt/ZrO_2 (a)	75
$Pt/SrTiO_3$ (a)	90
Pt/TiO_2 (a)	90
Pt/SnO_2 (a)	80
Pt/TiO_2 (b)	100
Pt/SiO_2 (b)	95
Colloidal Pt	85

Hydrogen can also be produced with these compounds instead of TEOA in the presence of a reduction catalyst, although the efficiencies are lower than that with TEOA. The rates and the quantum yields of the hydrogen production with $FlBr_4$ are shown in Table III. The result that ethanol and phenol also served as reducing agents indicates that the excited states of these dyes have relatively strong oxidating power.

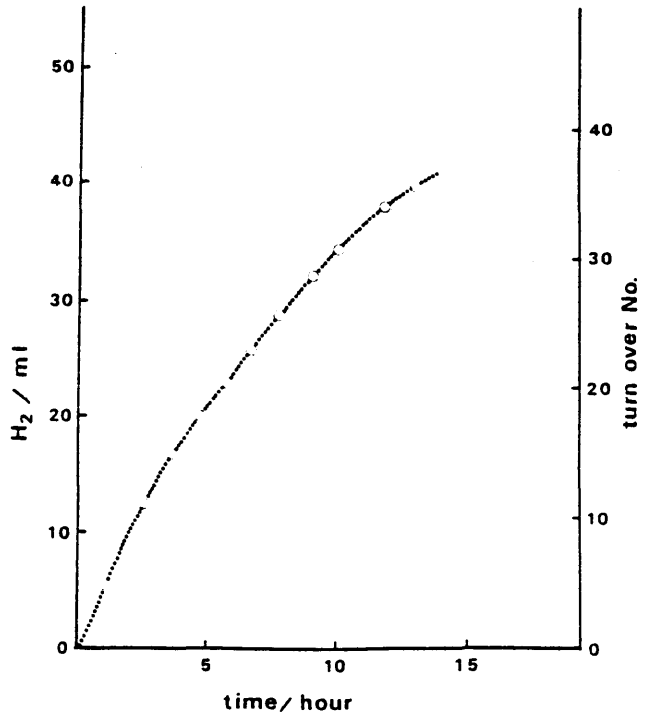

Figure 3. – Overall hydrogen production and turn-over number of the dye in Eosin-Y ($FlBr_4$)-Pt/SiO_2-TEOA system as a function of the visible light illumination time. Light source: 500-W Xe lamp ($\lambda > 470$ nm). $FlBr_4$: 5×10^{-3} M, TEOA: 10^{-1} M, pH = 12.5 (10 ml aq. soln).

Table III. – Hydrogen production with eosin-Y ($FlBr_4$) and various reducing agents. (a) 10^{-1} M, (b) 50 vol%. Reduction catalyst: Pt/SiO_2.

Red. Agent	H_2 Production	
	Rate (μl/h)	Q.Y.
TEOA (a)	7,800	9×10^{-2}
TEA (a)	630	7×10^{-3}
EDTA (a)	1,300	1.5×10^{-2}
Ethanol (b)	110	1×10^{-3}
Phenol (a)	1	1×10^{-5}
H_2O	0	0

Time Behavior of Intermediate Species

The initial efficiency of hydrogen production with FlI_4 and TEOA is rather high compared with the other homogeneous systems. The photofading of dyes, however, occurs and the reaction rate decreases gradually during prolonged irradiation. Figure 3 shows the change in the hydrogen production rate and the turn-over number of the dye in the $FlBr_4$-Pt/SiO_2-TEOA system. The rate after 10 hours of irradiation was about a half of the initial rate. The turn-over numbers of Fl, $FlBr_4$ and FlI_4 in the presence of Pt/SiO_2 and TEOA, were about 400, 120 and 30, respectively, showing the catalytic nature of these reactions and the tendency that the dyes substituted with heavier halogen atoms are more easily decomposed. These values, however, depend on various conditions such as light intensity, reduction catalyst and pH, so that these might be improved with better conditions.

Imamura *et al.* reported that halogenated fluorescein dyes are photochemically dehalogenated by visible light and ring system remains [9a(b), 20, 21]. They investigated the mechanism of this process by using γ-ray irradiation and a flash photolysis technique [9a(d), 22, 23]. According to their results, the semi-reduced dyes produced absorb the light around 400 nm and dehalogenation proceeds successively, resulting in the fluorescein formation. Even in the presence of a reduction catalyst, the same reactions seem to proceed, although its rate is much slower than that in the absence of a reduction catalyst. Curves (*a*) and (*c*) in Figure 4 represent the absorption spectra of the FlI_4 solution before and after prolonged irradiation, respectively. The peak position of (*c*) corresponds to that of the absorption spectrum of Fl [21]. Curve (*d*) shows the absorption intensity of Fl whose molar amount was same as that of FlI_4 used on (*a*). From the absorption intensities of (*c*) and (*d*), it is known that about 70% of the FlI_4 was converted to Fl under these conditions (*see* the caption of Figure 4). For the rest of FlI_4 (30%), ring system might have been decomposed. Halide ions (0.5 M) were added the solution in an attempt tp prevent the dehalogenation, but no effect was observed.

Curve (*b*) in Figure 4 represents the absorption spectrum of FlI_4 in the absence of a reduction catalyst just after 10 seconds irradiation. The intensity of the main peak decreases and a new peak emerges around 415 nm. This new peak is assigned to the semi-reduced dye [9a(b), (c), (d)]. In order to elucidate the reaction mechanism, we measured the time behavior of these peaks. In Figure 5-(A) are shown the time course of the transient absorptions at 415 nm of the semi-reduced radical. In the absence of a reduction catalvst, this

Table I. – Quantum yields of hydrogen production and intersystem crossing. (*a*) Na salt, (*b*) pH = 12.5 aq. soln. (*c*) Dye: 5×10^{-3} M, Pt/SiO_2, TEOA: 10^{-1} M. (*d*) The initial values. (*e*) Reported by P. G. Bowers and G. Porter [15]. (*f*) Reported by M. S. Chan and J. R. Bolton [16].

Dye(*a*)	Abs. peak (nm) (*b*)	H_2 production (*c*)		Intersystem crossing	Redox potential(*f*)
		(ml/h) (*d*)	Q. Y.	Q. Y. (*e*)	$E_{1/2}$(V)
(1) Fl	490	0.62	0.74×10^{-2}	0.05 ± 0.02	−0.58
(2) $FlCl_2$	503	1.4	1.7×10^{-2}	–	–
(3) $FlCl_2(OCOCH_3)_2$	503	3.6	4.3×10^{-2}	–	–
(4) $FlBr_2$	506	7.1	8.5×10^{-2}	0.49 ± 0.07	–
(5) $FlBr_2Hg$	506	7.1	8.5×10^{-2}	–	–
(6) $FlBr_2(NO_2)_2$	518	0.019	2.3×10^{-4}	–	−0.12
(7) $FlBr_4$	518	7.8	9.4×10^{-2}	0.7 ± 0.1	−0.58
(8) FlI_4	526	10.0	12×10^{-2}	1.07 ± 0.13	−0.29

section. Fluorescein itself can serve as the sensitizer with a low efficiency $\Phi_{H_2} = 0.006$, but the efficiency of hydrogen production increases drastically with halogen atom substitution. Quantum yields of triplet formation (Φ_T) of these dyes in alkaline aqueous solution which were reported by P. G. Bowers and G. Porter [15], are also shown in the same table. Φ_T increases with heavier halogen substitution because of the heavy atom effect on intersystem crossing. Φ_{H_2} increases with Φ_T, suggesting that hydrogen is produced by way of the triplet states of these dyes. However, Φ_{H_2} for $FlBr_2(NO_2)_2$ is smaller than that for the other dyes, although it is expected that Φ_{isc} will be as high as that of $FlBr_2$. This is probably because the redox potential of the semi-reduced radical of this dye is much more positive than that of the others, and may not be enough to reduce a proton. The redox potential of ground state $FlBr_2(NO_2)_2$ is more positive than that of the others as shown in Table I [16].

Although the components of the present hydrogen-producing systems are similar to those of other systems based on dye sensitization of semiconductors which are composed of a dye and Pt/TiO_2, [5, 17] these reaction mechanisms are quite different from each other. Table II shows the relative activities of various kinds of reduction catalysts on hydrogen production in the $FlBr_2$-TEOA system. Here the rate for Pt/TiO_2 (Aerosil) was normalized to 100. Neither remarkable nor systematic changes depending on the energy levels of supporting semiconductors were observed. Moreover both Pt/SiO_2 and colloidal Pt can serve as reduction catalysts. The existence of semiconductor is not indispensable in the present systems although that is necessary in the hydrogen production systems based on dye sensitization of semiconductors [5, 17]. The efficiency of hydrogen production in the present case might be determined mainly by the catalytic activity of platinum. This independence on the catalyst is different from results obtained using photoelectrochemical cells, as will be discussed later.

Another characteristic of the present systems is that the reaction is efficient and relatively stable in the high pH region. The maximum rate was obtained in the pH region, 11-13 as is shown in Figure 2. In this pH region, the proton concentration is so small that reduction of water molecules must occur pather than that of protons. From an energetic point of view, the former process is much more difficult than the latter, but the reaction rates for neutral and acidic solutions are lower and decreŒase faster than that for alkaline solution. This result suggests that the intermediate species of this reaction is stable and its formation yield is high in the alkaline region. On the other hand fluorescein and its halogenated derivatives are known to be photo-reduced, forming very stable semi-reduced dyes in aqueous alkaline solution in the presence of a reducing agent [9]. All the results described above indicate that the reductive quenching of the excited triplet state dye is the first reaction step and forms the semi-reduced radical which plays the role of the intermediate in the present hydrogen production reaction. This will be discussed later.

Besides TEOA, several other sacrificial reducing agents such as TEA [18] and EDTA [9-(a), 19], and some organic compounds such as ethanol and phenol [9-(c)] are known to be able to reduce fluorescein derivatives to the semi-reduced radicals.

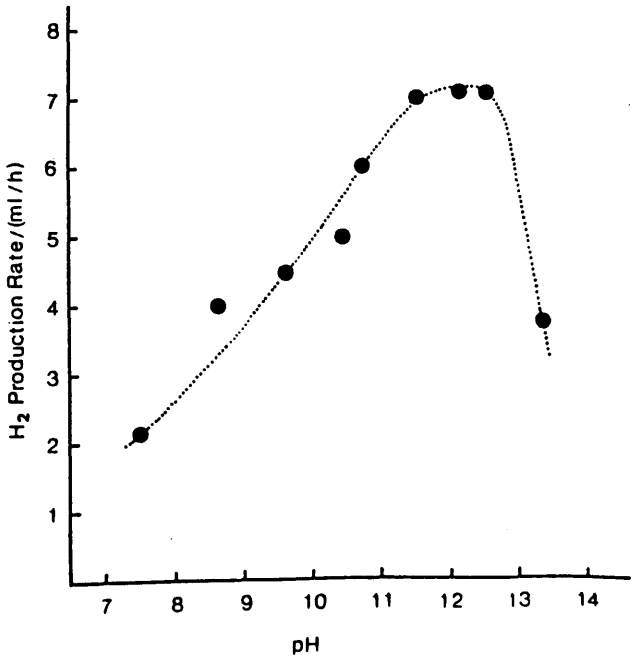

Figure 2. – pH dependence of the initial rate of hydrogen production. $FlBr_2$: 5×10^{-3} M, Pt/TiO_2, TEOA : 5×10^{-1} M.

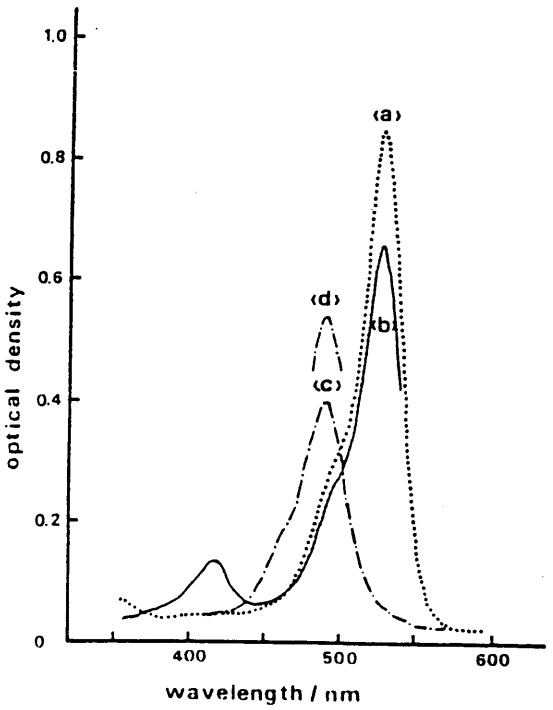

Figure 4. – Absorption spectra of erythrosin (FII_4) in the presence of TEOA. (*a*) Before irradiation, (*b*) After irradiation for 10 seconds in the absence of Pt/SiO_2, (*c*) After irradiation for 30 hours in the presence of Pt/SiO_2. (*d*) Absorption intensity of Fluorescein (Fl) whose molar amount is same as that of FII_4 on curve (*a*). Light source: 500-W Xe lamp ($\lambda > 470$ nm). FII_4: 9.5×10^{-6} M, TEOA: 10^{-3} M, pH = 12.5, path length of the cell: 1 mm.

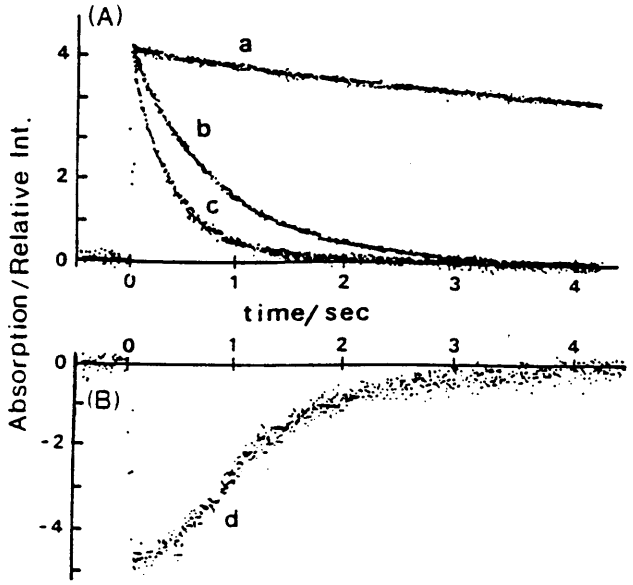

Figure 5. – Transient absorption of erythrosin (FII_4) in the presence of TEOA. (A) Observed at 415 nm (semi-reduced dye). (B) Observed at 545 nm (ground state dye). (*a*) In the absence of colloidal Pt. (*b*), (*c*) and (*d*) In the presence of 10^{-4} M, 2×10^{-4} M and 10^{-4} M colloidal Pt, respectively.

radical decayed very slowly [curve(*a*)] and the lifetime was estimated to be more than 15 seconds. Curves (*b*) and (*c*) are the decay curves in the presence of colloidal Pt. With increasing the concentration of colloidal Pt, the radical disappears faster. Figure 5-(B) represents the time behavior of the original ground state dye in the presence of colloidal Pt observed at 545 nm. From these curves, it can be seen that the amount of the original ground state dye decreased with excitation and the semi-reduced radical was formed. In the presence of Pt the radical disappeared and the original dye was recovered, although the radical has a very long lifetime in the absence of a reduction catalyst. Consequently, we can conclude that this semi-reduced dye is the intermediate species in the present hydrogen production process and recovers to the original dye releasing an electron to the Pt catalyst on which hydrogen is produced. This type of reaction, the reductive quenching of excited dye, was extensively studied for $Ru(bipy)_3^{2+}$ by Sutin *et al.* and Whitten *et al.* [10].

PHOTOELECTROCHEMICAL PROPERTIES

We constructed relatively efficient photoelectrochemical cells by using the present fluorescein derivatives and TEOA. Interestingly, they showed very high photovoltages (V_{op}) amounting to 1 V, and the quantum efficiencies of the short circuit current (I_{sc}) for monochromatic light, which are defined as follows,

$$\Phi_{I_{sc}} = \frac{\text{(number of electron flown in the cell)}}{\text{(number of incident photons)}}, \qquad (2)$$

were rather high, 0.01-0.20.

Photoelectrochemical cells using dyes can be roughly classified into two categories [24]. One is based on the sensitization effect of the dye adsorbed on the semiconductor electrode [25], and the other is based on the photochemical reaction of the dye in the bulk solution [26], the latter is called photogalvanic cell. The present systems seem to correspond to the latter case containing an irreversible reducing agent [27, 28], because the long-lived semi-reduced dye might play an important role in the current generation as well as in the hydrogen production system described previously. In fact, a platinum plate can also serve as the light electrode instead of semiconductors. This property is characteristic of a photogalvanic cell [24]. Table IV shows the values of V_{op} and $\Phi_{I_{sc}}$ in the cell, ⟨semiconductor or Pt (light) | $FIBr_4$-TEOA | Pt (dark)⟩, with various light electrode materials. V_{op} does not depend greatly on the kind of light electrode. Here, the following two points are to be noted. (*a*) Either a semiconductor or Pt can work as the electron acceptor from the semi-reduced dye, and $\Phi_{I_{sc}}$ for the semiconductor is rather larger than that for platinum. It is well known that electrons are separated efficiently from holes in the space charge layer of semiconductors because of the rectification effect of the Schottky barrier. Due to this effect, the back electron transfer from an electrode to the oxidized dye is suppressed more efficiently for semiconductors than for metals. This may be the reason why $\Phi_{I_{sc}}$ for semiconductors is higher than that for the metal (Pt). (*b*) The photopotential of each light electrode is more negative than -1.0 V vs SCE. Actually the potential value of the anodic oxidation of the semi-reduced radical for $FIBr_4$ was measured to be more negative than -1.2 V vs SCE under the same conditions [29]. Because the hydrogen production potential with pH = 12.6 is about -0.99 V vs SCE, hydrogen production is possible in any case. These results indicate that the semi-reduced dye can give an electron to either a semiconductor or Pt in the hydrogen production system using a Pt/(semi-

Table IV. – Dependence of light electrode materials on open voltage and short circuit current. Dye: $FlBr_4$ (5×10^{-4} M), Reducing agent: TEOA (10^{-2} M), Na_2SO_4 (0.2 M), pH = 12.6.

Electrode	Open Voltage (V)	V vs SCE	Q.Y. of I_{sc}
TiO_2	0.95	−1.12	0.14
ZnO	1.02	−1.19	0.18
SnO_2	0.99	−1.16	0.21
Pt	0.86	−1.02	0.091

Table V. – Open voltage and quantum yield of short circuit current using various fluorescein derivatives as sensitizers. Light electrode: SnO_2, Dye: 5×10^{-4} M, Reducing agent: TEOA (10^{-2} M), Na_2SO_4: 0.2 M, pH = 12.6.

Dye	Open Voltage (V)	V vs SCE	Q.Y. of I_{sc}
Fl	1.01	−1.17	0.014
$FlCl_2$	1.01	−1.15	0.055
$FlBr_2$	1.05	−1.17	0.13
$FlBr_4$	0.99	−1.16	0.21
FlI_4	1.01	−1.16	0.099

conductor) reduction catalyst, and moreover the potential of Pt loaded on the semiconductor, whose Fermi level is more positive than the hydrogen production potential, becomes negative enough for hydrogen production under irradiation. These agree with the results obtained in the previous section where the hydrogen production efficiency is almost independent on the kind of a supporting materialof Pt.

The solid curve in Figure 6 shows the time dependence of the photocurrent. The current rises and decays very slowly when the light is turned on or off, taking several minutes to become constant. This behavior agrees with that of a typical photogalvanic cell with an irreversible reducing agent [28], and is explained as follows. The long-lived semi-reduced dye formed in the bulk solution diffuses to the surface of the electrode (semiconductor or Pt), initiating the electron transfer and the current rises. On the other hand, we reported previously that the hydrogen production from the system composed of rose bengal, Pt/TiO_2 and EDTA is based on the dye-sensitization effect of the semiconductor [5]. Actually the time response of the current produced in the cell composed of ZnO, Pt, rose bengal and EDTA as the light electrode, a dark electrode, a sensitizer and a reducing agent is very fast (<ms) and is shown in Figure 6 (dotted curve). The response time of dye-sensitized semiconductor cells is known to be very fast, because the electron transfer occurs from the adsorbed excited dye to a semiconductor electrode [25].

We also investigated the dependence of V_{op} and I_{sc} on the kinds of the fluorescein derivatives. The results are shown in Table V. V_{op} is not very sensitive to the kind of dye, which means that each semi-reduced radical has the almost same oxidation potential. $\Phi_{I_{sc}}$ also increased with heavy-atom substitution except FlI_4. FlI_4 is easily decomposed as described previously, so that the apparent quantum yield might be small. There is also an interesting aspect that $\Phi_{I_{sc}}$ is larger than Φ_{H_2} in these systems.

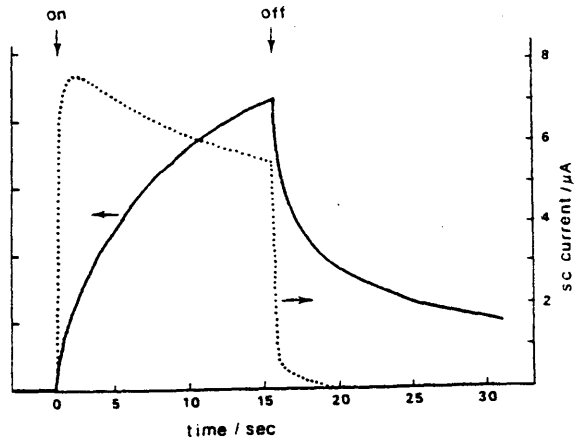

Figure 6. – Change of photocurrent vs. time. Light electronde potential: 0.4 V vs SCE. Solid curve: ⟨ZnO|eosin-Y, TEOA|Pt⟩ pH = 12.6, 518 nm irradiation. Dotted curve ⟨ZnO|rose bengal, EDTA|Pt⟩. pH = 6.0, 620 nm irradiation.

REACTION MECHANISM

From the above discussions, the reaction mechanism of the present system would be described as follows.

$$\mathrm{Dye} \xrightarrow{h\nu} {}^1\mathrm{Dye}^*; \quad (3) \qquad \text{(Bulk)}$$

$${}^1\mathrm{Dye}^* \rightarrow {}^3\mathrm{Dye}; \quad (4)$$

$${}^3\mathrm{Dye} \xrightarrow{\mathrm{Red}} \mathrm{Dye}^- + \mathrm{Red}^+; \quad (5)$$

$$\mathrm{Red}^+ \rightarrow \mathrm{Decomposition}; \quad (6)$$

$$\mathrm{Dye}^- \xrightarrow[\text{or Pt}]{\text{Semiconductor}} \mathrm{Dye} + e^- \quad (7) \qquad \textit{(Interface)}$$

Here Red and e^- represent a reducing agent and an electron, respectively. The lifetimes of the triplet states(T_1) of the fluorescein derivatives studied here are several orders of magnitude larger than those of the first excited singlet states (S_1). For example, the lifetimes of S_1 and T_1 of $FlBr_4$ are 3.6 ns [30] and 1.7 ms [31], respectively, in deoxygenated ethanol at room temperature. The processes, (3)-(6), occur in the bulk of the solution. The semi-reduced dye, which has a very long lifetime, diffuses to the surface of a reduction catalyst or an electrode to which the semi-reduced dye transfers an electron being oxidized into the original dye. The transferred electron generates electricity in the photo-electrochemical cell and is also used for the reduction of water in the hydrogen-producing system.

As was indicated in the previous section, the radical can transfer an electron to either semiconductor or Pt electrode ald the efficiencies are almost the same. Thus the electron transfer might also occur to both the semiconductor surface and particulate Pt loaded on the semiconductor surface in the hydrogen production system using Pt/(semiconductor) photocatalyst as the reduction catalyst. However, when semiconductor alone was used, little hydrogen is produced. This indicates that semiconductor is used as the electron carrier to the Pt site, as was suggested by Grätzel *et al.* in the $Ru(bipy)_3^{2+}$-methylviologen (MV^{2+})-$Pt/TiO_2/RuO_2$ system [1-(g)], and TiO_2 itself is not a good catalyst for hydrogen production. We have reported that both forms of TiO_2 (rutile and anatase) can reduce water efficiently [32]. Moreover as is shown in Table IT, the potential of the working electrode

becomes more negative than that required for hydrogen production, even for SnO_2. This indicates that electrons are injected into the conduction band of SnO_2, resulting in a enormous negative shift (-1.16 V vs SCE). The situation seems similar to that in the system of a powdered semiconductor whose conduction band is located below the redox level of H^+/H_2 in the dark, since hydrogen is produced very efficiently even by using Pt/TiO_2 (rutile), or Pt/SnO_2.

In Figure 8 is shown the schematic picture of the hydrogen production process. This is a so-called two-component system, i. e., electron relay free system [7], and the dye serves as both a sensitizer and an electron relay [26-28]. This process is similar to that of photogalvanic cells [25], so that we may call this a photogalvanic-type hydrogen-producing system.

The components of this system are very similar to those of a dye-sensitized semiconductor system, but the reaction mechanisms are quite different from each other. The latter process can be explained as follows [5].

$$\text{Dye} \xrightarrow{h\nu} \text{Dye}^*, \tag{8}$$

$$\text{Dye}^* \xrightarrow[\text{semiconductor}]{} \text{Dye}^{+\cdot} + e_{cb}^-, \tag{9}$$

$$\text{Dye}^{+\cdot} \xrightarrow{\text{Red}} \text{Dye} + \text{Red}^{+\cdot}, \tag{10}$$

$$\text{Red}^{+\cdot} \rightarrow \text{decomposition}, \tag{11}$$

Here e_{cb}^- represents an electron in the conduction band of the semiconductor. This electron is used for the reduction of water and the current as well. In this case the excited dye is quenched by the oxidative electron transfer to the semiconductor, so that only the dye adsorbed on the semiconductor surface and the dye that exists in the diffusion layer formed by the excited state dye can participate in the electron transfer. However most dye molecules exist in the bulk solution [5]. Consequently the apparent quantum yield of hydrogen production becomes low even if the electron transfer occurs efficiently between the semiconductor and the adsorbed dye (or the dye in the diffusion layer). However, in the photogalvanic-type hydrogen-producing system, the excited dye is quenched by the reductive process forming a very stable radical, so that almost all the dye molecules in the solution can participate in the electron transfer. This is the reason why the quantum yield is high in this system.

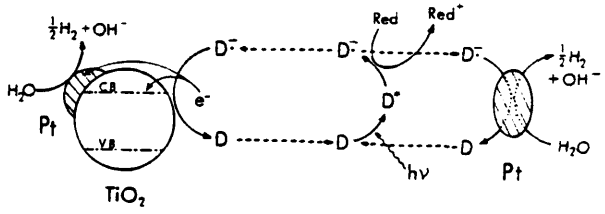

Figure 7. – Schematical illustration of the hydrogen-producing process for halogenated fluorescein derivatives in the presence of a reduction catalyst and a reducing agent.

Φ_{H_2} of the most efficient system studied (FII_4) is 0.12 and is almost equal to that of one of the most efficient three-component systems, $Ru(bipy)_3^{2+} - MV^{2+} - Pt/PVA$ in the presence of EDTA, 0.13 [33]. The other two-component systems were reported by several researchers, for instance, $Ru(bipy)_3^{2+} - PtO_2$ [34], proflavine-Pt/PVA [7] and chromium(III) complexes-Pt/PVA [35] in the presence of TEA, EDTA or TEOA, and EDTA, respectively. However, hydrogen production in the present system is more efficient than that in other relatively stable two-component systems. For instance, the rate for $FIBr_4$ is several times larger than that for proflavine. The quantum efficiency for the chromium complexes is almost the same as for $FIBr_4$, but the turn-over number of chromium complexes is very small, about 4. A comparison of these hydrogen production systems is summarized in Table VI.

Conclusion

Efficient hydrogen-producing systems can be constructed by using halogenated fluorescein derivatives. The excited Œdye is quenched by reductive electron transfer, forming a very stable semi-reduced dye which also serves as an electron relay. A photogalvanic cell can be also constructed. These two are based on the same process. These are efficient in the high pH region, which indicates that the intermediate radical has relatively strong oxidating power, because the reduction of H_2O, which is more difficult than that of H^+, proceeds under these conditions. Therefore, there might be the possibility of applying them to other reductive reactions, especially

Table VI. – Comparison of characteristics of hydrogen-producing systems. (*) Visible light from a 500-W Xe lamp filtered with a 470-nm cutoff filter for the $FIBr_4$ system, a 390-nm filter for the proflavine system and a 440-nm filter for the $Ru(bipy)_3^{2+}$ systems, respectively. (b), (c) The experimental conditions were the same as those of reference [7] and [1-6], respectively. (d) Dye-sensitized Pt/TiO_2 system [5]. (e) See the note(36).

Dye	Absorption peak (nm)	Electron relay	Redox catalyst	H_2 production (a) rate (ml/h)	pH	Reducing agent
Eosin-Y ($FIBr_4$)	518	–	Pt/TiO_2	7.8	12.5	TEOA
			Pt-PVP	6.6		
Proflavine (b)	445	–	Pt-PVP	2.4	7.0	TEOA
$Ru(bipy)_3^{2+}$ (c)	452	MV^{2+}	Pt-PVP	2.9 (e)	5.0	EDTA
$Ru(bipy)_3^{2+}$ (d)	452	–	Pt/TiO_2	0.1	5.0	EDTA

in alkaline solution. Moreover the spectral properties can be easily controlled by substitution, which is a characteristic feature of these kinds of organic dyes.

There are, however, still two serious problems to be solved. One is the instability of the dye. The other is the weak oxidating power of the dye in the excited state. If we can succeed in synthesizing a stable dye with a more positive reduction potential in the excited state, this method will become more promising.

Acknowledgment

We thank to Drs. Y. Sakaguchi, J. Nakamura and H. Hayashi at the Institute of Chemical and PhysicŒal R Research for the kind help for the measurement of flash photolysis experiment, and Dr. M. Matsumura and Professer H. Tsubomura at Osaka University for the gift of ZnO sinter disks, and Drs. R. D. McKelvey and J. Moore for the careful reading of the manuscript.

REFERENCES AND NOTES

[1] For example: (*a*) G. N. Schrauzer, and T. D. Guth, *J. Amer. Chem. Soc.*, **99**, 7189 (1977). (*b*) F. T. Wagner, and G. A. Somorjai, *Nature*, **285**, 559 (1980). (*c*) S. Sato, and J. M. White, *Chem. Phys. Lett.*, **72**, 83 (1980). (*d*) T. Kawai, and T. Sakata. *Chem. Phys. Lett.*, **72**, 87 (1980). (*e*) J. M. Lehn, J. P. Sauvage, and R. Ziessel, *Nouv. J. Chim.*, **4**, 623 (1980). (*f*) K. Domen, S. Naito, M. Soma, T. Ohnishi, and T. Tamaru, *J.C.S. Chem. Commun.*, 543 (1980). (*g*) D. Duonghong, E. Borgarello, and M. Grätzel, *J. Amer. Chem. Soc.*, **103**, 4685 (1981).

[2] For example: (*a*) J. M. Lehn, and J. P. Sauvage, *Nouv. J. Chim.*, **1**, 449 (1977). (*b*) Moradpour, E. Amouyal, P. Keller, and H. Kagan, *Nouv. J. Chim.*, **2**, 547 (1978). (*c*) A. I. Krasna, Photochem. *Photobiol.*, **29**, 267 (1979). (*d*) K. Kalyanasundaram, and M. Grätzel, *Angew. Chem. Int. Ed. Engl.*, **18**, 701 (1979). (*e*) J. M. Lehn, J. P. Sauvage, and E. Ziessel, *Nouv. J. Chim.*, **4**, 355 (1980). (*f*) P. Keller, A. Moradpour, E. Amouyal, and H. B. Kagan, *Nouv. J. Chim.*, **4**, 377 (1980). (*g*) E. Borgarello, J. Kiwi, E. Pelizzetti, M. Visca, and M. Grätzel, *J. Amer. Chem. Soc.*, **103**, 6324 (1981). (*h*) J. Hawecker, J. M. Lehn, and R. Ziessel, *Nouv. J. Chim.*, **7**, 271 (1983). (*i*) Y. Degani, and I. Willner, *J.C.S. Chem. Commun.*, 710 (1983).

[3] (*a*) K. Kalyanasundaram, and M. Grätzel, *Helv. Chim. Acta*, **63**, 478 (1980). (*b*) A. Harriman, and M.-C. Richoux, *J. Photochem.*, **14**, 253 (1980). (*c*) E. Borgarello, K. Kalyanasundaram, Y. Okuno, and M. Grätzel, *Helv. Chim. Acta*, **64**, 1937 (1981). (*d*) T. Shimidzu, T. Iyoda, Y. Koide, and N. Kanda, *Nouv. J. Chim.*, **7**, 21 (1983).

[4] J. R. Darwent, and G. Porter, *J.C.S. Chem. Commun.*, 145 (1981). (*b*) J. R. Darwent, *J.C.S. Faraday Trans.* **2**, **77**, 1703 (1981). (*c*) J. D. Spikes, *Photochem. Photobiol.*, **34**, 549 (1981). (*d*) K. Kalyanasundaram, E. Borgarello, D. Dunghong, and M. Grätzel, *Angew. Chem.*, **93**, 1012 (1981). (*e*) K. Kalyanasundaram, E. Borgarello, and M. Grätzel, *Helv. Chim. Acta*, **64**, 362 (1981). (*f*) E. Borgarello, K. Kalyanasundaram, M. Grätzel, and E. Pelizzetti, *Helv. Chim. Acta*, 65, 243 (1982). (*g*) D. H. M. W. Thewissen, A. H. A. Tinnemans, M. Eeuwhorst-Reinten, K. Timmer, and A. Mackor, *Nouv. J. Chim.*, **7**, 195 (1983). (*h*) E. Borgarello, W. Erbs, M. Grätzel, and E. Pelizzetti, *Nouv. J. Chim.*, **7**, 195 (1983).

[5] K. Hashimoto, T. Kawai, and T. Sakata, *Nouv. J. Chim.*, **7**, 249 (1983).

[6] K. Hashimoto, T. Kawai, and T. Sakata, *Chem. Lett.*, 709 (1983).

[7] K. Kalyanasundaram, and M. Grätzel, *J.C.S. Chem. Commun.*, 1137 (1979).

[8] For example, M. Koizumi, and Y. Usui, *Mol. Photochem.*, **4**, 57 (1972) and references therein.

[9] (*a*) A. H. Adelman, and G. Oster, *J. Amer. Chem. Soc.*, **78**, 3977 (1956). (*b*) M. Imamura, *Bull. Chem. Soc. Jpn.*, **31**, 962 (1958). (*c*) E. F. Zwicker, and L. I. Grossweiner, *J. Phys. Chem.*, **67**, 549 (1963). (*d*) K. Kimura, T. Miwa, and M. Imamura, *Bull. Chem. Soc. Jpn.*, **43**, 1337 (1970).

[10] For example: (*a*) C.-T. Lin, W. Böttcher, M. Chou, C. Creutz, and N. Sutin, *J. Amer. Chem. Soc.*, **98**, 6536 (1976). (*b*) C. Creutz, N. Sutin, and B. S. Brunschwig, *J. Amer. Chem. Soc.*, **101**, 1297 (1979). (*c*) P. J. De Laive, B. P. Sullivan, T. J. Meyer, and D. G. Whitten, *J. Amer. Chem. Soc.*, **101**, 4007 (1979).

[11] B. Kreutler, and A. J. Bard, *J. Amer. Chem. Soc.*, **100**, 2239 (1978).

[12] H. Hirai, Y. Nakao, and N. Toshima, *J. Macromol. Sci. Chem.*, A13, 727 (1979).

[13] T. Sakata, and T. Kawai, *Nouv. J. Chim.*, **5**, 279 (1981).

[14] Y. Sakaguchi, and H. Hayashi, *H. Chem. Phys.*, in press.

[15] P. G. Bowers, and G. Porter, *Proc. Roy. Soc.*, Ser. A, **299**, 348 (1967).

[16] M. S. Chan, and J. R. Bolton, *Solar Energy*, **24**, 561 (1980).

[17] T. Kajiwara, K. Hashimoto, T. Kawai, and T. Sakata, *J. Phys. Chem.*, **86**, 4516 (1982).

[18] G. Ostep, G. K. Oster, and G. Karg, *J. Phys. Chem.*, **66**, 2514 (1962).

[19] Y. Momose, K. Uchida, and M. Koizumi, *Bull. Chem. Soc. Jpn.*, **38**, 1601 (1965).

[20] M. Imamura, *Bull. Chem. Soc. Jpn.*, **30**, 250 (1957).

[21] M. Imamura, and M. Koizumi, *Bull. Chem. Soc. Jpn.*, **29**, 913 (1956).

[22] K. Kimura, T. Miwa, and M. Imamura, *Bull. Chem. Soc., Jpn.*, **43**, 1329 (1970).

[23] K. Kimura, T. Miwa, and M. Imamura, *Chem. Commun.*, 1619 (1868).

[24] H. Tsubomura, *Photochemistry and Energy Conversion*. Tokyo Kagaku Dojin, (1980).

[25] For example: (*a*) H. Gerischer, and H. Tributch, *Ber. Bunsenges. Phys. Chem.*, **72**, 437 (1968). (*b*) K. Hauffe, and J. Range, *Z. Naturforsch.*, **23b**, 736 (1968). (*c*) R. Memming, *Photochem. Photobiol.*, **16**, 325 (1972). (*d*) T. Watanabe, A. Fujishima, O. Tatsuoki, and K. Honda, *Bull. Chem. Soc. Jpn.*, **49**, 8 (1976). (*e*) H. Tsubomura, M. Matsumura, Y. Nomura, and T. Amamiya, *Nature*, **261**, 402 (1976).

[26] For example: (*a*) E. Rabinowitch, *J. Chem. Phys.*, **8**, 551 (1940). (*b*) T. Sakata, Y. Suda, J. Tanaka, and H. Tsubomura, *J. Phys. Chem.*, **81**, 537 (1977). (*c*) M. Kandko, and A. Yamada, *J. Phys. Chem.*, **81**, 1213 (1977).

[27] (*a*) M. Eisenberg, and H. P. Silverman, *Electrochim. Acta*, **5**, 1 (1961). (*b*) N. Kamiya, and S. Okawara, *J. Electrochem. Soc. Jpn.*, **37**, 81 (1969).

[28] H. Tsubomura, Y. Shimoura, and S. Fujiwara, *J. Phys. Chem.*, **83**, 2103 (1979).

[29] Unpublished data.

[30] G. R. Fleming, A. W. E. Knight, J. M. Morris, R. J. S. Morrison, and G. W. Robinson, *J. Amer. Chem. Soc.*, **99**, 4306 (1977).

[31] C. A. Parker, "*Advances in Photochemistry*", Wiley (Interscience), New York, (1964), Vol. 2, p. 305.

[32] T. Sakata, and T. Kawai, *Chem. Phys. Lett.*, **80**, 341 (1981).

[33] J. Kiwi, and M. Grätzel, (*a*) *J. Amer. Chem. Soc.*, **101**, 7214 (1979). (*b*) *Nature*, **281**, 657 (1979).

[34] P. J. Delaive, B. P. Sullivan, T. J. Meyer, and D. A. Whitten, *J. Amer. Chem. Soc.*, **400**, 4007 (1979).

[35] R. Ballardini, A. Juris, G. Varani, and V. Balzani, *Nouv. J. Chim.*, **4**, 563 (1980).

[36] The hydrogen production efficiency is rather small compared to that of the literature[1-(a)], probably because of the particle size effect of Pt colloid on the hydrogen production efficiency as was reported by J. Kiwi, and M. Grätzel, *Nature*, **281**, 657 (1979).

Photocatalytic Reactions of Hydrocarbons and Fossil Fuels with Water. Hydrogen Production and Oxidation

Kazuhito Hashimoto, Tomoji Kawai,† and Tadayoshi Sakata*

Institute for Molecular Science, Myodaiji Okazaki 444, Japan *(Received: July 19, 1983; In Final Form: January 31, 1984)*

Photocatalytic H_2 production from several aliphatic and aromatic compounds with water was investigated with powdered Pt/TiO_2 catalyst suspended in solution. Various fossil fuels such as coal, tar sand, and pitch also reacted with water, producing both H_2 and CO_2 from an early stage of irradiation. The photocatalytic oxidations of their model compounds, especially a linear hydrocarbon and benzene, were studied in the presence of silver ion as an electron acceptor. For aliphatic hydrocarbons, they are oxidized to alcohols, aldehydes, and carboxylic acids, successively. CO_2 was found to be formed through the "photo-Kolbe" type of reaction of carboxylic acids produced, which explained well the result of the complete decomposition of *n*-hexadecane. For benzene, we could detect phenol, catechol, hydroquinone, and muconic acid. On the basis of these results, the possibility of the direct oxidation of benzene by photogenerated holes and its ring-opening process peculiar to the photocatalytic reaction are discussed. The main reaction path for CO_2 production was suggested in which the benzene ring opens not by way of phenol and catechol, but by way of the intermediates whose reactivities are much larger than that of benzene.

Introduction

Recently, various photocatalytic reactions with powdered semiconductors were actively studied. Our studies have concentrated on H_2 production from water and various organic compounds with metal or metal oxide loaded TiO_2 as a photocatalyst,[1-8] where organic compounds serve as electron donors and H_2 is produced from water. These organic compounds were oxidized to CO_2 finally when platinized TiO_2 was used as a photocatalyst.

On the other hand, the photocatalytic oxidations of hydrocarbons in the presence of O_2 as an electron acceptor are reported by several researchers.[9-13] For aliphatic hydrocarbons, Bard et al. reported that small amounts of alcohols were produced and CO_2 was the main product.[9] For the oxidation of an aromatic hydrocarbon it has been considered that the photogenerated holes are scavenged by water at first forming ·OH radical, and the oxidation begins by the hydroxylation of the aromatic ring with ·OH radical and proceeds to CO_2 production eventually.[9-12] However, no detailed consideration of the mechanism of oxidation processes has been proposed. Moreover, O_2 may form $\cdot O_2^-$ and $\cdot HO_2$ which might contribute to the oxidation processes of a hydrocarbon, and O_2 itself sometimes participates in the oxidation processes.[9-14] Silver ion, however, serves as an electron acceptor, being reduced to the metal, and does not affect the oxidation of these compounds, so that this electron acceptor seems a good choice for investigation of the mechanism of oxidation.

Here we investigated the H_2-producing reactions of these aliphatic and aromatic compounds with water. In these cases CO_2 was also produced even at an early stage of irradiation. This phenomenon is quite different from that for the alcohol–water system in which the main oxidation product is an aldehyde, and CO_2 is produced only after irradiation for a long time.

In order to elucidate this phenomenon, we carried out product analysis for the photocatalytic reactions of the aliphatic and aromatic hydrocarbons. On the basis of these results, we discuss their oxidation processes.

We have also extended this subject to photocatalytic H_2 production from liquid water and some natural fossil fuels such as coal, tar sand, and pitch, since these fossil fuels are composed of aliphatic and aromatic hydrocarbons.[15]

Experimental Section

Several kinds of powdered TiO_2 ([1] Nippon Aerosil Co., Ltd., P-25, anatase, average grain size 300 Å, [2] Katayama Kagaku Co., Ltd., rutile, 1000 Å, [3] Kojundo Kagaku Co., Ltd., rutile, several micrometers) were used. The results obtained were almost the same regardless of the species of TiO_2. Other powdered semiconductors ($SrTiO_3$, WO_3, SnO_2, Fe_2O_3) were purchased from Kojundo Kagaku Co., Ltd. For the experiments on the oxidation reactions in the presence of Ag^+ as an electron acceptor, powdered semiconductors were used without further treatment. For the H_2 production experiments, the surface of these TiO_2 powders was modified with Pt (4 wt %) photochemically.[16,17]

A bituminous coal produced in Japan was ground into powder (0.1 g) and physically mixed with Pt/TiO_2 (0.3 g) in an agate mortar. Athabasca tar sand (Syncrude) adhering to the surface of sands, produced in Canada, and a pitch (the residue on distillation of Kafuji oil) produced in China were used without any treatments. Various aliphatic hydrocarbons and aromatic compounds were purchased from Katayama Kagaku or Tokyo Kasei (special grade) and were used without further purification. $AgNO_3$ or Ag_2SO_4 (Wako Pure Chemical Industries, Ltd.) was also used without further purification.

The photocatalyst (0.3 g) and a fossil fuel (0.1 g) or a hydrocarbon (0.1–1 g) were suspended in a deaerated water (30 mL) in a 280-mL Pyrex glass bulb which passes light of wavelength

† Present address: Osaka University, Institute of Scientific and Industrial Research, Mihogaoka Ibaraki, Osaka 567, Japan.

(1) T. Kawai and T. Sakata, *J. Chem. Soc., Chem. Commun.*, 695 (1980).
(2) T. Kawai and T. Sakata, *Nature (London)*, **286**, 5772 (1980).
(3) T. Sakata and T. Kawai, *Nouv. J. Chim.*, **5**, 279 (1981).
(4) T. Sakata and T. Kawai, *Chem. Phys. Lett.*, **80**, 341 (1981).
(5) T. Kawai and T. Sakata, *Chem. Lett.*, 81 (1981).
(6) T. Kawai and T. Sakata, *J. Chem. Soc., Chem. Commun.*, 1047 (1979).
(7) T. Kawai and T. Sakata, *Nature (London)*, **282**, 5736 (1979).
(8) T. Sakata, T. Kawai, and K. Hashimoto, *Chem. Phys. Lett.*, **88**, 50 (1982).
(9) I. Izumi, W. W. Duun, K. O. Wilbiurn, Fu-Ren F. Fun, and A. J. Bard, *J. Phys. Chem.*, **84**, 3207 (1980).
(10) M. Fujihira, Y. Satoh, and T. Osa, *Nature (London)*, **293**, 5829 (1981).
(11) M. Fujihira, Y. Satoh, and T. Osa, *J. Electroanal. Chem.*, **126**, 277 (1981).
(12) M. Fujihira, Y. Satoh, and T. Osa, *Chem. Lett.*, 1053 (1981).
(13) I. Izumi, Fu-Ren F. Fun, and A. J. Bard, *J. Phys. Chem.*, **85**, 218 (1981).
(14) C. D. Jaeger and A. J. Bard, *J. Phys. Chem.*, **83**, 3146 (1979).
(15) For example: (a) H. H. Lowry, "Chemistry of Coal Utilization", Vol. 1, Wiley, New York, 1945, p 2; Supplement, 1962. (b) P. L. Walker, Jr., F. Rusinko, Jr., and L. G. Austin, "Advances in Catalysis", Vol. 11, Academic Press, New York, 1959, p 133.
(16) B. Kraeutler and A. J. Bard, *J. Am. Chem. Soc.*, **100**, 4317 (1978).
(17) K. Hashimoto, T. Kawai, and T. Sakata, *Nouv. J. Chim.*, 7, 249 (1983).

0022-3654/84/2088-4083$01.50/0

TABLE I: Hydrogen Production Rates[a]

reactant	H_2 production rate, μmol/h: acidic–neutral[b]	alkaline
(a) Aliphatic Hydrocarbon		
n-pentane	4.4	8.4
n-heptane	6.6	11
isooctane	2.4	9.4
n-paraffin	1.2	2.3
polyethylene	1.0	3.9
(b) Aromatic Compound		
benzene	4.0	36
phenol	4.1	33
pyridine	2.7	31
(c) Fossil Fuel[c]		
coal	1.3	9.0
tar sand	0.5	10
pitch	1.0	10

[a] Light source: 500-W Xe lamp. Photocatalyst: Pt/TiO_2. [b] See note 27. [c] Initial rate.

longer than 320 nm. The glass bulb was irradiated from the bottom side for several hours to several tens of hours with a white light from a 500-W Xe lamp (USHIO, UXL500). All the experiments were done at room temperature. The temperature of the solution was about 40–50 °C during the irradiation.

The gaseous reaction products were trapped at −196 or −55 °C and analyzed by a quadrupole mass spectrometer (Anelva, AGA-360) and a sensitive manometer (Datametrics, barocel pressure sensor) as described previously.[1] The reaction products in the aqueous phase were analyzed by a steam gas chromatograph (Okura Denki, Model 103) and a liquid chromatograph (Japan Spectroscopic Co., Ltd., Familic-100) and a gas chromatograph (Okura Denki, Model 701).

Results and Discussion

Aliphatic Compounds. Hydrogen Production from Aqueous Solutions of Hydrocarbons. In Table Ia are shown the rates of H_2 production from mixtures of water and several aliphatic hydrocarbons with a white light ($\lambda > 320$ nm) from the 500-W Xe lamp. When NaOH was added to the solution (5 N), the rates became about 2–4 times larger than those without NaOH. The quantum yields of the H_2 production in these systems are on the order of 10^{-2}–10^{-3}. One of the characteristic features of these systems is that CO_2 is produced even from an early stage of irradiation.

These are the reactions of water with organic compounds, in which the organic compounds are oxidized eventually to CO_2 and water is reduced, producing H_2.[1-8] We tried the complete decomposition of *n*-hexadecane ($C_{16}H_{34}$), one of the linear saturated hydrocarbons which are difficult to oxidize. The expected reaction is described by the following equation:

$$C_{16}H_{34} + 32H_2O \rightarrow 16CO_2 + 49H_2 \qquad (1)$$

$$\Delta G^\circ = 1232 \text{ kJ/mol}$$

The result is shown in Figure 1. The gaseous products are H_2 and CO_2 as is expected from eq 1. Other products were not detected in the gas phase. The total amounts of H_2 and CO_2 produced were 4.14 and 1.3 mmol, respectively. The amounts of H_2 and CO_2 predicted by eq 1 and the initial amount of *n*-hexadecane, 85 μmol, are 4.16 and 1.36 mmol, respectively, in excellent agreement with the experiment. This supports reaction 1 for the complete decomposition of *n*-hexadecane. Another interesting result is that the ratio of H_2 to CO_2 is always about 3 at each sampling point as seen in this figure. This implies that the ratio of H_2 to CO_2 is constant, about 3, during the decomposition of the reaction intermediates of *n*-hexadecane.

Bard et al. demonstrated the formation of ·OH radical on TiO_2 photocatalyst under illumination by using the spin-trapping method.[14] The radical was suggested to play an important role in the oxidation of hydrocarbons.[9-14] Assuming the involvement of

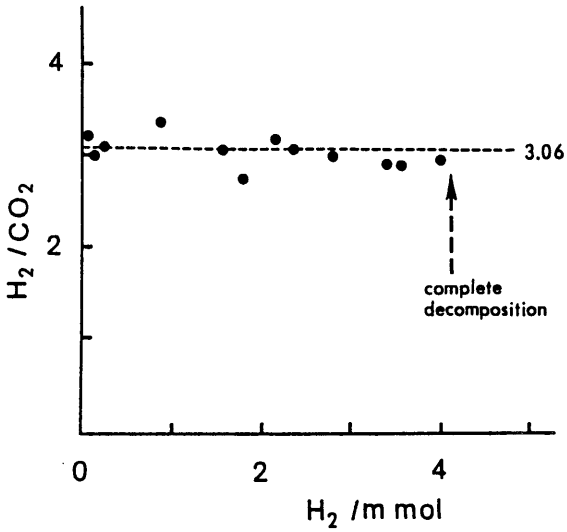

Figure 1. Ratio of hydrogen to carbon dioxide produced during the complete decomposition of *n*-hexadecane ($C_{16}H_{34}$). Light source: 1-kW Xe lamp. Photocatalyst: Pt/TiO_2. Total irradiation time: ~700 h.

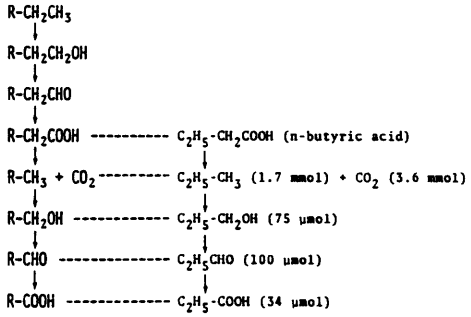

Figure 2. Photocatalytic oxidation process of a linear saturated hydrocarbon and the oxidation products from *n*-butyric acid. Light source: 1-kW Xe lamp. Photocatalyst: TiO_2 in the presence of $AgNO_3$. Irradiation time: 19 h.

the ·OH radical, our result for *n*-hexadecane could be explained by eq 2–9.

(I) formation of an alcohol and a carboxylic acid

$$H_2O + p \rightarrow \cdot OH + H^+ \qquad (2)$$

$$H^+ + e \rightarrow {}^1/_2H_2 \qquad (3)$$

$$RCH_2CH_3 + 2\cdot OH \rightarrow RCH_2CH_2OH + H_2O \qquad (4)$$

$$RCH_2CH_2OH \rightarrow RCH_2CHO + H_2 \qquad (5)$$

$$RCH_2CHO + H_2O \rightarrow RCH_2COOH + H_2 \qquad (6)$$

$$2 \times [(2) + (3)] + (4) + (5) + (6)$$

$$RCH_2CH_3 + 2H_2O \rightarrow RCH_2COOH + 3H_2 \qquad (7)$$

(II) decomposition of a carboxylic acid (photo-Kolbe reaction)[18-21]

$$RCH_2COOH \rightarrow RCH_3 + CO_2 \qquad (8)$$

(III) total reaction

$$RCH_2CH_3 + 2H_2O \rightarrow RCH_3 + 3H_2 + CO_2 \qquad (9)$$

As seen in eq 9, three H_2 molecules and one CO_2 molecule are produced along with a decrease of one in the carbon number. This process is shown in Figure 2. When the above reactions (eq 4–6

(18) B. Kraeutler and A. J. Bard, *J. Am. Chem. Soc.*, **100**, 2239 (1978).
(19) B. Kraeutler, C. D. Jaeger, and A. J. Bard, *J. Am. Chem. Soc.*, **100**, 4903 (1978).
(20) B. Kraeutler and A. J. Bard, *J. Am. Chem. Soc.*, **100**, 5985 (1978).
(21) T. Sakata, T. Kawai, and K. Hashimoto, *J. Phys. Chem.*, in press.

and 8) are assumed to proceed successively, the result in Figure 2 is explained well. This assumption means that the intermediate products of this reaction, RCH_2CH_2OH, RCH_2CHO, and RCH_2COOH, are oxidized much faster than the saturated hydrocarbons.

Product Analysis. In order to find evidence to support the previous reaction scheme, we carried out the photocatalytic reaction of *n*-pentane (40 vol %), one of the simpler hydrocarbons, in an aqueous medium in the presence of silver ion (5 mmol). In this case the photo-Kolbe type of reaction proceeds through H atom extraction from acids, aldehydes, or alcohols instead of the addition of H atom produced by the reduction of water.[21] O_2 production besides CO_2 was also observed at an early stage of irradiation. The total amount of O_2 produced was 0.83 mmol after 14-h irradiation. This indicates that the oxidation of *n*-pentane is not efficient and is in competition with the oxidation of water. The main product in the aqueous phase was acetic acid with about 60 μmol produced after 40-h irradiation. Small amounts of propionic acid, acetaldehyde, ethanol, methanol, and several unknown products were also detected. This result seems to support the reaction scheme described by eq 2–8.

We also investigated the decomposition of *n*-butyric acid (n-C_3H_7COOH) (10 vol %) in an aqueous medium in the presence of silver ion (5 mmol). After 19-h irradiation, *n*-propyl alcohol (75 μmol), propionaldehyde (102 μmol), and propionic acid (34 μmol) were produced as the main products as well as propane (1.7 mmol) and CO_2 (3.6 mmol). This result is shown in Figure 2. Besides the above products, small amounts of ethanol (0.92 μmol), acetaldehyde (6.0 μmol), and acetic acid (4.6 μmol) were detected. Moreover, O_2 was not produced for the decomposition of *n*-butyric acid, which indicates that *n*-butyric acid is oxidized more easily than *n*-pentane through the photocatalytic process. Taking all these results into account, we conclude that an aliphatic hydrocarbon is oxidized mainly according to eq 2–8 successively, because the intermediate products are much more reactive than the starting material. Thus, one oxidation cycle makes three H_2 molecules and one CO_2 molecule as shown in eq 9.

We have described above only the simplest and probably the main path. There are, however, many other paths besides that. For example, according to the above reaction scheme, simple hydrocarbons such as methane, ethane, and propane are expected to be produced in the gas phase. However, such hydrocarbons were barely detected even at the last stage of reaction for the complete decomposition of *n*-hexadecane. This fact suggests that the H_2 attached to a carbon chain are attacked rather randomly by ·OH radicals to produce various alcohols with many OH groups. Such a reaction is more favorable to H_2 production than to hydrocarbon production.[4,21]

Aromatic Compounds. Hydrogen Production. Several aromatic compounds also serve as the electron donor for the reaction of the present photocatalytic H_2 production with Pt/TiO_2 as is shown in Table Ib. The rates in the alkaline region are also about 5–10 times larger than those without NaOH. They depend on the concentration of the hydrocarbons. For example, the rate takes a maximum value at the volume ratio of benzene to water of about 1/30. As the ratio increases, it decreases remarkably and H_2 cannot be detected with pure benzene. The alcohol–water mixture is in marked contrast to the benzene–water mixture, because the rate increases with larger concentrations of the alcohols and it takes a maximum value for the pure alcohol such as methanol and ethanol. In the case of aromatic hydrocarbons, CO_2 is also produced from an early stage of irradiation. For example, in the case of benzene the ratio of H_2 to CO_2 was about 2.5. When NaOH was added to the solution, a trace amount of phenol (H_2/phenol > 1000) was produced.

Direct Oxidation of Benzene by Photogenerated Holes. It has been considered that the oxidation of benzene also starts by the hydroxylation of the benzene ring the same as the oxidations of aliphatic hydrocarbons.[9-12] However, we will propose the possibility of the direct oxidation of benzene by photogenerated holes in the valence band of TiO_2. It can be ensured from several reasons described below. At first, biphenyl (180 μmol) was produced from deaerated pure benzene with Ag_2SO_4 (0.5 mmol) and TiO_2 powder after 170 h irradiation, although no gaseous product was detected in this case. The production rate of biphenyl was slow, which can be explained by the following two reasons: (a) The ionization potential of pure benzene is much larger than that in aqueous solution because of the small stabilization energy of benzene cation radical in pure benzene. (b) The concentration of silver ion is small because Ag_2SO_4 is hardly dissolved in it. Thus, it is considered that the direct oxidation in water occurs more easily and faster. Secondly, Aikawa and Sukigara reported the measurement of the mobility and the electrical charge of photosensitive particles in a dielectric liquid with a photoelectrical transient technique.[22] They observed that a negative charge was accumulated on TiO_2 powder suspended either in benzene water mixture or in pure benzene under UV light irradiation. The magnitude of the electrical negative charge of TiO_2 powder in water–benzene mixture was only 2 times larger than that in pure benzene. This suggests that photogenerated holes were scavenged by both water and benzene molecules. On the other hand the half-wave potential of the anodic oxidation of benzene in acetonitrile was reported to be 2.54–2.62 V vs. NHE.[23,24] In general, the potential value starting an oxidation is about 0.3 V more negative than a half-wave potential. Thus, if the value is assumed to be approximately the same as that in a neutral aqueous solution, the oxidation of benzene would start from around 2.2–2.3 V vs. NHE. Since the valence band edge position of TiO_2 is reported to be 2.4[25]–2.8[26] V vs. NHE at pH 7,[27] the direct electron transfer from benzene molecule in a neutral aqueous solution to the photogenerated holes in TiO_2 seems to be possible.

It has been established by pulse radiolysis that benzene radical cation reacts rapidly (≤0.1 μs) with water to give hydroxycyclohexadienyl radical,[28] which leads to simultaneous formation of phenol[29,30] and hydroxymucondialdehyde (HMD)[31-34] in the presence of O_2. Taking all these facts into consideration, we conclude that the direct oxidation of benzene by photogenerated holes (eq 10) also proceeds in competition with ·OH radical addition to the benzene ring (eq 11). Both reactions yield the hydroxycyclohexadienyl radical, which is the primary intermediate of the present photocatalytic reaction.

Oxidation Process of Benzene. Benzene is mainly oxidized to CO_2 with several other minor products. CO_2 is also produced from an early stage of irradiation. Thus, the intermediate oxidation products should be much more reactive than benzene by the same reasoning as was done for the decomposition of aliphatic compounds. We carried out product analysis for several aromatic compounds in the presence of 1 mmol of silver ion (0.5 mmol of Ag_2SO_4).[35] The relative reactivities of these compounds can be

(22) Y. Aikawa, T. Takahashi, and M. Sukigara, *J. Chem. Soc. Jpn., Chem. Ind. Chem.*, 292 (1984).
(23) J. W. Loveland and G. R. Dimeler, *Anal. Chem.*, 33, 1196 (1961).
(24) E. S. Pysh and N. C. Yang, *J. Am. Chem. Soc.*, 20, 2124 (1963).
(25) K. Honda, A. Fujishima, and T. Inoue, "Hydrogen Energy Progress", T. N. Veziroglu, K. Fueki, and T. Ohta, Eds., Proceedings of the 3rd World Hydrogen Energy Conference, Tokyo, Japan, Pergamon Press, Oxford, 1980, pp 753–63.
(26) H. Gerischer, "Solar Energy Conversion", Topics in Applied Physics, Vol. 31, B. O. Seraphin, Ed., Springer-Verlag, West Berlin, 1979.
(27) In these experiments, the solution was not buffered, so that the pH changes continuously during the photolysis. For example, in the case of benzene with silver ion, the pH changed from 5.0 to 1.5 for 100-h irradiation. Therefore, the valence band edge is more positive than the value in the text under this condition, but this shift makes the direct oxidation of benzene easier.
(28) P. Neta and R. W. Fessenden, *J. Am. Chem. Soc.*, 99, 163 (1977).
(29) M. K. Eberhardt, *J. Am. Chem. Soc.*, 103, 3876 (1981).
(30) M. P. Irion, W. Fuss., and K.-L. Kompa, *Appl. Phys.*, B27, 191 (1982).
(31) I. Loeff and G. Stein, *J. Chem. Soc.*, 2623 (1963).
(32) L. M. Dorfman, I. A. Taub, and R. E. Bühler, *J. Chem. Phys.*, 36, 3051 (1962).
(33) I. Balakrishnan and M. P. Reddy, *J. Phys. Chem.*, 76, 1273 (1972).
(34) N. Jacob, I. Balakrishnan, and M. P. Reddy, *J. Phys. Chem.*, 81, 17 (1977).
(35) In these experiments 1 mmol of silver ion was added to the solution. First O_2 and CO_2 were produced, and H_2 started evolving instead of O_2 after 50–100 h of irradiation. We analyzed the products in the liquid phase at this time.

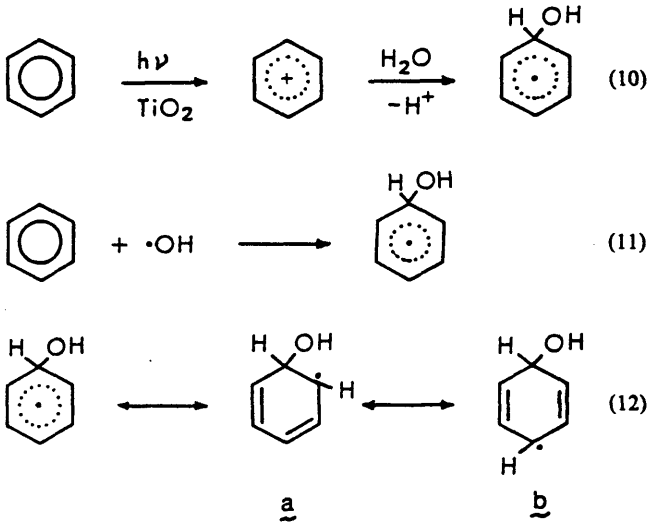

also determined from the rates of O_2 production.[36] The results are shown in Table II. In these experiments the concentrations of the reactants were equalized in order to compare their reactivities.[37] Although there were other unknown peaks, only the species which could be assigned are shown. Phenol, catechol, and muconic acid were produced in an aqueous solution of benzene. Muconic acid and catechol were detected as the oxidation products of catechol and phenol, respectively. Since muconic acid produces CO_2 by the photo-Kolbe reaction, these results suggest that the oxidation proceeds partially by way of phenol, catechol, and muconic acid (Figure 3, path 7 → 8 → 9) and that muconic acid is oxidized to produce CO_2. In fact, it is known that phenol is easily oxidized to muconic acid via catechol by peracetic acid in the metal-catalyzed reaction.[38] However, it can be considered that the main path of CO_2 production exists besides that. This is expected for the following three reasons: (a) Muconic acid could not be detected for the photocatalytic reaction of phenol although it could for that of benzene. (b) Much more hydroquinone was produced than catechol for the decomposition of benzene whereas these quantities were nearly equal for the decomposition of phenol. (c) The total amount of CO_2 produced for the photocatalytic reaction of benzene is about 3 times larger than those for phenol and catechol.

Moreover, the initial production rate of CO_2 from saturated aqueous solutions of benzene is also 2 or 3 times larger than those from aqueous solutions of phenol and catechol. In Table III are shown the initial rates of CO_2 production for aqueous solutions of various compounds in the presence of 1 mmol of silver ion. Due to the poor activity of these compounds, O_2 was also produced. The O_2 production rate is also shown in this table. The rate of CO_2 production from muconic acid is much larger than those from other aromatic compounds,[37] so that if the benzene ring opening occurs accompanied by muconic acid formation, CO_2 will be produced easily by the successive decomposition of muconic acid. The experimental result shows that lots of CO_2 is produced even at an early stage of the reaction for the decomposition of benzene. Therefore, if the benzene ring opening occurs mainly by way of phenol and catechol, it has to be assumed that the reactivities of phenol and catechol should be much larger than that of benzene. However, the reactivities of these compounds are in the order of

$$\text{catechol} > \text{benzene} > \text{phenol} \qquad (13)$$

which was determined from the O_2 production rates. This means that the above assumption is not reasonable and the path 7 → 8 → 9 is a minor one.

On the other hand, in the radiolysis of the aqueous benzene solution under O_2, it is known that O_2 is added to hydroxycyclohexadienyl radical as follows:

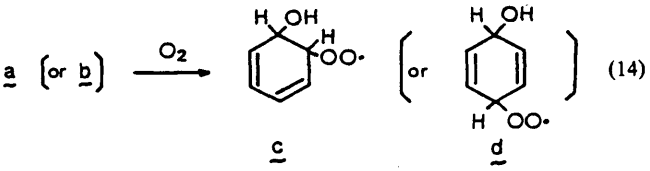

c and d give phenol with H_2O, or the ring opens by way of c or d, forming hydroxymucondialdehyde (HMD).[31-34] This ring-opening process is in competition with the phenol formation. Phenol and HMD are both "primary" products in the sense that their formation does not involve any of the stable reaction products as intermediates. The existence of O_2 is indispensable for both the benzene ring opening and the phenol formation.[31] Thus, in the case of the present photocatalytic oxidation reaction, it may be considered that a similar path also exists (Figure 3, path 11 → 12 → 13) besides phenol formation. In this case intermediate products do not have an aromatic nature. Since they are alcohols, aldehydes, and acids, they are oxidized easily to CO_2 successively

TABLE II: Photocatalytic Oxidation Products after Consuming 1 mmol of Silver Ion[a]

	products, μmol		
	gas phase		
reactant	O_2	CO_2	liquid phase
benzene	8.0	110	biphenyl (3.0), phenol (21), catechol (1), hydroquinone (13), muconic acid (1.0)
phenol	24	27	catechol (17), hydroquinone (23), muconic acid (none)
catechol	0.6	38	muconic acid (3.5)
hydroquinone	3.4	98	muconic acid (none)
muconic acid	5.0	380	

[a] Light source: 1-kW Xe lamp. Irradiation time: 50–100 h. Photocatalyst: TiO_2. Ag_2SO_4: 0.5 mmol. See note 37.

TABLE III: Initial Rates of Carbon Dioxide and Oxygen Production in the Presence of Silver Ion[a]

	initial production rate, μmol/h	
reactant[b]	O_2	CO_2
benzene	2.1	13
phenol	7.8	5.4
catechol	0.3	7.9
hydroquinone	0.4	2.4
muconic acid	(5.0)[c]	71

[a] Ag_2SO_4: 0.5 mmol. [b] Reactant: 1.3 mmol. Light source: 1-kW Xe lamp. Photocatalyst: TiO_2. [c] See note 37.

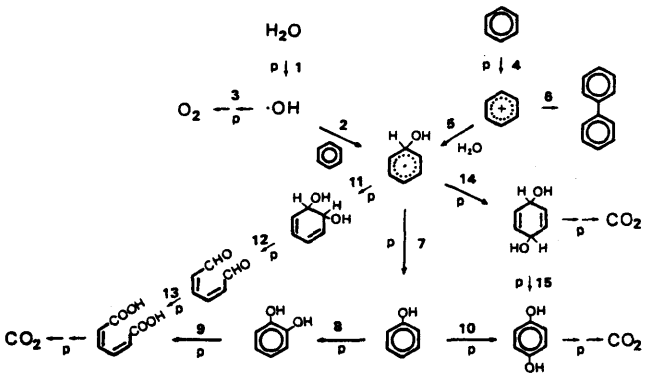

Figure 3. Reaction scheme of photocatalytic oxidation of benzene in water.

On the other hand, in the radiolysis of the aqueous benzene solution under O_2, it is known that O_2 is added to hydroxycyclohexadienyl radical as follows:

(36) The O_2 production is in competition with the oxidation of reactants as shown in Figure 3. Thus, a large O_2 production rate corresponds to a poor activity of a reactant.

(37) The solubility of benzene in water is about 0.205 wt % at 50 °C (J. A. Riddick and W. B. Bunger, "Organic Solvents", 3rd ed., Wiley, New York, 1970, p 107), which corresponds to 1.3 mmol/50 mL of aqueous solution, so that the same molar amounts of the other compounds were added to 50 mL of neutral water. However, the solubility of muconic acid in water is much lower than that of benzene, so that the reactivity of muconic acid cannot be compared to those of others by the O_2 production rate.

(38) A. J. Pandell, *J. Org. Chem.*, **41**, 3992 (1976).

TABLE IV: Amounts of Carbon Dioxide and Oxygen Produced by Photocatalytic Decomposition of Aqueous Solution of Benzene in the Presence of Silver Ion[a]

	SnO_2	WO_3	TiO_2	$SrTiO_3$	Fe_2O_3
CO_2, μmol	140	160	110	30	3
O_2, μmol	0	60	10	70	0

[a] Light source: 1-kW Xe lamp. Irradiation time: 65 h. Ag_2SO_4: 0.5 mmol. See note 40.

as described in the previous section. These processes are different from the radiolysis because the phenol formation and the ring opening occur even in the absence of O_2. Although it may be premature to speculate on the detailed mechanism, all the experimental results could be explained well with the following process; that is, the hydroxycyclohexadienyl radical is oxidized further by photogenerated holes of TiO_2 and the reaction proceeds as follows:

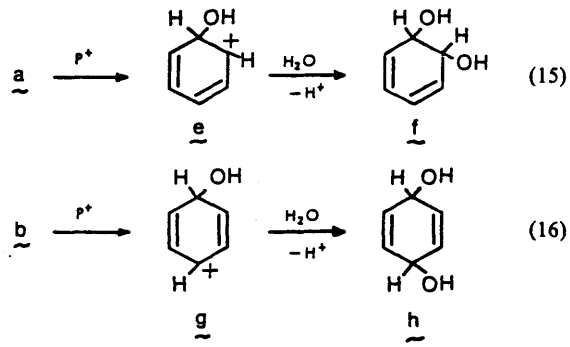

(15)

(16)

The possibility of ·OH addition to a and b can be ruled out, because in the radiolysis experiment the existence of O_2 is indispensable for the formation of phenol and HMD.[31] Equations 15 and 16 correspond to the O_2 addition process in the radiolysis, but here hydroxycyclohexadienyl radical is oxidized by photogenerated holes instead of O_2.

As is well-known 1,2 diol is easily oxidized, breaking the C–C bond to yield an aldehyde which is much more easily oxidized than benzene. Thus, muconic acid forms from f (Figure 3, path 11 → 12). The muconic acid thus formed is easily oxidized to CO_2.

1,4 diol (h) may be also decomposed partially, but the main reaction is probably the formation of hydroquinone (Figure 3, path 15). The experimental result that much more hydroquinone was produced than catechol can be also explained well by the above consideration.

The formation of phenol can be thought of as proceeding mainly by the direct oxidation of hydroxycyclohexadienyl radical by photogenerated holes (Figure 3, path 7), because H_2 atom extraction by ·OH radical is very difficult.[31] Fujihira et al. reported that phenol is the main product of the photocatalytic oxidation of acidic aqueous benzene solution in the presence of O_2.[10] This is quite different from the present result, in which the main product is CO_2 (110 μmol) more than phenol (21 μmol). This discrepancy might be explained as follows. Reaction 14 also proceeds in the presence of O_2 besides reactions 15 and 16, and the phenol formation from c or d may be catalyzed by acids.[39]

Various oxidation processes of benzene are schematically illustrated in Figure 3 and are summarized as follows. Benzene forms hydroxycyclohexadienyl radical with both the ·OH radical addition (path 1, 2) and the direct oxidation by photogenerated holes (path 4, 5) proceeding in parallel, and this radical is oxidized to phenol (path 7) or muconic acid (path 11 → 12 → 13) by holes. Muconic acid is oxidized to CO_2. CO_2 is also produced partially by the further oxidation of phenol (path 7 → 8 → 9 → 11).

Photocatalytic Oxidation of Benzene with Various Powdered Semiconductors. When certain types of powdered semiconductors were used instead of TiO_2, CO_2 and O_2 were produced under irradiation from benzene–water mixtures in the presence of Ag^+.

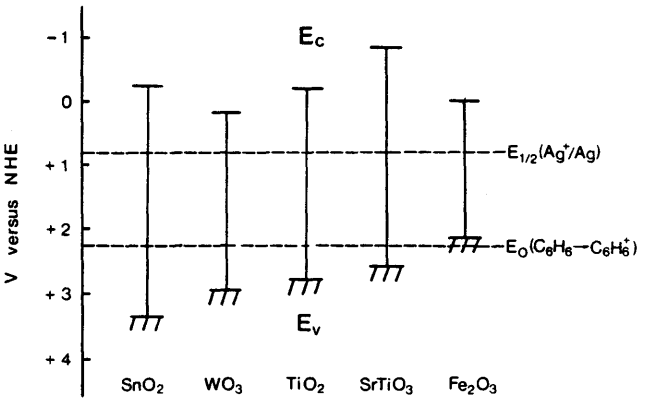

Figure 4. Band edge positions of various semiconductors at pH 7 vs. NHE.[27] Half-wave redox potential of Ag^+/Ag ($E_{1/2}$) and the potential where the oxidation of benzene occurs (E_0) are also illustrated (see the text).

The results and the energy levels of the semiconductors used are shown in Table IV and Figure 4,[27] respectively. In addition to the energy levels of semiconductors, the efficiencies of these reactions were also dependent on the lifetime of the minority carrier, surface states, and the adsorption and catalytic properties of the surface of reaction sites. Roughly speaking, however, the comparison between the rates of the CO_2 production and the energy levels of the semiconductors indicates that a semiconductor having a stronger oxidation power (the valence band position is more positive) leads to a higher yield of CO_2.[40] This may be explained by using the result obtained in the previous section. Namely, the direct oxidation of both benzene and the hydroxycyclohexadienyl radical by photogenerated holes is easier with a semiconductor possessing a deeper valence band, and this results in greater CO_2 production. Moreover, the ratio of CO_2 production to O_2 production is also dependent on the type of semiconductor. These reactions compete with each other. According to the mechanism described previously, a semiconductor with a deeper valence band should give a higher ratio of CO_2 to O_2 since the direct oxidation of benzene (path 4) becomes more efficient under this condition. In fact, the general tendency in Table IV agrees with this explanation.

Fossil Fuels. We applied the present H_2-producing method to the gasification of natural fossil fuels; that is, the fossil fuels were used as the electron donors for photocatalytic reactions. The model compounds of the fossil fuels are composed of unit structures connected by aliphatic hydrocarbons. The unit structures consist of aromatic and condensed aromatic compounds.[15] Thus, it can be considered that these photocatalytic reactions are the extensions of the present subject. Sato et al. reported that coal (Texas lignite) reacted with water vapor to form H_2 and CO_2 by irradiation of Pt/TiO_2.[41]

In Table Ic are shown the initial H_2 production rates from mixtures of fossil fuels and water. In these cases neither silver ion nor O_2 was added to the solution. The rates were about 1 μmol/h in the neutral region in the case of any coal, tar sand, or pitch. However, the rate increased remarkably, about 10 times, when NaOH was added to the solution. The quantum yields of these H_2-producing reactions in the alkaline region correspond to about 0.5% at 380 nm. When D_2O was used instead of H_2O for the aqueous suspension of coal, D_2 was 86% of the hydrogen gas produced, DH 10%, and H_2 4%. This result indicates that water is reduced through the photocatalytic process and the fossil fuels serve as electron donors. H_2 was the only gaseous reaction

(39) For example, J. H. Baxendale and J. Magee, *Discuss. Faraday Soc.*, **14**, 160 (1953).

(40) For rigorous comparison of the oxidation rates, we have to use the quantum yields of the reactions, although their measurements are difficult in these systems. For example, the band gap of SnO_2 is much larger than those of the others, so that the absorbed photon number is smaller. This means that the quantum yield of CO_2 production rate for the SnO_2 system may be much larger than those for other systems. However, this tendency agrees with the consideration in the text.

(41) S. Sato and J. M. White, *Ind. Eng. Chem. Prod. Res. Dev.*, **19**, 542 (1980).

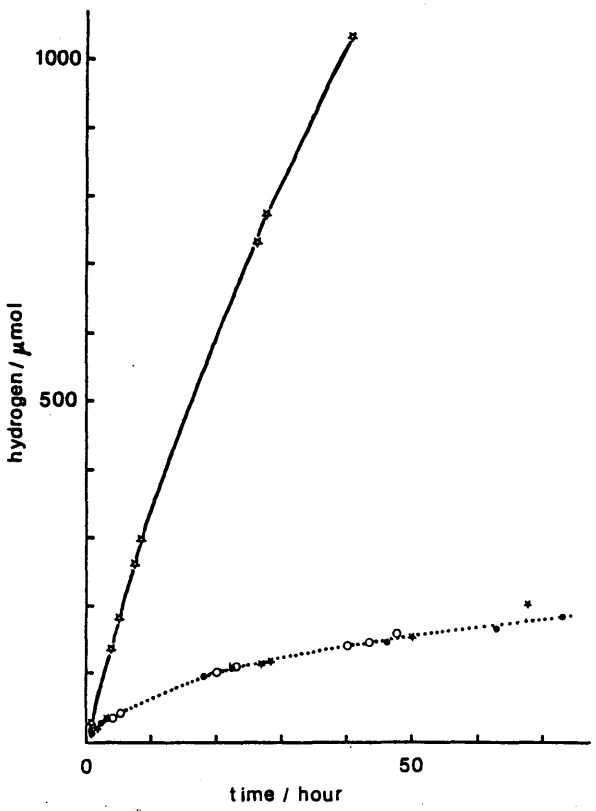

Figure 5. Hydrogen productions from water with phenol and fossil fuels: (☆) phenol, (★) pitch, (○) tar sand, (●) coal, 1 N NaOH solution. Light source: 500-W Xe lamp. Photocatalyst: Pt/TiO_2.

product in alkaline solutions, while CO_2 was also produced without NaOH. The ratio of H_2 to CO_2 was also about 2–3. However, the reaction rate decreases gradually under irradiation. This tendency is quite different from that of a pure organic compound. Figure 5 represents the H_2 production from the aqueous solution of phenol vs. time (solid line). In this case the rate does not decrease remarkably after 30-h irradiation. Furthermore, the rate did not show any change after leaving this reaction bulb as it was for over 1 month under room light. This same property is observed for the alcohol–water and glucose–water mixtures and suggests that this photocatalyst is rather stable under irradiation even in a concentrated alkaline solution. However, the situation is quite different for fossil fuel–water mixtures. The dotted line in Figure 5, which represents the H_2 production from fossil fuel–water mixtures, shows that the rates decrease gradually under irradiation. The rates after 40-h irradiation were 10 times smaller than those during an early stage of irradiation. Even after the photocatalyst was filtered and was mixed again with a fresh coal, the rate did not recover. These results suggest that the activity of the photocatalyst itself was reduced in these cases. One of the main reasons for these results may be explained by the effect of various metal ions, for instance Fe ion, which are contained in fossil fuels. They might be adsorbed on the surface at TiO_2 and serve as a recombination center of electrons and holes, which would decrease the photocatalytic activity. For example, the rate of H_2 production from an ethanol–water mixture with Fe-adsorbed TiO_2 (Fe/TiO_2) was about half of that with TiO_2 alone.

Conclusion

It was shown that fossil fuels and hydrocarbons can produce H_2 by reacting with water at room temperature with the aid of light energy and a semiconductor photocatalyst. Several interesting organic compounds are found to be produced for the photocatalytic reactions of hydrocarbons. The mechanisms of CO_2 production from the aqueous solutions of a linear saturated hydrocarbon and benzene are presented. These compounds are oxidized to acids and the photo-Kolbe type of reaction occurs, producing CO_2. Generally speaking, if the intermediate products from a hydrocarbon to a corresponding acid are more reactive than the starting material, they are oxidized successively, resulting in CO_2 as a main product.

Registry No. TiO_2, 13463-67-7; Pt, 7440-06-4; Ag^+, 14701-21-4; H_2, 1333-74-0; O_2, 7782-44-7; CO_2, 124-38-9; $C_{16}H_{34}$, 544-76-3; *n*-pentane, 109-66-0; *n*-heptane, 142-82-5; isooctane, 540-84-1; polyethylene, 9002-88-4; benzene, 71-43-2; phenol, 108-95-2; pyridine, 110-86-1; catechol, 120-80-9; hydroquinone, 123-31-9; muconic acid, 505-70-4.

Reprinted from The Journal of Physical Chemistry, 1984, 88, 2344.

Heterogeneous Photocatalytic Reactions of Organic Acids and Water. New Reaction Paths besides the Photo-Kolbe Reaction

Tadayoshi Sakata,* Tomoji Kawai,† and Kazuhito Hashimoto

Institute for Molecular Science, Myodaiji, Okazaki 444, Japan *(Received: June 27, 1983)*

The heterogeneous photocatalytic reactions of acetic, propionic, and butyric acids were studied on several kinds of powdered semiconductors, mainly TiO_2. The influence of Ag^+ as an electron acceptor, and the dependence of the reactions on the kind of semiconductor and pH, were investigated. The ratio of yields of hydrogen to hydrocarbon depends strongly on pH. At neutral or alkaline pH, hydrocarbon stops being evolved and only hydrogen is evolved. It is concluded that the pH dependence of the valence band position of the semiconductor and the concentration of OH^- ion control the reaction paths. From the pH dependence of methane production from acetic acid the valence band of anatase is estimated to be located more deeply by 0.1 eV than that of rutile. The results of product analysis and the complete decomposition of acetic acid to CO_2 show that there exist new reaction paths in which water is an oxidizing agent. Reaction schemes of these organic acids are proposed.

Introduction

The photocatalytic reactions of powdered semiconductors have been investigated because of their potential application to the direct conversion of solar energy into chemical energy.[1] One of the most important applications is the water-splitting reaction.[2] Other photocatalytic reactions such as oxidation of cyanide,[3,4] sulfite,[4] acetate,[5] hydrocarbons,[6-9] and other substances[10] have been investigated. Recent studies from this laboratory have shown photocatalytic hydrogen production from the reactions of water with various organic compounds such as alcohols,[11,12] carbohydrates,[13] hydrocarbons,[14] fossil fuels,[14] artificial high polymers,[15,16] and biomasses[15,16] with powdered semiconductor photocatalysts. In these reactions, organic molecules are oxidized and water is reduced to produce hydrogen. In several cases hydrogen production is very efficient.[11,12] On the other hand, hydrocarbon formation was reported by Bard et al. by the photocatalytic decomposition of organic acids such as acetic acid.[17-22] They also observed methyl radical as an unstable intermediate during the photocatalytic reaction of acetic acid.[22] Sato reported photocatalytic synthesis of ethane from acetic acid in the vapor phase.[23] Recently Yoneyama et al. investigated the factors influencing product distribution in the photocatalytic decomposition of aqueous acetic acid on platinized TiO_2.[24] They found that the relative yield of ethane to methane produced was high when the decomposition rate was high and that the amount of CO_2 produced exceeded that of methyl radical consumed in thee formation of methane and ethane. They also found that the ratio of yields of ethane to methane increased linearly with illumination intensity. In these reactions organic acids are decomposed into hydrocarbons and CO_2. Water was not thought to be involved in the main reactions. However, we have found that these reactions depend strongly on pH. In alkaline medium organic acids produce only hydrogen. In order to clarify the reaction mechanism, we analyzed the reaction products quantitatively in the aqueous medium. In this report we would like to discuss new reaction paths besides Kolbe type ones for the photocatalytic decomposition of organic acids and on the involvement of water in the reaction.

Experimental Section

Materials. Acetic acid (CH_3COOH, glacial, special grade, Katayama Chemicals), $CH_3COONa{\cdot}3H_2O$ (Special grade, Katayama Chemicals), propionic acid (guaranteed reagent, Katayama Chemicals), *n*-butyric acid (guaranteed reagent, Katayama, Chemicals), NaOH (guaranteed reagent, Kanto Chemicals), ethanol (guaranteed reagent, 99.5%, Kanto Chemicals), and deuterated water (D_2O, 99.75%, Merck) were used without further purification. The TiO_2 powders were undoped rutile (TiO_2(r), grain size: 0.2 μm, 99.99%, Furuuchi Ltd.), doped rutile (produced from the undoped rutile by heating under a hydrogen atmosphere of 200 torr at 600 °C for 1 h), and undoped anatase (TiO_2(a), grain size: 0.15 μm, Fuji Titanium Ltd., TP-2, 99.9%). Powdered WO_3 (99.99%, Furuuchi Ltd.), $SrTiO_3$ (99.9%, grain size: 1.7 μm, Soekawa Chemicals), and Fe_2O_3 (Katayama Chemicals, 99.9%) were also used. Pt was deposited by illuminating each powdered semiconductor (1.0 g) suspended in a water–ethanol solution (20% aqueous solution, 200 mL) of K_2PtCl_6 (0.182 g) with white light from a 500-W Xe lamp through Pyrex. In a similar way, various metals (Pd, Rh, Au, Cu, Ag) were deposited

† Present address: Osaka University, Institute of Scientific and Industrial Research, Mihogaoka, Ibaraki 567, Osaka, Japan.

(1) See, e.g.: (a) T. Freund and W. P. Gomes, *Catal. Rev.*, **3**, 1 (1969); (b) A. J. Bard, *J. Photochem.*, **10**, 59 (1979); (c) A. J. Bard, *Science*, **207**, 139 (1980), and references therein; (d) M. Grätzel, *Ber. Bunsenges. Phys. Chem.*, **84**, 981 (1980); (e) M. Grätzel, *Acc. Chem. Res.*, **14**, 376 (1981).
(2) See, e.g.: (a) A. Fujishima and K. Honda, *Bull. Chem. Soc. Jpn.*, **44**, 1148 (1971); *Nature (London)*, **238**, 37 (1972); (b) G. N. Schrauzer and T. D. Guth, *J. Am. Chem. Soc.*, **99**, 7189 (1977); (c) H. Yoneyama, M. Koizumi, and H. Tamura, *Bull. Chem. Soc. Jpn.*, **52**, 3449 (1979); (d) J. M. Lehn, J. P. Sauvage, and R. Ziessel, *Nouv. J. Chim.*, **4**, 623 (1980); (e) T. Kawai and T. Sakata, *Chem. Phys. Lett.*, **72**, 87 (1980); (f) S. Sato and J. M. White, *ibid.*, **72**, 85 (1980); (g) K. Domen, S. Naito, H. Soma, T. Ohnishi, and K. Tamaru, *J. Chem. Soc., Chem. Commun.*, 543 (1980); (h) F. T. Wagner and G. A. Somorjai, *J. Am. Chem. Soc.*, **102**, 5494 (1980); (i) D. Dounghong, E. Borgarello, and M. Grätzel, *ibid.*, **103**, 4685 (1981); (j) K. Kalyanasudaram, E. Borgarello, and M. Grätzel, *Helv. Chim. Acta*, **64**, 362 (1981).
(3) S. N. Frank and A. J. Bard, *J. Am. Chem. Soc.*, **99**, 303 (1977).
(4) S. N. Frank and A. J. Bard, *J. Phys. Chem.*, **81**, 1484 (1977).
(5) B. Krauetler and A. J. Bard, *J. Am. Chem. Soc.*, **100**, 5985 (1978).
(6) I. Izumi, W. W. Dunn, K. O. Wilbourn, Fu-Ren F. Fan, and A. J. Bard, *J. Phys. Chem.*, **84**, 3207 (1980).
(7) M. Fujihira, Y. Sato, and T. Osa, *Nature (London)*, **293**, 206 (1981).
(8) M. Fujihira, Y. Sato, and T. Osa, *Chem. Lett.*, 1053 (1981).
(9) S. Sato and J. M. White, *Chem. Phys. Lett.*, **70**, 131 (1980).
(10) See, e.g.: (a) T. Watanabe, T. Takizawa, and K. Honda, *J. Phys. Chem.*, **81**, 1845 (1977); (b) M. Miyake, H. Yoneyama, and H. Tamura, *Bull. Chem. Soc. Jpn.*, **50**, 411 (1977); (c) T. Inoue, A. Fujishima, S. Konishi, and K. Honda, *Nature (London)*, **277**, 637 (1979); (d) T. Kanno, T. Oguchi, H. Sakuragi, and K. Tokumaru, *Tetrahedron Lett.*, **21**, 4673 (1980); (e) M. A. Fox and C. Chen, *J. Am. Chem. Soc.*, **103**, 6757 (1981).
(11) T. Kawai and T. Sakata, *J. Chem. Soc., Chem. Commun.*, 694 (1980).
(12) T. Sakata and T. Kawai, *Chem. Phys. Lett.*, **80**, 341 (1981).
(13) T. Kawai and T. Sakata, *Nature (London)*, **286**, 474 (1980).
(14) T. Sakata and T. Kawai, *J. Synth. Org. Chem., Jpn.*, **39**, 589 (1981).
(15) T. Kawai and T. Sakata, *Chem. Lett.*, 81 (1981).
(16) T. Sakata and T. Kawai, *Nouv. J. Chim.*, **5**, 279 (1981).
(17) B. Kraeutler and A. J. Bard, *J. Am. Chem. Soc.*, **99**, 7729 (1977).
(18) B. Kraeutler and A. J. Bard, *J. Am. Chem. Soc.*, **100**, 2239 (1978).
(19) B. Kraeutler and A. J. Bard, *J. Am. Chem. Soc.*, **100**, 5985 (1978).
(20) B. Kraeutler and A. J. Bard, *Nouv. J. Chim.*, **3**, 31 (1979).
(21) I. Izumi, Fu-Ren F. Fan, and A. J. Bard, *J. Phys. Chem.*, **85**, 218 (1981).
(22) B. Kraeutler, C. D. Jaegger, and A. J. Bard, *J. Am. Chem. Soc.*, **100**, 4903 (1978).
(23) S. Sato, *J. Chem. Soc., Chem. Commun.*, 26 (1982).
(24) H. Yoneyama, Y. Takao, H. Tamura, and A. J. Bard, *J. Phys. Chem.*, **87**, 1417 (1983).

0022-3654/84/2088-2344$01.50/0

on the powdered TiO_2 (rutile, doped) in water–ethanol solution of the corresponding chlorides or nitrate ($PdCl_2$, $RhCl_3$, $AuCl_3$, $CuCl_2$, $AgNO_3$). The solution was decolorized as the deposition of the metals onto the TiO_2 surface occurred. The powdered TiO_2 loaded with the metal was washed several times with distilled water and dried at 60 °C in the air for 1 day. Even after this treatment, a small amount of organics was found to be left on the photocatalyst. This was confirmed by the fact that a small amount of H_2 and CO_2 was produced when its suspension in distilled water was irradiated with a 500-W Xe lamp. The evolution rate was on the order of 1–2 μmol/h in the beginning and decreased with time. In order to remove this organic impurity, the photocatalyst in pure water was irradiated for 1 or 2 days before the experiment.

Apparatus, Photolysis, and Product Analysis. A 500-W Xe lamp (Ushio, UXL 500) or a 1000-W Xe lamp (Ushio, UIC-1001C3) operated at 500 W was used as the light source. The powdered semiconductor photocatalyst (0.30 gr) was suspended in a deaerated aqueous solution of an organic acid in a 280-mL Pyrex bulb, which transmits light of wavelength longer than 320 nm. When the glass bulb was irradiated from the bottom with white light from the 500-W Xe lamp, gas bubbles evolved. Gaseous reaction products were trapped at −196 or −40 °C and analyzed by a quadrupole-mass spectrometer (Anelva, AGA-360) as described previously.[12] The mass-spectrometric analysis of the gaseous products which could not be trapped at −196 °C showed that hydrogen and methane were the main products in the photocatalytic reaction of acetic acid under acidic conditions. The ratio of methane to hydrogen was determined by comparing the intensity ratio of their mass spectra with those of a known mixture of H_2 and CH_4 (1:1). Their quantities were determined from the pressure by using a sensitive manometer (Datametrics Inc., Barocel pressure sensor). For the determination of the CO_2 quantity in a mixture with a hydrocarbon such as ethane, NaOH was used to remove the CO_2. When the mixed gas was passed through a layer of NaOH pellets in a glass tube several times, all the CO_2 was absorbed by the NaOH layer and only the hydrocarbon remained without being absorbed. Then the quantity of hydrocarbon was determined from the pressure and that of CO_2 from the difference of the pressures before and after the NaOH treatment.

The pH of the aqueous solution of organic acids was controlled by using NaOH. The pH was measured with a pH meter (Iwaki Glass, pH/ion meter 225). For the analysis of reaction products in an aqueous medium a steam carrier gas chromatograph (Okura Denki, Model 103) and a liquid chromatograph (Japan Spectroscopic Co., Ltd., Familic-100) were used.

For the complete decomposition of acetic acid, 136 mg of $CH_3COONa{\cdot}3H_2O$ (1.02 mmol) was dissolved in 20 mL of distilled water. As the photocatalyst, TiO_2(a)/Pt (300 mg) was used. The pH of the solution was 8.4 at the beginning of the reaction. At the end of the reaction, where hydrogen and carbon dioxide almost stopped evolving, the pH of the solution was 9.5. Carbon dioxide produced was partly absorbed in the alkaline aqueous medium and was liberated by adding excess nitric acid to the solution.

Results and Discussion

Hydrogen and Hydrocarbon Production from Organic Acids. Bard et al. investigated the photocatalytic reaction of organic acids with powdered TiO_2/Pt.[5,17-22] They confirmed the following reaction and called it the photo-Kolbe reaction:

$$RCOOH \rightarrow RH + CO_2 \quad (1)$$

One of the characteristic features of this reaction with powdered semiconductors is that RH is the main product and R–R, the dimer ·R, is a byproduct.[18] This seems to be a result of the large surface area of the powdered semiconductor, which causes the surface concentration of ·R to be so small that RH is formed more easily than R–R.

We measured the production rates of H_2 and RH from the photodecomposition of several organic acids with TiO_2(r)/Pt. The results are shown in Table I. As seen in this table, the hydrogen production rate is high and cannot be neglected even compared with the production rate of RH. This result suggests that reactions other than reaction 1 are taking place. Additional evidence that supports this conclusion is the pH dependence of the photocatalytic decomposition of acetic acid, as is shown in Table II. The ratio of H_2 to CH_4 depends strongly on pH: The higher the pH, the larger the ratio gets. At pH 14, almost pure hydrogen evolved, and methane was hardly produced. Interestingly, hydrogen is also evolved in pure acetic acid. Bard et al. proposed the following reactions for acetic acid:[5,17-22]

$$CH_3COOH \rightarrow CH_4 + CO_2 \quad (2)$$

$$2CH_3COOH \rightarrow C_2H_6 + 2CO_2 + H_2 \quad (3)$$

The main reaction is reaction 2, and reaction 3 is a minor one. Actually, ethane formation is minor compared with that of methane. For instance, C_2H_6/CH_4 is 0.21 at pH 2.1. Although eq 3 explains hydrogen formation, more hydrogen is always produced than ethane: At pH 2.1 the ratio of H_2 to C_2H_6 is 4.3 and at pH 14 it is more than 500. A similar pH dependence was observed for the photocatalytic reaction of propionic acid. As shown in Table III, the ratio of H_2 to C_2H_6 is 0.1 at pH 2.2 and 590 at pH 13.

Analysis of Reaction Products in Aqueous Medium in the Presence of Ag^+. It is very important to know the reaction products in the aqueous medium besides the gaseous products in order to clarify the reaction mechanism. The photocatalytic reactions were carried out by adding Ag^+ ($AgNO_3$) as a strong electron acceptor.[25,26] In the presence of Ag^+, the reactions

TABLE I: Production Rate of Hydrogen and Hydrocarbon by the Photocatalytic Decomposition of Organic Acids[a]

reactant	pH	H_2, μmol/10 h	RH, μmol/10 h
CH_3COOH	1.4	160	156
C_2H_5COOH	1.6	154	1470
n-C_3H_7COOH	1.6	334	996
n-C_4H_9COOH	1.9	523	1018

[a] 30 mL of a water–organic acid (6:1) mixture with 300 mg of TiO_2 (rutile, doped)/Pt was irradiated with a 500-W Xe lamp.

TABLE II: Dependence of Hydrogen and Methane Production Rate on pH for the Photocatalytic Decomposition of Acetic Acid in Aqueous Medium[a]

pH	H_2, μmol/h	CH_4, μmol/h	H_2/CH_4
2.1	23	119	0.19
5.4	23	28	0.82
6.2	25	10	2.5
7.5	51	3.3	15
8.8	57	0.5	110
11.8	43	<0.08	>500

[a] 30 mL of a water-acetic acid mixture (6:1 in volume) with 300 mg of TiO_2 (rutile, doped)/Pt was irradiated with a 1-kW Xe lamp (operated at 500 W). The pH of each solution, which was controlled by adding NaOH or H_2SO_4, hardly changed after each experimental run (1-h irradiation).

TABLE III: Dependence of Hydrogen and Ethane Production Rate on pH for the Photocatalytic Decomposition of Propionic Acid in Aqueous Medium[a]

pH	H_2, μmol/10 h	C_2H_6, μmol/10 h	H_2/C_2H_6
2.2	154	1470	0.1
4.2	127	641	0.2
7.0	80	92	0.9
9.0	95	0.7	135
13	47	0.08	590

[a] 30 mL of a water-propionic acid mixture (6:1 in volume) with 300 mg of TiO_2 (rutile, doped)/Pt was irradiated with a 1-kW Xe lamp (operated at 500 W).

TABLE IV: Reaction Products of the Photocatalytic Reactions of Acetic, Propionic, and Butyric Acids in the Presence of Ag^+ [a]

run	reactant	pH of soln	irradn time, h	gaseous products		products in aq medium [b]	
				compd	amt, μmol	compd	amt, μmol
1	CH_3COOH	2.0	21.8	CH_4	491	CH_3OH	66
				C_2H_6	408	C_2H_5OH	5.6
				CO_2	2935	$(CH_3)_2CO$	1.8
						CH_3COOCH_3	7.9
						C_2H_5COOH	65
2	C_2H_5COOH	2.2	45.3	CH_4	16	CH_3CHO	203
				C_2H_6	2276	C_2H_5OH	130
				CO_2	5231	CH_3COOH	67
						$CH_3COOC_2H_5$	89
						n-C_4H_9COOH (n-valeric acid)	27
						C_4H_9COOH (methylethylacetic acid)	39
3	C_3H_7COOH	2.2	18.8	C_3H_8	1680	CH_3CHO	6.0
				CO_2	3570	C_2H_5OH	0.9
						CH_3COOH	4.6
						C_3H_7OH	75
						C_2H_5CHO	102
						C_2H_5COOH	34

[a] Aqueous solutions of each organic acid and $AgNO_3$ (2 mL of organic acid and 1.0 g of $AgNO_3$ in 30 mL of distilled water) with 300 mg of powdered TiO_2 (rutile, undoped) were irradiated with a 500-W Xe lamp. [b] Products in the aqueous medium were detected by a steam carrier gas chromatograph. For the photocatalytic reaction of acetic acid, 80 μmol of glycolic acid and 430 μmol of succinic acid were detected by a liquid chromatograph in a separate experiment (10-h irradiation in the presence of Ag^+).

proceed very easily with TiO_2 alone. Since electrons in the conduction band are consumed to reduce Ag^+, hydrogen was not evolved under these conditions. Table IV shows the results of product analyses for three organic acids, acetic acid, propionic acid, and butyric acid. The quantity of CO_2 evolved is enormous, as shown in Table IV. For acetic acid, CO_2 is produced by reaction 2 and the following reaction, which is a modification of reaction 3:

$$2CH_3COOH + 2Ag^+ \rightarrow C_2H_6 + 2CO_2 + 2Ag + 2H^+ \quad (4)$$

From reactions 2 and 4, the total quantity of CO_2 is expected to be equal to the quantity of $CH_4 + 2C_2H_6$. However, as is calculated from the results in Table IV, the ratio of CO_2 to $CH_4 + 2C_2H_6$ is 2.2 for the photocatalytic reaction of acetic acid. A similar discrepancy was also reported by Yoneyama et al.[24] This result also indicates the existence of other reactions in which water is involved. The formation of ·OH, one of the intermediates of oxidation of water, was reported by Bard et al. on powdered TiO_2 suspended in water under UV irradiation.[27] ·OH radical is known to have a strong oxidation power and to oxidize various organic compounds, extracting hydrogen from them.[28] Many of the reaction products are explained reasonably by assuming the involvement of this radical. For instance, the formations of CH_3OH from CH_3COOH, C_2H_5OH from C_2H_5COOH, and C_3H_7OH from C_3H_7COOH can be explained easily by the following reaction:[29]

$$\cdot R + \cdot OH \rightarrow ROH \quad (5)$$

When one takes into account these reactions, the products in aqueous medium in Table IV, for instance, those from n-butyric acid, are explained as follows:

$$C_3H_7COOH + p \rightarrow \cdot C_3H_7 + CO_2 + H^+ \quad (6)$$

$$H_2O + p \rightarrow \cdot OH + H^+ \quad (7)$$

$$\cdot C_3H_7 + \cdot OH \rightarrow C_3H_7OH \quad (8)$$

$$(\text{or } \cdot C_3H_7 + p \rightarrow C_3H_7^+,\ C_3H_7^+ + H_2O \rightarrow C_3H_7OH + H^+ \text{[29]}) \quad (9)$$

$$C_3H_7OH + 2p \rightarrow C_2H_5CHO + 2H^+ \quad (10)$$

$$C_2H_5CHO + H_2O + 2p \rightarrow C_2H_5COOH + 2H^+ \quad (11)$$

$$C_2H_5COOH + p \rightarrow \cdot C_2H_5 + CO_2 + H^+ \quad (12)$$

$$\cdot C_2H_5 + \cdot OH \rightarrow C_2H_5OH \quad (13)$$

$$(\text{or } \cdot C_2H_5 + p \rightarrow C_2H_5^+,\ C_2H_5^+ + H_2O \rightarrow C_2H_5OH + H^+ \text{[29]}) \quad (14)$$

$$C_2H_5OH + 2p \rightarrow CH_3CHO + 2H^+ \quad (15)$$

$$CH_3CHO + H_2O + 2p \rightarrow CH_3COOH + 2H^+ \quad (16)$$

Here p represents a photogenerated hole in the valence band. The decomposition of propionic acid is explained by eq 12–16. Actually, for the photocatalytic reaction of propionic acid, methane was evolved and the quantity was increased with irradiation time as shown in Table VI, which was explained reasonably the accumulation of acetic acid (eq 16) and its decomposition.[5,17-22] As shown in Table IV, the ratio of CO_2/RH is greater than unity: CO_2/CH_4 is 5.9 for CH_3COOH, CO_2/C_2H_6 is 2.3 for C_2H_5COOH, and CO_2/C_3H_8 is 2.1 for C_3H_7COOH. This suggests that the oxidation of the organic acids proceeds further.

Formation of Organic Acids Having Longer Carbon Chains. Most of the oxidation products in aqueous medium can be explained by the reaction with ·OH[27] and $\cdot CH_3$.[22] Besides these oxidation products, organic acids having longer carbon chains than the starting material were detected as reaction products. For example, C_2H_5COOH is formed from CH_3COOH and n-

(25) H. Hada, H. Tanemura, and Y. Yonezawa, *Bull. Chem. Soc. Jpn.*, **51**, 3154 (1978).
(26) T. Kawai and T. Sakata, "Proceedings of the 7th International Congress on Catalysis", Kodansha Ltd., Tokyo, 1981, p 1198.
(27) C. D. Jaeger and A. J. Bard, *J. Phys. Chem.*, **83**, 3146 (1979).
(28) For instance, J. H. Merz and W. A. Waters, *J. Chem. Soc.*, 2427 (1949).
(29) Another possible explanation of alcohol formation is the oxidation of R· into the carbonium ion, R^+, which reacts easily with water to produce the alcohol as follows:

$$R\cdot + p \rightarrow R^+ \quad (A)$$

$$R^+ + H_2O \rightarrow ROH + H^+ \quad (B)$$

Reaction A seems to be possible on TiO_2 under irradiation. For instance, the ionization potential of methyl radical ($\cdot CH_3$) in the aqueous medium is estimated to be 6.2 eV by using Born's equation with 9.8 eV[30] as the ionization potential of methyl radical in the gas phase and the assumed radius of 2 Å for CH_3^+.[31] This value corresponds to 1.7 V vs. NHE (normal hydrogen electrode) when −4.5 eV is taken as the electron energy of NHE from the vacuum.[32] This estimation suggests that the photogenerated holes in the valence band of TiO_2 have enough power to oxidize methyl radical.

(30) L. Golob, N. Jonathan, A. Morris, M. Okuda, and K. J. Ross, *J. Electron Spectrosc.*, **1**, 506 (1972/1973).
(31) L. Pauling, "The Nature of the Chemical Bond", 3rd ed., Cornell University Press, Ithaca, NY, 1960.
(32) F. Lohmann, *Z. Naturforsch. A*, **22**, 843 (1967).
(33) K. Hashimoto, T. Kawai, and T. Sakata, unpublished data.

TABLE V: Reaction Products of the Photocatalytic Reactions of Acetic Acid, in the Absence of Ag^+ [a]

run	irradn time, h	photocatalyst[d]	pH of aq medium	gaseous products		products in aq medium[e]	
				compd	amt, μmol	compd	amt, μmol
1[b]	162	TiO_2(a,u)/Pt	2.1	H_2	1271	CH_3OH	8.8
				CH_4	3541	C_2H_5OH	1.1
				C_2H_6	112	$(CH_3)_2CO$	1.3
				CO_2	4572	C_2H_5COOH	12.0
2[c]	112	TiO_2(a,u)/Pt	7.4	H_2	5548	CH_3OH	2.3
				CH_4	8.2	C_2H_5OH	1.9
				CO_2	894	$(CH_3)_2CO$	10.0
						C_2H_5COOH	2.0
3[c]	112	TiO_2(a,u)/Pt	13.0	H_2	3262	CH_3OH	1.5
				CH_4	0	C_2H_5OH	0.7
				CO_2	0[a]	$(CH_3)_2CO$	0.9
						C_2H_5COOH	0
4[c]	247	TiO_2(r,d)/Pt	7.4	H_2	945	CH_3OH	2.0
				CH_4	0	C_2H_5OH	0.9
				CO_2	72	$(CH_3)_2CO$	2.3
						C_2H_5COOH	1.4

[a] Aqueous solution of acetic acid or sodium acetate with 300 mg of TiO_2 (rutile or anatase)/Pt was irradiated with a 500-W Xe lamp. [b] 2 mL of acetic acid in 30 mL of distilled water. [c] 0.5 g of sodium acetate in 30 mL of distilled water. The pH of the solution was controlled by adding NaOH. [d] a = anatase, r = rutile, d = doped, u = undoped. [e] Products in the aqueous medium were detected by a steam carrier gas chromatograph.

C_4H_9COOH and $C_2H_5CH(CH_3)COOH$ are formed from C_2H_5COOH as shown in Tables IV and V. The production of C_2H_5COOH from CH_3COOH would be explained by the following reactions:

$$\cdot CH_3 + CH_3COOH \rightarrow CH_4 + \cdot CH_2COOH \quad (17)$$

or

$$\cdot OH + CH_3COOH \rightarrow H_2O + \cdot CH_2COOH \quad (18)$$

$$\cdot CH_2COOH + \cdot CH_3 \rightarrow C_2H_5COOH \quad (19)$$

Because $D_0(HO-H) = 5.09$ eV $> D_0(CH_3-H) = 4.38$ eV,[34] reaction 18 is favorable thermodynamically. Here $D_0(A-B)$ represents the bond dissociation energy of A–B. Reaction 17 is supported by the experimental result that CH_4 is formed in the photocatalytic reaction of CH_3COOH in D_2O in the presence of a strong electron acceptor such as Ag^+ (see the next section). By analogy with reaction 19, formation of glycolic acid and succinic acid is expected by the following reactions:

$$\cdot CH_2COOH + \cdot OH \rightarrow HOCH_2COOH \quad (20)$$

$$\cdot CH_2COOH + \cdot CH_2COOH \rightarrow HOOCC_2H_4COOH \quad (21)$$

Actually, glycolic acid and succinic acid were produced (80 and 430 μmol, respectively, after 1-h irradiation in the presence of Ag^+).

For the photocatalytic reaction of C_2H_5COOH, the formation of $\cdot C_2H_4COOH$ is possible according to the following reactions, which are similar to eq 17 and 18:

$$\cdot C_2H_5 + C_2H_5COOH \rightarrow C_2H_6 + \cdot C_2H_4COOH \quad (22)$$

or

$$\cdot OH + C_2H_5COOH \rightarrow H_2O + \cdot C_2H_4COOH \quad (23)$$

But, unlike the case of acetic acid, isomeric radicals, $\cdot CH_2CH_2COOH$ and $CH_3\dot{C}HCOOH$, are expected to be formed in this case. The following reactions, analogous to eq 19, are possible:

$$\cdot CH_2CH_2COOH + \cdot C_2H_5 \rightarrow n\text{-}C_4H_9COOH \quad (24)$$

$$CH_3\dot{C}HCOOH + \cdot C_2H_5 \rightarrow C_2H_5CH(CH_3)COOH \quad (25)$$

Actually, both compounds were detected in the aqueous medium. As shown in Table IV, α-methylbutyric acid ($C_2H_5CH(CH_3)COOH$) is produced in higher yield than *n*-valeric acid (*n*-C_4H_9COOH). This is reasonable since the α-hydrogen of CH_3CH_2COOH is extracted more easily by $\cdot OH$ or $\cdot C_2H_5$ than the β-hydrogen. The formation of C_2H_5COOH, and succinic acid from CH_3COOH and *n*-C_4H_9COOH and $C_2H_5CH(CH_3)COOH$ from C_2H_5COOH, is interesting from the viewpoint of organic synthesis because the number of carbons is increased in the products compared with that in the starting material.

Two Reaction Paths for Methane Formation. As is shown in Table IV, methane is produced even in the presence of Ag^+. Since the concentration of hydrogen atoms would be negligibly small under these conditions, methane formation by combination of a hydrogen atom and a methyl radical would be unlikely. The photocatalytic decomposition of acetic acid in heavy water ($CH_3COOH:D_2O$ = 1:20 in volume, pH 2.1) in the presence of Ag^+ showed that the main component of the produced methane was not CH_3D but CH_4. The ratio of CH_3D to CH_4 was 1:13.[36] This result demonstrates clearly that the hydrogen in methane does not come predominantly from water, but from the methyl group in acetic acid by the hydrogen abstraction reaction 17.

On the other hand, in the absence of a strong electron acceptor such as Ag^+ or O_2, the main reaction path for methane formation is thought to be the reaction of a methyl radical with a hydrogen atom produced on Pt:[19]

$$\cdot H + \cdot CH_3 \rightarrow CH_4 \quad (26)$$

Actually, mainly CH_3D is produced from CH_3COOH in heavy water. The ratio of CH_3D to CH_4 was 14:1. This result shows that the main reaction path for methane formation is reaction 28 in the absence of a strong electron acceptor.[36] In the absence of Ag^+, the ratio of C_2H_6 to CH_4 is 0.1–0.2 with TiO_2(r)/Pt, while the ratio is increased to 0.83 in the presence of Ag^+ (see Table IV), indicating that C_2H_6 is formed comparably with CH_4. This result suggests that the reaction rate of hydrogen abstraction (eq 17) is slower than that of reaction 26. Thus, the presence of Ag^+ changes reaction paths. The most important result is that the reaction path of methane formation is controlled by the presence of Ag^+ from reaction 26 to 17.

Photocatalytic Reaction of Acetic Acid and Propionic Acid in the Absence of Ag^+. In the absence of a strong electron acceptor such as Ag^+, hydrogen evolution takes place instead of reduction of Ag^+. Since the photocatalytic activity of TiO_2 alone is not high for this reaction, platinized TiO_2 (anatase) was used. The results for acetic acid at three different pHs is shown in Table V and

(34) R. C. Weast, Ed., "CRC Handbook of Chemistry and Physics", CRC Press, Boca Raton, FL, 1979, p F238.

(35) The bond dissociation energy of $H-CH_2COOH$ is not known. If the value for $H-CH_2COCH_3$ ($D_0(H-CH_2COCH_3) = 4.26$ eV) is approximated as the bond dissociation energy of $H-CH_2COOH$, the enthalpy change for the reaction is found to be −0.12 eV.

(36) T. Kawai, K. Hashimoto, and T. Sakata, unpublished.

TABLE VI: Reaction Products of the Photocatalytic Reactions of Propionic Acid in the Absence of Ag^+ [a]

run	irradn time, h	photocatalyst[b]	gaseous products		products in aq medium[c]	
			compd	amt, μmol	compd	amt, μmol
1	63	TiO_2(a,u)/Pt	H_2	813	CH_3CHO	1.5
			C_2H_6	2674	C_2H_5OH	2.0
			CO_2	3221	CH_3COOH	9.2
					n-C_4H_9COOH	32.0
					$CH_3(C_2H_5)CHCOOH$	34.0
2	165	TiO_2(a,u)/Pt	H_2	2361	CH_3CHO	1.5
			C_2H_6	7067	C_2H_5OH	2.8
			CO_2O_2	9578	CH_3COOH	9.8
					n-C_4H_9COOH	62
					$CH_3(C_2H_5)CHCOOH$	86

[a] Aqueous solution of propionic acid (2 mL in 30 mL of distilled water) with 300 mg of TiO_2 (anatase)/Pt was irradiated with a 500-W Xe lamp. [b] a = anatase, u = undoped. [c] Products in the aqueous medium were detected by a steam carrier gas chromatograph.

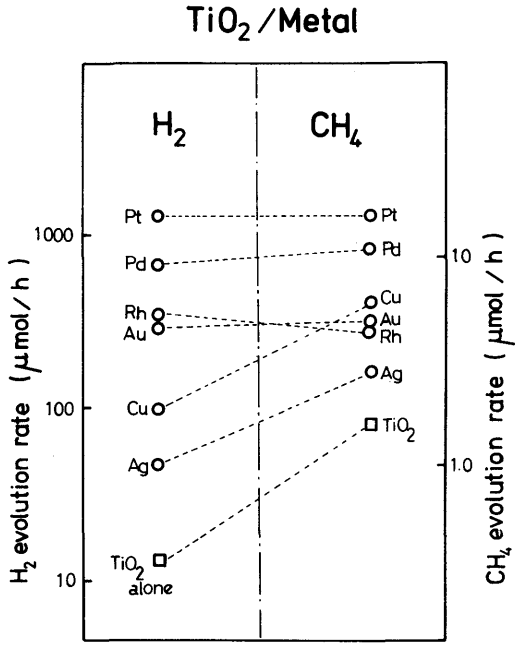

Figure 1. Correlation between hydrogen production rate from an ethanol–water mixture (1:1 in volume) and methane production rate from an acetic acid–water mixture (1:6 in volume) with various TiO_2 (rutile, doped)/metal photocatalysts; 30 mL of a water–ethanol (or acetic acid) mixture with 300 mg of TiO_2/metal photocatalyst was irradiated with a 1-kW Xe lamp (operated at 0.5 kW).

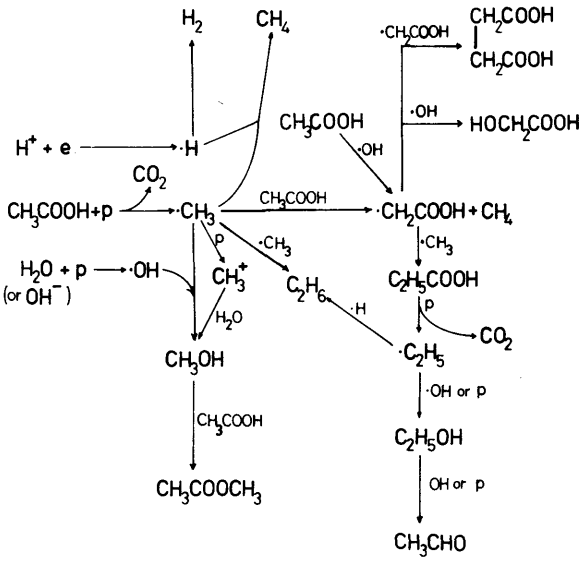

Figure 2. Reaction scheme of photocatalytic reactions of acetic acid in aqueous medium with powdered TiO_2 photocatalysts.

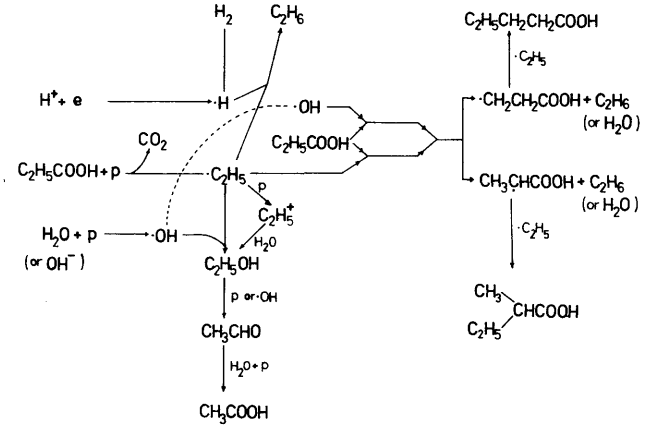

Figure 3. Reaction scheme of photocatalytic reactions of propionic acid in aqueous medium with powdered TiO_2 photocatalysts.

that for propionic acid at a single pH is shown in Table VI. When the reaction products are compared with those in Table IV, it is apparent that they are almost the same, indicating that Ag^+ does not influence the kinds of reaction products. However, the quantity of the products in the aqueous medium is very small in the absence of Ag^+. It does not depend on the kind of TiO_2, i.e., rutile or anatase. It was also confirmed by using Ag/TiO_2 instead of Pt/TiO_2 that it was not caused by the catalytic effect of Ag which was deposited on the TiO_2 surface during the reduction of Ag^+. This result is explained reasonably as follows. In the presence of Ag^+, photoexcited electrons are consumed for the reduction of Ag^+. However, in the absence of Ag^+, H· is formed on the surface of Pt on TiO_2. These adsorbed hydrogen atoms are used for methane formation (see reaction 26) as well as the production of hydrogen molecules. This suppresses reactions 5 and 19–21, which lead to the production of CH_3OH, C_2H_5COOH, $HOCH_2COOH$, and $HOOCC_2H_4COOH$, respectively.

On the other hand, reaction 26 is suppressed in the presence of Ag^+, which promotes reactions 5 and 19–21. In the presence of Ag^+, ethane production is also promoted, as seen in Table IV. A similar situation exists in the photocatalytic reaction of propionic acid. Table VI shows the result of product analysis for the photocatalytic reaction of propionic acid. The quantities of C_2H_5OH, CH_3CHO, and CH_3COOH produced in run 2 of Table VI are very small compared with those in run 2 in Table IV, even though more CO_2 is produced in the former case. This would also be explained by the difference in the reaction paths in the presence and absence of Ag^+.

Figure 1 shows the dependence of the hydrogen evolution rate from ethanol–water (1:1) mixture (left-hand side) and the methane evolution rate from acetic acid–water mixture (right-hand side) on the kind of metal which is supported on the powdered TiO_2 (rutile). As seen from this figure, there is a correlation between the photocatalytic activity of hydrogen evolution and that of methane evolution. This also suggests the importance of reaction 26.

Another interesting observation is that the quantities of C_2H_5OH, CH_3CHO, and CH_3COOH are not increased with irra-

diation time (runs 1 and 2 in Table VI), whereas valeric acid accumulates. This indicates that C_2H_5OH, CH_3CHO, and CH_3COOH are reaction intermediates and have already arrived at steady states. In Figures 2 and 3 the reaction paths are shown for the photocatalytic reactions of CH_3COOH and C_2H_5COOH, respectively.

Dependence of the Reactions on pH. As was described in the previous section, the influence of pH on the gaseous products is remarkable. A similar effect is also observed in the products in the aqueous medium. For instance, C_2H_5COOH and CH_3OH are produced more at pH 2.1 than at pH 7.4 and 13.0 as is shown in Table V. In the case of CH_3COOH, CH_4 formation is suppressed with increasing pH, and the ratio of H_2/CH_4 depends on pH. This result might be explained by taking into consideration the dependence of the energy levels of TiO_2 on pH.

As to methane formation, eq 2 is thought to consist of the following elementary reactions:

$$CH_3COOH \rightarrow CH_3COO^- + H^+ \quad (27)$$

$$CH_3COO^- + p \rightarrow CH_3COO\cdot \quad (28)$$

$$CH_3COO\cdot \rightarrow \cdot CH_3 + CO_2 \quad (29)$$

$$\cdot CH_3 + \cdot H \rightarrow CH_4 \quad (26)$$

or

$$\cdot CH_3 + CH_3COOH \rightarrow CH_4 + \cdot CH_2COOH \quad (17)$$

Since the bond dissociation energy of $CH_3COO\cdot \rightarrow \cdot CH_3 + CO_2$ is −0.87 eV, reaction 29 is expected to proceed spontaneously if $CH_3COO\cdot$ does not interact strongly with the TiO_2 surface and the difference between the interaction energy of $CH_3COO\cdot$ and that of $\cdot CH_3$ is less than 0.87 eV. The rate constant for this process in hydrocarbon solvents is estimated to be 1.6×10^9 s^{-1} at 60 °C,[37] which indicates that the decarboxylation is very rapid.

Since the bond dissociation energy $D_0(CH_3-H)$ is as much as 4.51 eV,[34] reaction 26 would proceed easily to the right-hand side even on the catalyst surfaces. Therefore, the rate-determining step for methane productions is thought reasonably to be reaction 28. Actually, the oxidation of CH_3COO^- is suggested to be very difficult in an aqueous medium by the following calculation.

Since the electron affinity of $CH_3COO\cdot$ is 3.36 eV[38,39] and the enthalpy of hydration of CH_3COO^- is 4.15 eV,[40] the enthalpy change of the following equation is 7.51 eV:

$$CH_3CO_2^-(aq) \rightarrow CH_3CO_2\cdot(gas) + e_{vac} \quad (30)$$

If we assume 0.5 eV tentatively as the stabilization energy for the process, $CH_3COO\cdot(gas) \rightarrow CH_3COO\cdot$ (on the TiO_2 surface in the aqueous medium), the ionization energy of CH_3COO^- in the aqueous medium is still as much as 7.01 eV. This corresponds to 2.51 V vs. NHE, assuming the electron energy for the normal hydrogen electrode (NHE) to be −4.50 eV.[32] Experimentally the critical potential for the oxidation of CH_3COO^- is 2.05–2.7 V vs. NHE.[41] From these values, the state density of electrons in the highest occupied level of CH_3COO^- is estimated to start from −6.55 to −6.9 eV vs. vacuum, because its threshold is thought to agree with the critical potential.

The energy levels of TiO_2 are well-known to depend on the pH of the electrolyte solution. The flat band potential of TiO_2 (rutile) depends on pH as follows:

$$U_{fb} = -0.11 - (kT/e)[pH] \text{ V vs. NHE}^{42}$$

If 0.10 eV is assumed for the energy difference between the Fermi level and the bottom of the conduction band, the edge of the valence band of rutile is expressed by the following equation, taking into account the band gap of 3.0 eV for rutile:

$$U_{vb} = +2.79 - (kT/e)[pH] \text{ V vs. NHE} \quad (31)$$

The energy structure of anatase is not clear, because of the difficulty of preparing an anatase electrode.

As seen in eq 31, the valence band is located deep and the photogenerated holes in the valence band have enough power to oxidize CH_3COO^-. However, the oxidation power of the photogenerated holes decreases with increasing pH, since the valence band is shifted in the negative direction according to eq 31. Therefore, at high pH, the oxidation of CH_3COO^- becomes difficult and the oxidation of OH^- ($OH^- + p \rightarrow \cdot OH$) begins to overwhelm that of CH_3COO^-, since the valence band of TiO_2 is located deeply enough to oxidize OH^- even under alkaline conditions.

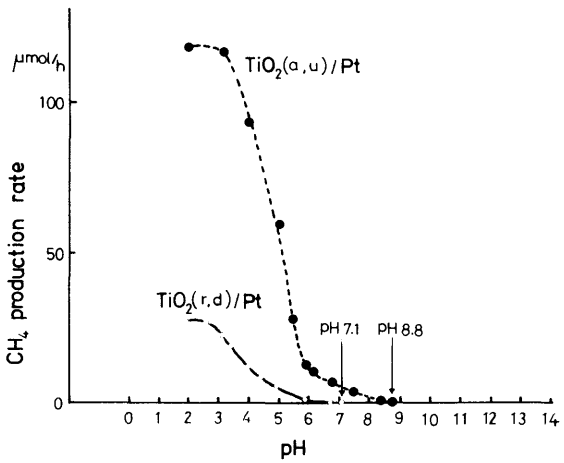

Figure 4. Dependence of methane production rate on pH for the photocatalytic decomposition of acetic acid in aqueous medium; 30 mL of a water–acetic acid mixture (6:1 in volume) with 300 mg of TiO_2/Pt was irradiated with a 500-W Xe lamp. The pH of the mixture, which was controlled by adding NaOH or H_2SO_4, hardly changed after each experimental run (1-h irradiation).

Figure 4 shows the dependence of CH_4 production rate on pH. As seen in this figure, CH_4 is not produced above pH 8.8 for anatase and pH 7.1 for rutile. The pH value above which methane formation is prevented relates presumably to the critical potential of the oxidation of CH_3COO^-. When the pH value of 7.1 for rutile is used in eq 31, 2.37 V vs. NHE is obtained as the potential of the valence band. This value seems to be reasonable compared to the critical potential of the oxidation of CH_3COO^- for metal electrodes. If direct oxidation by the photogenerated hole in the valence band is assumed, this potential is thought to be equal to the critical potential for the oxidation of CH_3COO^- on the TiO_2 (rutile) surface in aqueous medium. If the critical potential of the oxidation of CH_3COO^- on the anatase surface is the same as that on the rutile surface, the valence band must be located at 2.37 V vs. NHE at pH 8.8. Since the valence band edge of rutile at pH 8.8 is estimated to be located at 2.27 V vs. NHE from eq 31, the oxidation power of anatase is stronger than that of rutile, which explains well the difference in the photocatalytic activity between them.

There might be another explanation for the decrease of CH_4 formation at higher pH, although the above energetical reason would be the most important. In a higher pH region, a lot of $\cdot OH$ radicals would be formed because of the high concentration of OH^-. Then, even when $\cdot CH_3$ is produced, it would be consumed not to produce CH_4 but to produce CH_3OH by the following reaction:

$$\cdot CH_3 + \cdot OH \rightarrow CH_3OH \quad (32)$$

Since methanol reacts efficiently with water on TiO_2 photocatalysts to produce hydrogen,[11] reaction 32 suppresses CH_4 formation. Thus, the reaction paths shown in Figure 2 are influenced by pH.

(37) W. Braun, L. Rajbenbach, and F. R. Eirich, *J. Phys. Chem.*, **66**, 1591 (1962).
(38) S. Tsuda and W. H. Hamil, "Advances in Mass Spectrometry", Vol. 3, W. L. Mead, Ed., The Institute of Petroleum, London, 1966, p 249.
(39) W. E. Wentworth, E. Chen, and J. C. Steelhammer, *J. Phys. Chem.*, **72**, 2671 (1968).
(40) H. Ohtaki, M. Tanaka, and S. Hunabashi, "Chemistry of Solution Reaction", Gakkai Publishing, Tokyo, 1982, p 216.
(41) A. J. Bard and H. Lund, Eds., Encyclopedia of Electrochemistry of the Elements", Vol. 12, Marcel Dekker, New York, 1978, p 266.
(42) M. Tomkiewicz, *J. Electrochem. Soc.*, **126**, 1505 (1979).
(43) H. P. Maruska and A. K. Ghosh, *Sol. Energy*, **20**, 443 (1978).
(44) R. Williams, *J. Vac. Sci. Technol.*, **13**, 12 (1976).

TABLE VII: Dependence of Photocatalytic Reactions of Acetic Acid on the Kind of Semiconductor[a]

gaseous products		products in aq medium	
compd	amt, μmol	compd	amt, μmol
	TiO_2(r,u)[b]		
CH_4	225	CH_3OH	30
C_2H_6	187	C_2H_5COOH	29
CO_2	1350		
	TiO_2(a,u)[c]		
CH_4	62	CH_3OH	58
C_2H_6	133	C_2H_5COOH	45
CO_2	570		
	WO_3		
CH_4	73	CH_3OH	117
C_2H_6	96	C_2H_5COOH	13
CO_2	617		
	$SrTiO_3$		
CH_4	33	CH_3OH	32
C_2H_6	47	C_2H_5COOH	4
CO_2	299		
	Fe_2O_3		
CH_4	2.7	CH_3OH	1.5
CO_2	3.0		

minor products: C_2H_5OH, $(CH_3)_2CO$, CH_3COOCH_3

[a] Aqueous solution of acetic acid (2.0 mL in 30 mL of distilled water) containing 1.0 g of $AgNO_3$ with various kinds of powdered semiconductors was irradiated for 10 h with a 500-W Xe lamp. [b] TiO_2(r,u) = rutile, undoped. [c] TiO_2(a,u) = anatase, undoped.

Similar situations might exist in the photocatalytic reaction of other organic acids.

Dependence of the Reactions on the Kind of Semiconductor. Table VII shows the results of product analysis for the photocatalytic reaction of acetic acid in the presence of Ag^+ with various kinds of powdered semiconductors. As shown in this table, the kind of reaction product does not depend on the kind of semiconductor photocatalyst but their distribution does: For instance, methanol is produced about 9 times as much as propionic acid for WO_3 and $SrTiO_3$, while the amount of propionic acid is nearly the same as that of methanol for TiO_2 (for both anatase and rutile). It seems to be closely related to the catalysis on the semiconductor surface and the oxidation power of the semiconductor. Further investigation is necessary.

Complete Decomposition of Acetic Acid in an Alkaline Medium and Involvement of Water in the Reaction. From the above discussion, we can conclude the existence of new reaction paths in which water is involved. For acetic acid, they consist of the following reactions:

$$2H^+ + 2e \rightarrow H_2 \quad (33)$$

$$H_2O + p \rightarrow \cdot OH + H^+ \quad (7)$$

$$(\text{or } OH^- + p \rightarrow \cdot OH)$$

$$CH_3COOH + p \rightarrow \cdot CH_3 + CO_2 + H^+ \quad (34)$$

$$\cdot CH_3 + \cdot OH \rightarrow CH_3OH \quad (32)$$

or

$$CH_3COOH + 2\cdot OH \rightarrow HOCH_2COOH + H_2O \quad (35)$$

In the next step, CH_3OH[11] and $HOCH_2COOH$ are decomposed:

$$CH_3OH + H_2O \rightarrow CO_2 + 3H_2 \quad (36)$$

$$HOCH_2COOH + H_2O \rightarrow 2CO_2 + 3H_2 \quad (37)$$

The overall reaction from the above is written as

$$CH_3COOH + 2H_2O \rightarrow 2CO_2 + 4H_2 \quad (38)$$

$$\Delta G^\circ = 78.5 \text{ kJ/mol}$$

In the low pH region, the contribution of reaction 2 is large. For instance, the ratio of reactions 2, 3, and 38 in run 1 (pH 2.1) in Table V was determined to be 88:5:7 from the quantities of CH_4, C_2H_6, and H_2 produced. This ratio explains the quantity of CO_2. This analysis seems to be reasonable, since the quantities of the reaction products accumulated in the aqueous medium are quite small compared with those of gaseous products. On the other hand, in the neutral or alkaline region, reaction 38 is dominant, as seen in Tables II and V.

In order to confirm reaction 38, the complete decomposition of acetic acid was carried out. A 1.02-mmol sample of CH_3COONa was dissolved in 20 mL of distilled water. At the end of the reaction, the total amount of hydrogen produced was 4.18 mmol and that of CO_2[45] was 1.98 mmol. These values agree well with the quantities expected from eq 38 and the initial quantity of sodium acetate (the calculated value; H_2: 4.06 mmol, CO_2: 2.03 mmol). This result demonstrates clearly that reaction 38 takes place under this condition.

Reaction 38 has two characteristic features: The first is that water is involved in the reaction as an oxidizing agent. The second is that a comparable amount of free energy is stored, whereas ΔG° is −52.3 kJ/mol in reaction 2. The non-Kolbe type electrode reaction of organic acids in which olefins and alcohols are produced is known as the Hofer–Moest reaction.[46] Since methanol and glycolic acid are produced as reaction intermediates in reaction 38, it has a close similarity to the Hofer–Moest reaction.

Registry No. *n*-C_4H_9COOH, 109-52-4; TiO_2, 13463-67-7; Pt, 7440-06-4; Ag^+, 14701-21-4; $AgNO_3$, 7761-88-8; WO_3, 1314-35-8; $SrTiO_3$, 12060-59-2; Fe_2O_3, 1309-37-1; OH^-, 14280-30-9; CH_4, 74-82-8; C_2H_6, 74-84-0; H_2, 1333-74-0; CH_3OH, 67-56-1; C_2H_5OH, 64-17-5; $(CH_3)_2CO$, 67-64-1; CH_3COOCH_3, 79-20-9; C_2H_5COOH, 79-09-4; CH_3CHO, 75-07-0; CH_3COOH, 64-19-7; $CH_3COOC_2H_5$, 141-78-6; C_3H_7OH, 71-23-8; C_2H_5CHO, 123-38-6; C_3H_7COOH, 107-92-6; sodium acetate, 127-09-3; water, 7732-18-5; rutile, 1317-80-2; anatase, 1317-70-0; succinic acid, 110-15-6; methylethylacetic acid, 116-53-0; glycolic acid, 79-14-1; propane, 74-98-6.

(45) The pH of the solution was 8.4 in the beginning of the reaction and 9.5 at the end. Therefore, part of the produced CO_2 (0.96 mmol) was absorbed in the aqueous medium. An excess amount of nitric acid was added to the solution to liberate the absorbed CO_2.

(46) H. Hofer and M. Moest, *Ann. Chem.*, **323**, 284 (1902).

MAGNETIC FIELD EFFECT ON THE FLUORESCENCE OF METHYLGLYOXAL

Kazuhito HASHIMOTO, Saburo NAGAKURA
The Institute for Solid State Physics, The University of Tokyo, Roppongi, Minato-ku, Tokyo 106, Japan

and

Junko NAKAMURA and Suehiro IWATA
The Institute of Physical and Chemical Research, Wako, Saitama 351, Japan

Received 27 April 1980; in final form 23 May 1980

In the presence of a magnetic field, the faster of the two slow components of the fluorescence of methylglyoxal decreases in intensity while the slower component is unaffected, and a new component with a lifetime of about 40 ns appears. The effect becomes weaker with increasing excitation energy.

1. Introduction

The magnetic field effect on fluorescence from excited singlet states of molecules in gaseous state was first found for CS_2 in 1974 [1]. Since then, studies of the effect have been extended to glyoxal [2–4], formaldehyde [5], and SO_2 [6]. These molecules belong to the small molecule case; for instance, CS_2 and SO_2 are classified into the small molecule strong coupling case and glyoxal and formaldehyde into the small molecule weak coupling case (see, for example ref. [7]). In order to elucidate the mechanism of the phenomenon, several theoretical studies have also been made [4,8–10]. In the present work, we have studied the magnetic field effect on the fluorescence of methylglyoxal, which is known to be a prototype molecule for the intermediate case [11,12] and is expected to show a magnetic field effect different from that for the small molecule case.

2. Experimental

A major amount of water was distilled off from a portion of 40% aqueous solution of methylglyoxal (Aldrich), and the residue was depolymerized and purified by trap to trap distillation. Sample pressures were measured with a Baratron capacitance manometer (MKS 222A). An N_2 laser pumped dye laser (Molectron UV-24, DL-14) was used as an exciting source. Fluorescence decay was studied with the single photon counting method and the time-resolved emission intensity was measured with the photon counting method.

3. Results and discussion

The fluorescence of methylglyoxal has been reported to be composed of two decay components [11,12], a fast one of about 10 ns decay time and a slow one with a multi-exponential decay of the order of μs. This phenomenon has been interpreted theoretically with the "reversible intersystem crossing" model or the "mixed state" model [11,13,14]. In the present study, the total fluorescence is found to be composed of more than two components; in the absence of a magnetic field:

$$F_{\text{total}}(0) = F_1 + F_2(0) + F_3 \; ; \qquad (1)$$

and in the presence of a magnetic field, H:

$$F_{\text{total}}(H) = F_1 + F_H(H) + F_2(H) + F_3 \; . \qquad (2)$$

Here the fluorescence component F_i ($i = 1–3, H$) is

written approximately with the pre-exponential factor (I_i) and the lifetime (τ_i) as follows:

$$F_i = I_i \exp(-t/\tau_i) . \quad (3)$$

Among the four components F_1, F_2, F_3 and F_H, F_2 and F_H are changed by application of a magnetic field, while F_1 and F_3 are not. The experimental results of the pressure, field strength and excitation energy dependences of the magnetic field effect upon the respective fluorescence components will be explained in sections 3.1–3.3.

3.1. Fast fluorescence component, F_1

The fast component, F_1 was observed both at higher (above 1 Torr) and lower (below 100 mTorr) pressures (1 Torr = 101.325/760 Pa). The lifetime of the fast fluorescence excited at 449.2 nm was observed to be 14 ns (τ_1^{ℓ}) at the lower pressure and to be 26 ns (τ_1^{h}) at the higher pressure. These values are in good agreement with those in the literature [11,12].

The F_1 component was examined for the magnetic field effect. The excitation wavelengths were chosen in such a way that this component was most prominent and was observed easily and accurately (449.2 nm at the higher pressure and 432.0 nm at the lower pressure). At the higher pressure, the fluorescence lifetime and intensity showed no changes by application of a magnetic field as high as 3 kG (1 G = 10^{-4} T). At the lower pressure, the lifetime was almost independent of the magnetic field and the pre-exponential factor did not change within experimental error.

3.2. Slow fluorescence components, F_2 and F_3

The slow fluorescence of an intermediate case molecule is known to be observed only at low pressures. Therefore, the present study was carried out at pressures of 5–100 mTorr. In the absence of an external magnetic field, the slow fluorescence slightly deviates from a single exponential decay curve, although it has hitherto been regarded as a single component [12]. The following analysis of the decay curve shows that the slow fluorescence consists of two components, F_2 and F_3.

Fig. 1 shows the slow fluorescence decay curve observed in the presence of a magnetic field. The curve in the absence of the field is also shown in fig. 1 for

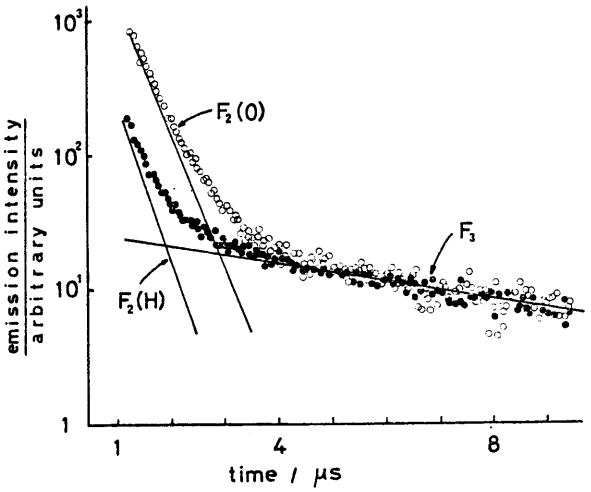

Fig. 1. Semilogarithmic plot of the slow fluorescence intensity (in arbitrary units) of methylglyoxal (22 mTorr) excited at 449.2 nm versus time: ○, in the absence of a magnetic field; ●, in the presence of a magnetic field of 1.1 kG.

the purpose of comparison. Both curves obtained independently by the single photon counting method were normalized in the time range longer than 4 μs after the excitation. This is because the following two experiments showed that neither the total intensity nor the lifetime was affected by the magnetic field in this time range. First, the total intensity in the time range of 4–24 μs after the excitation was measured by the gated photon counting method, and secondly, the lifetime was measured in the same time range by the delayed single photon counting method.

The results show that the slow fluorescence consists of two components, the relatively faster component (F_2) which is sensitive to the external magnetic field and the slower component (F_3) which is independent of the field. Concerning F_2 excited at 449.2 nm, the pre-exponential factor, I_2, is reduced to about one fourth in the presence of a magnetic field of 1.1 kG.

We studied the field strength dependence of $I_2(H)/I_2(0)$, the ratio between the pre-exponential factors with and without a magnetic field at constant excitation energy. The $I_2(H)/I_2(0)$ value decreases with increasing field strength below 1 kG. Above 1 kG, the value is almost constant up to 8 kG. Therefore, the magnetic field effect is saturated at a rather weak magnetic field (weaker than 1 kG).

The pressure dependence of $I_2(H)/I_2(0)$ was measured at several pressures in the range of 5–100 mTorr. The ratio was found to be constant at all the pressures examined (0.25 for excitation at 449.2 nm). This result indicates that the observed magnetic field effect is due to an intramolecular process.

The ratio between the lifetimes of F_2 with and without magnetic field, $\tau_2(H)/\tau_2(0)$, is slightly dependent on the sample pressure. The ratio is equal to unity at very low pressure (5–10 mTorr) and reduces to 0.9 at 20–100 mTorr.

The pressure dependence of the observed lifetimes of F_2 and F_3 satisfied the Stern–Volmer relation at various excitation wavelengths in the range 449.2–401.0 nm. From an analysis of the Stern–Volmer plots, the collision-free lifetimes and self-quenching constants (C_q) of F_2 and F_3 were determined. Both quantities are dependent on the excitation energy for F_2 [12] (see fig. 2), but not for F_3. Fig. 2 reveals that both excitation energy dependences show opposite trends to each other. To our knowledge, the present study is the first observation of an excitation energy dependence of the magnetic field effect on fluorescence.

3.3. New fluorescence component, F_H

In addition to the main and prominent magnetic field effect on the intensity of F_2, closer examination of the decay curves (fig. 3) shows that the overlapping

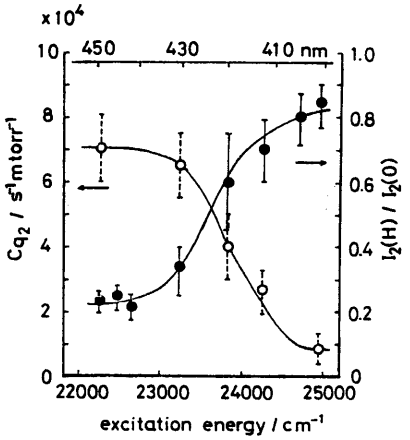

Fig. 2. Plots of $I_2(H)/I_2(0)$ (•) and the self-quenching constant, C_q for F_2 (○) versus excitation energy in the presence of a magnetic field of 3.5 kG.

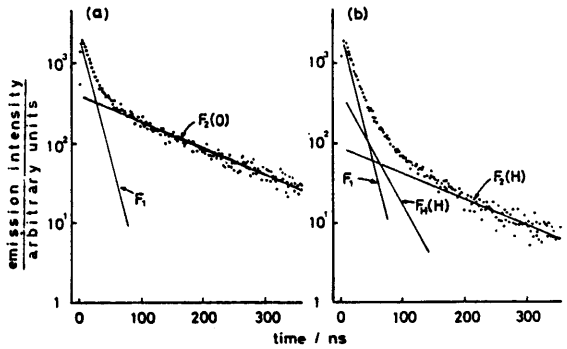

Fig. 3. Semilogarithmic plot of the initial fluorescence intensity (in arbitrary units) of methylglyoxal (100 mTorr) excited at 449.2 nm versus time: (a) in the absence of a magnetic field; (b) in the presence of a magnetic field of 1.1 kG.

part of the decay curve between the F_1 and F_2 components cannot be represented by their simple superposition in the presence of a magnetic field (fig. 3b). In the absence of a magnetic field, the total decay curve in the time range of the overlapping part is satisfactorily analyzed as a simple sum of F_1 and F_2 (see fig. 3a), because the contribution of the F_3 component to the decay curve is safely disregarded; in this time range, the following relations are satisfied: $I_2(0)/I_3 \geqslant 200$, $I_2(H)/I_3 \geqslant 50$, and τ_3 is longer than several μs on the excitation at 449.2 nm. From an analysis of the decay curve in the presence of a magnetic field based on the fact that τ_1 does not change and τ_2 reduces to 90% by an external magnetic field of 1 kG, it is found that a new, fourth component, F_H, exists as shown in fig. 3b. The lifetime of F_H excited at 449.2 nm is 40 ns and remains constant within experimental error upon changing the sample pressure from 5 to 100 mTorr.

3.4. Spectra of the F_2 and F_3 components and phosphorescence

The time-resolved emission spectra in the gaseous state were observed by the gated photon counting method. The result is shown in fig. 4a. The spectrum at high pressure (presumably that of the fast fluorescence, F_1^h) reported by Yardley et al. [15] is also shown in fig. 4 for the purpose of comparison. The spectrum of F_2 is similar to that of F_1^h. By application of a magnetic field, its shape does not change, but its intensity decreases uniformly to one fourth in the

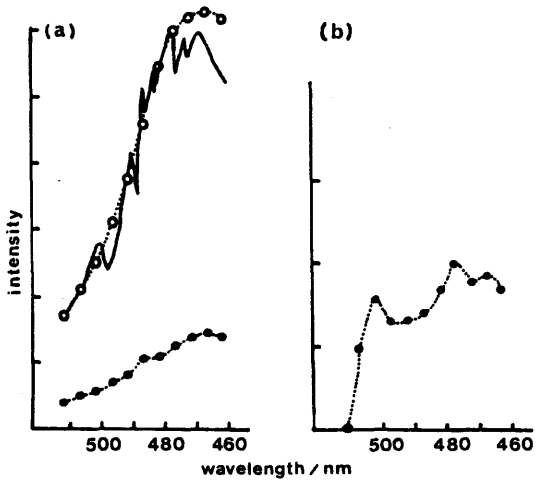

Fig. 4. Emission spectra of methylglyoxal (100 mTorr) excited at 449.2 nm: (a) ○, the spectrum of F_2 in the absence of a magnetic field; •, the spectrum of F_2 in the presence of a magnetic field of 1.1 kG ——, the spectrum of F_1^h in the absence of a magnetic field (from ref. [15]); (b) the spectrum of F_3 (in the absence and in the presence of a magnetic field).

whole wavelength region. The spectrum of F_3 shown in fig. 4b is somewhat different from those of F_2 and F_1^h, and its shape and intensity are both independent of the magnetic field.

The thermalized phosphorescence spectrum at 100 mTorr was measured by the gated photon counting method (delay time 30 μs, gate width 20 μs). Neither the intensity nor the shape of the spectrum is affected by the magnetic field within experimental error.

The large decrease of F_2 in the presence of a magnetic field may be compensated for by the appearance of the new fluorescence component, F_H. The F_H component may be slow fluorescence characteristic of the intermediate case molecule, which is enhanced and turns out to appear in a weak magnetic field.

The F_3 component cannot be regarded as fluorescence due to the reversible intersystem crossing characteristic of the intermediate case molecule, since its spectrum is different from those of F_2 and F_1^h. The F_3 component may be an emission from a hidden electronic level near 420 nm, which may probably be related to the irregularities of the excitation energy dependences of the magnetic field effect and the self-quenching constant shown in fig. 2.

References

[1] A. Matsuzaki and S. Nagakura, Chem. Letters (1974) 675; Bull. Chem. Soc. Japan 49 (1974) 359.
[2] A. Matsuzaki and S. Nagakura, Chem. Phys. Letters 37 (1976) 204.
[3] H.G. Kuttner, H.L. Selzle and E.W. Schlag, Israel J. Chem. 16 (1977) 264.
[4] A. Matsuzaki and S. Nagakura, Helv. Chim. Acta 61 (1978) 675.
[5] N.I. Sorokin, N.L. Lavrik, G.I. Skubnevskaya, N.M. Bazhin and Yu.N. Molin, Dokl. Akad. Nauk SSSR 345 (1979) 657.
[6] V.I. Makalov, N.L. Lavrik, G.I. Skubnevskaya and N.M. Bazhin, React. Kinet. Catal. Letters 12 (1979) 225.
[7] P. Avouris, W.M. Gelbert and M.A. El-Sayed, Chem. Rev. 77 (1977) 793.
[8] P.R. Stannard, J. Chem. Phys. 68 (1977) 3932.
[9] H.L. Selzle, S.H. Lin and E.W. Schlag, Chem. Phys. Letters 62 (1979) 230.
[10] M. Lombardi, R. Jost, C. Michel and A. Tramer, Chem. Phys. 46 (1980) 273.
[11] R.A. Coveleskie and J.T. Yardley, Chem. Phys. 9 (1975) 275.
[12] R. van der Werf, E. Schutten and J. Kommandeur, Chem. Phys. 16 (1976) 151.
[13] R. van der Werf and J. Kommandeur, Chem. Phys. 16 (1976) 125.
[14] F. Lahmani, A. Tramer and C. Tric, J. Chem. Phys. 60 (1974) 4331.
[15] R.A. Coveleskie and J.T. Yardley, J. Am. Chem. Soc. 97 (1975) 1667.

Journal of Luminescence 24/25 (1981) 763–766
North-Holland Publishing Company

EXTERNAL MAGNETIC FIELD EFFECT ON THE FLUORESCENCE OF GLYOXAL

J. Nakamura, K. Hashimoto* and S. Nagakura*

The Institute of Physical and Chemical Research
Wako, Saitama
Japan

Fluorescence decay curves of glyoxal at low pressures were analyzed by measuring external magnetic field effect on the single vibronic level time-resolved fluorescence spectra. The observed multi-component decays were found to be the overlaps of four emissions, F_0, F_1, F_2 and F_3, from different origins. Excitation energy dependence of the magnetic field effect on these four emissions suggested a mechanism of singlet- triplet energy transfers among three electronic excited states, S_1, T_1 and T_2.

INTRODUCTION

Glyoxal vapor at low pressures shows a fluorescence with a single-exponential decay when excited to the vibrationless lowest excited singlet state S_1 (0$^0_0$). Accumlated spectroscopic knowledges indicate that this molecule is a prototype of "weak coupling small molecule" case.[1]. The same molecule behaves, however, like an "intermediate case molecule" when excited with a light shorter than 455 nm; the fluorescence observed at the normal fluorescing region (e.g. at 482 nm) shows a multi-exponential decay.

We have studied the external magnetic field effects on the SVL fluorescence of glyoxal, and found out the relations between the quenching patterns of the fluorescence decay under the existence of a magnetic field and the type of interactions among the singlet and triplet states.

EXPERIMENTAL

Glyoxal monomer was obtained from dried polymer by the usual method. Neat glyoxal of 20 to 500 mtorr was filled in a pyrex sample cell of 50 mm i.d., cross-shaped with a photon trap. The sample pressures were monitored with a capacitor-type manometer(Baratron MKS 222A). The cell was set between the poles of a magnet which feeds a magnetic field of 700 to 7000 Gauss to the sample. Glyoxal was excited in the range of 455.3 to 380 nm with an N_2 laser pumped dye laser (Molectron 24, DL14). Time-resolved spectra of fluorescence and phosphorescence and time-profiles of the individual single vibronic transitions were recorded with a single-photon counting system combined with a Boxcar integrator. Schematic arrangement of the apparatus is shown in Fig. 1.

RESULTS AND DISCUSSIONS

The decay curves of fluorescence were found to become more and more deviated from the single-exponential decay with increasing energy of excitation. From the analysis of multi-component decays observed with and without a magnetic field, we

* Present address: The Institute for Molecular Science, Okazaki, Japan

0 022–2313/81/0000–0000/$02.75

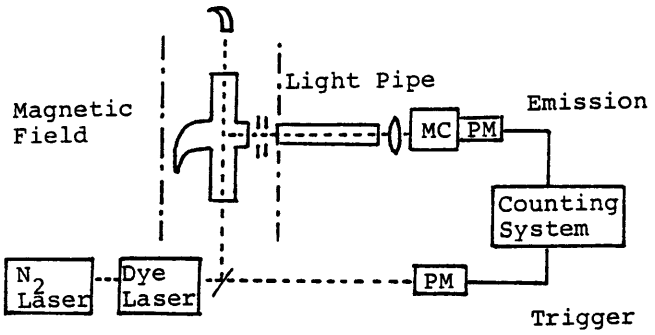

Fig.1
Schematic diagramm of the apparatus used for the observation of external magnetic field effect on the emissions of glyoxal.

deduced at most four components of fluorescence. The time-resolved spectra for each of the components indicated further that the multi-component decay usually observed at the normal region with a low spectral resolution is a result of accidental overlap of independent series of fluorescences with essentially single- exponential decays. We designate these four types of fluorescence as F_0, F_1, F_2 and F_3 in order of their lifetimes ($^2F_0$ is the shortest).

According to the number of components in the decay curves, the whole region of S_1 state is classified into four parts. The behaviors of quenching by the application of a magnetic field are also characteristic to the four regions. The results are summarized as follows. (As the effect saturates at a weak magnetic field, the strength of the field , denoted as H≠0 in the figures, was fixed to 3.5 kG.)

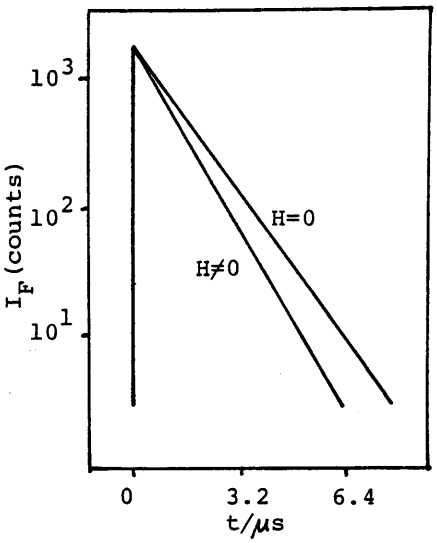

Fig.2 Time-profile of fluorescence
Glyoxal 190 mtorr.
Excitation at 455.3 nm (0_0^0)
Observation at 482 nm (8_1^0)

Case I. Excitation at 455.3 nm (0_0^0)

This case has been reported by many authors, yet an observed time-profile of fluorescence is shown in Fig.2 for the purpose of comparison. Main features of this case are; 1) emission spectrum is composed of the direct transitions from the excited 0_0^0 state to the vibrational levels in the ground state, S_0, 2) application of a magnetic field quenches the fluorescence in its lifetime but not in the initial intensity, 3) the rate of quenching, $\tau(H\neq0)/\tau(H=0)$, is pressure dependent.

Case II. Excitation at 455 nm ~ 435 nm

As has been pointed out,[2] the excitation to a certain level in this region causes a bi-exponential decay as the self quenching constant is bigger for the vibrational levels than for the 0_0^0 (Au) state. Here, F_1 is the direct emission from the excited level and F_2 is the indirect emission from 0_0^0 state which is gradually populated by the collision induced vibrational relaxation from the excited level. F_1 is slightly quenched in lifetime and F_2 is also quenched considerably in lifetime by the application of a weak magnetic field as shown in

Fig. 3. The decaytime of F_1 is equal to the risetime of F_2.

Case III. Excitation at 435 nm ~ 420 nm

We have three components in this case, F_1, F_2 and F_3. F_1 is again the direct emission from the excited level to the levels in the ground state and is quenched with a magnetic field in lifetime. It should be noted that the collision-free lifetime of F_1 in this case is shorter than that for F_1 in Case II.[2] F_2 shows a complicated behavior, as shown in Fig. 4. The time-resolved spectrum for this component clearly showed that F_2 is the indirect emission from the 0_0^0 state, the result being evidenced by the observation of rise in F_2 (though overlapped with a weak F_1 peak). The effect of a magnetic field appears, however, mainly as the decrease in the initial intensity ($I(H\neq0)/I(H=0) = 0.5\sim0.7$). On the contrary. quenching in lifetime is far smaller than in the cases I and II and the rate $\tau(H\neq0)/\tau(H=0)$ does not necessarily depend on the sample pressure. F_3 appears in Cases III and IV as a weak but long-lived emission. The lifetime of F_3 varies with the excitation energy and the observing wavelength.

The behaviors of these three components are similar with those of intermediate case molecules such as methylglyoxal.[3]

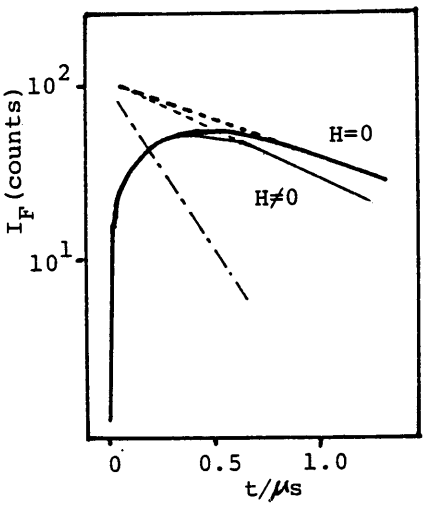

Fig. 3. Time-profile of fluorescence (F_2) in Case II.
Glyoxal 500 mtorr
Excitation at 440.3 nm (8_0^1)
Observation at 455.3 nm (0_0^0)
-.-. line indicate the rise-time of F_2.

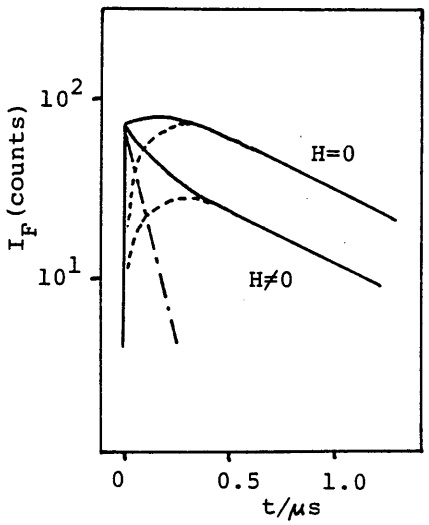

Fig. 4. Time-profile of fluorescence (F_2) in Case III.
Glyoxal 500 mtorr
Excitation at 422.7 nm ($4_0^1 8_0^1$)
Observation at 455.3 nm (0_0^0).
-.-.line indicates the decay of direct emission F_1 which overlaps the indirect emission F_2 with rise and decay.

Case IV. Excitation at 420 nm ~ 380 nm

A characteristic feature in Case IV is, as has been reported [4], the appearance of a very fast decay component, F_0 (fast fluorescence in Ref. 4). We show a typical result of Case IV in Fig.5. The time-resolved spectra are for the excitation at 415.1 nm where no fast decay had been observed. Spectrum A with a relatively low pressure sample shows that the direct emission from 422.7 nm level, as well as from the excited level, to the ground state is predominant just after

the excitation. Spectra B and C, taken at initial and later parts of decay after the excitation, show that the excited level itself is not the origin of emission but the fast and slow decays observed are composed of F_1 and F_2 of Case III excited at 422.7 nm. These results imply that the energy in the excited level is redistributed in a very short time (<7 ns) to the underlying level of the same symmetry by collision.

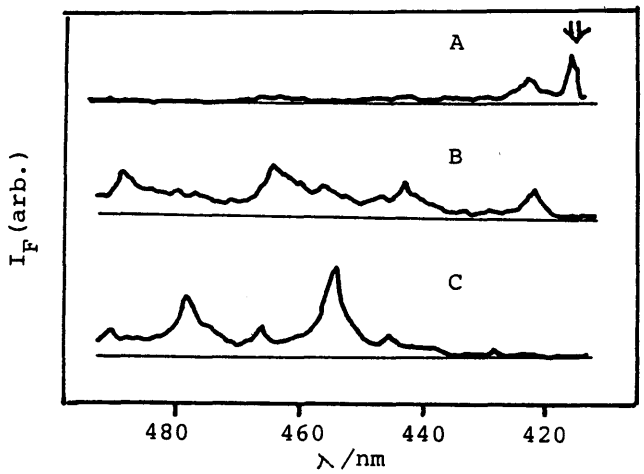

Fig. 5. Time-resolved fluorescence spectra.
Excitation at 415.1 nm ($2^1_0 8^1_0$)
as indicated with an arrow.
A; Glyoxal 50 mtorr. 0~200 ns after the excitation.
B; Glyoxal 500 mtorr. 0~200 ns after the excitation.
C; Glyoxal 500 mtorr. 500~1300 ns after the excitation.

Glyoxal has been expected to behave as an intermediate case molecule by the excitation in its higher energy state because the number of vibrational levels in T_1 state becomes large enough to cause the appreciable coupling between S_1 and T_1 states.[4] The complicated and rapid changes in the time-profile and manner of magnetic quenching observed here can not be interpreted in terms of the coupling with T_1.

We have worked out a new mechanism which interprete the whole phenomena observed in this study. The mechanism includes a postulation of a second triplet state, presumably $T_2(\pi,\pi^*)$ state, coupling with S_1 state below 435 nm and the energy transfers among the vibronic levels of S_1, T_1 and T_2 states.

REFERENCES

[1] Michel, C., and Tramer, A., Lifetimes of the S_1 state of glyoxal, Chem. Phys. 42 (1979) 315.
[2] Beyer, R.A., Zittel, P.F., and Lineberger, W.C., Relaxation of glyoxal, J. Chem. Phys. 62 (1975) 4016.
[3] Hashimoto, K., Nakamura, J., and Nagakura, S., Magnetic field effect in methylglyoxal, Chem. Phys. Lett., 74 (1980) 228.
[4] Van der Werf, R., Schutten, E., and Kommandeur, J., Fluorescence in glyoxal, Chem. Phys. 11 (1975) 281.

PHOTOCHEMICAL DIODE MODEL OF Pt/TiO_2 PARTICLE AND ITS PHOTOCATALYTIC ACTIVITY

T. SAKATA, T. KAWAI and K. HASHIMOTO
Institute for Molecular Science, Myodaiji, Okazaki 444, Japan

Received 28 December 1981; in final form 20 February 1982

The photocatalytic properties of a powdered semiconductor loaded with metal catalyst are discussed using a photochemical diode model. The rate of hydrogen evolution depends on particle size and correlates with irreversibility of oxidation of reactants. Only a small amount of Pt (smaller than 1/100 monolayer on TiO_2) is required to produce a remarkable effect on photocatalytic activity.

1. Introduction

Photocatalytic effects of semiconductors have been under investigation for some time because of their potential application to the direct conversion of solar energy into chemical energy [1]. Research in this field is now making rapid progress. During the past several years surface modification of powdered semiconductors such as TiO_2, $SrTiO_3$ and CdS by the addition of Pt, Pd or RuO_2 has been found to increase the photocatalytic activity of the semiconductor 10–10^3 times [2–7]. We have demonstrated that the photocatalytic activity of TiO_2 is greatly increased by supporting metal or metal oxide catalysts such as Pt and RuO_2 on TiO_2 [6–14]. By means of these surface-modified photocatalysts water can be split into oxygen and hydrogen [4,7,8]. Furthermore, hydrogen evolution is achieved with high efficiencies by reducing water with various organic compounds such as carbon [6,9], alcohols [12,13], carbohydrates [7], amino acids [10], fatty oil [10,11], fossil fuels [14], various biomasses [10,11], and artificial polymers [10,14] which act as electron donors. Similar effects are commonly observed among other semiconductors such as CdS. GaP, MoS_2, WS_2, etc. [14]. It is important to elucidate the mechanism of the photocatalytic reactions on these powdered semiconductors loaded with metal catalysts. In this report we describe the electronic structure of the particulate semiconductor (TiO_2)/metal diode, the size effect on hydrogen evolution, the correlation between the hydrogen evolution rate and the irreversibility of oxidation of substrate molecules, and the supporting effect of Pt on powdered semiconductors.

2. Experimental

As a photocatalyst, powdered TiO_2 (≈0.2 μm diameter, 99.99%, Furuuchi Ltd.) whose surface was modified with Pt was used. TiO_2 was reduced at 600°C for 2 h under a hydrogen atmosphere (200 Torr) until it became pale blue. This reduction treatment increases the photocatalytic activity, probably because it increases the donor (Ti^{3+}) concentration, resulting in enhanced n-type semiconductivity in TiO_2. Pt was then deposited photochemically on the surface of the reduced TiO_2 by illuminating powdered TiO_2 (5 g) suspended in a water–ethanol solution (20% aqueous solution, 100 ml) of K_2PtCl_6 (0.5 g) with a 500 W Xe lamp (Ushio, UXL 500) [2,13]. The TiO_2/Pt photocatalyst made in this way was used throughout the following experiment. The photocatalyst (TiO_2/Pt, 0.3 g) was suspended in a deaerated aqueous solution of an organic compound (ethanol was used in the present study as a typical organic compound for hydrogen evolution) [13] in a 280 ml Pyrex glass bulb which transmits light of wavelengths longer than 320 nm. When the glass bulb was irradiated from the bottom with white light from the 500 W Xe lamp,

0 009-2614/82/0000–0000/$ 02.75

gas bubbles evolved. Gaseous reaction products were trapped at −197 or −40°C and analysed by a quadrupole mass spectrometer (Anelva, AGA-360) as described previously [6]. The mass-spectrometric analysis of the gaseous products which could not be trapped at −197°C showed that hydrogen was the main component. The quantity of hydrogen gas was determined from the pressure using a sensitive manometer (Data Metrics Inc., barocel pressure sensor).

To measure the dependence of the hydrogen evolution rate on the photocatalyst size, the following four kinds of TiO_2 were used: a single crystal (reduced under a H_2 atmosphere of 400 Torr for 2 h, rutile, Nakazumi Crystal Ltd., 10 mm × 10 mm × 1.5 mm); TiO_2 powder of 70 μm average grain size made by crushing the single crystal; and TiO_2 powders of 0.2 μm (rutile, 99.99%, Furuuchi Ltd.) and of 0.04 μm average grain size (rutile, Mitsubishi Metal Corp.). The single crystal was ohmically contacted with a Pt plate (10 mm × 10 mm × 0.1 mm) at the back using a gallium–indium alloy to make a TiO_2/Pt photochemical diode. The TiO_2 powders were mixed with platinum black (10% weight ratio to TiO_2) in an agate mortar to make TiO_2/Pt photocatalysts.

3. Results and discussion

3.1. "Photochemical diode" model of powdered semiconductor photocatalysts and its electronic structure

Nozik [15], considering the photochemical properties of a metal/semiconductor diode, designated it a "photochemical diode". Although he was referring to a wafer of the semiconductor ohmically contacted with a metal layer at the back, a small, metal-loaded, semiconductor particle can be considered to have essentially the same properties. This suggestion has been put forward by several authors including us [4, 6,16,17], although a detailed analysis has not yet been carried out. Actually, as we shall show, fundamental properties of powdered semiconductor photocatalysts can be explained on the basis of the photochemical diode model.

Fig. 1 shows the electronic structure of a TiO_2/Pt particle in a neutral aqueous solution. In constructing this diagram we used the following values: the work

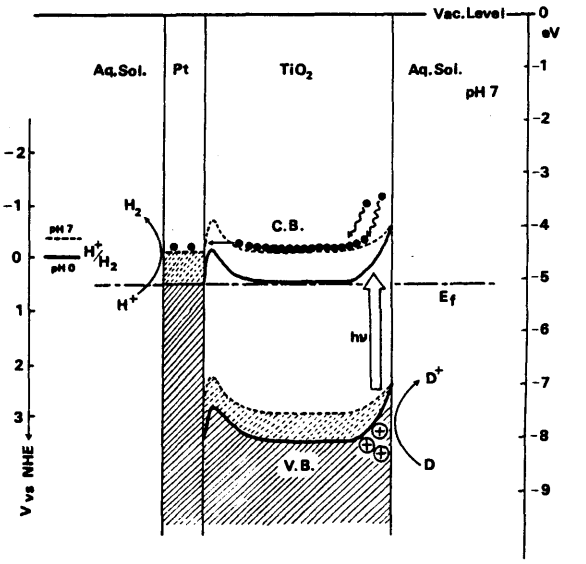

Fig. 1. The energy structure of the photocatalyst, TiO_2/Pt, in an electrolyte solution (pH = 7). The barrier height at the metal–semiconductor interface is modified by the image force of the metal. The solid lines show the energy levels in the dark and the dotted lines those under illumination.

function of Pt, 5.6 eV [18]; the electron energy for the normal hydrogen electrode (NHE), −4.5 eV from the vacuum level [19]; the Fermi level of an aqueous solution (pH = 7), 0.3 V versus NHE ‡; the flat band potential of TiO_2 at pH = 7, −0.5 V versus NHE [20]; the band gap of TiO_2, 3.0 eV. As can be seen in this diagram, the barrier height at the TiO_2/electrolyte interface is estimated to be ≈0.8 eV in the dark. The width of the space charge layer (d) is in the range 220–700 Å, assuming a carrier density of 10^{18}–10^{19} cm^{-3}. In order to estimate the energy structure under illumination, the photovoltage of the TiO_2/Pt slurry electrode was measured [21]. This photovoltage was −0.6 V (the voltage of the light electrode against that of the dark one) in the water–alcohol (methanol or ethanol) mixture, indicating a decrease of the band bending at the interface together with an upper shift of the conduction band inside the particle under illumination. The energy structure of

‡ Determined experimentally by measuring the electrode potential of the Pt electrode immersed in the solution. Its potential immersed in slurries in the dark showed +0.3 V versus NHE.

the photocatalyst under illumination is shown by the dotted lines in fig. 1.

It can be seen from fig. 1 that hydrogen evolution becomes possible due to the upper shift of the Fermi level of Pt under illumination. In fact, hydrogen evolution is quite efficient in water–alcohol systems [12, 13]. A band bending of 0.3–0.4 eV is still expected under illumination and at this space charge layer, electrons and holes would be separated. The hydrogen evolution rate was found to depend on the wavelength when monochromatic light was used to excite the semiconductor. The evolution rate is small at the bandgap wavelength of TiO_2 (410 nm) and grows to a maximum at 380 nm, similar to the wavelength dependence of the photocurrent observed for a single-crystal electrode [22]. This result indicates that the charge separation at the space charge layer of a TiO_2/Pt powdered photocatalyst is important in hydrogen evolution. Based on this photochemical diode model, oxidation should take place at the semiconductor surface (reduction at the metal surface) for an n-type semiconductor/metal diode, and at the metal surface (reduction of the semiconductor surface) for a p-type.

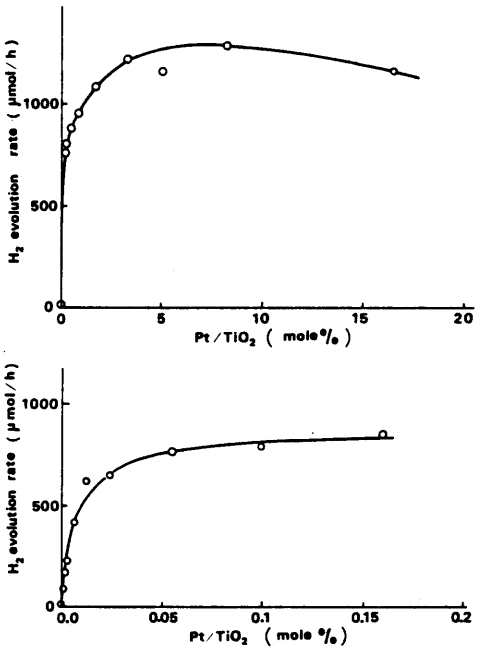

Fig. 2. Dependence of hydrogen evolution rate on the amount of Pt supported photochemically on TiO_2. Water: 15 ml, ethanol: 15 ml, TiO_2/Pt: 300 mg, irradiation with a 500 W Xe lamp.

3.2. Catalytic effect of Pt on semiconductor surface

The hydrogen evolution rate depends on the kind of metal which is supported on the powdered semiconductor surface. For instance Pt, Pd or Rh increase the hydrogen evolution rate 20–100 times, whereas Fe on TiO_2 suppresses evolution. This remarkable dependence is considered to arise partly from the catalytic effect of metals on hydrogen evolution. For instance, Pt, Pd and Rh are well known as good electrode materials, being $\approx 10^4$ times more active than the Ti electrode for hydrogen evolution [23]. In order to investigate the supporting effect of Pt on TiO_2, the amount of Pt on a fixed amount of TiO_2 was varied. Fig. 2 shows the dependence of the hydrogen evolution rate on the amount of Pt. It will be observed that the rate for the Pt/TiO_2 photocatalyst (5 mole% Pt) is $\approx$100 times larger than that for TiO_2 alone and shows a maximum at $\approx$5 mole% Pt on TiO_2. It will also be observed that the rate is not sensitive to decreasing amounts of Pt. In fact, the activity of the photocatalyst is maintained even at as small a ratio of Pt to TiO_2 as 0.0005, below which it decreases rapidly as illustrated in fig. 2b. At the ratio Pt/TiO_2 = 0.0005, Pt is expected to form a 0.01 monolayer on the TiO_2 surface, assuming uniform deposition and a surface area for powdered TiO_2 of 10 m^2/g (the average particle size of TiO_2 is 0.2–0.4 μm). It is remarkable that so small an amount of Pt (10^{-2} monolayer) is sufficient to produce good photocatalytic activity. It should be noted that application of the photochemical diode model to such a weakly loaded semiconductor particle might be difficult. It is clear, as the plot in fig. 2a demonstrates, that the catalytic activity of semiconductors in hydrogen evolution is strongly enhanced by loading with metal.

3.3. Size effect of photocatalytic activity

Fig. 3 shows the dependence of the rate of hydrogen evolution on the particle size (or surface area) of TiO_2 in an ethanol–water (1 : 1) mixture. This plot shows that the evolution rate is very small, 2 μmol/h, for a sandwich-like diode (diamond in fig. 3) composed of a TiO_2 single crystal (10 mm × 10 mm × 1.5 mm) and a Pt plate (10 mm × 10 mm × 0.1 mm) with an

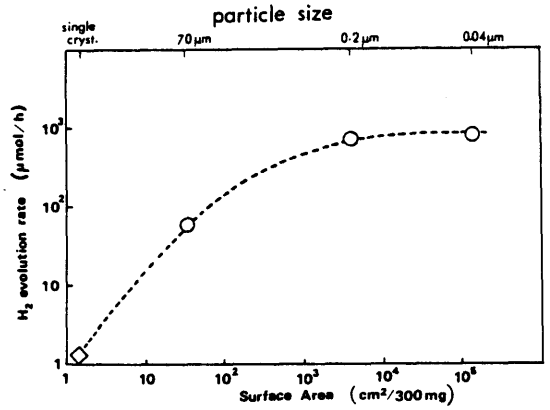

Fig. 3. Dependence of hydrogen evolution on the particle size and surface area of powdered (○) or single-crystalline (◇, 10 mm × 10 mm × 0.8 mm) TiO_2.

ohmic contact, whereas it is more than 800 μmol/h (400 times greater) for photocatalysts with a particle size smaller than 0.4 μm.

At first sight it would appear that this increase is a result of the increased surface area of the photocatalyst, as in the case of thermal catalysts. However, a complete explanation must take other factors into consideration. In the photoelectrode reaction with a TiO_2 single crystal and a light source like a 500 W Xe lamp, the rate-determining step is known to be not the photoanodic reaction (surface reaction) but the supply of photogenerated holes to the surface. In this case the anodic photocurrent increases linearly with increasing light intensity. Therefore the anodic reaction (oxidation) is limited not by the surface area of TiO_2 but by the light intensity. Furthermore, the photocurrent of the electrochemical cell,

$\langle TiO_2 |$ ethanol–water (1 : 1), 1 M KCl $| Pt \rangle$,

is small due to the small band bending of TiO_2 under short-circuit conditions, and is ≈100 μA with a 500 W Xe lamp. This photocurrent corresponds to a hydrogen evolution rate of 2 μmol/h in fair agreement with the experimental value, 1 μmol/h, for the TiO_2 single-crystal–Pt plate photochemical diode (see fig. 3).

The following explanations may be advanced for the improved efficiency of charge separation, as shown by the data in fig. 3, for a small particle TiO_2/Pt photocatalyst compared to a photochemical diode composed of a TiO_2 single-crystal–Pt plate. First, for a given quantity of photocatalyst the smaller the size of the semiconductor particle, the larger the total volume of the space charge layer, where electrons and holes separate efficiently. Secondly, electrons and holes easily reach the surface within their lifetime, since they are most reactive at the surface. Thirdly, if active centers of some sort are assumed to play an important role in the photoanodic reaction, a powdered semiconductor composed of small particles is likely to contain more of such centers than a single-crystal semiconductor. Finally, from the viewpoint of the cathodic reaction, the larger the surface area of supported Pt the more efficiently hydrogen will evolve, since hydrogen evolution is a dark reaction and proportional to the surface area of the electrode.

3.4. Correlation between the efficiency of hydrogen evolution and the irreversibility of the surface reaction

The first step in photoelectrochemical energy conversion is charge separation at the space charge layer of the semiconductor. In this regard the irreversibility of the surface reactions is important when a semiconductor powder or a dye is used as a photocatalyst. Table 1 shows the rate of hydrogen evolution with TiO_2/Pt as photocatalyst and various electron donors. For H_2O, $S_2O_3^{2-}$, I^- and Fe^{2+}, the evolution rate is quite small even though all these donors, except H_2O, are easily oxidised. In addition, it is very high for methanol, ethanol, ethylene glycol and glycerol, which are not readily oxidised. However, alcohols are known

Table 1
Correlation between hydrogen evolution rate and the reversibility of the reactions

	Reactant (electron donor)	H_2 evolution rate (μmol/10 h) [a]
reversible system	H_2O	<1
	Fe^{2+}	1
	$S_2O_3^{2-}$	6
	I^-	<1
irreversible system	CH_3OH	9000
	C_2H_5OH	8000
	glycerol	7500
	ethylene glycol	5800

[a] 500 W Xe lamp: irradiation for 10 h. Photocatalyst: TiO_2/Pt (300 mg).

to show a current-doubling effect and decompose irreversibly, releasing two electrons to n-type semiconductors. Therefore with TiO_2 photocatalysts, they are easily converted to aldehyde, carboxylic acid and finally into CO_2. This reaction sequence is thought to be highly irreversible, and hence favorable to an efficient hydrogen evolution. On the other hand, the quantum yield of hydrogen evolution is very small, ≈0.02%, for the decomposition of water into H_2 and O_2. Since the oxidation products of water, ·OH, $\cdot O_2H$ and O_2, are good electron acceptors, they are reduced easily to water [24]. This is probably the main reason why the quantum yield is so small. Similarly, oxidation of I^-, Fe^{2+} and $S_2O_3^{2-}$ is probably highly reversible.

In the photoanodic reaction of a water–alcohol mixture at a TiO_2 electrode, water is oxidized competitively with alcohols [13,25]. However, O_2 is not detected at all with TiO_2 powder photocatalysts. The difference results from the fact that oxidation and reduction proceed simultaneously on the same particle surface in the latter case, whereas they proceed separately at the different electrodes in the former case. Hence the existence of back reactions in the small-particle system is of the utmost importance.

References

[1] K.I. Zamaraev and V.N. Parmon, Catal. Rev. 22 (1980) 261.
[2] B. Kraeutler and A.J. Bard, J. Am. Chem. Soc. 100 (1978) 2239.
[3] J.M. Lehn, J.P. Sauvage and R. Ziessel, Nouv. J. Chim. 4 (1980) 623.
[4] K. Kalyanasundaram, E. Borgarello and M. Grätzel, Helv. Chim. Acta 64 (1981) 362.
[5] S. Sato and J.M. White, Chem. Phys. Letters 72 (1980) 83.
[6] T. Kawai and T. Sakata, Nature 282 (1979) 283.
[7] T. Kawai and T. Sakata, Nature 286 (1980) 474.
[8] T. Kawai and T. Sakata, Chem. Phys. Letters 72 (1980) 87.
[9] T. Kawai and T. Sakata, J. Chem. Soc. Chem. Commun. (1979) 1048.
[10] T. Kawai and T. Sakata, Chem. Letters (1981) 81.
[11] T. Sakata and T. Kawai, Nouv. J. Chim. 5 (1981) 279.
[12] T. Kawai and T. Sakata, J. Chem. Soc. Chem. Commun. (1980) 694.
[13] T. Sakata and T. Kawai, Chem. Phys. Letters 80 (1981) 341.
[14] T. Sakata and T. Kawai, J. Syn. Org. Chem. Japan 39 (1981) 589.
[15] A.J. Nozik, Appl. Phys. Letters 30 (1977) 567.
[16] A.J. Bard, J. Photochem. 10 (1979) 59.
[17] S. Sato and J.M. White, J. Catal. 69 (1979) 128.
[18] D.E. Eastman, Phys. Rev. B2 (1970) 1.
[19] F. Lohmann, Z. Naturforsch. A22 (1967) 843.
[20] M. Tomkiewicz, J. Electrochem. Soc. 126 (1979) 1505.
[21] W.W. Dunn, Y. Aikawa and A.J. Bard, J. Electrochem. Soc. 128 (1981) 222.
[22] H. Yoneyama, H. Sakamoto and H. Tamura, Electrochim. Acta 20 (1975) 341.
[23] J. O'M. Bockris and A.K.N. Reddy, Modern electrochemistry (Plenum Press, New York, 1974) p. 1238.
[24] C.D. Jaeger and A.J. Bard, J. Phys. Chem. 83 (1979) 3146.
[25] M. Miyake, H. Yoneyama and H. Tamura, Chem. Letters (1976) 635.

Radiation Effects Letters, 1982, Vol. 67, pp. 129-133
0142-2448/82/6705-0129$6.50/0

Printed in the United States of America

NEUTRAL PARTICLE EMISSION FROM ZINC OXIDE SURFACE INDUCED BY HIGH-DENSITY ELECTRONIC EXCITATION

T. NAKAYAMA and N. ITOH
Department of Crystalline Materials Science, Faculty of Engineering, Nagoya University, Furo-cho, Chikusa-ku, Nagoya 464, Japan
T. KAWAI, K. HASHIMOTO and T. SAKATA
Institute for Molecular Science, Myodaiji, Okazaki 444, Japan

Abstract---Emission of neutral zinc and oxygen atoms and oxygen molecules emitted from zinc oxide surface by laser irradiation have been measured. It is found that the emission intensity starts to increase when the laser intensity exceeds a certain threshold value, indicating that the particle emission is a high density electronic excitation effect. The energy spectrum of emitted particles is found not to follow the Maxwellian distribution.

It is known that bombardments of insulators by energetic ions cause neutral atom ejection, the yield of which is several orders of magnitude larger than that predicted on the basis of elastic collision cascade theory.[1),2)] This process has been ascribed to the high density electronic excitation effect in ion tracks in solids and much attention has been paid on the mechanism of the conversion of energy possessed as the high density electronic excitation to the kinetic energy that causes atomic ejection. Such energy transfer from high density electronic excitation to the atomic motion has been also known to cause the enhancement of chemical etching in ion tracks.[3)] Irradiation with high intensity laser above the fundamental absorption edge of a solid is also expected to cause high density electronic excitation near the surface. It has been shown that high-density excitation in ion tracks causes the same luminescence lines as those observed by high-intensity laser irradiation.[4)] Thus we may expect that the laser annealing[5)] is process similar to the high-density electronic excitation effect in ion tracks. Following three mechanisms for atomic motion under high density electronic excitation have been proposed. (1) Thermal model,[6),7)] namely enhancement of the atomic motion in the molten zone near the surface. (2) Ion explosion model,[8)~10)] namely enhancement of atomic motion due to coulombic field induced in positively charged core formed along the axis of ion tracks. (3) Plasma model,[11)~13)] namely enhancement of the atomic motion due to the softening of atomic bonds in crystals and due to the screening of coulombic field in high density electron-hole plasma.

So far no report has been published on neutral particle emission due to laser-induced high density electronic excitation of insulators.

We have undertaken the studies of neutral particle emission induced from zinc oxide (ZnO) by nitrogen-laser. The band gap of ZnO is 3.2 eV and is smaller than the resonance energy of nitrogen laser (3.68 eV). High-intensity-laser-induced particle emission mainly from metal surface has been reported already.[14] The ion emission from metal surface, which has been studied extensively in 1960's, takes place at a laser intensity larger more than 100 times than that used in the present investigation. High intensity laser irradiation of metals is known to cause neutral particle emission that exhibits a Maxwellian distribution with an effective temperature between the melting and boiling points of the target materials.[15)~16)] This phenomenon has been ascribed to the thermal effect, namely laser-induced atom evapolation from molten zone at the surface.

In the present letter we report the results of experimental observation of neutral particles emission from ZnO by nitrogen-laser irradiation. The dependence of the emission intensity on the laser intensity was found to exhibit a threshold laser intensity, above which the neutral particle emission is observed. The neutral particle emission reported in the present paper is ascribed to a high-density electronic-excitation effect. The energy spectra were shown not to follow the Maxwellian distribution.

Experimental arrangement is basically the same as described elsewhere.[18)] A specimen of ZnO single crystal (MRC), with a size of 10 × 10 × 2 mm, was etched by dilute solution of hydrochloric acid and was mounted on a sample holder equipped with a heating system. The surface of the specimen was cleaned by bombardment with Ar^+ ions and was annealed subsequently. The sample holder was placed at the center of an ultrahigh vacuum chamber, the base pressure of which is 2×10^{-9} Torr. The specimen was bombarded with 10 ns light pulses generated from a nitrogen laser (Molectron UV 22). The repetition rate was varied from 1 to 25 s^{-1}. The laser spot on the sample was about 5×10^{-3} cm^2. The laser power was calibrated with a power meter (ED - 100), and the maxmum laser power density was determined to be about 10^7 W/cm^2. Laser light was incident on the sample at an angle of 45° to the surface normal. Metallic neutral density filters (Oriel) were used to change the intensity of the laser light.

Emitted neutral particles were analyzed with a quadrupole mass spectrometer (UTi 100C) equipped with an ionizer and were detected with a channeltron. The flight path for the time-of-flight analysis was 7 cm. Signals amplified by an amplifier (PAR Model 115) were stored in a transient recorder (Kawasaki M-500T) and were averaged with a signal averager (Kawasaki TMC-400). The averaged time-of-flight signal was recorded on a oscilloscope (Tektronix465) or an X-Y recorder (Riken Denshi D72 BP).

The results of the mass spectroscopic analysis indicate that nitrogen-laser irradiation emits Zn, O and O_2 by nearly the same yield. In order to decide whether O is generated in the ionizer or emitted from the surface, we measured the intensity ratio of O to O_2 when O_2 gas was introduced into the spectrometer. The obtained ratio was 0.2 and was much smaller than the ratio obtained when ZnO was irradiated with laser light. Thus we consider that both O and O_2 are emitted from the surface of ZnO by laser irradiation.

The dependence of the emission intensity of Zn, O and O_2 on the laser-intensity are shown in Fig. 1. Clearly, the emission intensity is zero at low laser intensities and starts to increase when the laser intensity exceeds a certain threshold value. Time-of-flight spectra of neutral zinc atoms emitted from ZnO were also measured and analyzed using the conventional method.[19] Observed spectra were corrected using the fact that the ionization efficiency in the ionizer is inversely proportional to the ion velocity. The relation between energy E and the differential emission intensity dY/dE of Zn atoms divided by $\sqrt{E}$, is shown in Fig. 2. In this plot the data points should fall on a straight line if the energy distribution follows the Maxwellian distribution:

$$\frac{dY}{dE} \propto \sqrt{E}\ \exp(-E/kT). \qquad (1)$$

If we assume that the plots at the highest energy region, namely above 0.3 eV, fit to a straight line, we obtain the effective temperature to be 3500 K. Thus the spectra may be regarded as the superposition of several components, each of which possesses various effective temperatures lower than 3500 K.

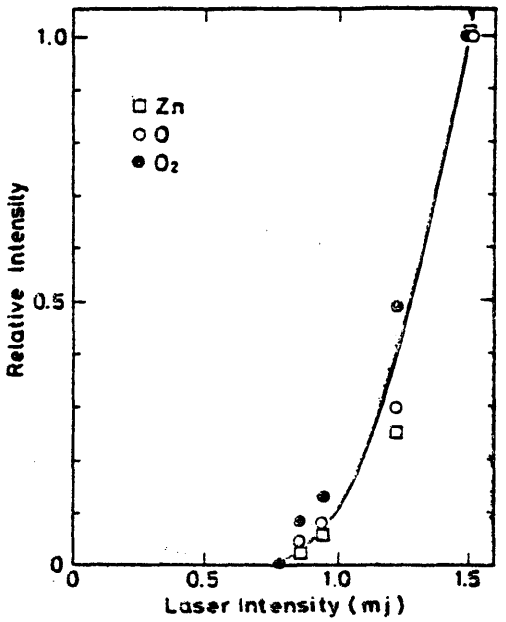

FIGURE 1, Laser intensity dependence of the relative neutral particle emission yield measured at room temperature.

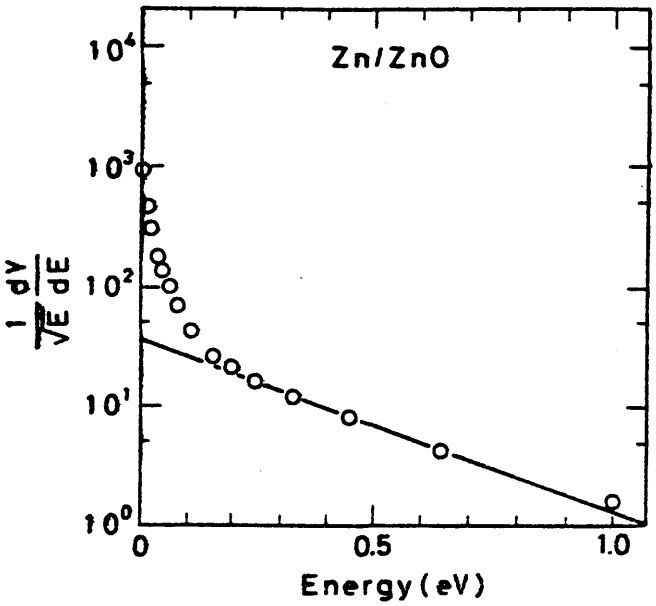

FIGURE 2, The energy spectrum of neutral zinc atoms emitted from ZnO at 210°C. The abscissa is energy E and the ordinate is the differential emission yield dY/dE, divided by $\sqrt{E}$.

The primary interaction of nitrogen laser light with ZnO is electronic excitation, or creation of electron-hole pairs. Moreover the experimental results of the intensity dependence indicate that the neutral particle emission takes place only by high-density electronic excitation. Among the mechanisms suggested for the electron-lattice energy transfer process at a high density, the ion-explosion model cannot be applicable to the laser-excitation case, since the laser irradiation causes a uniform electron-hole distribution over a large irradiated area. Seiberling et al.[1] have measured the energy spectra of neutral particles from UF_4 emitted by high energy ion bombardments and obtained the Maxwellian distribution with an effective temperature much higher than the melting point. Based on the comparison of the time required for the heat transfer with the electron-lattice relaxation time, they argued against the thermal model and invoked the thermalized ion-explosion model. The result of the present investigation that the spectra consist of components having an effective temperature higher than the melting point of ZnO (2250 K) may suggest that the thermal model, in addition to the ion-explosion model, may not be applicable. Thus we are inclined to ascribe the photo-induced particle emission to the formation of the electron-hole plasma. A modified plasma model will be presented in a forthcoming paper.

In conclusion we have shown that neutral particle emission from ZnO occurs when photo-excited above a certain threshold excitation density. Similar results have been obtained for TiO_2 and GaP, which will be published shortly.

The authors wish to thank to Mr. Ichikawa for his assistance. This work was supported by the Joint Study Program (1980 - 1981) of the Institute for Molecular Science and was partially supported by Grant-in-Aid for Science Research from Ministry of Education.

REFERENCES

1. L. E. Seiberling, J. E. Griffith and T. A. Tombrello, Rad. Effects 52, 201 (1980).
2. J. E. Griffith, R. A. Weller, L. E. Seiberling and T. A. Tombrello, Rad. Effects 51, 223 (1980).
3. R. L. Fleisher, P. B. Price and R. M. Walker, Nuclear Tracks in Solids (Univ. of California Press, Berkeley, 1975).
4. Y. Mitsushima and N. Itoh, Rad. Effects 51, 185 (1980).
5. C. W. White and P. S. Peercy (eds.) Laser and Electron Beam Processing of Materials (Academic Press, New York, 1980).
6. J. Bøttiger, J. A. Davies, J. L'ecuyer, N. Matsunami and R. W. Ollerhead, Rad. Effects 49, 119 (1980).
7. R. W. Ollerhead, J. Bøttiger, J. A. Davies, J. L'ecuyer, H. K. Haugen and N. Matsunami, Rad. Effects 49, 203 (1980).
8. W. L. Brown, W. M. Angustyniak and L. J. Lanzerotti, Phys. Rev. Letters 45, 1632 (1980).
9. R. L. Fleisher, P. B. Price and R. M. Walker, J. Appl. Phys. 36, 3645 (1965).
10. W. L. Brown, W. M. Augustyniak, E. Brody, B. Cooper, L. J. Lanzerotti, A. Ramirez, R. Evatt and R. E. Johnson, Nucl. Inst. Methods 170, 321 (1980).
11. I. B. Khaibullin, E. I. Shtyrkov, M. M. Zaripov, R. M. Bayazitov, and M. F. Galjautdinov, Rad. Effects 36, 225 (1978).
12. J. A. Van Vechten, R. Tsu and F. W. Saris, Phys. Letters 74A, 417 and 422 (1979).
13. J. A. Van Vechten, Phys. Rev. B23, 5543 and 5551 (1981).
14. J. F. Ready, Effects of high-power laser radiation (Academic Press, New York, 1971).
15. R. A. Olstad and D. R. Olander, J. Appl. Phys. 46, 1499 (1975).
16. R. A. Olstad and D. R. Olander, J. Appl. Phys. 46, 1509 (1975).
17. A. T. Prengel, J. Dehaven, E. J. Johonson, and P. Davidovits, J. Appl. Phys. 48, 3551 (1977).
18. T. Kawai and T. Sakata, Chem. Phys. Letters 69, 33 (1980).
19. H. Overeijnder, M. Szymonski, A. Haring and A. E. De Vries, Rad. Effects 36, 63 (1978).

—コミュニケーション—

n 型半導体表面に担持した RuO_2 と Pt の触媒作用について

坂田 忠良*, 川合 知二*, 橋本 知仁*

The Catalytic Properties of RuO_2 and Pt on n-type Semiconductors

Tadayoshi SAKATA*, Tomoji KAWAI*, and Kazuhito HASHIMOTO*

RuO_2 は酸化触媒としてよく知られている．この数年，RuO_2 は光触媒的水の分解のための触媒としてよく用いられてきた．われわれはすでに RuO_2/TiO_2, $RuO_2/TiO_2/Pt$ が水の光分解に活性を示すことを示した[1,2]．最近 Grätzel のグループは $RuO_2/TiO_2/Pt$ コロイドを用いて，310 nm で 30 %の量子効率を持つ大変効率のよい光触媒の開発に成功したことを報告している[3]．彼らはまた，$RuO_2/CdS/Pt$ が可視光で水を分解しうるとしている[4]．このような光触媒において，RuO_2 は常に酸化触媒，Pt は水素発生の還元触媒として考えられてきた．

われわれは n-型半導体上におけるこれらの触媒の役割を明らかにするため，TiO_2 や CdS 単結晶上に少量の RuO_2 や Pt を塗布あるいは蒸着し，その光電化学的挙動を測定した．

Fig. 1 の（a）はよく知られた TiO_2 単結晶の水（1 M KCl）中での電流－電圧曲線を示す．（b），（c）は，RuO_2 蒸気にさらすことによって RuO_2 を TiO_2 表面に沈着させたものの電流－電圧曲線である．RuO_2 をつけることによって光アノード電流の著しい減少がみられる．ほとんど目に見えないくらいつけたとき（曲線（b））でも著しい効果があることから，RuO_2 の光吸収によって TiO_2 に到達する光量が減少するのではなく，RuO_2 が TiO_2 表面で再結合中心として働いているためであることを示唆している．次に興味あるのは，フラットバンドポテンシャル近くの電位では，カソード電流が増大していることである．これは，RuO_2 が酸化触媒としてのみでなく，還元の触媒として働くことを示している．実際 RuO_2 が水素発生の良好な触媒であることは Amouyal らによって示されている[5]．もし，RuO_2 が酸素発生触媒として働いているのならば，光触媒の作動電位と考えられる $-0.3 \sim -0.5$ V *vs.* SCE の電位領域で光アノード電流は増加してもよいはずである．結果は逆で，電流はカソード方向に流れている．このことは，水の完全分解においては，RuO_2 が還元触媒として働くことを示唆している．このことをさらに確めるために中戸，坪村らによって行われたと同じ方式で光起電力の測定を行った[6]．1 cm × 1 cm × 0.1 cm の単結晶 TiO_2 上に Pt と RuO_2 をおのおの別の領域につけ，光照射時に電位がどのようにシフトするかを測定する方法である．水の中では，RuO_2, Pt の電位は，光照射によって負に移動する．このことは Pt と RuO_2 に電子が流れこみ，そのフェルミレベルが負に移動したことを示す．同様な光起電力の挙動は，CdS 単結晶上の RuO_2, Pt に対してもみられた．

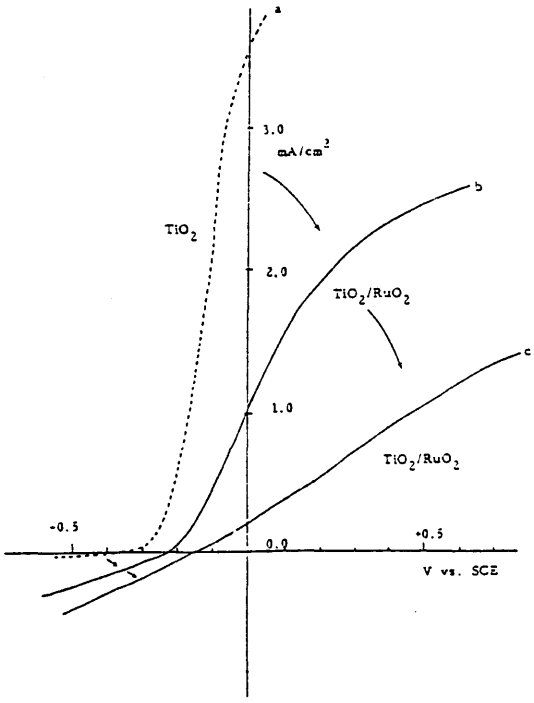

Fig. 1 The effect of RuO_2 deposition on the current-voltage curve of a TiO_2 single crystal electrode under illumination. Curve a: TiO_2, curve b: TiO_2/RuO_2 (very small amount of RuO_2, the layer of RuO_2 deposited is not visible to the naked eyes), curve c: TiO_2/RuO_2 (further deposition, the thickness is estimated to be several hundred angstroms). Electrolyte solution: 1M KCl, N_2 bubbled. Sweeping rate of voltage: 1 mV/s

これらの事実から，水の完全分解に際しては 1）RuO_2 は Pt と同様再結合センターとして，2）また，Pt と同様水素発生の触媒作用をすることができると推論できる．

このような還元触媒としての役割は，粉末半導体を使

* 分子科学研究所（〒444 岡崎市明大寺町）Institute for Molecular Science (Myodaiji, Okazaki 444)

Table 1 Hydrogen evolution from ethanol-water mixture (1:1) by using various particulate TiO_2 photocatalysts. Experimental conditions; Light sourcs: 500 W Xe lamp, each photocatalyst; 300 mg, water: 15 cm^3, ethanol: 15 cm^3

photocatalyst	H_2 evolution rate (μmol/h)
TiO_2	2.3
TiO_2/RuO_2	79
TiO_2/Pd	230
TiO_2/Pt	564

Table 2 Catalytic role of RuO_2

(photo)Catalyst	Reaction	Catalytic Role of RuO_2
	$H_2O \longrightarrow H_2 + 1/2\ O_2$	H_2 evolution
RuO_2/TiO_2 (or CdS)	Org.compd. $+ H_2O \longrightarrow H_2$ [a]	catalyst
RuO_2/TiO_2(or CdS)/Pt	Strong Oxid. $+ H_2O \longrightarrow O_2$ [b][c]	O_2 evolution catalyst

a) Organic compound: various alcohols, carbohydrates, organic acids, aminoacids, hydrocarbons, EDTA---

b) Strong oxidizing agent: Ag^+, $S_2O_3^{2-}$, $Co^{3+}(NH_3)_5$, and $Ru(bipy)_3^{3+}$

c) RuO_2 works surely as an oxygen evolution catalyst especially when the semiconductor (TiO_2 or CdS) is not excited.

った水素発生の実験からも推測される．Table 1 には，エタノール，水混合系からの水素発生の速度を示す．この表からわかるように，RuO_2 はかなりよい光触媒活性を示している．この系においては，エタノールの酸化は容易であり，水素発生が律速段階と考えられるので，RuO_2 の還元触媒効果を示していると考えられる．RuO_2 は金属的伝導体であることから TiO_2 や，CdS と接触したとき，還元サイトとなることは容易に理解できるところである．

しかし，中戸，坪村らの実験が示すように強いアクセプターが存在するとき，n 型半導体上の金属は酸化触媒として働くことが考えられる[6]．実際，Ag^+, $S_2O_8^{2-}$, $Co^{3+}(NH_3)_5$, Fe^{3+}, $Ru(bipy)_3^{3+}$ 等をアクセプターとした酸素発生はこのことを考えることによって説明される．このような強い電子受容体の存在は，アノーデックバイヤスと同等に考えられ，電子は優先的に，これらの電子受容体の還元に使われ，正孔は光触媒上に残る．その結果 n 型半導体上の金属の電位は正に移動することが考えられる．中戸，坪村はアノーデックバイヤス下では，TiO_2 上の金属（Au）が，酸素発生電位にまで移動することを示した．微粒子系においても，強い電子受容体が存在する場合，n 型半導体上の RuO_2 は O_2 発生の触媒として働くことが予想される．このようなことを考えると，Table 2 に示したように，RuO_2 の触媒としての働きは二つに分類されることがわかる．

文　献

1) T. Kawai and T. Sakata, *Chem. Phys. Lett.* **72**, 87 (1980).
2) T. Kawai and T. Sakata, *Nature* **286**, 474 (1980).
3) D. Duonghong, E. Borgarello and M. Grätzel, *J. Amer. Chem. Soc.* **103**, 4685 (1981).
4) K. Kalyanasundaram, E. Borgarello and M. Grätzel, *Helv. Chim. Acta* **64**, 362 (1981).
5) E. Amouyal, P. Keller and A. Moradpour, *J. C. S. Chem. Comm.*, 1019 (1980).
6) Y. Nakato and H. Tsubomura, *Israel J. Chem.* **22**, 180 (1982).

(Received Oct. 12, 1982 ; Accepted Oct. 29, 1982)

別　刷

日本化学会誌 (化学と工業化学)

NIPPON KAGAKU KAISHI 1984

Journal of the Chemical Society of Japan, Chemistry and Industrial Chemistry

社団法人　日本化学会

論文特集「光化学反応とその応用」

（日本化学会誌，1984，（2），p. 277～282）

半導体微粒子光触媒の構造と反応性

（1983年8月10日受理）

川合知二*・坂田忠良**・橋本和仁**・川合真紀***

半導体微粒子光触媒の反応性を決めている要因を明らかにし，可視光で効率よく働く光触媒を設計する目的で，種々の半導体粉末の電子構造と，水と有機物からの水素発生反応活性との関連を調べた。その結果，第一近似として，微粒子の価電子帯，伝導帯と反応分子のレドックスレベルとの相対位置で活性が支配される事が示された。また，光電析法で調製した白金担持 TiO_2 微粒子光触媒の表面構造，電子構造を電子顕微鏡，XPS を用いて調べ，白金が豹の斑点のように 100 Å 程度の大きさで TiO_2 上に数多く分散していることがわかった。この構造の特徴が酢酸の分解反応でのレドックス機構を促進していること，また，不可逆的に分解する有機物と水からの水素発生に有効であることを示した。さらに，微粒子光触媒の特徴を半導体光電極と比較して議論し，その類似点と相違点を明らかにした。

1 緒　　言

近年，太陽エネルギー変換の観点から半導体微粒子を用いた水の光触媒的分解の研究がさかんに行なわれている。このような反応の活性を上げるためには，光触媒の反応性が触媒の電子構造，表面構造によって，どのように支配されているかを知ることが重要となる。本研究は高分解能電子顕微鏡，X線光電子分光法，電気化学的方法を用いて半導体微粒子の表面構造，エネルギー構造を知り，反応性との関係を明らかにしようとするものである。

TiO_2 粉末に白金，RuO_2 などを担持した光触媒を水と有機物の存在下で光照射すると，価電子帯（O：2p）の正孔によって有機物が酸化されるとともに，伝導帯（Ti：3d）の電子によって水が還元され水素が発生する[1]。固体の炭素[2]，アルコール類[3]，炭水化物[4]，タンパク質，脂肪，人工高分子[5]など種々の有機物が分解され電子供与体として働くことがわかってきた。本研究においては水とアルコールからの水素発生，水と酢酸からのメタン発生を代表的な反応例として取り上げた。

はじめに種々の半導体粉末を用いて，水とアルコールからの水素発生，酢酸からのメタン発生効率を調べ半導体の電子構造と反応活性との関係を考察した。つぎに用いた半導体微粒子の表面構造，とくに，担持した白金の状態を電子顕微鏡，XPS によって調べ反応に与える影響を考察した。このような表面の構造を反映する反応系の例として同位体を用いた酢酸の分解反応の実験を行なった。さらに，溶液で用いる還元剤の種類を変化させて，その酸化されやすさと反応性との関連を調べた。最後に微粒子光触媒と光電極の相違について考察した。

大阪大学産業科学研究所，567　茨木市美穂丘
** 分子科学研究所，444　岡崎市明大寺町西郷中
*** 東京大学理学部化学科，113　東京都文京区本郷
現在 大阪ガス株式会社総合研究所，554 大阪市此花区酉島

1) 川合知二，坂田忠良，現代化学，**No. 118**，52(1981)；有合化，**39**，589(1981).
2) T. Kawai, T. Sakata, *Nature*, **282**, 283(1979).
3) T. Kawai, T. Sakata, *J. Chem. Soc., Chem. Commum.*, **19**, 694(1980)；T. Sakata, T. Kawai, *Chem. Phys. Lett.*, **80**, 341(1981).
4) T. Kawai, T. Sakata, *Nature*, **286**, 474(1980).
5) T. Kawai, T. Sakata, *Chem. Lett.*, **1981**, 81；T. Sakata, T. Kawai, *Nouv. J. Chim.*, **5**, 279(1981).

2 実　　験

2.1 光触媒の調製

以下の二つの異なった白金の担持法を用いた。

1) **光電析法**[6]：TiO_2/Pt 系におもに用いた。TiO_2 粉末と 0.1～5 wt% の K_2PtCl_6 をメタノール水溶液（1：1）に懸濁し，スターラーでかきまぜながら光照射し，白金を TiO_2 上に析出させた。

2) **混練法**[2)~4)]：所定の半導体粉末と 10 wt% の白金ブラックをめのう乳鉢で混練して調製した。この方法は溶けやすい不安定な半導体粉末にも適用できるため，種々の半導体粉末触媒の活性を比較するのに適した白金担持法である。

半導体粉末は以下のものを用いた。

TiO_2, CdS, SiC（片山化学），MoS_2, WO_3（関東化学），GaP, Si, CdSe（高純度化学），Fe_2O_3（三津和化学），$MoSe_2$（レアメタリック）

2.2 反　　応

このように作製した光触媒（300 mg）を 280 ml のパイレックス製フラスコに入れ水-エタノール（1：1，40 ml）中に懸濁させ排気脱ガスしたのち，500W キセノンランプ（ウシオ電機）で光照射した。発生した水素はガスクロマトグラフによって定量した。酢酸からのメタン発生は酢酸-水（1：1，40 ml）中で行ない，発生メタン，二酸化炭素は質量分析計で定性，圧力計で定量

6) B. Kraeutler, A. J. Bard, *J. Am. Chem. Soc.*, **100**, 4317(1978).

を行なった。メタン中の重水素分布は質量分析計で決定した。

電子顕微鏡像の観察は，日本電子製 JEM-200 CX を用いて行なった。試料は，光触媒を水に懸濁し，その一部を表面を酸化物イオン衝撃処理したニトロセルロース膜に乗せ，真空排気することにより作製した。

XPS の測定は高分解能装置（ヒューレットーパッカード社製，HP 5950 A 分解能 (200 meV)）を用い，半導体粉末触媒を金板の表面に塗布して測定を行なった。

3 結　果

3.1 半導体のエネルギー構造と反応性

太陽光で効率よく働く光触媒の条件を知る目的で，可視光を吸収し，なおかつ様々な伝導帯 (C.B.)，価電子帯 (V.B.) の位置をもついくつかの半導体粉末を用いて光触媒反応を試みた。反応系としては緒言で述べたように，（1） エタノール-水系からの水素発生と，（2） 酢酸の分解，メタン発生反応を選んだ。エタノールは水素発生効率の高い還元剤[3]，また，酢酸はエタノールよりも酸化されにくい有機物として選んだ[7]。これらの反応は以下のような酸化還元反応である。

（1） エタノール-水系[3)8)]

a） $CH_3CH_2OH + 2p \longrightarrow CH_3CHO + 2H^+$

b） $2H_2O + 2e \longrightarrow H_2 + 2OH^-$

（2） 酢酸系 (3.3 項を参照)

a） $CH_3COOH + p \longrightarrow \cdot CH_3 + CO_2 + H^+$

b） $H^+ + \cdot CH_3 + e \longrightarrow CH_4$

または

b′） $\cdot CH_3 + CH_3COOH \longrightarrow CH_4 + \cdot CH_2COOH$

b′) は Ag^+ などの電子アクセプターの存在下.

図1に種々の半導体のエネルギー準位を C.B. の高い順に示し同時にエタノール-水系での水素発生速度を示す。この図からわかることは，大まかな傾向として，TiO_2, CdS, MoS_2 のように C.B. の下端が H^+/H_2 より上にあるか，またはほとんど等しく，価電子帯の位置も適当に深い半導体を中心とした，いわば火山型の活性序列を示しており，C.B. の下端が H^+/H_2 より低い WO_3, Fe_2O_3 など，また，V.B. の位置の浅い GaP, Si などは活性が低い。

酢酸の分解反応においても同様な考え方で活性の説明はできる。実験で得られた活性序列は，

$$TiO_2 \gg WO_3 > Fe_2O_3 \gg CdS \approx MoS_2 = 0$$

Ag^+ を電子受容体として存在させると，

$$TiO_2 \approx WO_3 > Fe_2O_3 \gg CdS \approx MoS_2 = 0$$

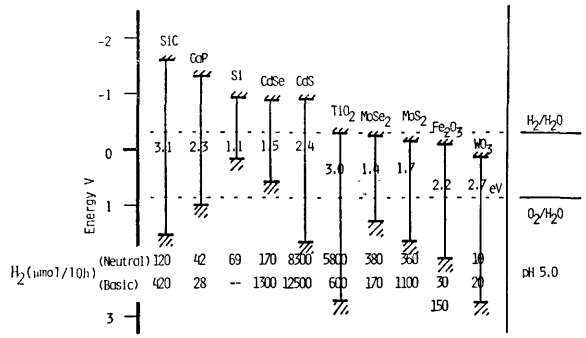

Fig. 1 The rate of H_2 production from water-ethanol mixture with various platinized semiconductor particles by the irradiation with 500 W Xe lamp

The figure includes band gap energy, conduction and valence band positions, and the rate of H_2 production in neutral and basic media.

であった。WO_3 は Ag^+ 存在下で初めて酢酸分解に TiO_2 と同じ程度の活性をもつ。量子効率は 380 nm の単色光に対して約 35% であった。

粉末の光触媒反応では，酸化反応と還元反応が両方とも効率よく一つの粒子内で起こらねばならない。酢酸はエタノールより酸化されにくいので（酸化電位+2.1～2.7 V vs. NHE[9)]），たとえ還元力のある CdS や MoS_2 でも酸化力が TiO_2 にくらべて低いため酢酸を酸化することができず，結果として全反応は進まない（図1参照）。WO_3 は C.B. の位置は低いが V.B. の位置は十分深いので（TiO_2 とおなじぐらい）Ag^+ のような電子受容体を共存させさえすれば酢酸は正孔によって酸化され，このプロセスにより CH_4 発生は TiO_2 と同じような活性で進行する。CdS や MoS_2 は酸化力の方が足りないので電子受容体共存下でも相変わらず反応は進行しない。

このように第一近似として，V.B., C.B. の位置でそれぞれ酸化力，還元力を予想できるが，微粒子光触媒での全反応の進行には同一粒子内で酸化還元の両反応が同時に効率よく起こる半導体が要求される。それには，C.B., V.B. の絶対的な位置でなく反応分子と半導体の組み合わせが重要で，酸化される分子の酸化電位，還元される分子の還元電位を半導体のバンドギャップの間にはさむことが必要条件となる。

3.2 TiO_2/Pt の表面構造と反応性

微粒子光触媒の反応性と表面構造，とくに担持金属の状態を知る目的で，もっともよく用いられる TiO_2/Pt 光触媒の表面を高分解能電子顕微鏡で観察し，その幾何学的状態を明らかにし，さらに XPS によって電子状態を調べた。

スターラーでかきまぜながら光電析法で調製した TiO_2/Pt の高分解能電子顕微鏡像では，Pt は TiO_2 と同じくらいのサイズでひとつかふたつ付着しているような構造ではなく，いわば“豹の斑点”のように数 10～100 Å ぐらいの大きさで TiO_2 (～0.5 μ) 上に数多く分散した構造をしていることがわかった（図2）。この構造は，混練法で調製した場合やスターラーかきまぜしない光電析法で調製した場合も同様であるが，白金粒子径が大きく，

7) B. Kraeutler, A. J. Bard, *J. Am. Chem. Soc.*, **100**, 2239, 5985(1978).

8) 主生成物としてアセトアルデヒドを検出したこと，純エタノールのみにおいても効率よくエタノールの酸化が起こることから，主反応としては(a)式を考え OH ラジカルの寄与などの副反応はここでは省いた．(b)式については，D_2O を用いた実験により水素が水から由来していることを確かめた，

9) A. J. Bard, H. Lund, “Encyclopedia of Electrochemistry of the Elements”, Vol. 12, Marcel Dekker Inc., New York (1978) p. 266.

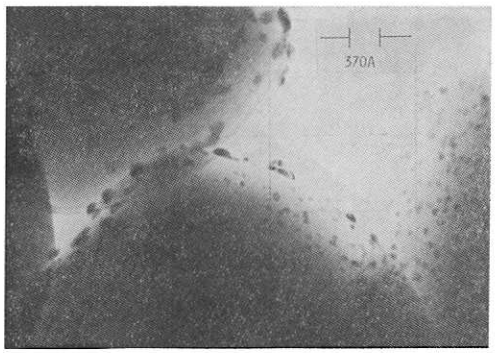

Fig. 2 Electron-micrograph of platinized TiO_2 (Pt :1 wt%) particle made by photo-electrochemical deposition method

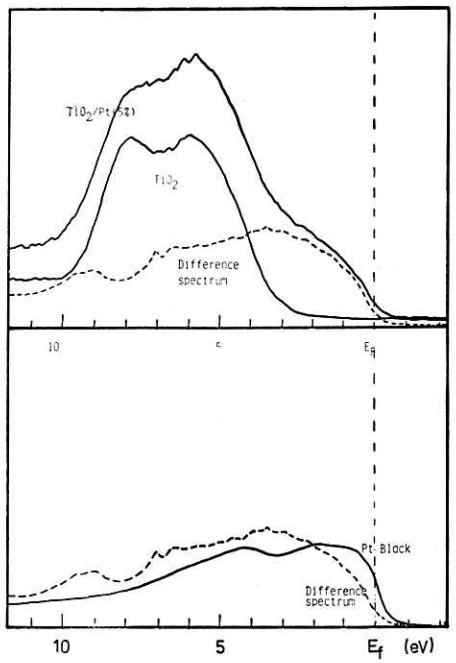

Fig. 3 X-ray photoelectron spectra of TiO_2 and TiO_2/Pt (5%) in the valence band region

The difference spectrum between TiO_2 and TiO_2/Pt, and the spectrum of Pt black are shown below.

数も少なくなり，後で述べるように光触媒反応の選択性に影響する。XPS スペクトルでは白金がよく分散された試料でも，TiO_2 の Fermi 面付近から白金のメタリックなバンドが立ち上がり，TiO_2 禁制帯のエネルギー領域に白金の満ちた価電子準位が存在する（図3）。しかし state density の形は白金ブラックとは異なっており，白金の valence 帯のピークは高 binding energy 側にずれている。その原因としては，白金が微粒子のため完全には金属的になっていないためと考えている。白金の担持量を増すと白金金属の状態密度分布に近づくからである。このことの光触媒効果への影響については今後の課題である。

Fermi レベルより 3 eV 下から TiO_2 の O : 2p による価電子帯がはじまる。このように TiO_2 粒子上に約 100 Å の間隔で白金が担持されている電子状態は図4のように表わされる。この特徴は酸化サイトである TiO_2 と還元サイトである白金が非常に

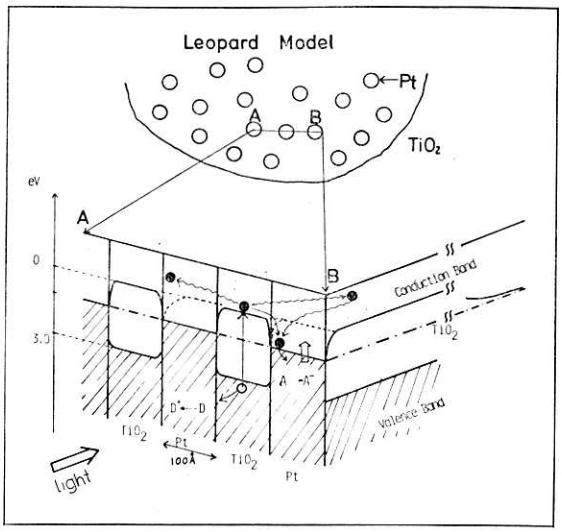

Fig. 4 Schematic model of a TiO_2/Pt particle

This figure includes the three dimensional energy structure for the region A-B on the particle, and the oxidation process by the hole on TiO_2 surface and the reduction process by electron on Pt surface.
The size and the distance of each Pt patch is taken to be 100 Å.
The barrier height at the metal-semiconductor interface is modified by the image force of the metal.

近接していることであり，しかも粒子表面がすべてほぼ均一にこのような斑点状の白金でおおわれていることである。反応分子が TiO_2 の正孔で酸化された場合，もし，この酸化生成物が再還元されにくいものであったり，すばやく分解してしまう不安定なものであれば，たとえ白金の還元サイトがすぐそばにあっても残された電子は白金上で有効に水素発生に使われる。しかし酸化された分子がラジカルのような中間的な形で安定に長寿命存在する場合は，これが生成した酸化サイトのすぐそばに白金があるため，この中間体は容易に再還元されてしまい水素発生は効率よく起こらない。

実際，このような表面構造の結果からすると，アルコールのように電流二倍過程[10]によって二電子酸化され，すぐ安定なアルデヒドになる系，また，カルボン酸のように中間ラジカル（$CH_3CO\dot{O}$；寿命 1ns[11]）がただちに分解してしまう反応系では白金が分散して担持された TiO_2 で反応が効率よく起こることがよく理解される。実際 TiO_2/Pt を用いるとエタノール-水からの水素発生量子効率は 60%，酢酸からのメタン発生では 30% におよぶことが波長 380 nm の単色光照射実験の結果がわかった。

3.3 TiO_2/Pt 粒子での酢酸の分解反応機構

豹の斑点状の TiO_2/Pt 触媒の構造的な特徴の反応選択性への影響は，酢酸の分解において見ることができた。TiO_2/Pt でのこの反応は光 Kolbe 反応として Bard らにより報告され[7]，CH_4 と CO_2 が選択的に生成する（前述の反応式）。電極による Kolbe 反応では C_2H_6 が多く生成する。この反応は，CH_3COOH

10) M. Miyake, H. Yoneyama, H. Tamura, *Chem. Lett.*, 1976, 635.
11) W. Braun, L. Rajbenbach, F. R. Eirich, *J. Phys. Chem.*, 66, 1951(1962).

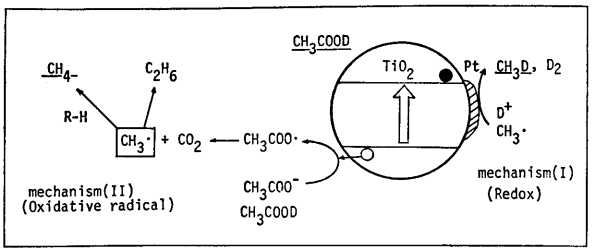

Fig. 5 The two different mechanisms of the decomposition of acetic acid (CH_3COOD) and the methane formation on a TiO_2/Pt particle

One is redox mechanism and the other is oxidative radical mechanism.

が TiO_2 の正孔により直接，または水の酸化で生じた OH ラジカルにより酸化され $CH_3COO\cdot$ を生じるところからはじまる。

図5に示すように，CH_3COOD（重水素化酢酸）を出発物質とすると，酸化されて $CH_3COO\cdot$ と D^+ を生成し，CO_2 を脱離したのち $\cdot CH_3$ を生じ，その後の機構としては，（1） レドックス機構；$CH_3\cdot$ と e と D^+ により CH_3D を生成，または，（2） ラジカル機構；$CH_3\cdot$ が酢酸の CH から H を引き抜き CH_4 を生成するという二つの異なった機構が考えられる。CH_3COOD を用いるとこの二つの機構が生成物の差（CH_3D と CH_4）として区別できる。白金がよく分散した光触媒では，CH_3D が 90% 以上の主生成物であった。混練法で調製すると白金の分散が悪くなるが，その光触媒を用いると約 20～30% CH_3D の生成比が減る。また白金の分散のよい光触媒でも Ag^+ を電子受容体として共存させると CH_4 が主生成物となる。

図5で理解されるように酸化サイトと還元サイトが離れていれば，酸化サイト（TiO_2）で生じた $CH_3\cdot$ はレドックス機構で CH_3D になるためには遠い還元サイトに移動しなければならず，この場合はむしろラジカル機構により CH_4 が生成してしまう。ここで用いている斑点状の TiO_2/Pt では酸化-還元サイトがきわめて接近（≈100 Å）して全体に分布していることのため，この光触媒に特有なレドックス機構の CH_3D 生成の効率を上げている。

3.4 水素発生の溶液依存性

表1にいくつかの有機物と水からの水素発生速度を有機物のイオン化ポテンシャルの小さい順にならべてある。この表から，水素発生効率は有機物のイオン化ポテンシャルだけでは決まらないことがわかる。アセトニトリルで水素発生が小さいのはイオン化ポテンシャルが大きすぎて酸化できないためであろう。実際，TiO_2 光電極による実験ではアセトニトリルは酸化できない。一方，イオン化ポテンシャルの小さい分子がよいとはかぎらない。*N*-メチルアニリンは容易に酸化され得るが，その結果生じるラジカルが安定であるため[12]，微粒子光触媒ではふたたび還元されてもとにもどってしまうため水素発生の効率が悪くなるものと思われる。

Table 1 The ionization potential of organic molecules and the H_2 production rate on TiO_2/Pt from water and these organic substances (H_2O : organic mole=1 : 1)

Substrate	Ionization potential	H_2 production rate (μmol/10 h)
N-Methylaniline	7.73	1
Toluene	8.85	10
Benzene	9.24	40
Octane	10.38	40
2-Propanol	10.48	4000
1-Propanol	10.48	3000
Ethanol	10.65	5500
Formaldehyde	10.80	4000
Methanol	10.85	6000
Acetic acid	10.87	2000
Formic acid	11.33	5000
Acetonitrile	12.20	10

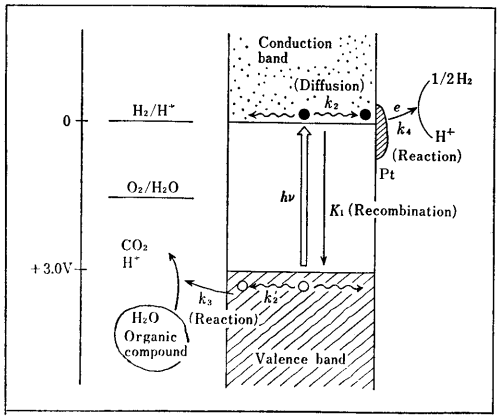

Fig. 6 Energy diagram of TiO_2/Pt particle on which the oxidation of water and organic substance and the hydrogen production proceed

3.5 半導体微粒子光触媒の特徴

本報で扱っている微粒子の光触媒反応は大きな半導体単結晶（1 mm～1 cm）を用いた光電極反応と共通点が多いが，微粒子特有の現象もみられる。図6に白金担持 TiO_2 を例にとり，そのエネルギー図と光触媒過程を模式的に表わしてある。光触媒過程は，（1） おのおのの粒子が光を吸収し，電子-正孔対を生じる。（2） 電子-正孔は拡散，または，電位勾配で移動する。（3） 微小粒子なのでただちに粒子表面に到達する。（4） 同時に再結合で消滅するものもある。（5） 表面で電子移動反応を起こす，として進行する。

この TiO_2/Pt 光触媒は TiO_2 陽極と白金陰極を用いる光電気化学セルとは，以下のように対比されるであろう（表2）。1) 光化学電池では酸化反応と還元反応が完全に分離された場所で起こるが，微粒子系では非常に接近した場所で起こる。2) 微粒子系では，多数の（$>10^{13}$ 個）微小な（0.5μ～300 Å）ミクロセルが独立して働き，反応を起こす有効な表面積が 10^4～10^5 倍も増加する。微粒子内で生成した電子，正孔は各粒子あたり数少なく，隔離されており失活せずにただちに表面に到達して反応を起

12) J. K. Kochi, "Free Radical", Vol. II, John-Wiley and Sons, New York (1973) p. 573.

Table 2 Comparison of particulate semiconductor photocatalyst with bulky single crystal semiconductor photoelectrode

		Bulky single crystal	Particle	Colloid (Molecule)
1	Size	1 cm-1 mm	⟶	1 μ-300 Å 10 Å
2	Number of electrodes	1	⟶	10^{13}～10^{19}
3	Reactive surface area	1 cm^2	⟶	10^5 cm^2
4	Redox reaction sites	Completely separated	⟶	Close
5	Space charge layer	Essential	⟶	Not essential
6	Reduction pretreatment	Necessary	⟶	Not necessary
7	Distribution of p(e)	Large number, Near surface	⟶	Small number, Uniform in a particle
8	P(e) Migration	Long	⟶	Short
9	Electrode	Fixed	Mobile	Mobile
10	Electrolyte	Necessary	⟶	Not necessary
11	Electrode potential	Fixed	⟶	Floating
12	Reactivity (No bias conditions)	Ethanol Acetic acid 1	⟶	10^3 10^4

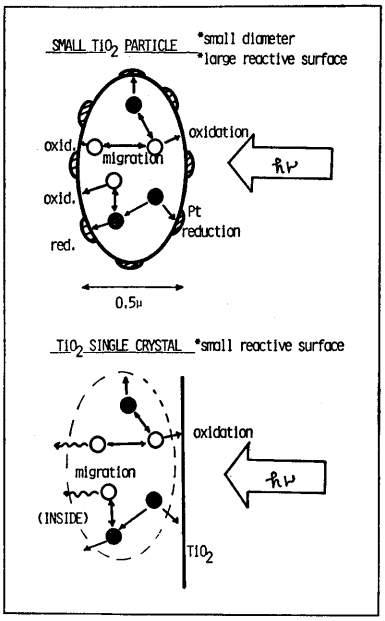

Fig. 7 Schematic representation of small particle of platinized TiO_2 as revealed in this study, and that of bulky TiO_2 single crystal

こす率が高い。3) TiO_2 光電極では還元処理をして space charge layer をつくり，電位を強制的にかけ電子，正孔を分離することができるが，粒子系では，径が小さくなると（数 100 Å），space charge layer による電荷分離の寄与はないと考えられ，表面での反応速度と電子，正孔の拡散，再結合までの寿命の関係が大事になる。還元処理をしない TiO_2 粒子でもよい活性を示す。

今回の研究の結果得られた光触媒の構造をもとに，模式的に TiO_2/Pt を表わしたのが図7であり，大きな単結晶とくらべて電子，正孔が効率よく表面に到達して白金または TiO_2 上で還元または酸化反応をすることがよく理解される（微粒子効果）。これに対して，電子-正孔の拡散距離より大きいサイズの TiO_2 結晶を用いると電子-正孔は内部で再結合を起こす確率が増し，有効に反応に用いられないことが示されている。

実際，表2に示されているように，水-エタノールからの水素発生，酢酸からのメタン発生で，微粒子系（5000～300 Å）では，1×1×10 mm の単結晶を用いた場合より，それぞれ 10^3～10^4 倍の高い効率を示すことがわかった。

Special Articles on
Photochemical Reactions and Applications

The Structure and the Reactivity of Particulate Semiconductor Photocatalyst

Tomoji KAWAI*, Tadayoshi SAKATA**, Kazuhito HASHIMOTO** and Maki KAWAI***

Institute of Scientific and Industrial Research, Osaka University ; Mihogaoka, Ibaraki-shi 567 Japan
** *Institute for Molecular Science ; Nisigo, Myodaijimachi, Okazaki-shi 444 Japan*
*** *Department of Chemistry, Faculty of Science, The University of Tokyo ; Hongo, Bunkyo-ku, Tokyo 113 Japan*
Present address : Osaka Gas Co., Research Cent.; Torishima, Konohana-ku, Osaka-shi 554 Japan

In order to elucidate the determining factors which control the reactivity of particulate semiconductor photocatalyst and to exploit a new material for the efficient photocatalyst, the relation between the electronic structure of the particle and the reactivity was studied through the hydrogen production from water-ethanol mixture and methane production from acetic acid. For H_2 production, Fe_2O_3 and WO_3, whose conduction band edge are below H^+/H_2, are poor photocatalysts in spite of their deep valence band positions. Si and GaP have conduciton band high enough for H_2 production, but valence band positions are not deep. For this reason, they are also poor photocatalysts for H_2 production from water-ethanol mixture. CdS, TiO_2 and MoS_2 have conduciton bands colse to H^+/H_2 and, furthermore, have moderate valence band position. These are efficient photocatalysts for H_2 production by visible and UV light. The activity of methane production from acetic acid could also be explained in the same manner.

Electron microscopic investigation of platinized TiO_2 particle revealed that platinum is deposited on the TiO_2 particle as many small spots, like a body of Leopard, the size of which are about 100 Å. The XPS spectrum showed that the edge of the filled state density distribution of Pt valence band coincides with the Fermi level of TiO_2. The oxidizing site, TiO_2, and reducing site, Pt, are very close to each other. Accordingly, if a molecule in solution is oxidized irreversibly into a stable chemical species, then the corresponding electron can be effectively used for the H_2 production.

The effect of this surface structure was observed in the decomposition of acetic acid to form methane, where "the redox mechanism" is dominant on the TiO_2 with highly dispersed Pt. Finally, the characteristic feature of small particlulate photocatalyst is compared with that of bulky semiconductor photoelectrode.

CHEMISTRY LETTERS, pp. 1449 - 1452, 1984.

PHOTOCATALYSIS OF ZINC SULFIDE MICROCRYSTALS IN REDUCTIVE HYDROGEN EVOLUTION IN WATER/METHANOL SYSTEMS

Shozo YANAGIDA,* Hiroshi KAWAKAMI, Kazuhito HASHIMOTO,† Tadayoshi SAKATA,† Chyongjin PAC, and Hiroshi SAKURAI††

Chemical Process Engineering, Faculty of Engineering, Osaka University, Suita, Osaka 565
†Institute for Molecular Scienece, Myodaiji, Okazaki 444
††Nara Technical College, Yata-cho, Yamatokoriyama 639-11

In photocatalytic H_2 evolution using an aq. methanol system, high quality microcrystalline(cubic) ZnS powders have been found to be active under an appropriate light intensity, which is comparable in activity with freshly prepared ZnS suspensions. Comparison of photoactivities of some commercial ZnS with their surface properties has revealed that the surface purity of ZnS plays an important role in the photocatalysis, while the luminescence observed at 445 nm for the high quality ZnS microcrystals was not affected in the presence of oxygen, diethylamine, or methylviologen.

Previously we reported that ZnS suspensions prepared *in situ* from aq. $ZnSO_4$ and Na_2S are very efficient as unmodified photocatalysts for UV light(λ>290 nm) photoredox reactions in aq. electron donor solutions; water is effectively reduced to evolve H_2 and some organic electron donors concurrently undergo one electron oxidation, leading to carbon-carbon bond formation via radical coupling reactions.[1,2] However, commercial ZnS powders for electroluminescence(Mitsuwa EL grade) showed little activity compared with the freshly prepared ZnS suspensions, and the colloidal parts of the freshly prepared ZnS seemed to play a decisive role in the photocatalysis. In fact, the acceleration of photochemical reactions by colloidal particles received much attention.[3-6] On the other hand, the reported value for the conduction band edge of ZnS, -1.74 V vs. SCE(pH 1),[7] suggests a strong reductive power of electron in the conduction band and also rationalizes the highly efficient H_2 evolution in the unmodified ZnS photocatalysis.

We now report that the high quality ZnS microcrystal dispersions are as active in photoreductive H_2 evolution as the freshly prepared ZnS suspensions.

In order to evaluate the photoelectron transfer activity of some commercial ZnS, the photoreductive H_2 evolution was investigated using an N_2 purged aq. methanol system. The physical properties of the examined ZnS, the reaction conditions, and the quantum yields measured on 313 nm irradiation are summarized in Table 1.

Compared with the quantum yield, 0.14, for the freshly prepared ZnS,[2] the commercially available CP grade ZnS powders have been found to have fairly good activities. Surprisingly, Nakarai GR grade ZnS crystals, which have the smallest surface area of the examined ZnS, show the highest activity. It should be noted that, under highly intense light like an internal UV irradiation, Nakarai ZnS powders blacken due to the photoformed metal Zn and gradually lose the activity. As we reported previously, Mitsuwa EL grade ZnS powders were confirmed to be ineffective in their activity without the blackening.

Observation by scanning electron microscopy reveals that Shimakyu ZnS powders are fine particles(Fig. 1a), Nakarai ZnS powders consist of crystalline

Table 1. The Physical Properties and the Photocatalytic Activity of Some Commercial ZnS Powders

ZnS	Purity %	Particle size μm	Surface[a] area/m^2g^{-1}	Crystal form[b]	Reaction conditions[c] ZnS/μmol	Quantum yield[d] $\Phi(1/2H_2)$ (react. time/h)[e]
Shimakyu (CP grade)	f)	<0.1[g]	14.4	c	104	0.055(5), 0.057(6)
Wako (CP grade)	-	<0.1[g]	7.0	c/h	150	0.017(5), 0.023(10)
Nakarai (GR grade)	99.99	av. 3	<1	c	108	0.093(5), 0.092(21)
Mitsuwa (EL grade)	h)	av. 2	43.2	c	125	0.003(10)

a) Determined by BET method. b) h, hexagonal; c, cubic. c) Methanol(3 ml) and water(1 ml) were used. d) Determined using a 2-hexanone actinometer by assuming that two photons produce one molecule of H_2 and corrected for light absorption by the suspended catalyst. e) Reactions were mostly carried out twice using the same reaction mixture. f) Contaminated with unknown crystalline salts, as determined by the X-ray diffraction pattern. g) Estimated by the scanning electron microscopy. h) Metallic impurity max. 5 ppm.[8]

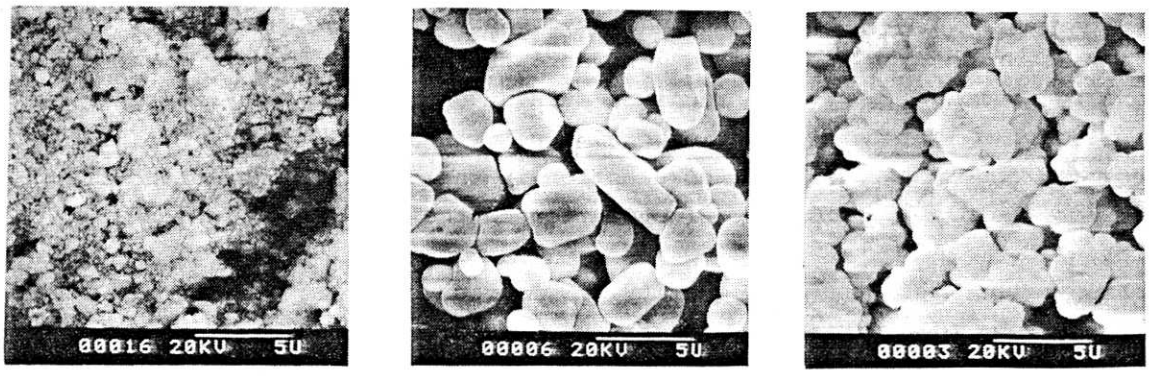

a b c

Fig. 1. Scanning electron micrographs of commercial zinc sulfide powders.
a: Shimakyu CP Grade, b: Nakarai GR Grade, c: Mitsuwa EL Grade.

particles(Fig. 1b), and Mitsuwa ZnS powders are porous particles, i.e., have the structure of second order particles composed of smaller particles(Fig. 1c). The porous structure explains the large surface area contrary to the apparent large particle size. These facts clearly indicate that the surface area is not necessarily an important factor affecting the photocatalytic activity.

Based on X-ray diffraction analysis, Nakarai ZnS powders were characterized to be cubic(sphalerite), both Mitsuwa and Shimakyu ZnS to be cubic contaminated by a small amount of hexagonal(wurtzite) form, and Wako ZnS to be a mixture of cubic and hexagonal forms. It is worth noting that Mitsuwa ZnS showed broad X-ray diffraction patterns.

The surfaces of Nakarai and Mitsuwa ZnS powders were investigated by ESCA. No substantial difference was observed in the spectra, indicating that the surface within a few nm are not different in composition. It should be mentioned that both ZnS powders were covered with oxygen atoms which were not removed even after heating at 400 °C for a period of 1 h followed by 0.5 h argon etching. This is probably due to the adsorbed O_2 which may diffuse into ZnS and/or the presence of oxidized ZnS species like ZnO on the surfaces.

The oxidative formation of ZnO on ZnS is supported by the photoacaustic spectra. As shown in Fig. 2, ZnO powders show a sharp onset at 400 nm, and the most effective ZnS powders obtained by evaporating to dryness the *in situ* prepared ZnS suspension(which involved Na_2SO_4) showing a sharp onset at 370 nm. The less active Wako ZnS have an onset at around 400 nm, indicating contamination by ZnO. The inactive Mitsuwa ZnS shows the spectrum which "tails" from 400 nm to 480 nm, indicating the presence of ZnO on the surface and/or the presence of surface defects attributable to metallic impurities(max 5 ppm).[8] Since the photo-generated electron-hole pairs should be trapped by such oxide surface or impurity levels and then inactivated, Mitsuwa ZnS was concluded to show little activity in the photocatalytic reaction.

Recently, Henglein and Gutierrez reported the photoluminescence of the colloidal ZnS and its quenching by electron donors and acceptors.[9] Since the most active Nakarai ZnS was found to show the strongest photoluminescence with a maximum at 445 nm under air at room temperature, the relationship of the luminescence with photoelectron transfer reactions was examined.

The decay of the luminescence shown in Fig. 3 was different in lifetime(τ) from that reported for the colloidal ZnS.[9] The photoluminescence can be divided roughly into two components, fast(τ_{fast}= 32 ns) and slow(τ_{slow}=610 ns) ones, whose spectra are different from each

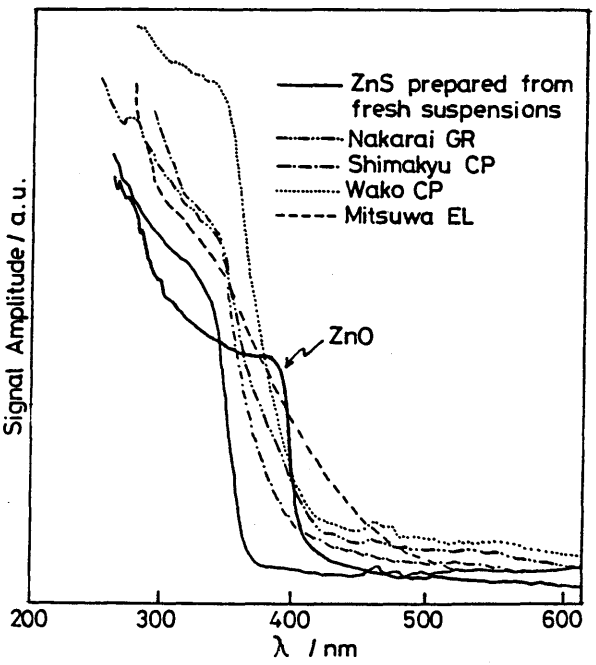

Fig. 2. Photoacaustic spectra of commercial ZnS powders.

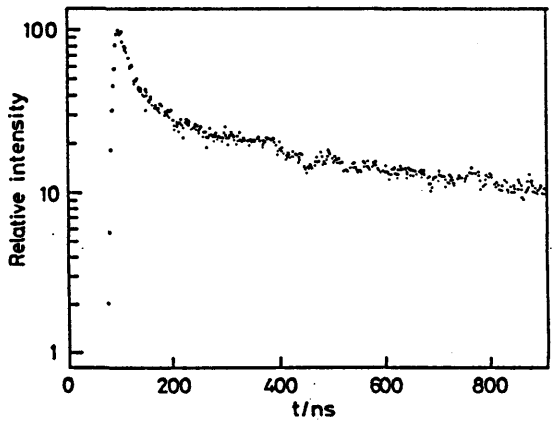

Fig. 3. Decay of Nakarai ZnS. Luminescence at 452 nm(under air at room temp). Light source: Pulsed N_2 laser, 6 ns, 337 nm.

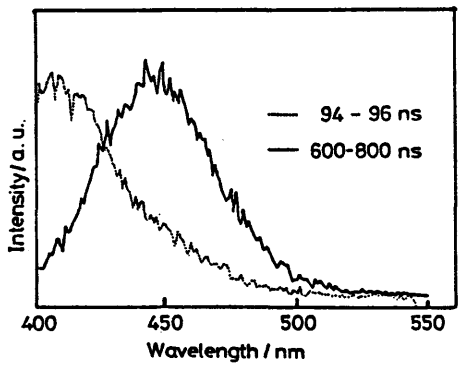

Fig. 4. Time-resolved luminescence spectra of Nakarai ZnS powder(under vacuum) observed with ns photon counting system.[11] Light source: Pulsed N_2 laser, 6 ns, 337 nm.

other as shown in Fig. 4. However, the decay of the luminescence was not affected by further desorption of air by heating *in vacuo* to 300 °C and by the introduction of air. Further, neither diethylamine nor methylviologen quenched the luminescence emitted on 337 nm excitation in water. These facts are inconsistent with a recent report on the colloidal ZnS system.[9] Since diethylamine is a good electron donor in the photocatalysis of ZnS,[10] the electron-hole pairs which give rise to photoluminescence should be indifferent to interfacial reactions. Another source of electron-hole pairs should play an important role in electron transfer reactions.

The authors thank to Dr. J. N. Moore for careful reading of the manuscript and to Dr. Hajime Nakamura (Goverment Industrial Research Institute, Osaka) for his help in taking photoacaustic spectra. This work was partly supported by a Grant-in-Aid for Scientific Research from the Ministry of Eductaion, Science and Culture of Japan and Joint Studies Program(1983) of the Institute for Molecular Science.

References

1) S. Yanagida, T. Azuma, and H. Sakurai, Chem. Lett., 1982, 1069.
2) S. Yanagida, T. Azuma, H. Kawakami, H. Kizumoto, and H. Sakurai, J. Chem. Soc. Chem. Commun., 1984, 21.
3) M. Grätzel, Acc. Chem. Res., 14, 376(1981).
4) A. Henglein, Ber. Bunsenges Phys. Chem., 86, 241, 301(1982).
5) J. Kuczynski and J. K. Thomas, J. Phys. Chem., 87, 5498(1983).
6) W. G. Becher and A. J. Bard, J. Phys. Chem., 87, 4888(1983).
7) F. -R. F. Fan, P. Leempoel, and A. J. Bard, J. Electrochem. soc., 130, 1866 (1983).
8) Based on the indication on the label of Mitsuwa ZnS.
9) A. Henglein and M. Gutierrez, Ber. Bunsenges. Phys. Chem., 87, 852(1983).
10) S. Yanagida, H. Kizumoto, and H. Sakurai, Unpublished work.
11) T. Yamanaka and I. Yamazaki, Annual Review of Insititute for Molecular Science, p. 131(1983).

(Received May 30, 1984)